



UNIL | Université de Lausanne

Unicentre

CH-1015 Lausanne

<http://serval.unil.ch>

Year : 2012

SURVIVAL RESPONSES IN STRESSED ORGANS

KHALIL Hadi

KHALIL Hadi, SURVIVAL RESPONSES IN STRESSED ORGANS

Originally published at : Thesis, University of Lausanne

Posted at the University of Lausanne Open Archive.
<http://serval.unil.ch>

Droits d'auteur

L'Université de Lausanne attire expressément l'attention des utilisateurs sur le fait que tous les documents publiés dans l'Archive SERVAL sont protégés par le droit d'auteur, conformément à la loi fédérale sur le droit d'auteur et les droits voisins (LDA). A ce titre, il est indispensable d'obtenir le consentement préalable de l'auteur et/ou de l'éditeur avant toute utilisation d'une oeuvre ou d'une partie d'une oeuvre ne relevant pas d'une utilisation à des fins personnelles au sens de la LDA (art. 19, al. 1 lettre a). A défaut, tout contrevenant s'expose aux sanctions prévues par cette loi. Nous déclinons toute responsabilité en la matière.

Copyright

The University of Lausanne expressly draws the attention of users to the fact that all documents published in the SERVAL Archive are protected by copyright in accordance with federal law on copyright and similar rights (LDA). Accordingly it is indispensable to obtain prior consent from the author and/or publisher before any use of a work or part of a work for purposes other than personal use within the meaning of LDA (art. 19, para. 1 letter a). Failure to do so will expose offenders to the sanctions laid down by this law. We accept no liability in this respect.



UNIL | Université de Lausanne

Faculté de biologie
et de médecine

Département de Physiologie

SURVIVAL RESPONSES IN STRESSED ORGANS

Thèse de doctorat ès sciences de la vie (PhD)

présentée à la

Faculté de biologie et de médecine
de l'Université de Lausanne

par

Hadi KHALIL

Maitrise-es Sciences de l'Université Libanaise, Beyrouth

Jury

Prof. François Pralong Président
Prof. Christian Widmann, Directeur de thèse
Prof. Marijke Brink expert
Prof. Dario Diviani expert

Lausanne 2012

Imprimatur

Vu le rapport présenté par le jury d'examen, composé de

<i>Président</i>	Monsieur Prof. François Pralong
<i>Directeur de thèse</i>	Monsieur Prof. Christian Widmann
<i>Experts</i>	Monsieur Prof. Dario Diviani
	Madame Prof. Marijke Brink

le Conseil de Faculté autorise l'impression de la thèse de

Monsieur Hadi Khalil

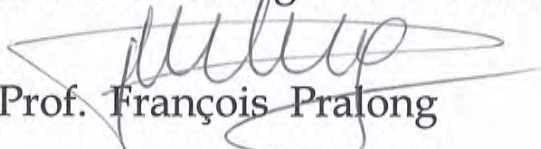
Master degree of Mediterranean Agronomic Institute of Chania, Greece

intitulée

SURVIVAL RESPONSES IN STRESSED ORGANS

Lausanne, le 7 décembre 2012

pour Le Doyen
de la Faculté de Biologie et de Médecine



Prof. François Pralong

Acknowledgements

I dedicate this work to my Mom. I would like to thank all my family for being with me even though you were far by distance; you were close, helpful and kept faith in me all the time. Thanks to all my friends who supported.

For my colleagues in the lab, who turned to be my best friends, and made the difficult PhD times very easy for me, I thank you all for your support. I would like to thank specifically Gilles Dubuis, you are an amazing person at all aspects, and you are always there for support whenever it is needed. I thank Nieves Peltzer, you are a great person and a remarkable team player, I enjoyed sharing many things together with you. David Barras and Alessandro Annibaldi I thank you for your interesting input and fruitful discussions in science and other aspects of life as well. Jiannick Petremand and Evrim Jaccard, I thank you for your kindness, for the assistance you offered, and for encouragement to learn the French language. I thank Mohammad Nemir, Corinne Berthonneche, Noureddine Loukili, Jiang-yan Yang, Natasha Bulat, Koshika Yadava and Nathalie Rosenblatt for their assistance.

This successful work would have never been completed without Christian Widmann who I thank for his instructions, guidance and support throughout the years of my PhD. I would like also to thank Professors Lucas Liaudet, Thierry Pedrazzini, Dario Diviani and Benjamin Marsland, I learned a lot from you and appreciated collaborating with you and participating in your lab meetings.

Thanks to the Jury members, Professors François Pralong, Marijke Brink and Dario Diviani, your questions and discussion were very helpful and precious.

Thanks to the French language expert “David Barras”, the English language expert “Nickolas Brosky” and thanks to Nieves and Mathieu for their input and corrections.

Thanks to Darko Maric (the efficient master), Aline Dousse and philippe Diderich, I wish you good luck in your current PhD studies.

For my new colleagues in the lab, Mathieu Heulot, Guliz Vanli, Issam Bilal and Elettra Santori, thank you and I wish you all the best in your PhD.

Table of content

Summary	1
Résumé	5
1. Introduction	9
1. Programmed cell death	11
1.1. Apoptosis	11
1.2. Necrosis and Necroptosis	12
2. Morphological properties of apoptotic cells	13
2.1. Cytoskeleton proteolysis and membrane blebbing	13
2.2. The nuclear envelope and nuclear fragmentation	13
2.3. DNA condensation and degradation	14
2.4. Fragmentation of organelles and shut down of transcription and translation	15
2.5. Clearing of apoptotic cell	15
3. Caspases	16
3.1. Caspase activation by extrinsic and intrinsic pathways	17
3.2. Caspase activation by Granzyme B	20
3.3. Inhibition of caspases and non-apoptotic functions of caspases	20
4. G proteins	22
5. RasGAP domains and function	23
6. Pro-survival Phosphoinositide 3- kinases (PI3K)/Akt pathway	26
7. Protein Kinase B (PKB/Akt)	27
7.1. Akt survival functions	28
8. NF- κ B family of transcription factors	30
8.1. NF- κ B-mediated signals	32
8.2. Regulation of NF- κ B signals	34
9. Heart	35
9.1. Reactivation of the fetal gene program	38
9.2. Myocardial cell death	38
9.3. Myocardial fibrosis	39
9.4. Sensing and transduction of hypertrophy signals	41
10. Physiological role of apoptosis	43
Reference list	44

2. Objectives	53
3. Results	57
• Part I	59
1-Introduction	59
2-Results	59
3-Contribution	59
4-Research article and supplemental data	61
• Part II	83
1-Introduction	85
2-Results	85
3-Contribution	85
4-Research article and supplemental data	87
• Part III	100
1-Introduction	102
2-Results	102
3-Contribution	102
4-Unpublished data	104
• Part IV	124
1-Introduction	126
2-Results	126
3-Contribution	126
4- Unpublished data	128
• Part V	169
1-Introduction	171
2-Results	171
3-Contribution	171
4. Discussion and perspectives	176
5. Methods	189

Figure List

Figure 1. Caspase family members and their activation	19
Figure 2. Pathways of caspase activation	21
Figure 3. Ras activation and RasGAP cleavage by caspase-3	24
Figure 4. Ras/PI3K/Akt pathway	29
Figure 5. Members of the NF- κ B, I κ B and IKK protein families	31
Figure 6. Canonical and non-canonical NF- κ B signaling	33
Figure 7. Development and progression of chamber hypertrophy	37

Summary

Summary

Apoptosis or programmed cell death is a regulated form of cell suicide executed by cysteine proteases, or “caspases”, to maintain proper tissue homeostasis in multicellular organisms. Dysregulation of apoptosis leads to pathological complications including cancer, autoimmunity, neurodegenerative, and heart diseases. Beside their known function as the key executioners of apoptotic cell death, caspases were reported to mediate non-apoptotic functions. In this report we study the survival signals conveyed through caspase-3-mediated cleavage of Ras GTPase-activating proteins (RasGAP). Ubiquitously expressed, RasGAP senses caspase activity and controls the cell death/survival switch. RasGAP is cleaved once at low caspase activity and the generated N-terminal fragment (fragment N) induces a survival response by activating Ras/PI3K/Akt pathway. However, high caspase activity associated with increased stress leads to fragment N cleavage into fragments that do not mediate any detectable survival signals.

In this thesis project we studied the role of fragment N in protecting stressed organs as well as in maintenance of their functionality. In response to stress in different organs, we found that mice lacking caspase-3 or unable to cleave RasGAP (Knock-In mice), and therefore unable to generate fragment N, were deficient in Akt activation and experienced increased apoptosis compared to wild-type mice. Augmented tissue damage and organ dysfunction in those mice highlight the importance of fragment N in activating Akt-mediated prosurvival pathway and in protection of organs during episodes of stress.

In parallel we investigated the role of fragment N in regulating the activation of transcription factor NF- κ B, a master regulator of inflammation. Sustained NF- κ B activation may be detrimental by directly causing apoptosis or leading to a persistent damaging inflammation response. We found that fragment N is a potent inhibitor of NF- κ B by favoring its nuclear export. Therefore, fragment N regulates NF- κ B activity and contributes to a controlled response as well as maintenance of homeostasis in stressed cells.

Importantly, these findings introduce new insights of how activated caspase-3 acts as a stress intensity sensor that controls cell fate by either initiating a fragment N-dependent cell resistance program or a cell suicide response. This identifies the pivotal role of fragment N in protection against patho-physiological damage, and

Summary

encourages the development of therapies which aim to increase cell resistance to vigorous treatment.

Résumé

Résumé

L'apoptose, ou mort cellulaire programmée, est une forme contrôlée de suicide cellulaire exécuté par des protéines appelées caspases, dans le but de maintenir l'homéostasie des tissus sains dans les organismes multicellulaires. Un mauvais contrôle de l'apoptose peut mener à des pathologies comme le cancer, la neurodégénération et les maladies cardiaques et auto-immunes. En dehors de leur rôle connu d'exécutrices de l'apoptose, les caspases ont aussi été identifiées dans d'autres contextes non-apoptotiques. Dans ce projet, nous avons étudié les signaux de survie émis par le résultat du clivage de RasGAP par la caspase-3. Exprimée de façon ubiquitaire, RasGAP est sensible à l'activité de caspase-3 et contrôle la décision de la cellule à entreprendre la mort ou la survie cellulaire. A un taux d'activité faible, la caspase-3 clive RasGAP, ce qui mène à la génération d'un fragment N-terminal, appelé Fragment N, qui induit des signaux de survie via l'activation de la cascade Ras/PI3K/Akt. Cependant, lorsque l'activité de la caspase-3 augmente, le fragment N est clivé, ce qui a pour effet d'éliminer ces signaux de survie.

Dans ce travail, nous avons étudié le rôle du Fragment N dans la protection des organes en état de stress et dans le maintien de leur fonctionnalité. En réponse à certains stress, nous avons découvert que les organes de souris n'exprimant pas la caspase-3 ou alors incapables de cliver RasGAP (souris KI), et de ce fait n'ayant pas la possibilité de générer le Fragment N, perdaient leur faculté d'activer la protéine Akt et démontraient un taux d'apoptose plus élevé que des organes de souris sauvages. Le fait que les organes et tissus de ces souris manifestaient de graves dommages et dysfonctions met en évidence l'importance du Fragment N dans l'activation des signaux de survie via la protéine Akt et dans la neutralisation de l'apoptose induite par la caspase-3.

En parallèle, nous avons investigué le rôle du Fragment N dans la régulation de l'activation de NF- κ B, un facteur de transcription clé dans l'inflammation. Une activation soutenue de NF- κ B peut être délétère par activation directe de l'apoptose ou peut mener à une réponse inflammatoire persistante. Nous avons découvert que le Fragment N, en favorisant l'export de NF- κ B depuis le noyau, était capable de l'inhiber très efficacement. Le Fragment N régule donc l'activité de NF- κ B et contribue au maintien de l'homéostasie dans des cellules stressées.

Résumé

Ces découvertes aident, de façon importante, à la compréhension de comment l'activation de la caspase-3 agit comme senseur de stress et décide du sort de la cellule soit en initiant une protection par le biais du fragment N, ou en induisant un suicide cellulaire. Cette étude définit le Fragment N comme ayant un rôle de pivot dans la protection contre des dommages patho-physiologiques, et ouvre des perspectives de développement de thérapies qui cibleraient à augmenter la résistance à divers traitements.

1. Introduction

1. Programmed cell death

“To seek the meaning of life, we should be interested in the meaning of death, how, when, and what’s next” Hadi Khalil

Programmed cell death (PCD) is a regulated form of cell suicide that is central to the development and homeostasis of multicellular organisms. Programmed cell death was reported at various developmental stages and three main morphologies of cell death are characterized, apoptotic cell death which is marked by cell shrinkage and extensive chromatin condensation, autophagic cell death distinguished by formation of autophagic vacuoles inside the dying cell, and necrotic cell death marked by rapid loss of plasma membrane integrity and therefore, release of the intracellular content (1;2).

1.1. Apoptosis

All tissues must be able to tightly control cell numbers and tissue size and to protect themselves from rogue cells that threaten homeostasis, a major player in this regulation is apoptosis. In the early 1970s, Kerr et al, observed a single-cell-death phenomenon that occurred in the dying cells of healthy tissues, as well as in cells associated with teratogenesis, neoplasia, tumor regression, atrophy, and involution. The term apoptosis, from Greek origins (apo=for, ptosis=falling), was chosen to describe the cellular process of programmed cell death (3). Apoptosis is characterized by a series of organized and tightly regulated dramatic perturbations to the cellular architecture that contribute not only to cell death, but also prepare cells for removal by phagocytes and prevent unwanted side immune responses (4). Two different structural stages characterize apoptotic cell death. The first stage is marked by nuclear and cytoplasmic condensation and breaking up of the cell into a number of membrane-bound ultrastructurally well-preserved fragments (blebs) known as apoptotic bodies (3;4). Apoptotic cells become rounded and retract from nearby cells, which resembles what happens when cells undergo mitosis. This is associated with, or followed closely by a prolonged period of dynamic plasma membrane blebbing, which frequently terminates in the ‘pinching off’ of many of these blebs as small vesicles called apoptotic bodies. In the second stage these apoptotic bodies, also known as “cellular debris”, are shed from epithelial-lined surfaces or are taken up and removed by other cells, typically by professional phagocytes

(macrophages) where they are rapidly degraded by lysosomal enzymes (3). Displayed “eat me” flags on the surface of intact apoptotic cells define them as targets of phagocytosis. The most characterized “eat me” flag is the exposure of the inner-membrane phosphatidylserine, beside other changes in surface sugars recognized by phagocyte lectins (3;5).

1.2. Necrosis and Necroptosis

Necrosis is a less tightly controlled passive form of cell death compared to apoptosis. Necrosis results as a consequence of overwhelming physico-chemical stress and does not take place of one well-described signalling cascade, but is the consequence of extensive crosstalk between several biochemical and molecular events at different cellular levels (6). Necrosis is characterized by organelle swelling, mitochondrial dysfunction, and the lack of typical apoptotic features (DNA condensation). Calcium and reactive oxygen species (ROS) are the main driving players during the propagation and execution phases of necrotic cell death, directly or indirectly provoking damage to proteins, lipids and DNA, which ends in disruption of cellular organelles and cell integrity. Necrotically dying cells induce pro-inflammatory signaling cascades by releasing inflammatory cytokines and by spilling their contents when they lyse (7). It is becoming clear that necrotic cell death is not uncontrolled as it is thought to be and that it may be an important cell death mode that is both pathologically and physiologically relevant, for instance necrosis is capable of killing tumour cells that have developed strategies to evade apoptosis (8). The term Necroptosis is used to define this particular type of programmed necrosis that depends on the serine/threonine kinase activity of receptor-interacting protein kinase 1 RIP1 which acts as a central initiator (9). Recent work showed that RIPK1-RIPK3 interaction induces cellular damage by necroptosis which drives mortality during TNF-induced systemic inflammatory response syndrome, an effect which was totally blocked by RIPK3 deletion (10).

2. Morphological properties of apoptotic cells

2.1. Cytoskeleton proteolysis and membrane blebbing

Major constituents of the cell cytoskeleton are cleaved by activated cysteine aspartic acid-specific proteases (caspases) during the apoptotic process. These substrates include components of microfilaments (actin, myosin, spectrins, α -actinin, gelsolin and filamin) microtubular proteins (tubulins, microtubule-associated proteins such as tau, cytoplasmic dynein intermediate chain and p150^{Glued}) and intermediate filament proteins (vimentin, keratins and nuclear lamins)(4). Proteolysis of cell skeleton components provokes cell shrinkage, rounding and retraction. In addition, weakening of the cell cytoskeleton favors dynamic membrane blebbing which is considered a distinctive feature of apoptosis defined by cytoplasm flow against unsupported areas of the plasma membrane. The small GTPase Rho (ROCK1) is a serine/threonine kinase which phosphorylates myosin light chain and regulates actin cytoskeleton dynamics, ROCK1 is a caspase substrate, which plays a role in this phase of apoptosis (11;12). Caspase-mediated proteolysis of the C terminus of ROCK1 constitutively activates the kinase leading to myosin light chain phosphorylation and contraction of actin bundles (13;14). Myosin-dependent contraction of cortical bundles of actin, leads to induction of blebs formation in cytoskeleton-weakened areas by pushing the cytosol against other areas of the cell cortex. In addition to membrane blebbing, the actin–myosin network is also suggested to play a role in the removal of apoptotic cells from epithelia, simultaneously stimulating neighboring cells to generate a network of actin–myosin cables. Upon contraction these cables effectively extrude the apoptotic cell from the epithelium and permit neighbouring cells to replace the gaps and to maintain epithelial integrity (15).

2.2. The nuclear envelope and nuclear fragmentation

Nuclear fragmentation is another major hallmark of apoptosis; it is the result of breakdown of the nuclear lamina and the collapse of the nuclear envelope. The proteolysis of lamins A, B and C by caspases is an initial and critical factor in these events (16). Lamin cleavage alone is not sufficient to cause nuclear fragmentation in the absence of the contractile force of the actin cytoskeleton, which plays an important role

in this event as well. The nuclear lamina is surrounded by a mesh of actin that is associated with the nuclear envelope. Because of such attachments, provoked reorganization of the actin–myosin system aids to tear the nucleus apart during the apoptotic process. Inhibition of ROCK1 myosin light chain kinase or inhibition of disruption of actin filaments prevents apoptosis-associated nuclear fragmentation (17). Finally, upon fragmentation, the microtubule-based cytoskeleton is implicated in the dispersal of nuclear fragments into plasma membrane blebs (18).

2.3. DNA condensation and degradation

Degradation of nuclear DNA into nucleosomal units forming a ladder of fragments is one of the first biochemical hallmarks to be identified of apoptotic cell death. It occurs in response to various apoptotic stimuli in a wide variety of cell types (19). This fragmentation process is driven by a specific DNase; caspase activated DNase (CAD); that cleaves chromosomal DNA in a caspase-dependent manner at internucleosomal sites. In proliferating cells CAD is found complexed with inhibitor of CAD (ICAD), which works as a specific chaperone for CAD and represses the activity of this endonuclease. When cells are subjected to apoptotic stimuli, caspase 3 cleaves ICAD to dissociate the CAD:ICAD complex, thereby resulting in the liberation of CAD and fragmentation of chromatin (20). However cells that lack ICAD or that express caspase-resistant mutant ICAD, although not showing DNA fragmentation, they do exhibit some other features of apoptosis and die, suggesting that ICAD although important is dispensable for apoptosis onset. Histone proteins wrapped around DNA to form nucleosomes, histone 2B (H2B) phosphorylation is found to be closely correlated with apoptotic chromatin condensation (21). Mammalian sterile-20 (MST1) kinase, which phosphorylates H2B, is cleaved and activated by caspase-3 during apoptosis and this also permits shuttling of MST1 to the nucleus (22). DNA degradation is important for avoiding unwanted immune activation since apoptosis-associated DNA degradation helps to prevent the accumulation of DNA that, if released into the extracellular space, could provoke autoimmune responses. This situation is seen in DNase-1 deficient mice, which displayed systemic lupus erythematosus; an autoimmune disease characterized by a defect in the apoptotic

process (23) and in mice embryos deficient in apoptotic DNA degradation, which displayed impaired thymic development (24).

2.4. Fragmentation of organelles and shut down of transcription and translation

Another characteristic of apoptosis is the fragmentation of cellular organelles, including the Golgi apparatus, the endoplasmic reticulum (ER) and the mitochondria, and their subsequent packaging into apoptotic bodies. The Golgi apparatus fragmentation appears to involve caspase-mediated cleavage of the Golgi-stacking protein GRASP65, (25). The ER is remodeled at late stage of the apoptotic process, and often surrounds condensed chromatin and is redistributed to apoptotic blebs; this process requires actin and the microtubule cytoskeleton (26). The mitochondrial network is also extensively fragmented during apoptosis, the permeabilization of mitochondrial outer membranes and the release of mitochondrial intermembrane space proteins is driven by the activation and conformational changes that occur in BAX (BCL-2-associated X protein) and/or BAK (BCL-2-antagonist/killer-1) during their assembly to mitochondrial pore (27;28). Caspases do not directly contribute to apoptosis-associated mitochondrial fragmentation; however, caspase-mediated proteolysis of the p75 subunit of complex I of the electron transport chain is found to play a role in the swelling and damaging of mitochondria, in addition to loss of mitochondrial transmembrane potential, decline in cellular ATP levels and the production of reactive oxygen species during apoptosis (29). Finally, the cleavage of multiple transcription factors (NFATc1 and NFATc2, NF- κ B p65), translation initiation factors (such as eIF2a, eIF3, eIF4B, eIF4E, eIF4G and eIF4H) and ribosomal proteins (RPP0 and p70S6K), suggests a rapid shut down of the transcription and translation processes during early stages of apoptosis (29;30).

2.5. Clearing of apoptotic cell

Probably the most important event in the apoptotic process is the removal of the dead cell by phagocytes (31). Removal of cells with their intact plasma membranes prevents the release of potentially damaging cellular constituents into the surrounding medium. The collapse of apoptotic cells into numerous apoptotic bodies happens most likely to safely break the cell apart into more manageable pieces for engulfment to ease the task

for phagocytes. Dying cells generate binding sites for phagocytes and release chemoattractant molecules, which aid cells of the immune system to coordinate the removal of the corpses. Chemoattractants like lysophosphatidylcholine are generated through the hydrolysis of membrane phosphatidylcholine by activation of Ca^{2+} -independent phospholipase-A2 (iPLA2), which in turn is activated through caspase-3-mediated cleavage (32). Other chemoattractant molecules were reported including the S19 ribosomal protein (33) and aminoacyl-tRNA synthetases (34). Phagocytosis of dying cells is achieved by phagocytes equipped with a group of receptors that specifically detect engulfment signals on the apoptotic cells. The best-characterized phagocytic ligand is the membrane phospholipid phosphatidylserine (PS). PS resides in the inner plasma membrane leaflet in healthy cells. PS translocation to the outer membrane leaflet in a caspase-dependent manner in apoptotic cells induces phagocytosis (35;36). Other possible ligands exposed on the surface of dying cells in a caspase-dependent manner were reported including oxidized low-density lipoprotein, Calreticulin (37) and the adhesion molecule ICAM3, a glycosylated member of the immunoglobulin superfamily (38). Besides integrins, several receptors were identified to recognize apoptotic cells based on carbohydrate signals including macrophage lectins (mannose-binding lectin) and lung surfactant proteins A and D (39). Under certain circumstances (presence of microorganism-derived peptides) antigens from ingested apoptotic cells can be presented on the surface of major histocompatibility complex (MHC) molecules of dendritic cells, and elicits T-cell responses, which might allow the immune system to respond to pathological infections that trigger apoptosis (40;41).

3. Caspases

Inducers of apoptosis are diverse and include death factors such as FasL (Fas ligand), TNF (tumor necrosis factor), and TRAIL (TNF-related apoptosis inducing ligand), growth factor starvation, genotoxic agents such as anti-cancer drugs, γ -irradiation and oxidative stress [5–8]. Regardless of the origin of the apoptotic stimulus, the commitment to apoptosis is mediated by the activation of caspases, a family of cysteine proteases normally present in healthy cells as inactive precursor enzymes (zymogens) with little or no protease activity (42). So far 14 members of the caspase family have been identified,

of which 7 members are implicated in apoptosis (Figure 1). Caspases are divided into three subfamilies. The first subfamily (group I) comprises caspases-1, -4, -5, and -12 play a role in the regulation of inflammatory responses. Caspase-1 and caspase-5 interact in a multiprotein complex; the so called as inflammasome, which is responsible for processing and maturation of pro-interleukin-1 β into active IL-1 β (43). The second subfamily (group II), is composed of caspases- 2, -8, -9 and -10 are known as initiator caspases. Caspase-8 can have pleiotropic effects since it may promote cell motility mediated by calpain activation (44) and macrophage differentiation by cleavage of the receptor-interacting protein (RIP), resulting in a downregulation of NF- κ B that is required during differentiation (45). Caspase-10 is implicated in the activation of NF- κ B-dependent pro-survival signaling pathways by a mechanism that is independent of its catalytic domain (46). The initiator caspases are activated by forming heteromeric complexes with accessory molecules such as a death factor receptor and its adaptor (death Inducing signaling complex DISC), or Apaf-1 and cytochrome C (apoptosome). This initiation step is followed by the cleavage and subsequent activation of downstream caspases (47). This is a third subfamily (group III) composed of caspase-3, -6 and -7 the so-called executioner (effector) caspases. Irrespective of the inducing stimulus and the initiator caspase implicated, the convergence point is the activation of the effector caspases, -3, -6 and -7. These enzymes execute the proteolysis events that are seen during the demolition phase of apoptosis. Three main ways of apoptosis-associated caspase activation have been established, these are the intrinsic, extrinsic and granzyme B- mediated pathways.

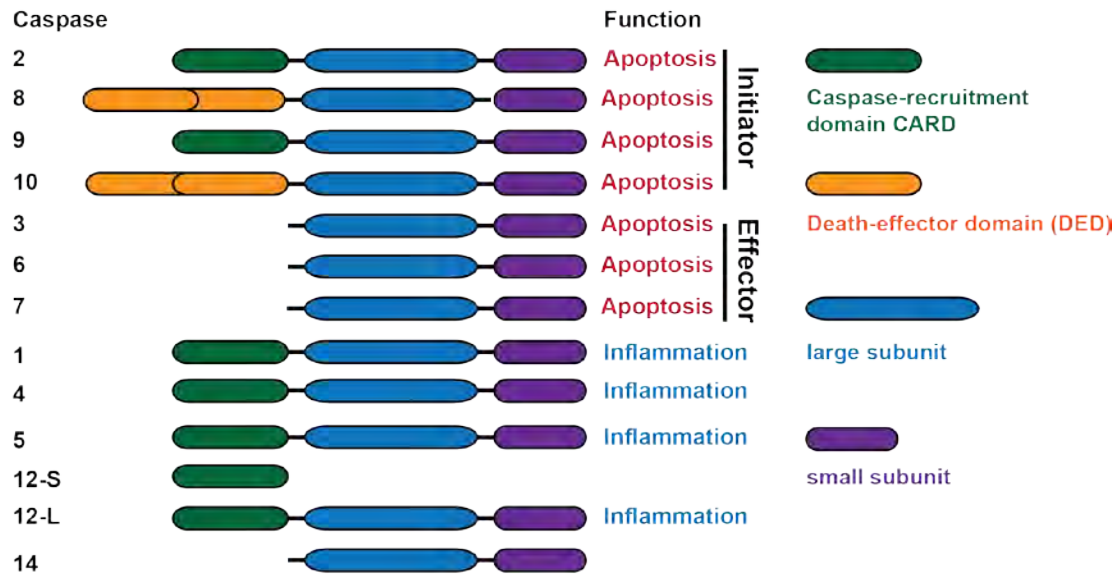
3.1. Caspase activation by extrinsic and intrinsic pathways

Caspase activation by the extrinsic pathway involves the binding of extracellular death ligands (such as FasL, TNF α or TRAIL) to transmembrane death receptors. Engagement of death receptors with their cognate ligands, generates homotrimeric ligand-receptor complex that provokes the recruitment of cytosolic adaptor proteins, such as the Fas-associated death domain protein (FADD) and caspase-8 or -10 forming an oligomeric death-inducing signalling complex (DISC) (48). Formation of the DISC complex in turn promotes caspase-8 autoprocessing and activation. Active caspase-8

then proteolytically processes and therefore activates caspase-3, 6 and -7 (Figure 2). The cellular FLICE-inhibitory proteins (c-FLIP) share a similar structure with caspase -8 but lack the active site residues, c-FLIP prevent activation of procaspase-8 at the DISC. However, upon stimulation c-FLIP is displaced and procaspase-8 activation takes place (49).

In the intrinsic pathway, diverse stimuli (DNA damage and ER stress) that induce stress or cell damage typically activate one or more members of the BH3-only pro-apoptotic family proteins that act as sentinels for cellular damage. BH3-only protein activation above a crucial threshold overcomes the inhibitory effect of the anti-apoptotic B-cell lymphoma 2 (Bcl-2) family members; this promotes the assembly of oligomers containing BAK and BAX within mitochondrial outer membranes and leads to mitochondrial outer membrane permeabilization (MOMP). MOMP permits the efflux of proapoptotic proteins, including cytochrome c, from the mitochondrial intermembrane space (IMS) which is a crucial event that drives initiator caspase activation and apoptosis. Upon release from mitochondria into the cytosol, cytochrome c binds to the apoptotic protease activating factor 1 (APAF1), inducing its conformational change, oligomerization and binding to ATP/dATP (50;51). This leads to the formation of what is called “apoptosome”, a caspase activation platform (comprising ~7 molecules of apoptotic protease-activating factor-1 (APAF1) and the same number of caspase-9 homodimers). The apoptosome recruits, dimerizes and activates caspase-9 (52). Active caspase-9 then propagates a proteolytic cascade of further caspase-3 and caspase-7 activation events. In addition, released proapoptotic mitochondrial IMS proteins, such as second mitochondria-derived activator of caspase (SMAC) also known as direct inhibitor of apoptosis (IAP)-binding protein with low pI (DIABLO), and the serine protease OMI also known as HtrA2 which are known to bind to and antagonize the inhibitor of apoptosis X-linked inhibitor of apoptosis protein (XIAP) (53;54). Endonuclease G is another mitochondrial IMS protein which is released after MOMP and that contributes to apoptosis through cleavage of nuclear DNA (Figure 2)(55).

A. Caspase family members



B. Caspase activation

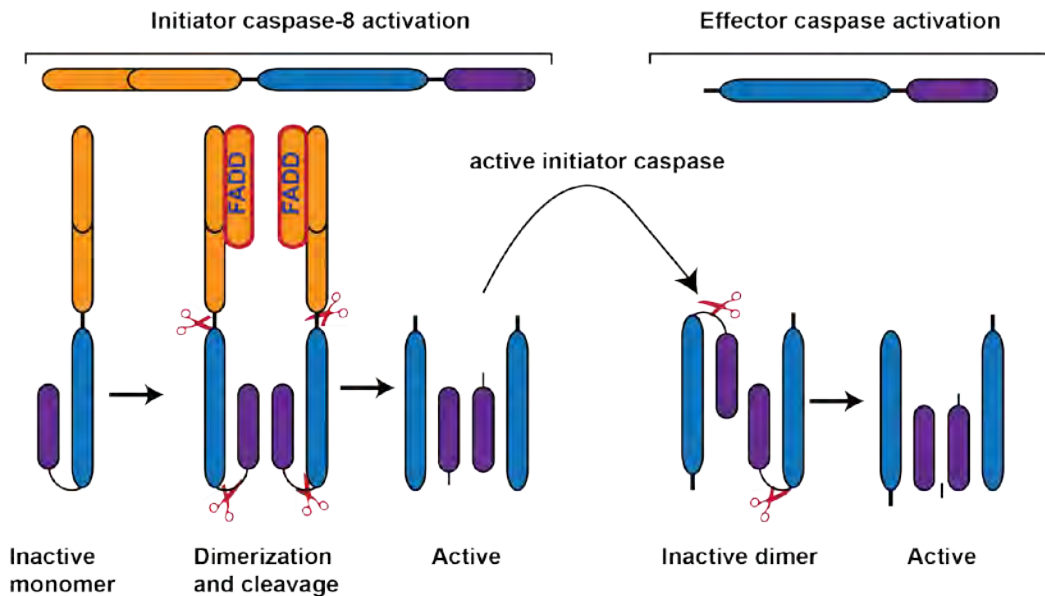


Figure 1. Caspase family members and their activation: Caspases (Cys Asp acid proteases) cleave their substrates after the Asp residue in tetrapeptide (X-X-X-Asp) motifs. **A.** Caspases confer apoptotic and non-apoptotic roles, such as cytokine maturation, inflammation and differentiation. Apoptotic caspases can be divided into two classes: initiator (2, 8, 9 and 10) and executioner caspases (3, 6, and 7). All caspases have a similar domain structure (pro-peptide, large and small subunits). The pro-peptide domain facilitates interaction with proteins that contain the same motif; pro-peptides identified are caspase recruitment domain (CARD) and the death effector domain (DED). **B.** Caspase activation is initiated through proteolytic cleavage between the large and small subunits to form a heterodimer.

The intrinsic and extrinsic apoptotic pathways are not totally disconnected (Figure 2); extrinsic death signals can crosstalk with the intrinsic pathway through caspase-8-mediated proteolysis of the BH3-only protein BID (BCL-2 homology 3 (BH3)-interacting domain death agonist). Truncated BID (tBID) can promote mitochondrial cytochrome c release and assembly of the apoptosome (56).

3.2. Caspase activation by Granzyme B

A third pathway leads to apoptosis is the granzyme B-dependent caspase activation. It involves the delivery of the protease granzyme B into the target cell through specialized granules that are released from cytotoxic T lymphocytes (CTL) or natural killer (NK) cells. CTL and NK granules contain numerous granzymes as well as a pore-forming protein, perforin which oligomerizes in the membranes of target cells to permit entry of the granzymes (Figure 2). Granzyme B, similar to the caspases, also cleaves its substrates after Asp residues and can process BID as well as caspase-3 and -7 to initiate apoptosis (57;58).

3.3. Inhibition of caspases and non-apoptotic functions of caspases

Even though caspase activation would certainly lead to apoptotic cell death in most situations, cells have developed several anti-apoptotic mechanisms to ensure cell survival, involving proteins of the Bcl2 family, which inhibit caspase activation (59), and members of the inhibitor of apoptosis (IAP) family which directly (XIAP) or indirectly (cIAP1/2) inhibit caspase activity (60;61). In addition, there are some exceptions where caspase cleaved substrates do not participate in the apoptotic process. Cleavage of PKC ϵ activates the enzyme and this in turn mediates the activation of antiapoptotic signals (62). Activation of B-cell receptor triggers caspase-mediated cleavage of the kinases Fyn and Lyn generating fragments that inhibit apoptosis (63;64). Caspase-3-cleaved c-terminal product of synphilin-1 was found to display anti-apoptotic properties (65). In addition, Ras GTPase activating protein (p120-RasGAP), a regulator of Ras and Rho signaling pathways, when cleaved by caspase-3 generates a potent anti-apoptotic response (66).

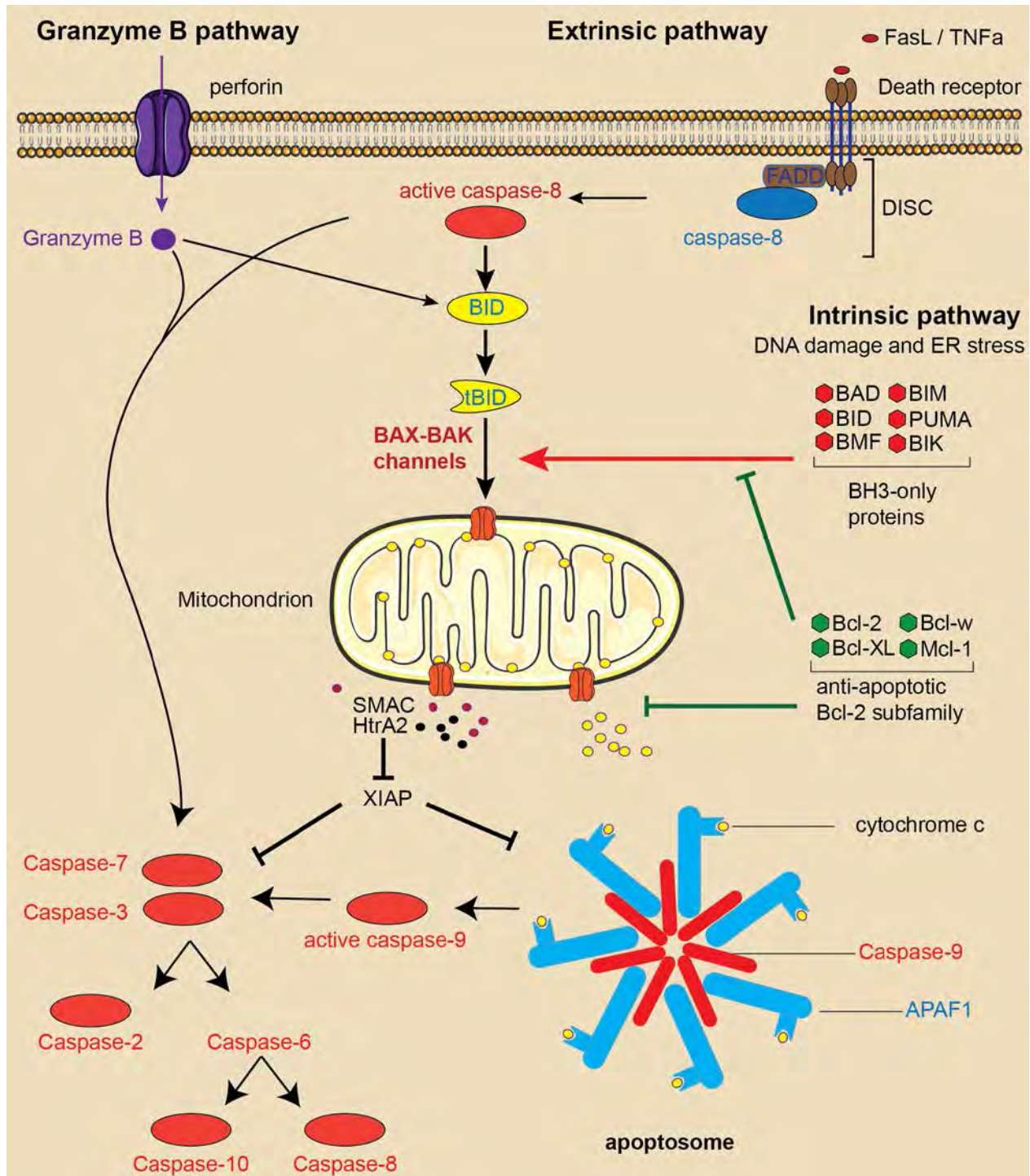


Figure 2. Pathways of caspase activation

4. G proteins

G proteins (guanine nucleotide-binding proteins) comprise a family of proteins involved in signal transmission; they transduce signals from many hormones, neurotransmitters, and signaling growth factors. GTPases are a superfamily of GTP-binding proteins with intrinsic GTPase activity. Members of this family are either heterotrimeric (large G proteins) or monomeric (small G-proteins) (67). Based on the homology in their sequences and similarity in their function, the small GTPase superfamily members are classified into five different subfamilies, including Ras, Rho, Rab, Ran, and Arf (ADP ribosylation factor) (68). The Ras subfamily proteins function as binary on/off switches to control many biological processes, this function is ensured by cycling between active GTP bound and inactive guanosine diphosphate (GDP)-bound conformations (Figure 3A). Guanine nucleotide exchange factors (GEFs) turn on Ras signaling by catalyzing the exchange from GDP-bound to GTP-bound state of the small G protein whereas GTPase-activating proteins (GAPs) terminate signaling by inducing GTP hydrolysis (69;70). Ras regulates signal transduction pathways by linking plasma membrane receptors to many essential and rate-limiting signals for growth and differentiation. Several effectors have been implicated in Ras mediated growth transformation and oncogenesis, including those of the Raf/mitogen-activated protein kinase (MAPK), PI3K/Akt, PLC/PKC, and GTPase Ral GEF cascades (71).

Activated Ras proteins elicit specific biological responses, by modifying the enzymatic activity of their bound effectors, changing their subcellular localization, or altering their interaction with other proteins. (Harvey) H-Ras, (Kirsten) K-Ras, and (Neuuroblastoma) N-Ras proteins are encoded by three highly related genes which were among the first identified human oncogenes. Mutations of these Ras genes are among the most common genetic changes in cancer, and are frequently observed in colorectal, pancreatic, and lung cancers. The mutationally altered Ras proteins are defective in their ability to recover their inactive, GDP-bound state, and instead remain constitutively active, transducing excessive signals that promote cancer cell proliferation and survival (72).

5. RasGAP domains and function

Various mammalian GAPs for Ras have been described, the first one to be isolated was p120-GAP (73). p120-RasGAP (Ras GTPase activating protein) is a regulator of Ras and Rho GTP-binding proteins, RasGAP accelerates the intrinsic GTPase activity of Ras, a process mediated by the C-terminal GAP domain. p120-RasGAP is a multi-domain protein and apart from being a regulator of Ras, its N-terminal domain contains a number of signaling modules such as Src Homology 3 (SH3) domain flanked by two Src Homology 2 (SH2) domains, a pleckstrin homology (PH) domain, and a calcium dependent phospholipid-binding domain (CaLB/C2 domain) (Figure 3B). These signaling modules mediate interaction with other signaling proteins and may act independently of Ras (68).

RasGAP controls Rho-mediated cytoskeletal reorganization through its SH3 domain (74). The SH2 domains bind to phosphorylated tyrosine kinase receptors such as PDGF and EGF and mediate associated signals. Both SH2 RasGAP domains are individually capable of binding p190-RhoGAP (a GAP protein specific for the Rho family of small GTPases). Members of the translation elongation factors family (eEF1A 1/2), involved in cell proliferation, were shown to interact with RasGAP SH2 domains (75).

The pleckstrin homology (PH) domain can bind to the GAP domain of RasGAP and interfere with Ras/RasGAP interaction. Indeed, the expression of isolated RasGAP PH domain specifically inhibits Ras-mediated signalling and transformation without affecting cellular growth (76). A calcium-dependent phospholipid-binding domain (CaLB/C2) follows the PH domain which binds Annexin-A6, a Ca^{+2} -regulated protein that forms a complex with RasGAP and induces Ras inactivation (77). The carboxy-terminal region contains the GAP domain of RasGAP catalyzes GTP hydrolysis, which is achieved by the direct chemical binding of the GAP protein to the active site of Ras and the immobilization of G-proteins switch regions. RasGAP stabilizes the catalytically important glutamine 61 of Ras and thus, the transitional state of Ras/RasGAP complex, which in turns coordinates the attacking water molecule.

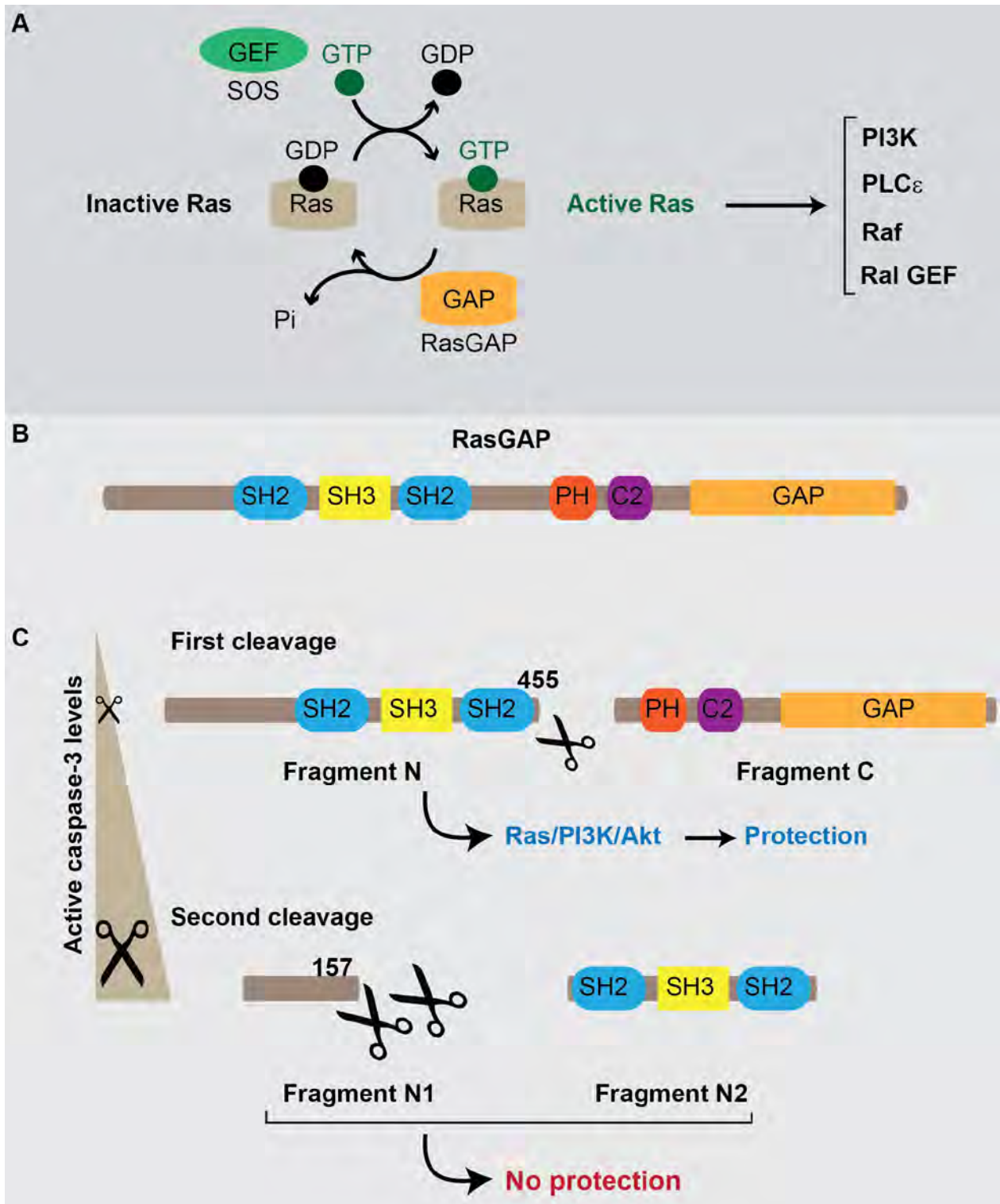


Figure 3: A Ras activation. B. RasGAP domains. C. RasGAP cleavage by caspase-3

Arginine 789 of RasGAP is positioned into the phosphate-binding site neutralizing the emerging negative charge of the α -phosphate during hydrolysis of the GTP to GDP. Oncogenic mutations at positions 12 and 13 of Ras sterically block the proper orientation of the Arg789 of RasGAP and the Glu61 of Ras preventing GTP hydrolysis. Therefore, Ras^{G12V}, Ras^{G13V} and Ras^{G61V} have oncogenic activity (73)

Ras is activated through the stimulation of tyrosine kinase/growth factor receptors and regulates diverse cellular responses through distinct signalling pathways such as Raf/MAPK/ERK, and PI3K/Akt, which are mainly involved in cell survival and proliferation. Therefore, RasGAP through regulating Ras, acts as an indirect regulator of those pathways. Additionally, RasGAP has an amino-terminal region similar in structure to “adaptor” proteins and to various non-catalytic domains, which may indicate that RasGAP can have other functions related or unrelated to its function as a regulator of Ras.

Aurora Kinase has been identified as a binding partner of RasGAP SH3 domain (78). The human Aurora kinase orthologs (HsAIRK-1 and HsAIRK-2) are proteins involved in proper cell division and are thus cell cycle-dependent. The activation, de-activation and degradation of these proteins are regulated by phosphorylation (cAMP-dependent protein kinase) and de-phosphorylation (protein phosphatase 1) (79). RasGAP regulates Aurora kinase orthologs by facilitating their association with kinases and phosphatases necessary for their regulation; indicating that RasGAP can be implicated in proliferation (78).

RasGAP and p190-RhoGAP interact through the SH2 domain of RasGAP, and are believed to be implicated in the actin cytoskeleton remodelling; constitutive association between these two GTPases is required for turnover and reorganization of stress fibers and focal adhesions. In addition, RasGAP knock out fibroblasts have dramatically reduced cell migration which implies that RasGAP is implicated in cell migration and cytoskeleton remodelling (80).

RasGAP plays also a pivotal role in the onset of apoptosis. RasGAP possesses two conserved caspase-3 cleavage sites (66). At low levels of caspase activity, RasGAP is

first cleaved at position 455. The N-terminal fragment (fragment N) generated by the cleavage activates Ras/PI3K/Akt potent anti-apoptotic pathway (81). Fragment N is crucial for cell survival in low stress conditions (82). However, at higher caspase activity, fragment N is further cleaved at position 157 and this abrogates its anti-apoptotic activity (83). At low levels of caspase activity, RasGAP is cleaved once into fragment N to protect cells from fully activating their executioner caspases. However, when caspase activity increases, fragment N is further cleaved, allowing the full caspase activation and apoptosis induction (Figure 3C). We assumed RasGAP to act as sensor of the level of stress within a cell instructed by caspase-3 activity, and therefore can act as a death/survival molecular switch (82).

6. Pro-survival Phosphoinositide 3- kinases (PI3K)/Akt pathway

PI3Ks are a family of lipid kinases identified by their ability to phosphorylate the 3'OH group of the inositol ring in inositol phospholipids. The PI3K family comprises eight members divided into three classes (class Ia-b, class II and class III) based on their sequence homology and substrate preference. Class I of PI3Ks are heterodimers made up of a catalytic subunit (α , β or δ) of 110 kD relative molecular mass (p110), and an adaptor/regulatory subunit (seven adaptor proteins generated by expression and alternative splicing of three genes p85 α , p85 β and p55 γ). Each of these adaptors contains two Src Homology (SH2) domains which allow binding to phosphotyrosines of receptor tyrosine kinase (RTK), such as platelet-derived growth factor receptor (PDGFR) and insulin receptor (IR) (84). Stimulated receptor tyrosine kinase (RTK) favors the recruitment of the p85 adaptor subunit, which induces allosteric activation of class Ia PI3Ks catalytic subunit. PI3K activation is also mediated by GTP-bound Ras (Ras·GTP), which can bind directly to the N-terminal region of p110 subunit, leading to PI3K activation (85;86). Son of sevenless (SOS) is a specific GEF for Ras; the proline rich carboxyl-terminal domain of SOS interacts with Src homology 3 (SH3) domain of growth factor receptor-bound protein 2 (Grb2). Grb2-SOS complexes are recruited to stimulated RTKs through the Src homology 2 (SH2) or Grb2. Recruitment of this complex to RTK stimulates the formation of Ras·GTP (87). Activated class I PI3Ks catalyze the

conversion of phosphatidylinositol-3,4-bisphosphate (PIP₂) to phosphatidylinositol-3,4,5-trisphosphate (PIP₃) (Figure 4) which is known to bind to leucine-rich FYVE domains (88), and highly basic pleckstrin homology (PH) domains. PH-containing proteins including the serine/threonine kinases, 3'-phosphoinositide-dependent kinase-1 (PDK-1) and protein kinase B (PKB also known as Akt) are the key mediators of RTK- class Ia PI3Ks signaling(89).

7. Protein Kinase B (PKB/Akt)

Akt is a serine/threonine kinase involved in the regulation of cell survival, proliferation, and metabolism and is activated by dual phosphorylation. Three isoforms (α , β and γ) of Akt were identified and they all contain an N-terminal PH domain, a central kinase domain containing phosphorylation site within the activation-loop at the residue Thr308, and a conserved regulatory serine phosphorylation site, Ser473 near the C terminus. The interaction of Akt PH-domain with 3'-phosphoinositide causes Akt translocation to plasma membrane, and imposes Akt conformational changes that expose its two main phosphorylation sites (90). PDK-1 is also recruited to the plasma membrane after PIP₃ generation. PDK-1 phosphorylates the Thr308 residue in Akt (91), which stabilizes the activation loop in an active conformation, Ser473 is then phosphorylated by mammalian target of rapamycin (mTOR) complex 2 (mTORC2) (92). Phosphorylation of Thr 308 is thought to be a prerequisite for kinase activation, but phosphorylation of the C-terminal Ser473 hydrophobic residue is required as well for full activation of Akt kinase (Figure 4). Phosphorylation of both Thr308 and Ser473 sites causes synergistic activation of Akt and is required for a high level of activation of the kinase (91). Phosphatidylserine (PS) interacts with Akt PH-domain outside the PIP₃-binding pocket, which is also required for the membrane binding and conformational changes to expose Thr308 for phosphorylation by PDK-1. The RD also interacts with PS and to a minimal extent to PIP₃, resulting in an open conformation, allowing Ser473 phosphorylation by mTORC2 (93).

7.1. Akt survival functions

A long list of Akt substrates have been identified in mammalian cells whose substrates act as regulators of apoptosis or cell growth (including protein synthesis and glycogen metabolism, and cell-cycle regulation). Substrates are phosphorylated within the same basic motif, RXXXS/T, these substrates include, glycogen synthase kinase (GSK3), a serine threonine kinase that regulate glycogen synthase function, the mammalian target of rapamycin (mTOR) complex 1 (mTORC1), which regulates translational machinery and protein synthesis, and endothelial nitric oxide synthase (eNOS), which catalyzes the generation of NO, an important protective molecule in the vasculature, and endothelial tissues. Activated Akt may translocate to the nuclear compartment and regulate transcription factors including cyclic AMP-responsive DNA-binding protein (CREB2) and eukaryotic transcription factor E2F in addition to many others. Anti-apoptotic signals by Akt include upregulation of anti-apoptotic proteins such as Mcl-1 (94), or by direct phosphorylation of downstream targets such as caspase-9, Bad, and mTORC1 (Figure 4).

Akt substrates involved in cell-death regulation include, murine double minute 2 (MDM2) which functions as E3 ubiquitin ligase and as inhibitor of p53. MDM2 is stabilized by Akt-mediated phosphorylation at Ser166 (95). Bcl-2 family member Bad is phosphorylated by Akt at Ser136, which decreases the binding of Bad to Bcl-xL at the mitochondrial membrane and increases its binding to 14-3-3 in the cytosol (96). Pim-1 is a proto-oncogenic serine-threonine kinase whose expression is induced by activated Akt. Besides its proliferative signaling, Pim-1 mediates cardioprotective effects through phosphorylation of multiple targets including Bad (97;98). Akt promotes the inactivation of caspase-9 downstream cytochrome c release by direct phosphorylation of caspase-9 at Ser196 (99). A variety of other transcription factors regulating cell survival were found to be regulated by Akt. Phosphorylated forkhead transcription factor FRKH (FOXO3a) is sequestered in the cytoplasm in the absence of phosphorylation; FOXO3a is localized to the nucleus and induces the expression target genes.

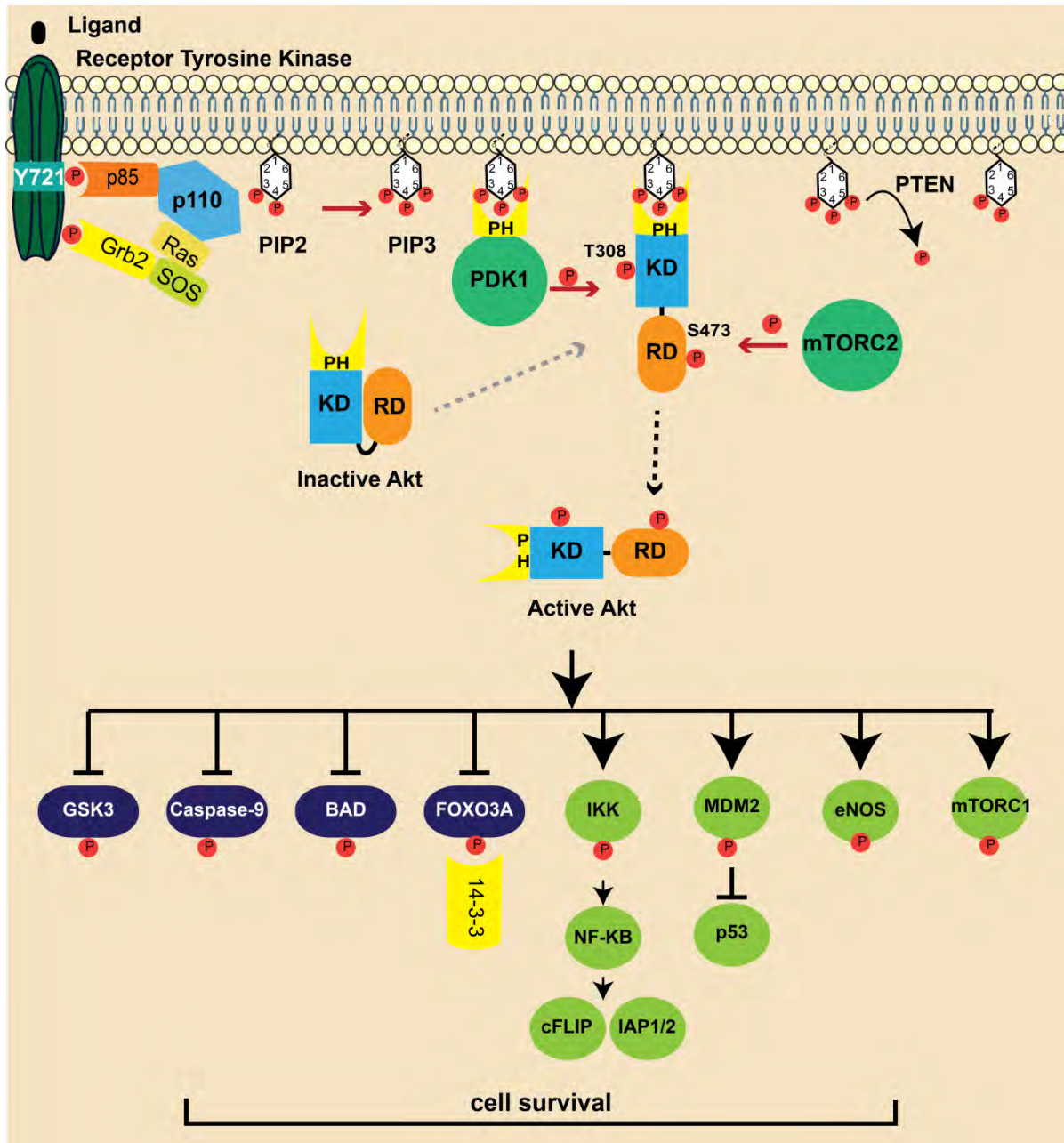


Figure 4. Ras/PI3K/Akt pathway: Activation of RTK by its ligand induces the recruitment of p85 of PI3K to phosphorylated tyrosine residues; this binding modulates and activates PI3K. On the other hand Grb2 can bind to phosphorylated tyrosine residue; Grb2 recruits SOS GEF which activates Ras, which in turn binds and activates PI3K p110 subunit. Activated PI3K catalyses the conversion of PIP2 to PIP3, which is recognized by the PH-domain of PDK1 and Akt, this favours the later proteins translocation to plasma membrane. PDK1 phosphorylates Akt at Thr308, mTORC2 phosphorylates Akt at Ser473. Activated Akt modulates different cellular processes by blocking or activating downstream targets through direct phosphorylation (mostly targets affecting the survival are listed). The phosphatase and tensin homolog (PTEN) dephosphorylates PIP3 to shut down the signaling cascade.

FOXO3a is known to positively regulate the expression of Fas L and Bim1 genes thus, Akt promotes the rescue from apoptosis through the inhibitory phosphorylation of FOXO3a (100).

Akt is considered as a signaling intermediate upstream of survival gene expression that is regulated by the transcription factor NF- κ B (cFLIP, IAP1/2). Akt has been shown to enhance the degradation of the I κ Bs (inhibitor of κ B) and to interact with the I κ B kinase β (IKK β) and induce its activation by phosphorylating the regulatory site at Thr23 (96;101). Therefore, Akt may promote survival either through direct phosphorylation of targets, or through the induction of anti-apoptotic genes.

8. NF- κ B family of transcription factors

Nuclear factor Kappa B (NF- κ B) was discovered and characterized as a transcription factor which binds to a site of immunoglobulin κ and is required for B lymphocyte-specific gene expression (102). However; subsequent studies showed that NF- κ B could be activated in various cells types (103). NF- κ B is ubiquitously expressed and serves as a critical regulator of the inducible expression of many genes (104). NF- κ B family in mammalian cells comprises five different members: p65 (RelA), RelB, c-Rel, NF- κ B1 (p50/p105) and NF- κ B2 (p52/p100). RelA, RelB, and c-Rel, are synthesized as transcriptionally active proteins; while p50/p105 (NF- κ B1) and p52/p100 (NF- κ B2) are synthesized as longer precursor molecules of 105 and 100 kDa respectively, these precursors are processed by proteolytic cleavage into the smaller, p50 and p52 transcriptionally active forms. Each member of NF- κ B family contains a conserved N-terminal (approximately 300 amino acids) region called the Rel-homology domain (RHD) This domain contains the DNA-binding and dimerization domains as well as the nuclear localization signal (NLS) (Figure 5) (104-107);(108). NF- κ B homo- or heterodimers are sequestered in the cytosol of unstimulated cells via noncovalent interactions with a class of inhibitory proteins called I κ Bs. I κ Bs are structurally related and have multiple copies of a 30–33 amino acid sequence the so called ankyrin (ANK) repeat at the C-terminal domain. The I κ B family comprises seven molecules [I κ B- α , I κ B- β , I κ B- ϵ , I κ B- ζ , Bcl-3, in addition to p100 and p105, which contain both RHD and ANK (Figure 5)].

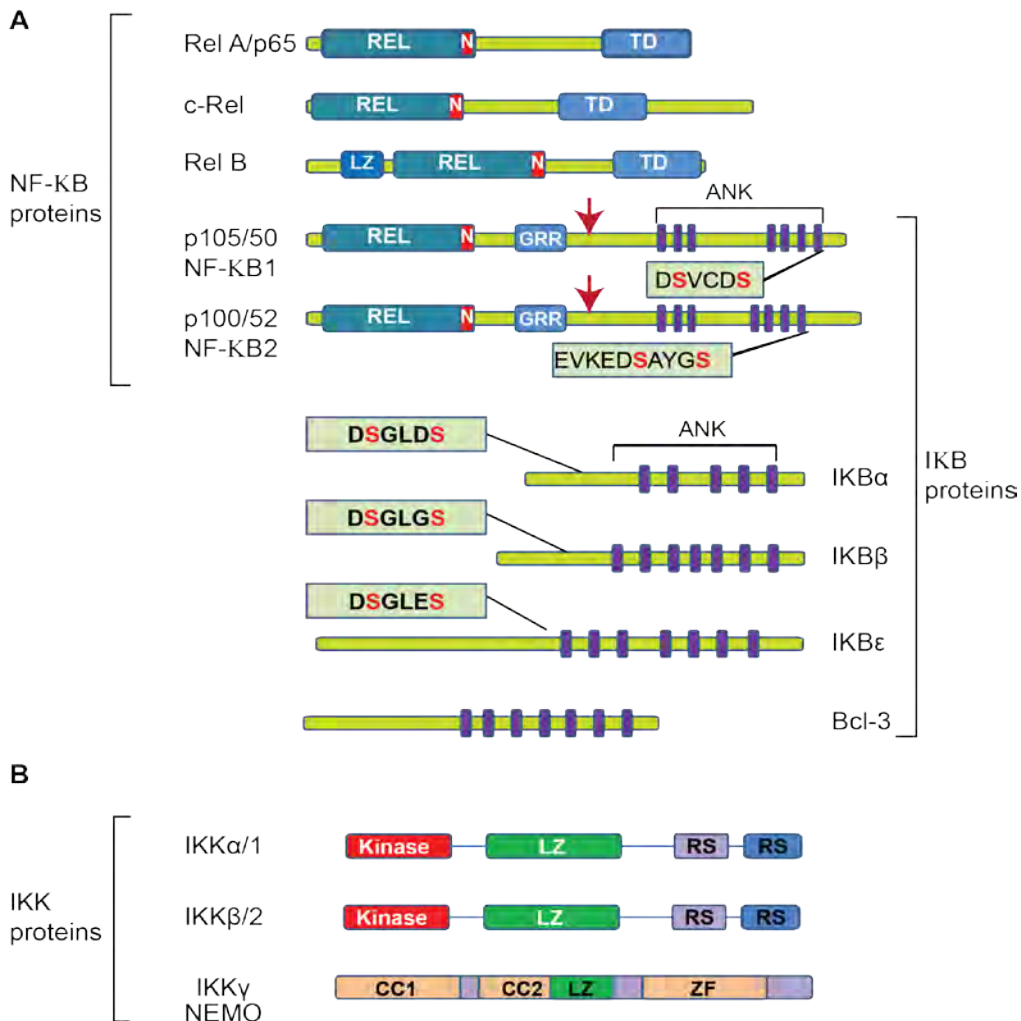


Figure 5. Members of the NF- κ B, I κ B and IKK protein families: **A.** Typical domains of NF- κ B and I κ B protein family members are presented. NF- κ B members have a structurally conserved amino-terminal Rel-homology domain (RHD). RelA, Rel B and c-Rel, have a carboxy-terminal non-homologous transactivation domain (TD). The precursor proteins p100 and p105 function both as I κ B proteins (contain ankyrin ANK repeats at the carboxyl terminus), while after processing by the proteasome 26S act as NF- κ B family members, known as p52 and p50 which contain RHDs at the amino terminus). Proteolytic processing sites of p100 and p105 are indicated by red arrows. The glycine-rich region (GRR) and the serine residues of inducible phosphorylation are required for the proteolysis. Beside p100 and p105, the inhibitor of NF- κ B (I κ B) family contains I κ B α , I κ B β , I κ B ϵ (two transcripts) and Bcl-3, identified by the presence of ankyrin (ANK) repeats. I κ B serine residues of induced phosphorylation of I κ B α , I κ B β and I κ B ϵ leading to their degradation are highlighted. **B.** The I κ B kinase (IKK) family members consists three members, the regulatory subunit IKK γ (Nemo) and two kinase subunits IKK α and IKK β . The two kinases IKK α and IKK β contain an N-terminal kinase domain and two C-terminal regulatory subunit flanked by LZ domain; BCL-3, B-cell lymphoma 3; CC, coiled-coil; HLH, helix-loop-helix; LZ, leucine-zipper, ZF, zinc-finger.

The specific interaction between the ANK repeats and the RHD is the defining feature of the interaction between NF- κ B-I κ B complexes, which inhibits nuclear translocation. However; different inhibitory properties of I κ Bs were reported, for instance I κ B α masks only one of the two NLS of NF- κ B dimer, whereas I κ B β masks the two NLS. Also, I κ B α but not I κ B β contains a functional nuclear export signal (NES) which is essential for export the NF- κ B-I κ B α complex back to the cytoplasm (104;109;110).

8.1. NF- κ B-mediated signals

NF- κ B regulates both innate and adaptive immune responses by turning on transcriptional programmes, which differ depending on the inducing stimulus and on the cell type that is mediating the response. NF- κ B is activated rapidly in response to a wide range of stimuli, including stress signals and pro-inflammatory cytokines, such as tumour-necrosis factor alpha (TNF α) and interleukin-1 (IL-1), as well as pathogen-induced TLRs (lipopolysaccharide (LPS), peptidylglycans, lipoproteins, unmethylated bacterial DNA and double-stranded RNA, which are recognized by toll like receptors TLR)(109). Signals that induce NF- κ B activation trigger the activation of the upstream I κ B kinase complex (IKK) which may contain the catalytic subunits IKK α , IKK β , in addition to a regulatory subunit IKK γ (also called NEMO) which depends on the pathway activated. Two distinct NF- κ B pathways (canonical and non-canonical Figure 6) are characterized based on the receptor stimulated, the subunits involved in the activated IKK complex, the phosphorylated I κ B member, and the induced NF- κ B dimer which targets specific downstream genes.

In the canonical NF- κ B signaling, activation of TNF receptor by TNF- α , results in TNF-receptor associated death domain (TRADD)-dependent recruitment of the complex I that contains TNF receptor associated factor 2 and 5 (TRAF2/TRAF5), receptor-interacting serine/threonine kinase (RIP1) and the cellular inhibitor of apoptosis protein 1 (c-IAP1) which is an E3 ubiquitin ligase that catalyzes the ubiquitination of RIPK1 and IKK γ (111) TRAF2 causes K63-linked ubiquitination of RIP1 which recruits IKK complex (IKK α -IKK β -IKK γ) to the receptor complex (112).

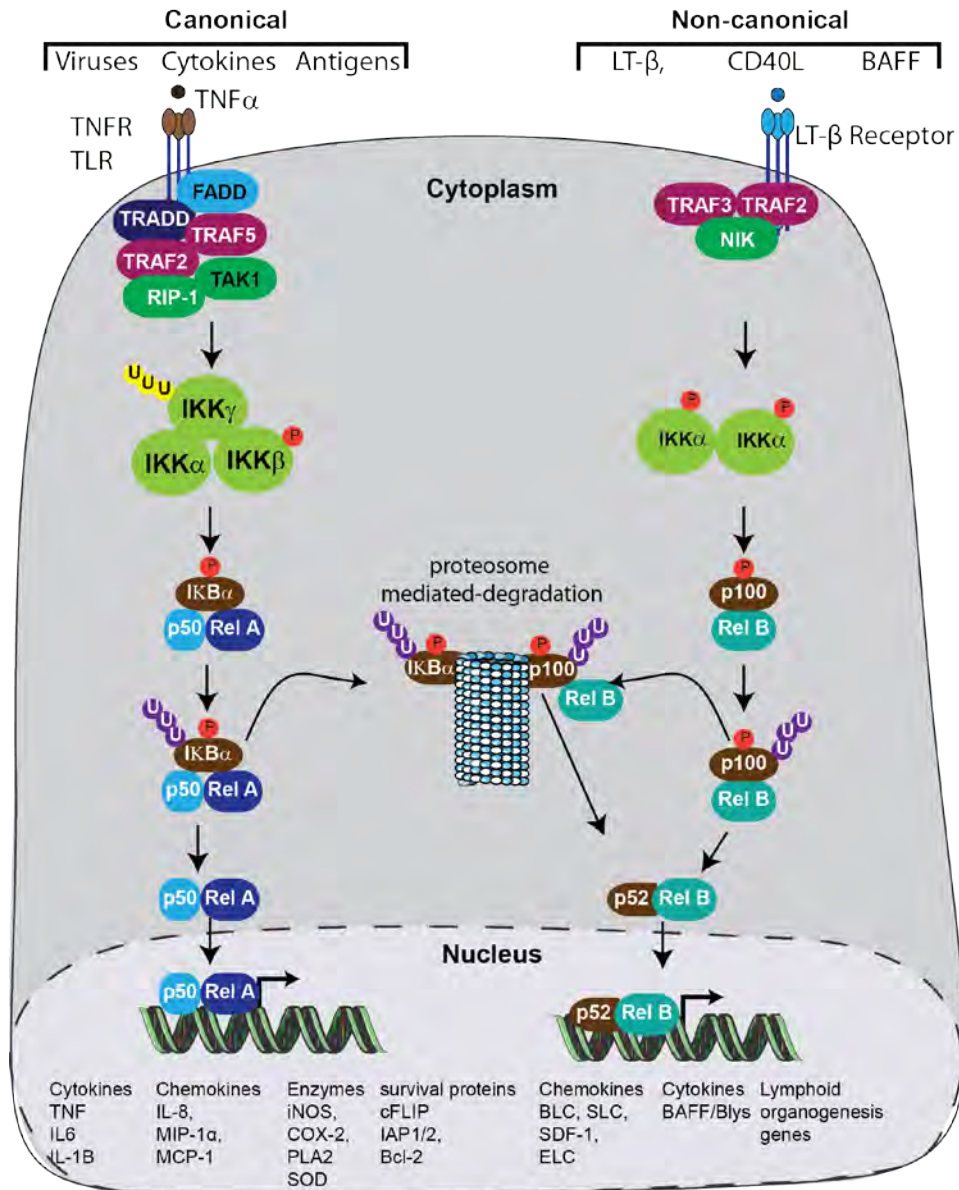


Figure 6. Canonical and non-canonical NF-κB signaling: In the canonical pathway IκBα is phosphorylated in an IKKβ- and NEMO-dependent manner, which results in the nuclear translocation of mostly p65-containing heterodimers. In the non-canonical pathway, it is induced by certain CD40L, BAFF and lymphotoxin-β (LT-β), which induces IKKα-mediated phosphorylation of p100. Degradation of IκBα releases the NF-κB heterodimers, which then migrate to the nucleus and regulate gene expression. BAFF, B-cell-activating factor belonging to the TNF family; BLC, B-lymphocyte chemoattractant; COX-2, cyclooxygenase 2; ELC, Epstein-Barr virus-induced molecule 1 ligand; IL-1b, interleukin-1b; iNOS, inducible nitric oxide synthase; LT, lymphotoxin; MCP-1, monocyte chemotactic protein-1; MIP-1a, macrophage inflammatory protein-1a; PLA2, phospholipase 2; SDF-1, stromal cell-derived factor-1a; SLC, secondary lymphoid tissue chemokine; SOD, superoxide dismutase. TLRs, Toll-like receptors.

TAK1-associated binding proteins 2 and 3 (TAB2 and TAB3) interact with TAK1 and TRAF2; leading to TAK1 activation that then phosphorylates IKK β and activates the IKK complex. IKK-dependent I κ B α -phosphorylation is followed by ubiquitination, which targets I κ B α to subsequent proteasome-mediated degradation (Figure 6); this allows p65 containing NF- κ B dimers to freely translocate into the nucleus and induce target gene expression (113;114).

The noncanonical NF- κ B signaling is regulated by TRAF3 and the NF- κ B-inducing kinase (NIK). Under resting conditions TRAF3 binds to NIK and mediates its ubiquitination and proteasomal degradation. After stimulation, TRAF3 itself undergoes degradation (mediated by TRAF2 and cIAP), thereby resulting in stabilization of NIK which phosphorylates IKK α to induce the phosphorylation and proteasomal processing of p100 (Figure 6), subsequently leading to the formation of p52-containing NF- κ B dimers (115)

8.2. Regulation of NF- κ B signals

NF- κ B signaling inhibition is mediated mainly by sequestering the NF- κ B dimers in the cytosol through the formation of NF- κ B-I κ B complexes. Post-translational modifications modulate NF- κ B signaling negatively or positively. These modifications take place upstream of the IKK-complex or directly on the NF- κ B members. For instance, the deubiquitinase A20 expression, which is induced by NF- κ B, removes the k63-linked polyubiquitin chain from Rip1 and IKK γ and thereby destabilizes the IKK-activating complex (116). Similar effects are mediated by CYLD (cylindromatosis), a tumour suppressor which inhibits both NF- κ B and JNK kinase activation by removing Lys63-linked polyubiquitin chains from BCL3, RIP1, TRAF2, TRAF6 and IKK γ (117). Dephosphorylation negatively regulates NF- κ B in non-stimulated cells, the association of the IKK-complex with protein phosphatase 2C β (PP2C β) or protein phosphatase 1 (PP1), renders the IKK-complex less active. In TNF- α and IL-1 β stimulated cells, protein phosphatase 2A (PP2A) enzyme complex associates and negatively regulates NF- κ B by dephosphorylating IKK, TRAF2 and NF- κ B. Interleukin-1 receptor-associated kinase 1

(IRAK1) is negatively regulated by tyrosine phosphatase SHP-1 (117). RelA polyubiquitination by COMMD1-SOCS1-Cullin-2 E3 ligase complex and PDLIM2 E3 ligase induce RelA proteasome-mediated degradation. In addition, PDLIM2 promotes the relocalization of RelA to transcriptionally silent promyelocytic leukemia nuclear bodies (PML body). The binding of RelA-NF- κ B complexes to DNA is negatively modulated by PIAS E3 ligase. Other post-translational modifications were reported to repress the transcriptional activity of NF- κ B; these include Rel A oxidation, nitration and deacetylation (116;118-121). Subsequent to NF- κ B stimulation, the expression of dominant negative adaptors MyD88s, SARM and IRAK-M are induced and negatively modulate the TLR signaling (116).

Although swift activation of NF- κ B is required for a successful immune response, such response should not last forever and thus it needs to be properly switched off to avoid tissue damage. Several human diseases result from both loss and gain of function in NF- κ B signaling. Inhibition of NF- κ B is accompanied by severe immune deficiency. Uncontrolled NF- κ B activation can lead to chronic inflammation; increase the risk of cancer, autoimmune diseases (e.g. rheumatoid arthritis), atherosclerosis (117;118;122).

9. Heart

The mammalian heart is a dynamic organ that functions as a mechanical pump; it grows and undergoes changes to accommodate alterations in workload. The heart experiences hypertrophic enlargement in response to physiological stimuli or pathological insults. Myocardial hypertrophy is characterized by an increase in the size (in length and/or width) of individual cardiac myocytes without an increase in the number of cells. This leads to an increase in heart muscle mass, which reflects a remodeling of the myocardium in response to biomechanical or neurohumoral stresses (123).

Heart failure is defined as a deficiency in the capability of the heart to adequately pump blood in response to systemic demands. Heart failure is a major cause of lethality worldwide; signs of heart failure include premature fatigue, dyspnoea, and/or oedema. Both biomechanical stresses could induce cardiac hypertrophy these include long

standing hypertension, myocardial infarction, ischemia associated with coronary artery disease, valvular insufficiency and stenosis (narrowing of the blood vessels), in addition to inherited mutation of genes encoding contractile proteins; as well as neurohumoral stresses induced by excessive release of hormones, cytokines and peptide growth factors at the level of the myocardium. Compensated hypertrophy (eccentric) is an adaptive response that aims to increase cardiac pump function and release ventricular wall tension. In the long term, adaptive hypertrophy turns to pathological hypertrophy (concentric) as being associated with maladaptive remodeling events including; reactivation of fetal gene program, cardiomyocyte death, alterations in cardiac extracellular matrix composition and fibrosis. Altogether these changes ultimately contribute to depressed contractile function and predisposes individuals to arrhythmia and sudden death (124).

In addition to hypertrophy, dilation is another type of cardiac enlargement which involves an increase in the size of the cavity of one or more chambers of the heart (Figure 7). Dilation can result from a growth response in which sarcomeres are predominantly added in series to individual myocytes. Conditions that directly damage the heart muscle, such as heart muscle inflammation (myocarditis) associated with viral infection and valvular regurgitation (incomplete opening of the valve) over time induce ventricular dilatation.

Cardiac hypertrophy is classified as eccentric or concentric based on pressure or volume overload on the heart. Eccentric hypertrophy, caused by volume overload, is characterized by increased heart-wall thickness and ventricular dilation but addition of new sarcomere *in-series* to the existing sarcomeres (Figure 7). Concentric hypertrophy, is imposed by pressure overload, and characterized by an increase in wall thickness with the deposition of new sarcomeres *in-parallel* to the existing sarcomeres; however, the chamber radius may not change (125). The thickened ventricle in these conditions is capable of generating greater forces and higher pressures, while the increased wall thickness maintains normal wall stress (124). Hypertrophic cardiomyopathy is an inherited class of hypertrophy and considered a genetic disease associated with weakness of the individual muscle fibers of the heart. Mutations in genes essential for

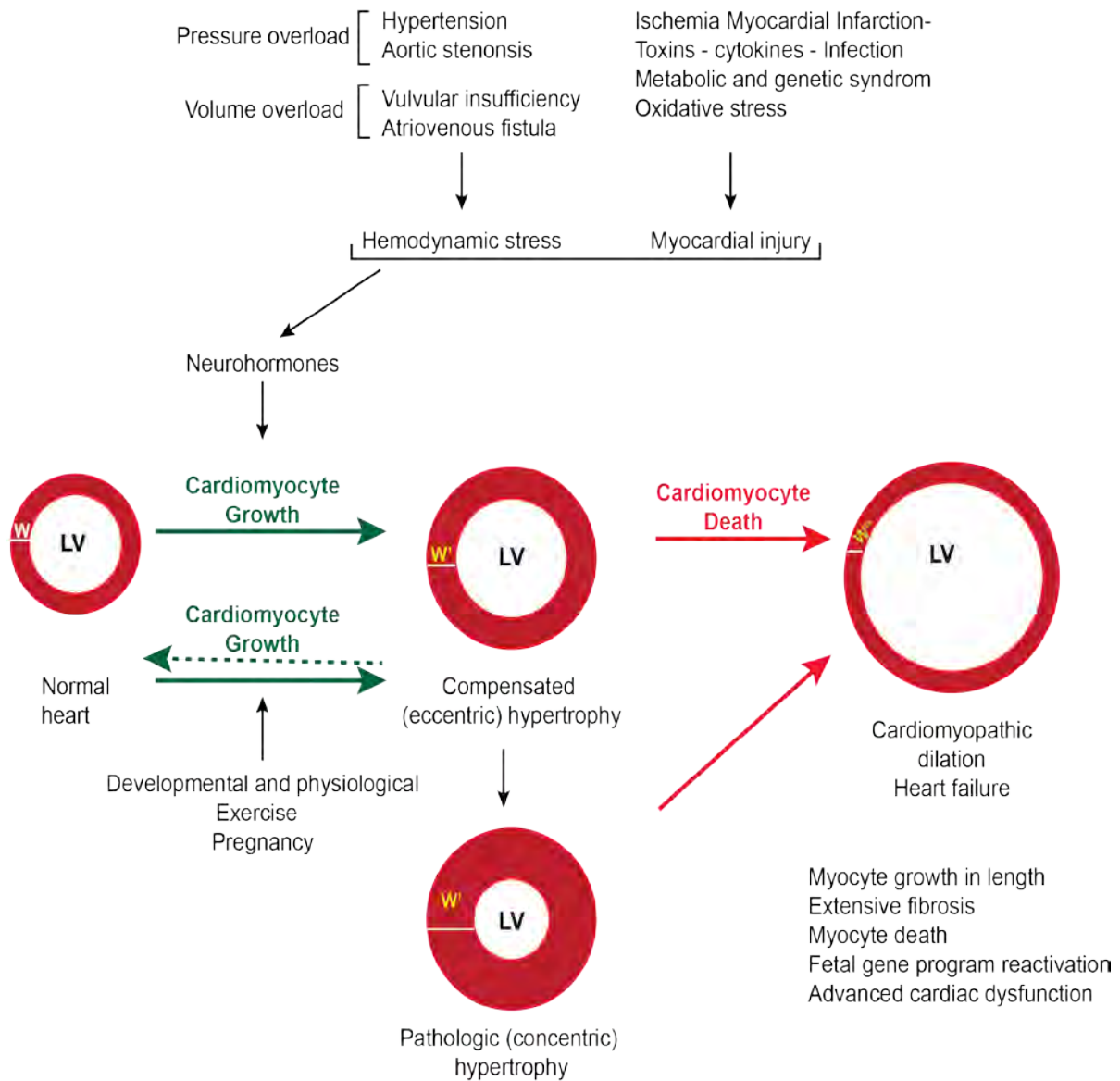


Figure 7. Development and progression of chamber hypertrophy

Neurohormonal activation by hemodynamic stress and/or myocardial injury transduces development of hypertrophy. Compensated (eccentric) cardiac hypertrophy is marked by a uniform increase in ventricular wall thickness ($W' > W$) and left ventricular chamber dimensions. During development and exercise the heart manifests this type of hypertrophy. Compensated hypertrophy can lead to pathologic (concentric) hypertrophy. Cardiomyocyte death leads to heart failure and cardiomyopathic dilation marked by larger LV chamber dimension and thinner wall ($W''' < W'$).

contraction of the heart muscle were reported in hypertrophic cardiomyopathy including the genes for myosin, troponin T, α -tropomyosin, cardiac myosin-binding protein-C, or the essential and regulatory light chains (126).

9.1. Reactivation of the fetal gene program

Cardiac hypertrophy is associated with the activation of the fetal gene program, and considered as one of the most consistent markers of cardiac hypertrophy. Fetal gene within this group include atrial natriuretic peptide (ANP) (127) and brain natriuretic peptide and (BNP), fetal type cardiac ion channels (hyperpolarization activated cyclic nucleotide-gated channel and T-type Ca^{2+} channel), some smooth muscle genes (smooth muscle α -actin and SM22 α) (128) and fetal isoforms of contractile proteins (skeletal α actin and β -myosin heavy chain)(129). The expression of sarcomeric proteins in the fetal heart undergoes major isoform switches at birth. In murine developing heart, β -myosin heavy chain (β -MHC) is the predominant isoform, but it is replaced by α -MHC after birth. This change in the MHC isoform seems to be an important process by which the heart adapts its mechanical performance and efficiency to the postnatal circulation. The mentioned fetal genes are abundantly expressed in fetal ventricles but become silent after birth; however, the expression of fetal gene is re-induced when the heart suffers pathological stress, and this expression is thought to play a key role in the molecular process underlying pathological cardiac remodeling. The best known transcription factors to regulate fetal gene expression include Nkx2.5, GATA4/6, myocyte enhancer factor (MEF)-2C, serum response factor (SRF) and nuclear factor of activated T-cells (NF-AT) (130;131).

9.2. Myocardial cell death

Numerous consequences of compensated myocardial hypertrophy may arise including alterations in intercellular matrix leading to interstitial fibrosis, loss of β -adrenergic receptor responsiveness, and changes in contractile protein isoforms. However, the defining irreversible cellular event is cardiomyocyte death. There is clinico-pathological evidence for all three forms of cell death (necrosis, apoptosis, and autophagy) in end-stage human cardiomyopathy. Cardiomyocyte necrotic death is suggested to take place

due to the increase of cardiomyocyte cross-sectional area (threefold), which overwhelms the physiological and physical limits of oxygen delivery to the center of the myocyte. In addition, mitochondria at the core of the cardiomyocyte become ischemic, with resulting diminished ATP-generating ability (132). Myocardial ischemia is caused by an inadequate blood supply, and thereby an inadequate supply of oxygen, glucose and fatty acids to the heart. In these conditions blood flow should be rapidly restored; otherwise massive cardiomyocyte death may follow, but it was noticed that reperfusion is also associated with cardiomyocyte death as well. It is not clear whether cell death takes place during reperfusion or after completion as a result of oxidative stress, which may induce both necrosis and apoptosis (133).

Myocardial apoptosis is an extremely rare event in the normal myocardium (0.001–0.002%); apoptotic rates in patients with end-stage dilated cardiomyopathy may reach 0.08–0.25%; however, the rate of cardiac myocyte apoptosis may increase dramatically in human heart diseases associated with cardiomyocyte drop-out, such as hypertrophic heart disease (134), dilated and ischemic cardiomyopathies (135), and arrhythmogenic right ventricular dysplasia (136). Inducible pro-apoptotic genes were detected in pressure-induced hypertrophy in mice and humans, such as Nix a BH3-only member of Bcl2 family protein (137). Cardiac-restricted expression of a conditional caspase-8 transgene showed that abnormal but low levels of cardiomyocyte apoptosis (0.023% vs. 0.002% in controls) are sufficient to cause lethal dilated cardiomyopathy. It seems that although the percentage of apoptotic cells is low, provided the fast rate of the apoptosis process (30 minutes) this can cause adverse and lethal complications. Relevant stimuli in heart failure probably include stretch (138), reactive oxygen species (H_2O_2 and peroxynitrite)(139), β 1-adrenergic agonists (138), cytoskeletal abnormalities (140), angiotensin II , proinflammatory cytokines and anthracycline drugs (141).

9.3. Myocardial fibrosis

Cardiac fibrosis is one of the pathologic features of heart failure beside cardiomyocyte hypertrophy and death. Cardiac fibrosis is characterized by excessive deposition of extracellular matrix proteins. Fibrosis increases myocardial stiffness a criterion related to

extracellular matrix (ECM) quality. ECM is a ground network of fibrillar collagens that is responsible for the integrity of myocardial structure and plays an important role in cardiac adaptation to diverse stresses, and promotes remodeling. The myocardial ECM is composed mainly of collagen type I (Col I) and collagen type III (Col III), which make scaffolding support for the myocytes and maintain the integrity of the heart. Collagen is a stable protein whose balanced turnover (synthesis and degradation) by cardiac fibroblasts is normally slow (estimated to be 80–120 days) (142). In the healthy heart transmission of the systolic contraction is facilitated by the scaffold of type I and type III fibrillar collagens, loss of collagen fibrils leads to ventricular dilation, myocyte slippage, and contractile dysfunction. Increase in interstitial collagen (accumulated perimysium) is associated with diastolic heart failure, whereas degradation of endomysial and perimysial components of the collagen scaffolding is associated with ventricular dilatation and systolic heart failure. Systolic and diastolic dysfunction could be predicted by evaluating the alteration of Col I and Col III levels and their Col I/Col III ratio which increase during dilated cardiomyopathy and heart failure (143) Therefore, modulation or balance between matrix protein synthesis and degradation is a crucial factor for cardiac remodeling and also in the pathophysiology of heart failure (144). Collagen turnover is maintained by matrix metalloproteinases (MMPs), whose activity is inhibited by their endogenous inhibitors tissue inhibitors of metalloproteinases (TIMPs). A fine balance between MMPs and TIMPs maintains the integrity of the matrix. MMP activity leads to enhanced ECM degradation, which may cause ventricular dilation (145).

One of the major features for the development of heart failure includes the transition of cardiac fibroblasts to myofibroblasts. These cells are defined by their dual functions: fibroblast-like in terms of ECM synthesis and smooth muscle myocyte-like in terms of migration. Myofibroblasts produce a different ECM than fibroblasts and modify the balance of MMPs and TIMPs to promote fibrosis. These changes in ECM modify the signals that cardiac myocytes receive from their scaffolding environment, leading to changes in gene expression associated with hypertrophy and contractile dysfunction. Myofibroblast collagen turnover is regulated by a number of growth factors such as Ang II, TGF- β 1, IGF-1, and TNF- α (146;147). The transition from compensated left

ventricular hypertrophy to heart failure is associated with degradation of ECM and changes in the collagen. Loss of the collagen network might cause loss of function by: interruptions in the collagen matrix that provides support, geometric alignment, and coordination of contraction by cardiomyocyte bundles; the loss of the normal interactions between endomysial components such as laminin and collagen with their receptors (dystroglycans and integrins) which is required for contractile synchrony and long-term cardiomyocyte homeostasis; the sliding displacement (slippage) of cardiomyocytes, leading to a decrease in the number of muscular layers in the ventricular wall and to LV dilation. The activation of the renin-angiotensin-aldosterone system (RAAS) and increased levels of active TGF- β 1 recruit smooth muscle cells, monocytes, and fibroblasts and stimulate wound repair program and ECM deposition, leading to perivascular fibrosis and amplification of the profibrotic state (148).

9.4. Sensing and transduction of hypertrophy signals

Extracellular signals are relayed through receptors to intracellular signal-transduction circuits to mediate the cardiac growth response. This is achieved by altering the levels of gene expression, increasing the rates of protein translation and decreasing the rates of protein degradation in the cytoplasm. Neurohumoral stimuli that are associated with the release of hormones, cytokines, chemokines and peptide growth factors are detected by heterotrimeric G proteins coupled receptors (GPCR) that have intracellular tyrosine kinase domains or that have intracellular serine/threonine kinase domains, and gp130 linked receptors. For instance the coupling of Angiotensin II, endothelin-1 and catecholamines (α -adrenergic) to receptors coupled with G proteins G α q/ α 11 subclass and associated with phospholipase C β (PLC β) induces the generation of diacyl glycerol (DAG), which functions as an intra-cellular ligand for protein kinase C (PKC). Once activated, PKC leads to the production and accumulation of inositol-1,4,5-trisphosphate(Ins(1,4,5)P₃)¹⁴. That is responsible for the mobilization of internal Ca²⁺ to the endoplasmic reticulum or the nuclear envelope. The increased levels of internal Ca²⁺ activate the dimeric Ca²⁺-dependent serine/threonine protein-phosphatase calcineurin, which binds to transcription factors of NF-AT family. Calcineurin dephosphorylates conserved serine residues at the N terminus of NF-AT, resulting in

NF-AT translocation to the nucleus and the activation of pro-hypertrophic genes expression including ANP, BNP and β -MHC (130;149).

Signaling mediators of cardiac hypertrophy include: mitogen-activated protein kinase (MAPK) which results in the dual phosphorylation and activation of p38, c-Jun N-terminal kinases (JNKs) and ERKs. p38 inhibition was reported to promote hypertrophic cardiomyopathy through upregulation of calcineurin-NFAT signaling (150). JNKs negatively regulate NF-AT and moreover, inhibition of JNKs by expressing a dominant negative form enhances the cardiac hypertrophic response. Phosphorylation of ERK1/2 causes cardiac hypertrophy (151). Activated PI3K induces Akt activation which induces the survival of cardiomyocytes, however Akt directly phosphorylates and inactivates GSK-3 β as well. Active GSK3 β negatively regulates hypertrophic transcriptional effectors, such as GATA4, β -catenin, c-Myc, NF-AT, c-jun, Stat, NF- κ B and the translation initiation factor eIF2B; all of these have been found to be involved directly or indirectly in the development of cardiac hypertrophy (123). Increased protein synthesis is a key feature of cardiac hypertrophy and likely underlies the increased cell and organ size observed. Akt activates mTOR which in turn leads to altered metabolism and increased cell growth, mediated by changes in gene transcription and translation (259, 288). mTOR can regulate protein synthesis through two pathways: mTOR phosphorylates and thereby inactivates eukaryotic initiation factor 4E-binding protein (eIF-4E BP1), leading to increased protein translation, mTOR also phosphorylates and activates p70S6 kinase, which is a short isoform of the ribosome S6 kinase 1 (S6K1); S6K1 and S6K2 increase ribosomal biosynthesis and protein translation (152). The inhibition of mTOR by rapamycin attenuates pathological cardiac hypertrophy and can reverse myocardial dysfunction (153)

Biomechanical signals are mediated through internal stretch-sensitive receptors. Cardiac myocytes detect mechanical deformation or stretch through an internal sensory apparatus including integrins heterodimeric transmembrane receptors (consisting of α - and β -subunits) that link the extracellular matrix to the intracellular cytoskeleton (154). The small LIM-domain protein MLP (muscle LIM protein), is thought to function as an

internal stretch sensor at the level of the Z-disc within each sarcomere through a complex of transducing proteins (155)

10. Physiological role of apoptosis

Apoptosis is a generalized but highly regulated cell response that is essential to eliminate unnecessary tissue and sculpting many tissues that develop during embryonic differentiation (such as the regression of inter-digital webs of the hands)(156). The ventricular and atrial compartments of the developing heart enlarge throughout development. This is due to high levels of apoptosis, which is observed in these chambers in the embryonic cardiomyocytes (E.11 and 16) and neonatal cardiomyocytes two days after birth (1). Apoptosis is responsible for the removal of the initially overproduced cells that fail to establish functional synaptic connections in the nervous system (157). Apoptosis has to be tightly regulated, otherwise it may lead to pathology. Insufficient apoptosis could lead to cancer where suppression of apoptosis plays a central role in for the development and progression of the disease. Therefore, apoptosis limits the proliferation of abnormal or damaged cells that could otherwise form malignant tumors (158). Autoimmune diseases may arise if apoptosis is deregulated, activated or auto-aggressive immune cells either during maturation in bone marrow and thymus, or in peripheral tissues are eliminated by apoptosis. Primarily those are auto-aggressive T cells that did not achieve productive antigen specificities, or over-proliferative B cells which consent with excess immunoglobulin production, leading to autoimmunity and other autoimmune diseases such as autoimmune lymphoproliferative syndrome (ALPS) (159;160). Excessive apoptosis leads to developmental defects and neurodegenerative diseases such as Parkinson's disease, Alzheimer's disease, Huntington's disease and amyotrophic lateral sclerosis (157;161).

Reference List

1. Fisher,S.A., Langille,B.L., and Srivastava,D. 2000. Apoptosis during cardiovascular development. *Circ. Res.* **87**:856-864.
2. Gregory,C. 2009. Cell biology: Sent by the scent of death. *Nature* **461**:181-182.
3. Kerr,D.J., Graham,J., Cummings,J., Morrison,J.G., Thompson,G.G., Brodie,M.J., and Kaye,S.B. 1986. The effect of verapamil on the pharmacokinetics of adriamycin. *Cancer Chemother. Pharmacol.* **18**:239-242.
4. Taylor,R.C., Cullen,S.P., and Martin,S.J. 2008. Apoptosis: controlled demolition at the cellular level. *Nat. Rev. Mol. Cell Biol.* **9**:231-241.
5. Fadok,V.A., Bratton,D.L., Frasch,S.C., Warner,M.L., and Henson,P.M. 1998. The role of phosphatidylserine in recognition of apoptotic cells by phagocytes. *Cell Death Differ.* **5**:551-562.
6. Galluzzi,L., and Kroemer,G. 2008. Necroptosis: a specialized pathway of programmed necrosis. *Cell* **135**:1161-1163.
7. Festjens,N., Vanden Berghe,T., and Vandenabeele,P. 2006. Necrosis, a well-orchestrated form of cell demise: signalling cascades, important mediators and concomitant immune response. *Biochim. Biophys. Acta* **1757**:1371-1387.
8. Zong,W.X., Ditsworth,D., Bauer,D.E., Wang,Z.Q., and Thompson,C.B. 2004. Alkylating DNA damage stimulates a regulated form of necrotic cell death. *Genes Dev.* **18**:1272-1282.
9. Christofferson,D.E., and Yuan,J. 2010. Necroptosis as an alternative form of programmed cell death. *Curr. Opin. Cell Biol.* **22**:263-268.
10. Duprez,L., Takahashi,N., Van,H.F., Vandendriessche,B., Goossens,V., Vanden Berghe,T., Declercq,W., Libert,C., Cauwels,A., and Vandenabeele,P. 2011. RIP kinase-dependent necrosis drives lethal systemic inflammatory response syndrome. *Immunity.* **35**:908-918.
11. Ohgushi,M., and Sasai,Y. 2011. Lonely death dance of human pluripotent stem cells: ROCKing between metastable cell states. *Trends Cell Biol.* **21**:274-282.
12. Samuel,M.S., and Olson,M.F. 2010. Dying alone: a tale of rho. *Cell Stem Cell* **7**:135-136.
13. Coleman,M.L., Sahai,E.A., Yeo,M., Bosch,M., Dewar,A., and Olson,M.F. 2001. Membrane blebbing during apoptosis results from caspase-mediated activation of ROCK I. *Nat. Cell Biol.* **3**:339-345.
14. Sebbagh,M., Renvoize,C., Hamelin,J., Riche,N., Bertoglio,J., and Breard,J. 2001. Caspase-3-mediated cleavage of ROCK I induces MLC phosphorylation and apoptotic membrane blebbing. *Nat. Cell Biol.* **3**:346-352.
15. Rosenblatt,J., Raff,M.C., and Cramer,L.P. 2001. An epithelial cell destined for apoptosis signals its neighbors to extrude it by an actin- and myosin-dependent mechanism. *Curr. Biol.* **11**:1847-1857.
16. Rao,L., Perez,D., and White,E. 1996. Lamin proteolysis facilitates nuclear events during apoptosis. *J. Cell Biol.* **135**:1441-1455.
17. Croft,D.R., Coleman,M.L., Li,S., Robertson,D., Sullivan,T., Stewart,C.L., and Olson,M.F. 2005. Actin-myosin-based contraction is responsible for apoptotic nuclear disintegration. *J. Cell Biol.* **168**:245-255.
18. Moss,D.K., Betin,V.M., Malesinski,S.D., and Lane,J.D. 2006. A novel role for microtubules in apoptotic chromatin dynamics and cellular fragmentation. *J. Cell Sci.* **119**:2362-2374.
19. Williams,J.R., Little,J.B., and Shipley,W.U. 1974. Association of mammalian cell death with a specific endonucleolytic degradation of DNA. *Nature* **252**:754-755.
20. Enari,M., Sakahira,H., Yokoyama,H., Okawa,K., Iwamatsu,A., and Nagata,S. 1998. A caspase-activated DNase that degrades DNA during apoptosis, and its inhibitor ICAD. *Nature* **391**:43-50.

21. Cheung,W.L., Ajiro,K., Samejima,K., Kloc,M., Cheung,P., Mizzen,C.A., Beeser,A., Etkin,L.D., Chernoff,J., Earnshaw,W.C. et al 2003. Apoptotic phosphorylation of histone H2B is mediated by mammalian sterile twenty kinase. *Cell* **113**:507-517.
22. Ura,S., Masuyama,N., Graves,J.D., and Gotoh,Y. 2001. Caspase cleavage of MST1 promotes nuclear translocation and chromatin condensation. *Proc. Natl. Acad. Sci. U. S. A* **98**:10148-10153.
23. Napirei,M., Karsunky,H., Zevnik,B., Stephan,H., Mannherz,H.G., and Moroy,T. 2000. Features of systemic lupus erythematosus in Dnase1-deficient mice. *Nat. Genet.* **25**:177-181.
24. Kawane,K., Fukuyama,H., Yoshida,H., Nagase,H., Ohsawa,Y., Uchiyama,Y., Okada,K., Iida,T., and Nagata,S. 2003. Impaired thymic development in mouse embryos deficient in apoptotic DNA degradation. *Nat. Immunol.* **4**:138-144.
25. Lane,J.D., Lucocq,J., Pryde,J., Barr,F.A., Woodman,P.G., Allan,V.J., and Lowe,M. 2002. Caspase-mediated cleavage of the stacking protein GRASP65 is required for Golgi fragmentation during apoptosis. *J. Cell Biol.* **156**:495-509.
26. Lane,J.D., Allan,V.J., and Woodman,P.G. 2005. Active relocation of chromatin and endoplasmic reticulum into blebs in late apoptotic cells. *J. Cell Sci.* **118**:4059-4071.
27. Karbowski,M., Norris,K.L., Cleland,M.M., Jeong,S.Y., and Youle,R.J. 2006. Role of Bax and Bak in mitochondrial morphogenesis. *Nature* **443**:658-662.
28. Kuwana,T., Bouchier-Hayes,L., Chipuk,J.E., Bonzon,C., Sullivan,B.A., Green,D.R., and Newmeyer,D.D. 2005. BH3 domains of BH3-only proteins differentially regulate Bax-mediated mitochondrial membrane permeabilization both directly and indirectly. *Mol. Cell* **17**:525-535.
29. Ricci,J.E., Munoz-Pinedo,C., Fitzgerald,P., Bailly-Maitre,B., Perkins,G.A., Yadava,N., Scheffler,I.E., Ellisman,M.H., and Green,D.R. 2004. Disruption of mitochondrial function during apoptosis is mediated by caspase cleavage of the p75 subunit of complex I of the electron transport chain. *Cell* **117**:773-786.
30. Luthi,A.U., and Martin,S.J. 2007. The CASBAH: a searchable database of caspase substrates. *Cell Death Differ.* **14**:641-650.
31. Savill,J., and Fadok,V. 2000. Corpse clearance defines the meaning of cell death. *Nature* **407**:784-788.
32. Lauber,K., Bohn,E., Krober,S.M., Xiao,Y.J., Blumenthal,S.G., Lindemann,R.K., Marini,P., Wiedig,C., Zobywalski,A., Baksh,S. et al 2003. Apoptotic cells induce migration of phagocytes via caspase-3-mediated release of a lipid attraction signal. *Cell* **113**:717-730.
33. Horino,K., Nishiura,H., Ohsako,T., Shibuya,Y., Hiraoka,T., Kitamura,N., and Yamamoto,T. 1998. A monocyte chemotactic factor, S19 ribosomal protein dimer, in phagocytic clearance of apoptotic cells. *Lab Invest* **78**:603-617.
34. Wakasugi,K., and Schimmel,P. 1999. Two distinct cytokines released from a human aminoacyl-tRNA synthetase. *Science* **284**:147-151.
35. Martin,S.J., Finucane,D.M., Amarante-Mendes,G.P., O'Brien,G.A., and Green,D.R. 1996. Phosphatidylserine externalization during CD95-induced apoptosis of cells and cytoplasts requires ICE/CED-3 protease activity. *J. Biol. Chem.* **271**:28753-28756.
36. Fadok,V.A., Voelker,D.R., Campbell,P.A., Cohen,J.J., Bratton,D.L., and Henson,P.M. 1992. Exposure of phosphatidylserine on the surface of apoptotic lymphocytes triggers specific recognition and removal by macrophages. *J. Immunol.* **148**:2207-2216.
37. Gardai,S.J., McPhillips,K.A., Frasch,S.C., Janssen,W.J., Starefeldt,A., Murphy-Ullrich,J.E., Bratton,D.L., Oldenborg,P.A., Michalak,M., and Henson,P.M. 2005. Cell-surface calreticulin initiates clearance of viable or apoptotic cells through trans-activation of LRP on the phagocyte. *Cell* **123**:321-334.
38. Moffatt,O.D., Devitt,A., Bell,E.D., Simmons,D.L., and Gregory,C.D. 1999. Macrophage recognition of ICAM-3 on apoptotic leukocytes. *J. Immunol.* **162**:6800-6810.

39. Hall,S.E., Savill,J.S., Henson,P.M., and Haslett,C. 1994. Apoptotic neutrophils are phagocytosed by fibroblasts with participation of the fibroblast vitronectin receptor and involvement of a mannose/fucose-specific lectin. *J. Immunol.* **153**:3218-3227.
40. Albert,M.L., Sauter,B., and Bhardwaj,N. 1998. Dendritic cells acquire antigen from apoptotic cells and induce class I-restricted CTLs. *Nature* **392**:86-89.
41. Bellone,M., Iezzi,G., Rovere,P., Galati,G., Ronchetti,A., Protti,M.P., Davoust,J., Rugarli,C., and Manfredi,A.A. 1997. Processing of engulfed apoptotic bodies yields T cell epitopes. *J. Immunol.* **159**:5391-5399.
42. Thornberry,N., and Lazebnik,Y.A. 1998. Caspases: enemies within. *Science* **281**:1312-1316.
43. Launay,S., Hermine,O., Fontenay,M., Kroemer,G., Solary,E., and Garrido,C. 2005. Vital functions for lethal caspases. *Oncogene* **24**:5137-5148.
44. Helfer,B., Boswell,B.C., Finlay,D., Cipres,A., Vuori,K., Bong,K.T., Wallach,D., Dorfleutner,A., Lahti,J.M., Flynn,D.C. et al 2006. Caspase-8 promotes cell motility and calpain activity under nonapoptotic conditions. *Cancer Res.* **66**:4273-4278.
45. Rebe,C., Cathelin,S., Launay,S., Filomenko,R., Prevotat,L., L'Ollivier,C., Gyan,E., Micheau,O., Grant,S., Dubart-Kupperschmitt,A. et al 2007. Caspase-8 prevents sustained activation of NF-kappaB in monocytes undergoing macrophagic differentiation. *Blood* **109**:1442-1450.
46. Sprick,M.R., Rieser,E., Stahl,H., Grosse-Wilde,A., Weigand,M.A., and Walczak,H. 2002. Caspase-10 is recruited to and activated at the native TRAIL and CD95 death-inducing signalling complexes in a FADD-dependent manner but can not functionally substitute caspase-8. *EMBO J* **21**:4520-4530.
47. Budihardjo,I., Oliver,H., Lutter,M., Luo,X., and Wang,X. 1999. Biochemical pathways of caspase activation during apoptosis. *Annu. Rev. Cell Dev. Biol.* **15**:269-290.
48. Peter,M.E., and Krammer,P.H. 2003. The CD95(APO-1/Fas) DISC and beyond. *Cell Death Differ.* **10**:26-35.
49. Krueger,A., Schmitz,I., Baumann,S., Krammer,P.H., and Kirchhoff,S. 2001. Cellular FLICE-inhibitory protein splice variants inhibit different steps of caspase-8 activation at the CD95 death-inducing signaling complex. *J Biol. Chem.* **276**:20633-20640.
50. Bossy-Wetzell,E., Newmeyer,D.D., and Green,D.R. 1998. Mitochondrial cytochrome c release in apoptosis occurs upstream of DEVD-specific caspase activation and independently of mitochondrial transmembrane depolarization. *EMBO J* **17**:37-49.
51. Zou,H., Henzel,W.J., Liu,X., Lutschg,A., and Wang,X. 1997. Apaf-1, a human protein homologous to *C. elegans* CED-4, participates in cytochrome c-dependent activation of caspase-3. *Cell* **90**:405-413.
52. Pop,C., Timmer,J., Sperandio,S., and Salvesen,G.S. 2006. The apoptosome activates caspase-9 by dimerization. *Mol. Cell* **22**:269-275.
53. Verhagen,A.M., Ekert,P.G., Pakusch,M., Silke,J., Connolly,L.M., Reid,G.E., Moritz,R.L., Simpson,R.J., and Vaux,D.L. 2000. Identification of DIABLO, a mammalian protein that promotes apoptosis by binding to and antagonizing IAP proteins. *Cell* **102**:43-53.
54. Suzuki,Y., Imai,Y., Nakayama,H., Takahashi,K., Takio,K., and Takahashi,R. 2001. A serine protease, HtrA2, is released from the mitochondria and interacts with XIAP, inducing cell death. *Mol. Cell* **8**:613-621.
55. Li,L.Y., Luo,X., and Wang,X. 2001. Endonuclease G is an apoptotic DNase when released from mitochondria. *Nature* **412**:95-99.
56. Luo,X., Budihardjo,I., Zou,H., Slaughter,C., and Wang,X. 1998. Bid, a Bcl2 interacting protein, mediates cytochrome c release from mitochondria in response to activation of cell surface death receptors. *Cell* **94**:481-490.

57. Medema,J.P., Toes,R.E., Scaffidi,C., Zheng,T.S., Flavell,R.A., Melief,C.J., Peter,M.E., Ofringa,R., and Krammer,P.H. 1997. Cleavage of FLICE (caspase-8) by granzyme B during cytotoxic T lymphocyte-induced apoptosis. *Eur. J Immunol.* **27**:3492-3498.
58. Thomas,D.A., Du,C., Xu,M., Wang,X., and Ley,T.J. 2000. DFF45/ICAD can be directly processed by granzyme B during the induction of apoptosis. *Immunity.* **12**:621-632.
59. Reed,J.C. 1998. Bcl-2 family proteins. *Oncogene* **17**:3225-3236.
60. Liston,P., Fong,W.G., and Korneluk,R.G. 2003. The inhibitors of apoptosis: there is more to life than Bcl2. *Oncogene* **22**:8568-8580.
61. Callus,B.A., and Vaux,D.L. 2007. Caspase inhibitors: viral, cellular and chemical. *Cell Death Differ.* **14**:73-78.
62. Basu,A., Lu,D., Sun,B., Moor,A.N., Akkaraju,G.R., and Huang,J. 2002. Proteolytic activation of protein kinase C-epsilon by caspase-mediated processing and transduction of antiapoptotic signals. *Journal of Biological Chemistry* **277**:41850-41856.
63. Ricci,J.E., Lang,V., Luciano,F., Belhacene,N., Giordanengo,V., Michel,F., Bismuth,G., and Auberger,P. 2001. An absolute requirement for Fyn in T cell receptor-induced caspase activation and apoptosis. *FASEB J* **15**:1777-1779.
64. Luciano,F., Herrant,M., Jacquelin,A., Ricci,J.E., and Auberger,P. 2003. The p54 cleaved form of the tyrosine kinase Lyn generated by caspases during BCR-induced cell death in B lymphoma acts as a negative regulator of apoptosis. *FASEB J* **17**:711-713.
65. Giaime,E., Sunyach,C., Herrant,M., Grosso,S., Auberger,P., McLean,P.J., Checler,F., and da Costa,C.A. 2006. Caspase-3-derived C-terminal product of synphilin-1 displays antiapoptotic function via modulation of the p53-dependent cell death pathway. *J Biol. Chem.* **281**:11515-11522.
66. Yang,J.-Y., and Widmann,C. 2001. Antiapoptotic signaling generated by caspase-induced cleavage of RasGAP. *MCB* **21**:5346-5358.
67. Grunicke,H.H., and Maly,K. 1993. Role of GTPases and GTPase regulatory proteins in oncogenesis. *Crit Rev Oncog.* **4**:389-402.
68. Pamonsinlapatham,P., Hadj-Slimane,R., Lepelletier,Y., Allain,B., Toccafondi,M., Garbay,C., and Raynaud,F. 2009. P120-Ras GTPase activating protein (RasGAP): a multi-interacting protein in downstream signaling. *Biochimie* **91**:320-328.
69. Bos,J.L., Rehmann,H., and Wittinghofer,A. 2007. GEFs and GAPs: critical elements in the control of small G proteins. *Cell* **129**:865-877.
70. Wittinghofer,A. 1998. Signal transduction via Ras. *Biol. Chem.* **379**:933-937.
71. Der,C.J., and Van,D.T. 2007. Stopping ras in its tracks. *Cell* **129**:855-857.
72. Malumbres,M., and Barbacid,M. 2003. RAS oncogenes: the first 30 years. *Nat. Rev. Cancer* **3**:459-465.
73. Wittinghofer,A. 1998. Signal transduction via Ras. *Biol Chem* **379**:933-937.
74. Leblanc,V., Tocque,B., and Delumeau,I. 1998. Ras-GAP Controls Rho-Mediated Cytoskeletal Reorganization through Its SH3 Domain. *Molecular and Cellular Biology* **18**:5567-5578.
75. Panasyuk,G., Nemazanyy,I., Filonenko,V., Negrutskii,B., and El'skaya,A.V. 2008. A2 isoform of mammalian translation factor eEF1A displays increased tyrosine phosphorylation and ability to interact with different signalling molecules. *Int. J Biochem. Cell Biol.* **40**:63-71.
76. Drugan,J.K., Rogers-Graham,K., Gilmer,T., Campbell,S., and Clark,G.J. 2000. The Ras/p120 GTPase-activating protein (GAP) interaction is regulated by the p120 GAP pleckstrin homology domain. *J Biol. Chem.* **275**:35021-35027.
77. Grewal,T., and Enrich,C. 2006. Molecular mechanisms involved in Ras inactivation: the annexin A6-p120GAP complex. *Bioessays* **28**:1211-1220.

78. Gigoux,V., L'Hoste,S., Raynaud,F., Camonis,J., and Garbay,C. 2002. Identification of Aurora kinases as RasGAP Src homology 3 domain-binding proteins. *J Biol. Chem.* **277**:23742-23746.
79. Walter,A.O., Seghezzi,W., Korver,W., Sheung,J., and Lees,E. 2000. The mitotic serine/threonine kinase Aurora2/AIK is regulated by phosphorylation and degradation. *Oncogene* **19**:4906-4916.
80. Kulkarni,S.V., Gish,G., van der Geer,P., Henkemeyer,M., and Pawson,T. 2000. Role of p120 Ras-GAP in directed cell movement. *J Cell Biol.* **149**:457-470.
81. Yang,J.-Y., and Widmann,C. 2002. The RasGAP N-terminal fragment generated by caspase cleavage protects cells in a Ras/PI3K/Akt-dependent manner that does not rely on NFκB activation. *JBC* **277**:14641-14646.
82. Yang,J.-Y., Michod,D., Walicki,J., Murphy,B.M., Kasibhatla,S., Martin,S., and Widmann,C. 2004. Partial cleavage of RasGAP by caspases is required for cell survival in mild stress conditions. *Mol. Cell Biol.* **24**:10425-10436.
83. Yang,J.-Y., Walicki,J., Michod,D., Dubuis,G., and Widmann,C. 2005. Impaired Akt activity down-modulation, caspase-3 activation, and apoptosis in cells expressing a caspase-resistant mutant of RasGAP at position 157. *Mol. Biol. Cell* **16**:3511-3520.
84. Fruman,D.A., Meyers,R.E., and Cantley,L.C. 1998. Phosphoinositide kinases. *Annu. Rev. Biochem.* **67**:481-507.
85. Downward,J. 1998. Ras signalling and apoptosis. *Curr. Opin. Genet. Dev.* **8**:49-54.
86. Marshall,C.J. 1996. Ras effectors. *Curr. Opin. Cell Biol.* **8**:197-204.
87. Chardin,P., Camonis,J.H., Gale,N.W., van,A.L., Schlessinger,J., Wigler,M.H., and Bar-Sagi,D. 1993. Human Sos1: a guanine nucleotide exchange factor for Ras that binds to GRB2. *Science* **260**:1338-1343.
88. Gaullier,J.M., Simonsen,A., D'Arrigo,A., Bremnes,B., Stenmark,H., and Aasland,R. 1998. FYVE fingers bind PtdIns(3)P. *Nature* **394**:432-433.
89. Blume-Jensen,P., and Hunter,T. 2001. Oncogenic kinase signalling. *Nature* **411**:355-365.
90. Franke,T.F., Kaplan,D.R., Cantley,L.C., and Toker,A. 1997. Direct regulation of the Akt proto-oncogene product by phosphatidylinositol-3,4-bisphosphate. *Science* **275**:665-668.
91. Alessi,D.R., Andjelkovic,M., Caudwell,B., Cron,P., Morrice,N., Cohen,P., and Hemmings,B.A. 1996. Mechanism of activation of protein kinase B by insulin and IGF-1. *EMBO J* **15**:6541-6551.
92. Sarbassov,D.D., Guertin,D.A., Ali,S.M., and Sabatini,D.M. 2005. Phosphorylation and regulation of Akt/PKB by the rictor-mTOR complex. *Science* **307**:1098-1101.
93. Huang,B.X., Akbar,M., Kevala,K., and Kim,H.Y. 2011. Phosphatidylserine is a critical modulator for Akt activation. *J Cell Biol.* **192**:979-992.
94. Wang,J.M., Chao,J.R., Chen,W., Kuo,M.L., Yen,J.J., and Yang-Yen,H.F. 1999. The antiapoptotic gene mcl-1 is up-regulated by the phosphatidylinositol 3-kinase/Akt signaling pathway through a transcription factor complex containing CREB. *Mol. Cell Biol.* **19**:6195-6206.
95. Ashcroft,M., Ludwig,R.L., Woods,D.B., Copeland,T.D., Weber,H.O., MacRae,E.J., and Vousden,K.H. 2002. Phosphorylation of HDM2 by Akt. *Oncogene* **21**:1955-1962.
96. Datta,S.R., Dudek,H., Tao,X., Masters,S., Fu,H., Gotoh,Y., and Greenberg,M.E. 1997. Akt phosphorylation of BAD couples survival signals to the cell-intrinsic death machinery. *Cell* **91**:231-241.
97. Miyamoto,S., Rubio,M., and Sussman,M.A. 2009. Nuclear and mitochondrial signalling Akts in cardiomyocytes. *Cardiovasc. Res* **82**:272-285.
98. Muraski,J.A., Rota,M., Misao,Y., Fransioli,J., Cottage,C., Gude,N., Esposito,G., Delucchi,F., Arcarese,M., Alvarez,R. et al 2007. Pim-1 regulates cardiomyocyte survival downstream of Akt. *Nat Med* **13**:1467-1475.

99. Cardone, M.H., Roy, N., Stennicke, H.R., Salvesen, G.S., Franke, T.F., Stanbridge, E., Frisch, S., and Reed, J.C. 1998. Regulation of cell death protease caspase-9 by phosphorylation. *Science* **282**:1318-1321.
100. Greer, E.L., and Brunet, A. 2005. FOXO transcription factors at the interface between longevity and tumor suppression. *Oncogene* **24**:7410-7425.
101. Ozes, O.N., Mayo, L.D., Gustin, J.A., Pfeffer, S.R., Pfeffer, L.M., and Donner, D.B. 1999. NF-kappaB activation by tumour necrosis factor requires the Akt serine-threonine kinase. *Nature* **401**:82-85.
102. Sen, R., and Baltimore, D. 1986. Multiple nuclear factors interact with the immunoglobulin enhancer sequences. *Cell* **46**:705-716.
103. Sen, R., and Baltimore, D. 1986. Inducibility of kappa immunoglobulin enhancer-binding protein NF-kappa B by a posttranslational mechanism. *Cell* **47**:921-928.
104. Baldwin, A.S., Jr. 1996. The NF-kappa B and I kappa B proteins: new discoveries and insights. *Annu Rev Immunol.* **14**:649-683.
105. Barnes, P.J. 1997. Nuclear factor-kappa B. *Int J Biochem. Cell Biol* **29**:867-870.
106. Verma, I.M., Stevenson, J.K., Schwarz, E.M., Van, A.D., and Miyamoto, S. 1995. Rel/NF-kappa B/I kappa B family: intimate tales of association and dissociation. *Genes Dev.* **9**:2723-2735.
107. May, M.J., and Ghosh, S. 1998. Signal transduction through NF-kappa B. *Immunology Today* **19**:80-88.
108. Kopp, E.B., and Ghosh, S. 1995. NF-kappa B and rel proteins in innate immunity. *Adv Immunol.* **58**:1-27.
109. Li, Q., and Verma, I.M. 2002. NF-kappaB regulation in the immune system. *Nat Rev Immunol.* **2**:725-734.
110. May, M.J., and Ghosh, S. 1998. Signal transduction through NF-kappa B. *IT* **19**:80-88.
111. Tang, E.D., Wang, C.Y., Xiong, Y., and Guan, K.L. 2003. A role for NF-kappaB essential modifier/IkappaB kinase-gamma (NEMO/IKKgamma) ubiquitination in the activation of the IkappaB kinase complex by tumor necrosis factor-alpha. *J Biol Chem* **278**:37297-37305.
112. Tada, K., Okazaki, T., Sakon, S., Kobayashi, T., Kurosawa, K., Yamaoka, S., Hashimoto, H., Mak, T.W., Yagita, H., Okumura, K. et al 2001. Critical roles of TRAF2 and TRAF5 in tumor necrosis factor-induced NF-kappa B activation and protection from cell death. *J Biol. Chem.* **276**:36530-36534.
113. Oeckinghaus, A., Hayden, M.S., and Ghosh, S. 2011. Crosstalk in NF-kappaB signaling pathways. *Nat. Immunol.* **12**:695-708.
114. Bonizzi, G., and Karin, M. 2004. The two NF-kappaB activation pathways and their role in innate and adaptive immunity. *Trends Immunol.* **25**:280-288.
115. Vallabhapurapu, S., Matsuzawa, A., Zhang, W., Tseng, P.H., Keats, J.J., Wang, H., Vignali, D.A., Bergsagel, P.L., and Karin, M. 2008. Nonredundant and complementary functions of TRAF2 and TRAF3 in a ubiquitination cascade that activates NIK-dependent alternative NF-kappaB signaling. *Nat. Immunol.* **9**:1364-1370.
116. Ruland, J. 2011. Return to homeostasis: downregulation of NF-kappaB responses. *Nat. Immunol.* **12**:709-714.
117. Wong, E.T., and Tergaonkar, V. 2009. Roles of NF-kappaB in health and disease: mechanisms and therapeutic potential. *Clin Sci (Lond)* **116**:451-465.
118. Ben-Neriah, Y., and Karin, M. 2011. Inflammation meets cancer, with NF-kappaB as the matchmaker. *Nat. Immunol.* **12**:715-723.
119. Karin, M., and Ben Neriah, Y. 2000. Phosphorylation meets ubiquitination: the control of NF-[kappa]B activity. *Annu Rev Immunol.* **18**:621-663.
120. Perkins, N.D. 2006. Post-translational modifications regulating the activity and function of the nuclear factor kappa B pathway. *Oncogene* **25**:6717-6730.

121. Schmukle,A.C., and Walczak,H. 2012. No one can whistle a symphony alone - how different ubiquitin linkages cooperate to orchestrate NF-kappaB activity. *J. Cell Sci.* **125**:549-559.
122. Courtois,G. 2005. The NF-kappaB signaling pathway in human genetic diseases. *Cell Mol. Life Sci.* **62**:1682-1691.
123. Heineke,J., and Molkenin,J.D. 2006. Regulation of cardiac hypertrophy by intracellular signalling pathways. *Nat Rev Mol Cell Biol* **7**:589-600.
124. Gupta,S., Das,B., and Sen,S. 2007. Cardiac hypertrophy: mechanisms and therapeutic opportunities. *Antioxid. Redox. Signal.* **9**:623-652.
125. Muhl,C., Dassen,W.R., and Kuipers,H. 2008. Cardiac remodelling: concentric versus eccentric hypertrophy in strength and endurance athletes. *Neth. Heart J* **16**:129-133.
126. Maron,B.J. 2002. Cardiology patient pages. Hypertrophic cardiomyopathy. *Circulation* **106**:2419-2421.
127. Izumo,S., Nadal-Ginard,B., and Mahdavi,V. 1988. Protooncogene induction and reprogramming of cardiac gene expression produced by pressure overload. *Proc. Natl. Acad. Sci. U. S. A* **85**:339-343.
128. Black,F.M., Packer,S.E., Parker,T.G., Michael,L.H., Roberts,R., Schwartz,R.J., and Schneider,M.D. 1991. The vascular smooth muscle alpha-actin gene is reactivated during cardiac hypertrophy provoked by load. *J Clin. Invest* **88**:1581-1588.
129. Izumo,S., Nadal-Ginard,B., and Mahdavi,V. 1988. Protooncogene induction and reprogramming of cardiac gene expression produced by pressure overload. *Proc Natl Acad Sci U S A* **85**:339-343.
130. Kuwahara,K., Nishikimi,T., and Nakao,K. 2012. Transcriptional regulation of the fetal cardiac gene program. *J Pharmacol. Sci.* **119**:198-203.
131. Barry,S.P., Davidson,S.M., and Townsend,P.A. 2008. Molecular regulation of cardiac hypertrophy. *Int. J Biochem. Cell Biol.* **40**:2023-2039.
132. Diwan,A., and Dorn,G.W. 2007. Decompensation of cardiac hypertrophy: cellular mechanisms and novel therapeutic targets. *Physiology. (Bethesda.)* **22**:56-64.
133. Gill,C., Mestrlil,R., and Samali,A. 2002. Losing heart: the role of apoptosis in heart disease--a novel therapeutic target? *FASEB J* **16**:135-146.
134. Hein,S., Arnon,E., Kostin,S., Schonburg,M., Elsasser,A., Polyakova,V., Bauer,E.P., Klovekorn,W.P., and Schaper,J. 2003. Progression from compensated hypertrophy to failure in the pressure-overloaded human heart: structural deterioration and compensatory mechanisms. *Circulation* **107**:984-991.
135. Narula,J., Haider,N., Virmani,R., DiSalvo,T.G., Kolodgie,F.D., Hajjar,R.J., Schmidt,U., Semigran,M.J., Dec,G.W., and Khaw,B.A. 1996. Apoptosis in myocytes in end-stage heart failure. *N. Engl. J Med.* **335**:1182-1189.
136. Mallat,Z., Tedgui,A., Fontaliran,F., Frank,R., Durigon,M., and Fontaine,G. 1996. Evidence of apoptosis in arrhythmogenic right ventricular dysplasia. *N. Engl. J Med.* **335**:1190-1196.
137. Yussman,M.G., Toyokawa,T., Odley,A., Lynch,R.A., Wu,G., Colbert,M.C., Aronow,B.J., Lorenz,J.N., and Dorn,G.W. 2002. Mitochondrial death protein Nix is induced in cardiac hypertrophy and triggers apoptotic cardiomyopathy. *Nat. Med.* **8**:725-730.
138. Cheng,W., Li,B., Kajstura,J., Li,P., Wolin,M.S., Sonnenblick,E.H., Hintze,T.H., Olivetti,G., and Anversa,P. 1995. Stretch-induced programmed myocyte cell death. *J Clin. Invest* **96**:2247-2259.
139. Ide,T., Tsutsui,H., Kinugawa,S., Suematsu,N., Hayashidani,S., Ichikawa,K., Utsumi,H., Machida,Y., Egashira,K., and Takeshita,A. 2000. Direct evidence for increased hydroxyl radicals originating from superoxide in the failing myocardium. *Circ. Res.* **86**:152-157.
140. Nikolova,V., Leimena,C., McMahan,A.C., Tan,J.C., Chandar,S., Jogia,D., Kesteven,S.H., Michalicek,J., Otway,R., Verheyen,F. et al 2004. Defects in nuclear structure and function promote dilated cardiomyopathy in lamin A/C-deficient mice. *J Clin. Invest* **113**:357-369.

141. Crow,M.T., Mani,K., Nam,Y.J., and Kitsis,R.N. 2004. The mitochondrial death pathway and cardiac myocyte apoptosis. *Circ. Res.* **95**:957-970.
142. Shirwany,A., and Weber,K.T. 2006. Extracellular matrix remodeling in hypertensive heart disease. *J Am. Coll. Cardiol.* **48**:97-98.
143. Lopez,B., Gonzalez,A., Querejeta,R., Larman,M., and Diez,J. 2006. Alterations in the pattern of collagen deposition may contribute to the deterioration of systolic function in hypertensive patients with heart failure. *J Am. Coll. Cardiol.* **48**:89-96.
144. Iwanaga,Y., Aoyama,T., Kihara,Y., Onozawa,Y., Yoneda,T., and Sasayama,S. 2002. Excessive activation of matrix metalloproteinases coincides with left ventricular remodeling during transition from hypertrophy to heart failure in hypertensive rats. *J Am. Coll. Cardiol.* **39**:1384-1391.
145. Creemers,E.E., Cleutjens,J.P., Smits,J.F., and Daemen,M.J. 2001. Matrix metalloproteinase inhibition after myocardial infarction: a new approach to prevent heart failure? *Circ. Res.* **89**:201-210.
146. Weber,K.T., Swamynathan,S.K., Guntaka,R.V., and Sun,Y. 1999. Angiotensin II and extracellular matrix homeostasis. *Int. J Biochem. Cell Biol.* **31**:395-403.
147. Rosenkranz,S. 2004. TGF-beta1 and angiotensin networking in cardiac remodeling. *Cardiovasc. Res.* **63**:423-432.
148. Berk,B.C., Fujiwara,K., and Lehoux,S. 2007. ECM remodeling in hypertensive heart disease. *J Clin. Invest* **117**:568-575.
149. Molkenin,J.D., Lu,J.R., Antos,C.L., Markham,B., Richardson,J., Robbins,J., Grant,S.R., and Olson,E.N. 1998. A calcineurin-dependent transcriptional pathway for cardiac hypertrophy. *Cell* **93**:215-228.
150. Braz,J.C., Bueno,O.F., Liang,Q., Wilkins,B.J., Dai,Y.S., Parsons,S., Braunwart,J., Glascock,B.J., Klevitsky,R., Kimball,T.F. et al 2003. Targeted inhibition of p38 MAPK promotes hypertrophic cardiomyopathy through upregulation of calcineurin-NFAT signaling. *J Clin. Invest* **111**:1475-1486.
151. Lorenz,K., Schmitt,J.P., Schmitteckert,E.M., and Lohse,M.J. 2009. A new type of ERK1/2 autophosphorylation causes cardiac hypertrophy. *Nat Med* **15**:75-83.
152. Harris,T.E., and Lawrence,J.C., Jr. 2003. TOR signaling. *Sci. STKE.* **2003**:re15.
153. McMullen,J.R., Sherwood,M.C., Tarnavski,O., Zhang,L., Dorfman,A.L., Shioi,T., and Izumo,S. 2004. Inhibition of mTOR signaling with rapamycin regresses established cardiac hypertrophy induced by pressure overload. *Circulation* **109**:3050-3055.
154. Ross,R.S., and Borg,T.K. 2001. Integrins and the myocardium. *Circ. Res.* **88**:1112-1119.
155. Knoll,R., Hoshijima,M., Hoffman,H.M., Person,V., Lorenzen-Schmidt,I., Bang,M.L., Hayashi,T., Shiga,N., Yasukawa,H., Schaper,W. et al 2002. The cardiac mechanical stretch sensor machinery involves a Z disc complex that is defective in a subset of human dilated cardiomyopathy. *Cell* **111**:943-955.
156. Jacobson,M.D., Weil,M., and Raff,M.C. 1997. Programmed cell death in animal development. *Cell* **88**:347-354.
157. Nijhawan,D., Honarpour,N., and Wang,X. 2000. Apoptosis in neural development and disease. *Annu. Rev. Neurosci.* **23**:73-87.
158. Lowe,S.W., and Lin,A.W. 2000. Apoptosis in cancer. *Carcinogenesis* **21**:485-495.
159. Opferman,J.T., and Korsmeyer,S.J. 2003. Apoptosis in the development and maintenance of the immune system. *Nat. Immunol.* **4**:410-415.
160. Opferman,J.T., Letai,A., Beard,C., Sorcinelli,M.D., Ong,C.C., and Korsmeyer,S.J. 2003. Development and maintenance of B and T lymphocytes requires antiapoptotic MCL-1. *Nature* **426**:671-676.

Introduction

161. Friedlander, R.M. 2003. Apoptosis and caspases in neurodegenerative diseases. *N. Engl. J Med.* **348**:1365-1375.

2. Objectives

Objectives

This PhD thesis was dedicated to study and characterize the molecular mechanisms that underlie the anti-apoptotic properties of RasGAP-derived fragment N both *in vitro* and *in vivo* mouse models. This work is divided into two main objectives. The first objective is addressed in parts I, II, and III, in which the results are described to validate the role of fragment N in protecting stressed organs such as heart, colon and skin. The second objective aims to understand the molecular pathways and cellular processes that may be regulated by fragment N including the inhibition of NF- κ B

Part I

This part summarizes the results showing the role of RasGAP cleavage and the generation of fragment N in protecting stressed skin, colon and heart. We show in caspase-3 knock-out mice and RasGAP D455A Knock-In mice, that the absence of fragment N leads to inability to activate Akt in response to stress, increased apoptosis, tissue damage, and organ dysfunction.

Part II

In this part we monitor the pattern of RasGAP cleavage in cardiomyocytes treated with peroxynitrite (PN), a potent nitrating and oxidizing agent generated during various pathological situations affecting the heart. A caspase-resistant form of fragment N efficiently protected cardiomyocytes against PN-induced cell death.

Part III (unpublished data)

We tested in an *in vivo* model the role of RasGAP and fragment N generation in protecting the heart suffering pressure overload induced by transverse aortic arch banding (TAC). The absence of fragment N in RasGAP D455A KI mice leads to a decline in the cardiac output and exacerbated myocardial cell death and fibrosis.

Part IV (unpublished data)

We assessed the cellular mechanisms by which fragment N blocks the activation of NF- κ B. The inhibitory activity of fragment N relies on the promotion of NF- κ B nuclear export and therefore, reduction of NF- κ B nuclear accumulation.

Part V

This chapter was dedicated to identify the binding partners of fragment N, Immunoprecipitation and mass spectrometry analysis showed few putative binding partners of fragment N. We validated the interaction between fragment N and the adaptor protein ShB (SH2-protein of β -cells), which operates downstream of several tyrosine kinase receptors.

3. Results: Part I

1. Introduction

RasGAP acts as a molecular sensor of caspase-3 activity within the cells due to its sequential cleavage. The first cleavage of RasGAP by low active caspase-3 generates N-terminal fragment (fragment N), which induces a potent anti-apoptotic response that relies on the activation of the prosurvival kinase Akt. Increased stress induces higher levels of active-caspase-3 which cleaves fragment N, this abrogates the protective signal and the cell eventually dies by apoptosis. The overexpression of a caspase-resistant form of fragment N *in vitro* protects various cell types against different stress stimuli (1-3). Moreover, in a transgenic mouse model, the expression of fragment N in pancreatic β -cell efficiently protected β -cell and increased their resistance to apoptosis inducing stimuli, without interfering with the physiological functions of the cells such as insulin secretion(4).

2. Results

We assessed the physiological role of RasGAP cleavage in relation to Akt activation. We investigated whether Akt is activated in mice lacking caspase-3 or unable to cleave RasGAP exposed to diverse pathophysiological insults in skin, colon and heart. We found that, the absence of RasGAP cleavage was correlated with greater organ dysfunction and increased apoptosis. This effect was due to the inability of those mice to activate the anti-apoptotic response mediated by Akt activation.

3. Contribution

This work has been published in the journal of Molecular and Cellular Biology (MCB). Experiments on the heart and colon, including animal breeding and treatment were done by me. Hemodynamic measurements have been performed together with Lucas Liaudet. Additionally, I carried out the biochemical analysis (Western blots, TUNEL assays) and quantifications of phosphorylated Akt in the heart. I also contributed to the writing and revising of the manuscript in collaboration with Christian Widmann.

Reference List

1. Yang,J.-Y., and Widmann,C. 2001. Antiapoptotic signaling generated by caspase-induced cleavage of RasGAP. *MCB* 21:5346-5358.
2. Yang,J.-Y., Michod,D., Walicki,J., Murphy,B.M., Kasibhatla,S., Martin,S., and Widmann,C. 2004. Partial cleavage of RasGAP by caspases is required for cell survival in mild stress conditions. *Mol. Cell Biol.* 24:10425-10436.
3. Yang,J.-Y., and Widmann,C. 2002. The RasGAP N-terminal fragment generated by caspase cleavage protects cells in a Ras/PI3K/Akt-dependent manner that does not rely on NFκB activation. *JBC* 277:14641-14646.
4. Yang,J.Y., Walicki,J., Jaccard,E., Dubuis,G., Bulat,N., Hornung,J.P., Thorens,B., and Widmann,C. 2009. Expression of the NH(2)-terminal fragment of RasGAP in pancreatic beta-cells increases their resistance to stresses and protects mice from diabetes. *Diabetes* 58:2596-2606.

Caspase-3 Protects Stressed Organs against Cell Death

Hadi Khalil, Nieves Peltzer, Joël Walicki, Jiang-Yan Yang, Gilles Dubuis, Noémie Gardiol, Werner Held, Paul Bigliardi, Benjamin Marsland, Lucas Liaudet and Christian Widmann
Mol. Cell. Biol. 2012, 32(22):4523. DOI: 10.1128/MCB.00774-12.
Published Ahead of Print 4 September 2012.

Updated information and services can be found at:
<http://mcb.asm.org/content/32/22/4523>

SUPPLEMENTAL MATERIAL

These include:
[Supplemental material](#)

REFERENCES

This article cites 51 articles, 24 of which can be accessed free at: <http://mcb.asm.org/content/32/22/4523#ref-list-1>

CONTENT ALERTS

Receive: RSS Feeds, eTOCs, free email alerts (when new articles cite this article), [more»](#)

Information about commercial reprint orders: <http://journals.asm.org/site/misc/reprints.xhtml>
To subscribe to to another ASM Journal go to: <http://journals.asm.org/site/subscriptions/>

Journals.ASM.org

Caspase-3 Protects Stressed Organs against Cell Death

Hadi Khalil,^a Nieves Peltzer,^a Joël Walicki,^a Jiang-Yan Yang,^a Gilles Dubuis,^a Noémie Gardiol,^b Werner Held,^b Paul Bigliardi,^{c*} Benjamin Marsland,^d Lucas Liaudet,^e and Christian Widmann^a

Department of Physiology^a and Ludwig Center for Cancer Research of the University of Lausanne,^b Faculty of Biology and Medicine, University of Lausanne, Lausanne, Switzerland, and Department of Dermatology,^c Department of Pneumology,^d and Department of Intensive Care Medicine,^e Centre Hospitalier Universitaire Vaudois and University of Lausanne, Lausanne, Switzerland

The ability to generate appropriate defense responses is crucial for the survival of an organism exposed to pathogenesis-inducing insults. However, the mechanisms that allow tissues and organs to cope with such stresses are poorly understood. Here we show that caspase-3-knockout mice or caspase inhibitor-treated mice were defective in activating the antiapoptotic Akt kinase in response to various chemical and environmental stresses causing sunburns, cardiomyopathy, or colitis. Defective Akt activation in caspase-3-knockout mice was accompanied by increased cell death and impaired survival in some cases. Mice homozygous for a mutation in RasGAP that prevents its cleavage by caspase-3 exhibited a similar defect in Akt activation, leading to increased apoptosis in stressed organs, marked deterioration of their physiological functions, and stronger disease development. Our results provide evidence for the relevance of caspase-3 as a stress intensity sensor that controls cell fate by either initiating a RasGAP cleavage-dependent cell resistance program or a cell suicide response.

Executioner caspases mediate cell death during apoptosis (45). Of these, caspase-3 has the ability to cleave the majority of the caspase substrates (43), and its activity is required for the induction of cell death in response to many apoptotic stimuli (1). While executioner caspases are indispensable for apoptosis, there are situations when their activation does not lead to death. For example, healthy dividing cells can weakly activate caspase-3 in response to mild stresses (47). Caspase-3 also participates, in an apoptosis-independent manner, in T and B cell homeostasis (35, 46), in microglia activation (6), in long-term depression (26), and in muscle (17), monocyte (44), embryonic stem cell (18), and erythroid cell (13) differentiation. However, it remains unclear how activation of caspase-3 under these conditions does not eventually lead to cell death (1, 24). Cells could have an intrinsic ability to tolerate low caspase activity by constitutively expressing antiapoptotic molecules, such as members of the inhibitors of the apoptosis protein family, or may stimulate antiapoptotic pathways in parallel to caspase activation (24). Alternatively, the caspases themselves might activate prosurvival pathways, in particular, when they are mildly stimulated. Indeed, there is evidence in cultured cells that caspase-3 mediates neuroprotection after preconditioning (30) and that caspase-3 activity turns on the antiapoptotic Akt kinase following partial cleavage of the RasGAP protein (47). Other caspase substrates that could potentially induce protective signals once cleaved include p27^{kip1} (14), Lyn (28), synphilin-1 (19), and Rb (42), yet the physiological importance of these cleaved substrates has not been evaluated to date.

In the present study, we have investigated the role played by caspase-3 and its substrate p120 RasGAP in the induction of the antiapoptotic Akt kinase in stressed tissues *in vivo*.

MATERIALS AND METHODS

Caspase-3-KO mice. B6.129S1-*Casp3*^{tm1Flv/J} caspase-3-knockout (KO) mice were purchased from the Jackson Laboratory (Bar Harbor, ME). The mice were genotyped using a mixture of the following three oligonucleotides: wild-type sense (GCG AGT GAG AAT GTG CAT AAA TTC), wild-type antisense (GGG AAA CCA ACA GTA GTC AGT CCT), and caspase-3-knockout antisense (TGC TAA AGC GCA TGC TCC AGA CTG). The

sizes of the amplified fragments are 320 bp for the wild-type allele and 300 bp for the caspase-3-knockout allele.

Generation of RasGAP D455A-knock-in (KI) mice. The strategy and methods used to create the targeting vector are presented in Fig. S1 in the supplemental material.

UV-B exposure and isolation of skin samples. Mice were shaved on both flanks, followed by depilation with depilatory cream (Veet), and 48 h later were anesthetized and illuminated with a Waldmann UV801 KL apparatus equipped with a Philips UV21 UV-B lamp (TL 20W/12RS). The doses of UV-B illumination were 0.05 and 0.3 J/cm² (i.e., 50 mJ/cm² and 300 mJ/cm², respectively), which were measured with a Waldmann Variocontrol dosimeter. In each case, only one side of the mouse was illuminated and the other side was used as a control (i.e., nonexposed skin). Mice were sacrificed 24 h after illumination. The lateral skin biopsy specimens (approximately 2 by 2 cm) were excised from each mouse, fixed in phosphate-buffered saline (PBS) and 4% Formol solution, and embedded in paraffin. The paraffin-embedded skin was cut into 4- μ m sections, deparaffinized, and stained with hematoxylin-eosin for histological observation.

Doxorubicin injection and hemodynamic measurements using left ventricular PV microcatheters. Eight-week-old mice were weighed and injected with a single intraperitoneal doxorubicin dose of 20 mg/kg of body weight using a 2-mg/ml doxorubicin solution (catalog number 733857-01; EBEWE Pharma) or injected with an equal volume of saline (catalog number 534534; B. Braun Medical AG). At 5 days postinjection, the animals were weighed again (the weight loss at that time was between 10 and 15%). The animals were anesthetized with an intraperitoneal in-

Received 8 June 2012 Returned for modification 9 July 2012

Accepted 29 August 2012

Published ahead of print 4 September 2012

Address correspondence to Christian Widmann, Christian.Widmann@unil.ch.

* Present address: Paul Bigliardi, NUHS/NUS and IMB/A*STAR, Singapore, Singapore.

H.K. and N.P. contributed equally to this article.

Supplemental material for this article may be found at <http://mcb.asm.org/>.

Copyright © 2012, American Society for Microbiology. All Rights Reserved.

doi:10.1128/MCB.00774-12

jection of 75 mg/kg ketamine and 10 mg/kg xylazine (the volume of injection was 10 μ l per g of mouse). A pressure-volume (PV) SPR-839 catheter (Millar Instruments, Houston, TX) was inserted into the left ventricle (LV) via the right carotid artery. After stabilization for 20 min, heart rate, LV systolic and end-diastolic pressures, and volumes were measured, and stroke volume, ejection fraction, and cardiac output were calculated and corrected according to *in vitro* and *in vivo* volume calibrations with a cardiac PV analysis program (PVAN3.2; Millar Instruments) (38, 39). End-systolic LV PV relationships were assessed by transiently reducing venous return by compressing the inferior vena cava, and LV contractility was assessed from the slope of the LV end-systolic PV relationship (end-systolic elastance), calculated using PVAN3.2, as detailed previously (21, 38). Hearts were isolated, cut into two pieces, and then either snap-frozen or fixed in 4% formalin for histology studies.

DSS-induced colitis and clinical score. Eight-week-old mice were given acidified water supplemented with 5% (wt/vol) dextran sodium sulfate (DSS; molecular weight, 400,000 to 600,000; MP Biomedicals, Illkirch, France) for 72 h and then given normal drinking water for four additional days. Mice were examined daily, and body weight, water consumption, occult blood, and diarrhea were measured. At day 7, mice were sacrificed, the colon length was measured, and a clinical score was estimated according to the procedure described by Ohkawara et al. (36). Percentage of weight loss was calculated by comparing the weight at day 0 and the weight of the mice at sacrifice. Scores were given according to the extent of weight loss: 0, no weight loss; 1, 1 to 5%; 2, 5 to 10%; 3, 10 to 15%; 4, >15%. Diarrhea was scored using a scale with values ranging from 0 to 4: 0, normal; 1, slightly loose feces; 2, loose feces; 3, semi-liquid stool; and 4, liquid stool. Fecal occult blood was detected using guaiac paper (ColoScreen Hemocult kit; Helena Labs, Beaumont, TX), and the associated scores were as follows: 0, none; 2, positive Hemocult result; and 4, gross bleeding. Colons were cut into three equal portions (proximal, middle, and distal), and each portion was further cut into three equal parts, two of which were snap-frozen in liquid N₂ and stored at -80°C for subsequent protein and RNA analysis, and the third portion was fixed in 4% formalin for histology analysis (paraffin sections).

Quantitation of active Akt- and active caspase-3-positive cells in heart, skin, and colon. Sections stained as described in the previous sections were scanned using an automated Nikon Eclipse 90i microscope equipped with Apo Plan $\times 20$ (0.75 pH 2 PM) and Apo Plan $\times 40/1.0$ DIC-H objectives and piloted with NIS-Elements Advance Research software (Nikon Instruments Inc., Melville, NY).

Three whole-heart sections were scanned at different levels, and the corresponding whole-section images were generated. The number of pAkt-positive cells was scored manually by counting the number of cells stained with the anti-phospho-Akt antibody (the samples were randomized prior to examination, and the person performing the counting was not aware of the experimental conditions). The total number of cells was determined by automatically scoring the number of nuclei (stained with the Hoechst 33342 dye) using the NIS-Elements AR program (Nikon). In order to minimize errors, all images were acquired with the same contrast (high), size and quality (1280 \times 960 pixels), exposure time (4', 6-diamidino-2-phenylindole [DAPI], 40 ms; fluorescein isothiocyanate [FITC], 300 ms), and gain (1 \times). The quantification threshold in the automated measurement menu was set at L32 for low and H236 for high, and the area was restricted to 0 to 0.5 μ m² out. In the image menu, the local contrast was set to 30, and in the image-background option, the background was set to 40 for DAPI and to 999 for FITC. Using the binary menu, the holes were filled using the fill holes option. This was performed to avoid multiple counting of the same nucleus. Touching nuclei were separated using the morpho separate objects option. The number of nuclei was displayed under automated measurement results—object data. Skin sections were scanned and analyzed similarly. Fifteen different fields were randomly taken from the proximal, middle, and distal sections of the colon and processed and analyzed as described above.

Apoptosis scoring. Apoptosis on histological slides was assessed by terminal deoxynucleotidyltransferase-mediated dUTP-biotin nick end labeling (TUNEL) assay (DeadEnd Fluorometric TUNEL system; catalog number G3250; Promega Switzerland), as per the manufacturer's protocol, and quantitated as described for the Akt staining in the previous section. Apoptosis *in vitro* counting was assessed by scoring the number of cells with pycnotic or fragmented nuclei after Hoechst 33342 staining (48).

Chemicals and antibodies. The quinolyl-valyl-O-methylaspartyl-[2,6-difluorophenoxy]-methyl ketone (Q-VD-OPh) caspase inhibitor was from MP Biomedicals (catalog number OPH109). Hexameric FasL (fusion protein between the Fas ligand and the Fc portion of IgG1) (20) was a kind gift from Pascal Schneider (University of Lausanne). The monoclonal and polyclonal anti-phospho-Ser473 Akt antibodies and the cleaved caspase-3-specific antibody were from Cell Signaling Technology (catalog numbers 4051, 9271, and 9664, respectively). The monoclonal anti-phospho-Ser⁴⁷³ Akt antibody was used on skin and colon sections as well as for Western blot assays, while the polyclonal anti-phospho-Ser⁴⁷³ Akt antibody was used on heart sections. The antibody recognizing total Akt was from Santa Cruz (catalog number sc-8312). The anti-RasGAP antibody was from Enzo Life Science (catalog number ALX-210-860-R100). Secondary antibodies (Cy3-coupled donkey anti-rabbit, horseradish peroxidase [HRP]-coupled donkey anti-rabbit, and HRP-coupled donkey anti-mouse antibodies) were from Jackson ImmunoResearch (catalog numbers 711-165-152, 715-035-152, and 715-035-150, respectively).

Protein extraction. Snap-frozen skin (0.3-cm² biopsy specimens), heart, and intestine tissue samples were crushed into powder in liquid nitrogen-dipped mortar and pestle and then suspended in 700 μ l lysis buffer (Tris-HCl, 50 mM; EDTA, 1 mM; EGTA, 1 mM; Triton X-100, 1%; dithiothreitol, 1 mM; sodium pyrophosphate, 5 mM; NaF, 50 mM; protease inhibitor cocktail tablet [1 tablet/40 ml buffer; catalog number 04 693 132 001; Roche]; phenylmethylsulfonyl fluoride, 1 mM; glycerol, 10%; pH 7.4). The samples were sonicated (amplitude, 80%; 5 s; twice). Protein concentration was measured by the Bradford assay using bovine serum albumin (BSA) as a standard. Lysates were mixed with an equal volume of 2 \times sample buffer (100 mM Tris-HCl [pH 6.8], 20% glycerol, 10% [vol/vol] β -mercaptoethanol, 4% [wt/vol] sodium dodecyl sulfate [SDS], and 0.02% bromophenol blue) and boiled for 5 min at 95°C before loading on SDS-polyacrylamide gels.

Western blotting. Western blotting was performed and quantitated as described previously (31).

Preparation of tissue section and immunohistochemistry. Mice were euthanized by cervical dislocation. The isolated organs (heart, skin, or intestine) were stored in PBS-4% Formol solution and embedded in paraffin. Four-micrometer sections were deparaffinized in toluene (catalog number 488555; Carlo Erba, Milan, Italy) and rehydrated using graded alcohol and distilled water. Antigen retrieval was performed by immersing sections in sodium citrate buffer (10 mM sodium citrate, pH 6), followed by heating in a microwave oven for 20 min (8 min at 800 W and 12 min at 400 W). Sections were cooled to room temperature and blocked using a 50 mM Tris-HCl, pH 7.6, 0.5% Tween 20, 0.2% BSA solution. The primary antibody was diluted (pAkt, 1/100; cleaved caspase-3, 1/200) in 50 mM Tris-HCl, pH 7.6, 0.5% Tween 20, 0.2% BSA and incubated with the slides for 1 h. Slides were washed 2 times for 10 min each time in 50 mM Tris-HCl, pH 7.6, 0.5% Tween 20. The fluorochrome-conjugated secondary antibody (Jackson Laboratory), diluted 1:300 in 50 mM Tris-HCl, pH 7.6, 0.5% Tween 20, 0.2% BSA, was incubated with the slides for another hour in the dark. Slides were then extensively washed (at least 6 times with one overnight washing step). The nuclei in the sections were then stained with 10 μ g/ml Hoechst 33342. Finally, the slides were mounted in Mowiol (catalogue number 81381; Fluka) at a concentration of 0.1 mg/ml in a solution made of 20% glycerol and 0.1% DABCO (diazobicyclo-octane; catalogue number 33480; Fluka).

Immunohistochemistry with tyramide signal amplification. Tyramide amplification of immunohistochemical signals using phospho-Akt-

specific antibodies was performed as described earlier (4). The primary antibody and the secondary HRP-coupled antibody were diluted 1/100 and 1/1,000, respectively.

Ethics statement. Experiments on the mice were carried out in strict accordance with the Swiss Animal Protection Ordinance (OPAn). The protocol was approved by the Veterinary Office of the state of Vaud, Switzerland (permit numbers 2055, 2056, and 2361).

MEF preparation. Mouse embryonic fibroblasts (MEFs) from KI and wild-type mice were initially prepared as described earlier by digesting embryonic day 14 embryos for 1.5 h in 0.05% trypsin (5). Using this protocol, MEFs could be generated from wild-type embryos, but none were obtained from the KI embryos (Fig. 5C). Reducing the incubation time in trypsin to 15 min, which presumably lessened a stressful situation on cells, however, allowed production of both wild-type and KI MEFs in more or less similar numbers (Fig. 5C).

Statistics. SAS/STAT (version 9.1) software (SAS Institute Inc., Cary, NC) was used to perform the statistical analyses. Unless otherwise stated, one-way analyses of variance were performed to determine the significance of the observed differences presented in the figures. Asterisks and NS in the figures indicate significant differences ($P < 0.05$) and no significant differences, respectively.

RESULTS

Mice lacking caspase-3 are impaired in their capacity to activate Akt in response to stress. Akt (also called PKB) is a downstream effector of phosphatidylinositol 3-kinase (PI3K) that mediates the survival responses of many cell types and tissues (40) and as such could be involved in stress survival responses across most, if not all, tissues. To determine whether Akt is activated in various tissues and organs in response to pathology-inducing stresses, mice were exposed to three different challenges: exposure of the skin to UV-B, injection of doxorubicin (an anticancer drug inducing cardiomyopathy), and administration of dextran sodium sulfate (DSS) via drinking water to induce colitis. In control skin, very few keratinocytes ($\sim 0.25\%$) expressed the active phosphorylated form of Akt (Fig. 1A). In response to mild UV-B exposure (0.05 J/cm^2), more than 10% of the keratinocytes had active Akt in their cytoplasm (Fig. 1A). In the hearts of untreated mice, cells expressing activated Akt were readily observed. Virtually all of these cells were cardiomyocytes, as determined by their shape and nucleus location (Fig. 1B). Under basal conditions (i.e., no treatment), the percentage of cells with active Akt was much higher in the heart ($\sim 6\%$) than in the epidermis. Doxorubicin increased the percentage of Akt-positive cardiomyocytes in a statistically significant manner to $\sim 10\%$ (Fig. 1B, gray bars). Akin to the situation encountered in the skin, very few cells in the colon epithelium ($\sim 0.7\%$) were found to be positive for active Akt (Fig. 1C). This percentage significantly increased to $\sim 1.2\%$ when colitis was induced by DSS (Fig. 1C, gray bars).

To determine whether Akt activation was dependent on caspase-3, we analyzed caspase-3-KO mice on the C57BL6 background. In this background, caspase-3-KO mice reach adulthood and breed (25). When the skin of these mice was exposed to UV-B, the number of keratinocytes with active Akt increased (Fig. 1A, lower right), suggesting that a caspase-3-independent mechanism can participate in the induction of protective signals in the epidermis. However, the UV-B-induced increase in the percentage of active Akt-positive keratinocytes in caspase-3-KO mice was much reduced compared to the situation observed in wild-type mice, and the increase was not statistically significant (Fig. 1A, black bars). This indicates that caspase-3 is required for a maximal Akt response in keratinocytes subjected to UV-B illumination. When

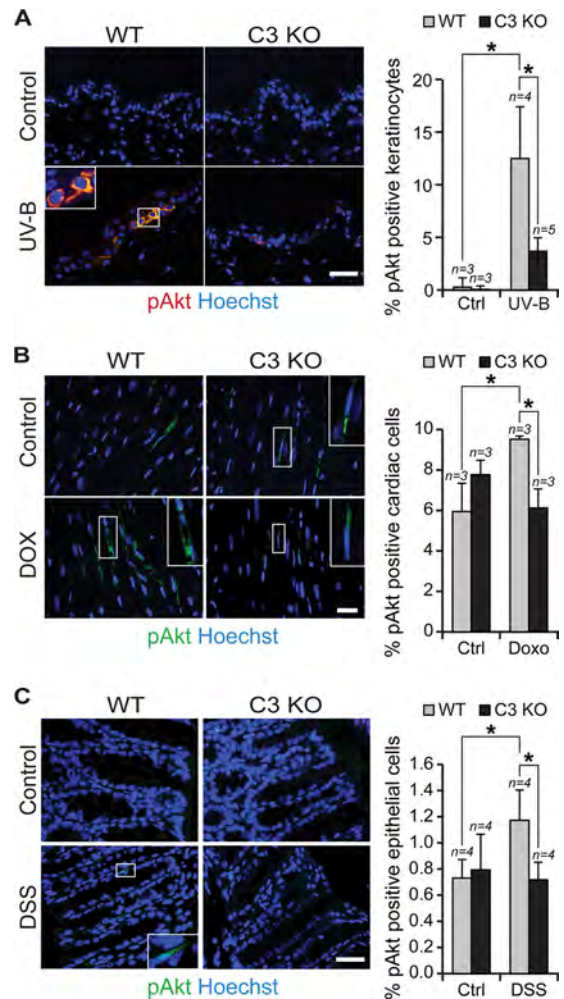


FIG 1 Defective stress-induced Akt activation in mice lacking caspase-3. The indicated numbers of wild-type (WT) and caspase-3-knockout (C3 KO) mice were subjected or not subjected to illumination of their skin with 0.05 J/cm^2 UV-B (A; 2 independent experiments), injection of 20 mg/kg doxorubicin (DOX or Doxo) (B; 2 independent experiments), or exposure to 5% DSS in the drinking water (C; 3 independent experiments) (see Materials and Methods for details). (A to C) Histological sections of the organs and tissues targeted by these stresses were then stained with an antibody recognizing the active phosphorylated form of Akt, and the percentage of phospho-Akt (pAkt)-positive cells was quantitated. Results correspond to the mean \pm 95% CI. The images shown are representative examples of sections labeled with the anti-phospho-Akt antibody (red or green staining) and with Hoechst 33342 (blue staining of the nuclei). Bars, 20 μm .

caspase-3-KO mice were treated with doxorubicin or DSS, the percentage of cells with active Akt in the targeted organs did not change compared to the nonchallenged situation (compare the gray and black bars in Fig. 1B and C), indicating that caspase-3 is strictly required for Akt activation in these tissues exposed to stress. To determine if stimulation of caspase-3 activity and not some other noncatalytic functions of the protease is necessary for stress-induced Akt activation, wild-type mice were injected with Q-VD-OPH, a broad-spectrum caspase inhibitor (10). Figures 2A and B show that this compound inhibited UV-B-induced caspase-3 activation in the skin. Q-VD-OPH was found to significantly decrease the ability of epidermal cells to stimulate Akt in response to UV-B (Fig. 2C), indicating that activation of caspases

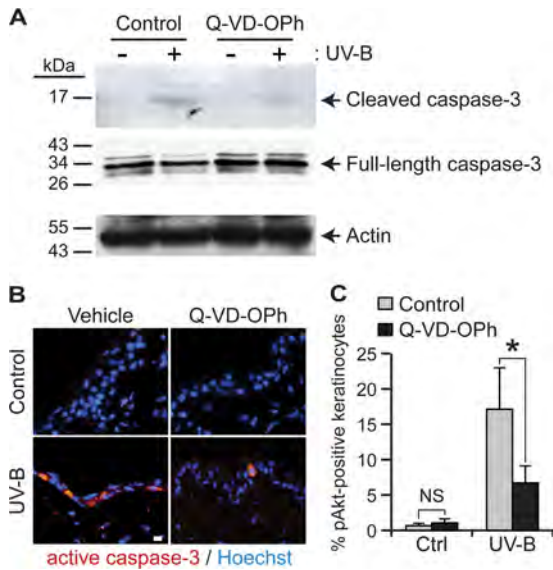


FIG 2 Pharmacological inhibition of caspases hampers UV-B-induced Akt activation in the epidermis. Wild-type mice were injected or not with 50 mg of the Q-VD-OPh caspase inhibitor per kg of mouse 15 min prior to UV-B exposure of the skin (0.3 J/cm^2 [A and B] and 0.05 J/cm^2 [C]). (A) Levels of cleaved active caspase-3, full-length inactive caspase-3, and actin were assessed by Western blotting. This experiment was repeated once with similar results. (B) Levels of active caspase-3 *in situ* were also visualized by immunofluorescence. Bar, $20 \mu\text{m}$. The pictures are representative images of data obtained with three mice per condition. (C) Levels of phosphorylated Akt were assessed as described in Fig. 1. Results correspond to the mean \pm 95% CI of 3 independent experiments ($n = 3$).

is required for the induction of the antiapoptotic Akt kinase in response to stress.

Increased stress-induced cell death and cell damage in mice lacking caspase-3. Impaired Akt activation in caspase-3-knockout mice may not lead to visible damage of the targeted tissues if the absence of caspase-3 prevents implementation of a cell death response. There are indeed situations where caspase-3 is mandatory for cell death. For example, beta cells from caspase-3-KO mice are fully resistant against streptozotocin-induced death, while beta cells from wild-type mice are not, leading to the development of diabetes (27). In other situations, cell death may still occur in the absence of caspase-3, either as a result of a nonapoptotic type of death or because apoptosis is mediated by other executioner caspases (e.g., caspase-7). In such cases, the absence of a caspase-3-mediated Akt activation might have detrimental consequences. To assess this point, we monitored the extent of stress-induced cell death in the skin and the heart of caspase-3-KO and wild-type mice.

In the skin of wild-type mice, UV-B induced the appearance of keratinocytes with a pycnotic nucleus and densely staining glassy cytoplasm—the so-called sunburn cells (see the inset in the lower left-hand panel in Fig. 3A)—which are apoptotic cells characteristic of those in damaged skin following UV exposure (12). The percentage of sunburn cells generated by UV-B in the skin of caspase-3-KO mice was significantly reduced compared to that in the skin of wild-type mice (Fig. 3A). Similarly, there were fewer TUNEL-positive keratinocytes in the UV-B-illuminated skin of caspase-3-KO mice than in the skin of wild-type mice (Fig. 3B). This indicates that caspase-3 is a main mediator of UV-B-induced

keratinocyte apoptosis. Cells can also die in a necrosis-like, nonapoptotic manner, in particular, when apoptosis pathways are altered (41). Keratinocytes dying in this way are characterized by their irregular shape, an eosinophilic cytoplasm, and hyperchromatic, condensed, and partly fragmented nuclei (3) (see the inset in the lower right-hand panel in Fig. 3A). UV-B dramatically increased the percentage of keratinocytes undergoing this type of death in the skin of caspase-3-KO mice compared to the skin of wild-type mice (Fig. 3A). When accounting for both apoptosis and necrosis-like deaths, there was more UV-B-mediated death recorded in the skin of caspase-3-KO mice than in the skin of wild-type mice ($8.1\% \pm 2.5\%$ versus $4.9\% \pm 1.2\%$; mean \pm 95% confidence interval [CI]).

Doxorubicin is a DNA-intercalating drug that induces both caspase-dependent and -independent cell death in various cell types (29), including cardiomyocytes (51). In response to doxorubicin injection, the percentage of cardiomyocytes undergoing apoptosis, as assessed with the TUNEL assay (see a representative example on the left-hand side of Fig. 3C), was significantly higher in caspase-3-KO mice than wild-type mice (Fig. 3C). It therefore appears that apoptosis induced by doxorubicin can be mediated by executioner caspases other than caspase-3, which is consistent with the observation that doxorubicin efficiently activates caspase-7 (11).

The increased susceptibility of caspase-3-KO mice to doxorubicin-induced cardiomyocyte apoptosis raised the possibility that the lack of caspase-3 affects survival of mice treated with doxorubicin. Figure 3D shows that caspase-3-KO mice survived doxorubicin treatment less efficiently than wild-type mice. This suggests that caspase-3 mediates a protective response in doxorubicin-treated animals that is required to counteract tissue damage induced in a caspase-3-independent manner.

In conclusion, the results presented in Fig. 1 to 3 show that, upon stress exposure, mice lacking caspase-3 are defective in the activation of the prosurvival Akt kinase and that this correlates with increased cell death, tissue damage, and even death of the animals.

Generation of mice expressing a caspase-3-resistant RasGAP mutant. *In vitro*, low caspase-3 activity leads to the cleavage of the p120 RasGAP protein into an amino-terminal fragment, called fragment N, that stimulates Akt in a Ras/PI3K-dependent manner (47, 50), preventing further caspase-3 activation and apoptosis (47). In the presence of high caspase-3 activity, fragment N is further cleaved into two additional fragments (fragments N1 and N2) that are unable to activate Akt (48). Notably, this second cleavage event does not take place if the first cleavage is prevented (49). Further, in the absence of caspase-3 in cells, other executioner caspases, such as caspase-6 and caspase-7, cannot cleave RasGAP (47). RasGAP is therefore a specific caspase-3 substrate. To assess the role of fragment N in Akt stimulation in stressed organs, we generated a KI mouse in which the first RasGAP cleavage site recognized by caspase-3 was destroyed by an aspartate-to-alanine substitution at position 455 (DTVA[455]G) (Fig. 4A and B); the construction of the targeting vector is shown in Fig. S1 in the supplemental material, and genetic analyses of the resulting mice are shown in Fig. 4B and C. This mutation does not affect the function of full-length RasGAP (47). Mice homozygous for the RasGAP^{D455A} allele (KI mice) are viable and fertile, grow normally (Fig. 4D), and show no obvious morphological alterations (Fig. 4E), histologic defects (data not shown), or hematologic abnor-

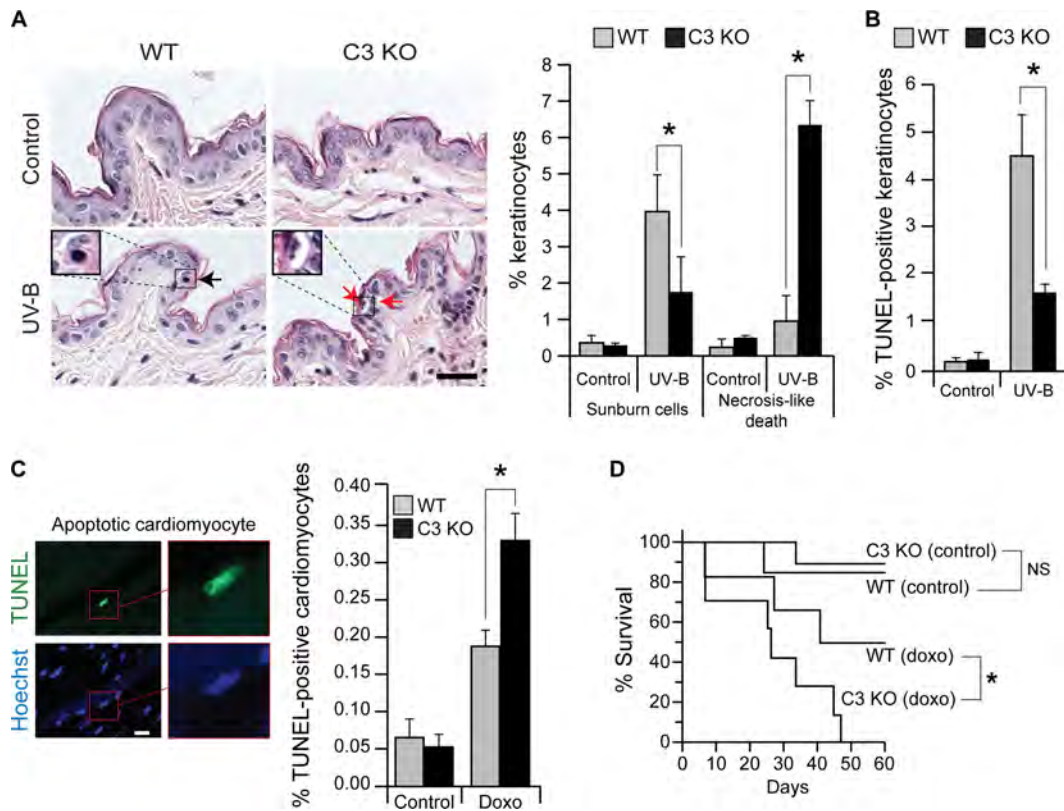


FIG 3 Increased stress-induced cell death and cell damage in mice lacking caspase-3. (A) Histological assessment of sunburn (black arrow) and necrotic-like (red arrows) cells in the epidermis (left and middle) of UV-B (0.05 J/cm^2)-irradiated mouse skin. Results correspond to the mean \pm 95% CI of measurements performed on 3 and 8 control and irradiated animals, respectively. Bar, $20 \mu\text{m}$. (B) Quantitation of TUNEL-positive keratinocytes following UV-B (0.05 J/cm^2) irradiation. Results correspond to the mean \pm 95% CI (3 animals per condition). (C) Apoptosis assessment by the TUNEL assay in cardiomyocytes from mice injected with 20 mg/kg doxorubicin 5 days earlier. A representative example of an apoptotic cardiomyocyte is shown on the left. Bar, $10 \mu\text{m}$. Results correspond to the mean \pm 95% CI (3 animals per condition). (D) Survival curves of 6 wild-type and 7 caspase-3-KO mice injected with 20 mg/kg doxorubicin (8 wild-type and 11 caspase-3-KO mice were used in the control noninjected groups). A Wilcoxon test of equality over strata (life-test procedure) was used to assess the significance of the observed difference.

malities (see Table S1 in the supplemental material). Expression of RasGAP, caspase-3, Akt, and actin was similar in given tissues and cells derived from wild-type and KI mice (Fig. 4F). The transmission of the mutated alleles occurred with normal Mendelian ratios (among 317 offspring obtained from breeding heterozygote +/D455A mice, 22.4% were +/+, 54.3% were +/D455A, and 23.7% were D455A/D455A).

As expected, fibroblasts derived from KI embryos were unable to cleave RasGAP in response to various apoptotic stimuli (Fig. 5A) and were more prone to apoptosis in response to these stimuli than control MEFs (Fig. 5B). Additionally, in contrast to what was observed with wild-type embryos, cells from KI embryos did not survive long-term trypsin digestion (Fig. 5C). MEFs from KI embryos were also impaired in their capacity to activate Akt in response to stress (Fig. 5D). The increased susceptibility of KI cells to death in response to stresses is consistent with the known ability of fragment N to stimulate Akt and inhibit apoptosis in cultured cell lines (47, 49, 50).

Mice that cannot cleave RasGAP at position 455 are unable to activate Akt in response to stress, and they experience increased apoptosis, tissue damage, and organ dysfunction. The KI mice were then used to assess the importance of RasGAP cleavage in Akt activation and in the protection of tissues and organs upon expo-

sure to the pathophysiological challenges described for Fig. 1. In response to low UV-B exposure (0.05 J/cm^2), Akt was activated in about 10% of keratinocytes of wild-type mice (Fig. 6A). Akt activation was, however, not observed when the skin was exposed to higher UV-B doses (0.3 J/cm^2) (Fig. 6A) that led to strong caspase-3 activation (Fig. 6B). It is known that low caspase-3 activity leads to fragment N generation, while high caspase-3 activity induces fragment N cleavage into fragments that are no longer able to activate Akt (48). In skin samples, all the RasGAP antibodies that we have tested lit up bands in the 35- to 55-kDa range, precluding visualization of fragment N (52 kDa) (Fig. 6C). These bands may be nonspecifically recognized by the RasGAP antibodies, but it is more likely that they correspond to RasGAP degradation products that are generated in keratinocytes en route to their final differentiation stage in the cornified layer, a process that is known to be associated with massive activation of epidermal proteases (8). Fragment N2, one of the caspase-3-generated products of fragment N (49), was, however, seen in samples derived from skin exposed to 0.3 J/cm^2 UV-B but not in samples derived from skin exposed to 0.05 J/cm^2 UV-B (Fig. 6C). These results indicate that Akt is not activated under conditions where fragment N2 is produced, i.e., when fragment N is degraded. In contrast to what was observed in wild-type skin, low doses of UV-B only marginally

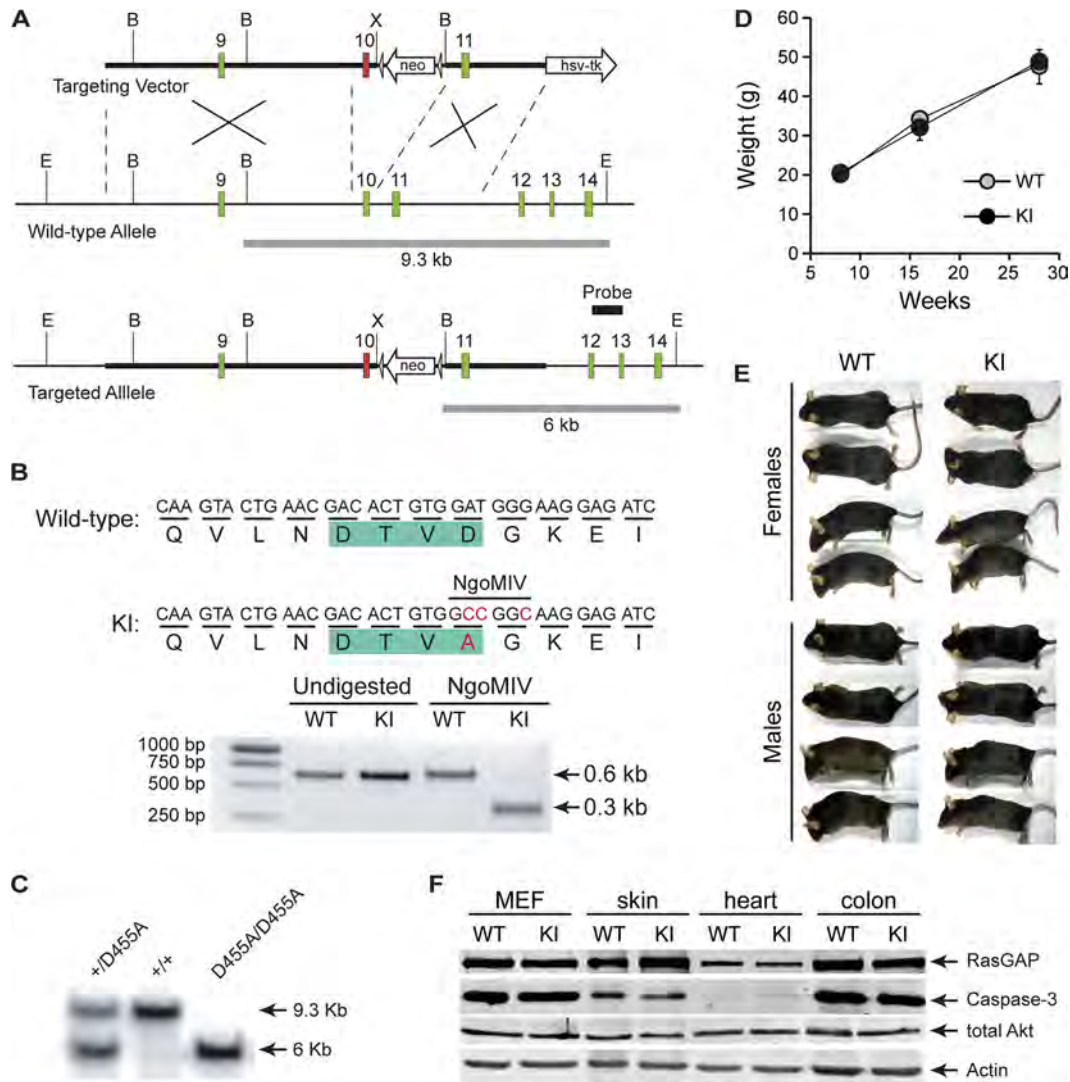


FIG 4 Generation of RasGAP^{D455A/D455A} knock-in mice. (A) The targeting vector consists of mouse RasGAP exons 9, 10, and 11. Exon 10 (indicated in red) bears the RasGAP D455A mutation. E, X, and B, EcoRV, XhoI, and BamHI, respectively; gray bars below the alleles, length of the BamHI/EcoRV fragments recognized by the probe (black bar) when genotyping by Southern blot is performed. (B) Detection of the D455A allele by PCR. The D455A allele bears a new NgoMIV restriction site encompassing the aspartate-to-alanine mutation (in red) within the caspase recognition site in RasGAP (in green). Genomic DNA was subjected to PCR amplification using primers flanking exon 10. The amplified fragments, after digestion with NgoMIV or not, were separated on a 1.5% agarose gel. The presence of the D455A mutation results in cleavage of the ~600-bp PCR fragment into two comigrating ~300-bp fragments. (C) Tail-purified genomic DNA was digested with EcoRV and BamHI and tested by Southern blotting using the probe shown in panel A. (D) The body weight of wild-type and RasGAP^{D455A/D455A} knock-in males was monitored at the indicated time points. Results correspond to the mean \pm 95% CI of at least 9 determinations per condition. (E) Images from anesthetized 10-week-old mice. (F) The expression of RasGAP, caspase-3, Akt, and actin in the indicated cell type and tissues was assessed by Western blotting.

and nonsignificantly activated Akt in keratinocytes from KI skin (Fig. 6A). This correlated with increased numbers of cells expressing active caspase-3 (Fig. 6B) and cells undergoing apoptosis (Fig. 6D). When the skin was exposed to higher UV-B doses (0.3 J/cm²), the extent of apoptosis in the skin of wild-type and KI mice was not significantly different, although there was a trend of a stronger apoptotic response in KI mice (Fig. 6D) that correlated with a tendency of KI mice to activate less Akt (compare the last two bars in Fig. 6A) but more caspase-3 (Fig. 6B) at high UV-B doses. Sunburn cells (see the example in Fig. 6E) were significantly augmented in the epidermis of 0.05-J/cm² UV-B-exposed KI skin compared to wild-type skin (Fig. 6E). The observed difference at higher UV-B doses (0.3 J/cm²) was, however, not statistically significant.

Doxorubicin induced the cleavage of RasGAP into fragment N in the heart of wild-type mice (Fig. 7A). As expected, this was not observed in KI mice (Fig. 7A). Following doxorubicin injection, the number of cardiomyocytes with activated Akt did not increase in KI mice (Fig. 7B). This was also associated with an increase in the number of apoptotic cells in the heart (Fig. 7C). In response to doxorubicin, KI mice had more impaired cardiac function as measured by hemodynamic parameters (see Table S2 in the supplemental material). Specifically, end-systolic elastance, which is derived from end-systolic pressure volume curves (Fig. 7D) and which is a direct (load-independent) measure of the heart contractile activity, was significantly decreased in KI mice treated with doxorubicin (Fig. 7D and E).

Finally, enterocytes from KI mice were also affected in their

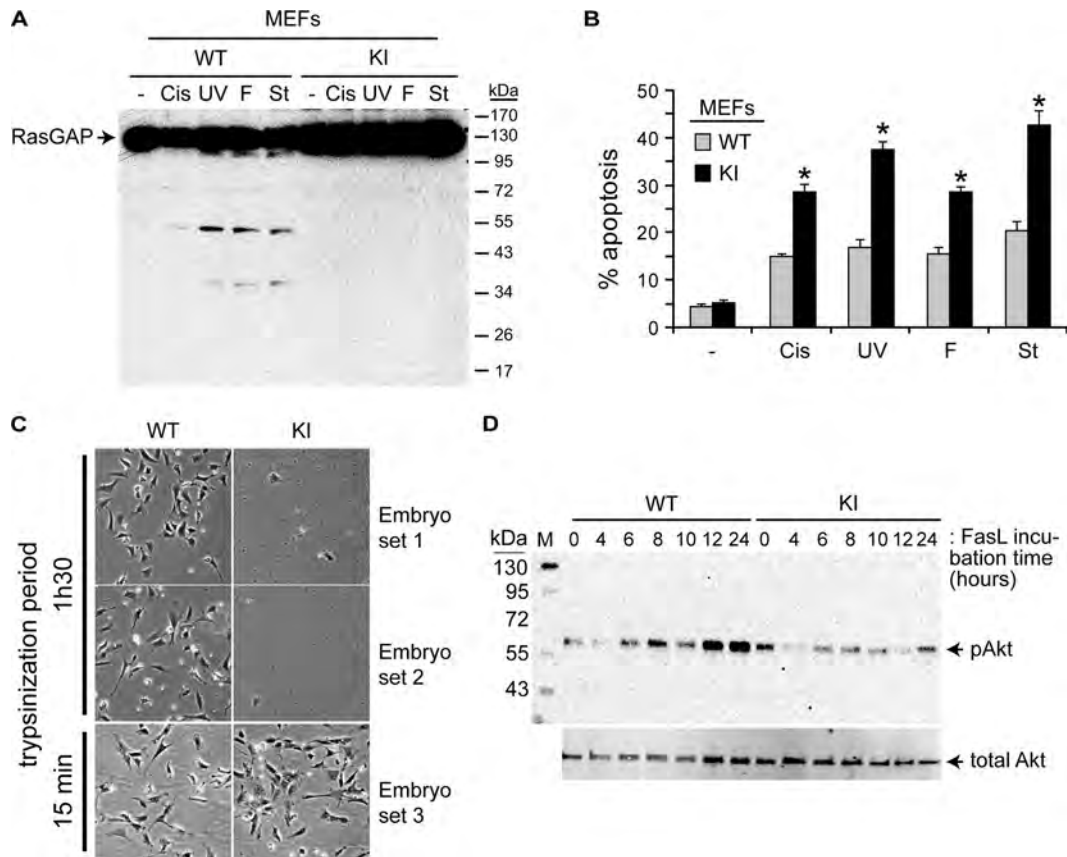


FIG 5 MEFs from RasGAP^{D455A/D455A} knock-in mice do not cleave RasGAP and are more sensitive to apoptosis. (A and B) Wild-type (WT) and KI MEFs were left untreated (–) or treated with 15 μ M cisplatin (Cis), 96 J/m² UV-C (UV), 15 ng/ml FasL (F), and 15 nM staurosporine (St). (A) Cells were lysed 24 h later and analyzed by Western blotting for the presence of RasGAP and its fragments using an anti-RasGAP polyclonal antibody. (B) Alternatively, apoptosis was scored. Results correspond to the mean \pm 95% CI of 3 independent experiments ($n = 3$). (C) Mouse embryonic cells 1 day after their isolation using a trypsinization period of 1 h 30 min or 15 min (see Materials and Methods for details). (D) Wild-type and KI MEFs were treated with 5 ng/ml FasL for the indicated periods of time. Cells were then washed twice with PBS and then incubated for an additional hour in Dulbecco modified Eagle medium at 37°C before lysis. Akt activation and total Akt expression were assessed by Western blotting. Lane M, molecular mass markers.

capacity to activate Akt in response to DSS (Fig. 8A), and this was accompanied by an increased apoptotic response compared to what was seen in wild-type mice (Fig. 8B). At the clinical level, DSS-induced colon damage was more pronounced, as assessed by colon shortening (Fig. 8C) and a more severe DSS-mediated colitis development in KI mice than wild-type mice (Fig. 8D).

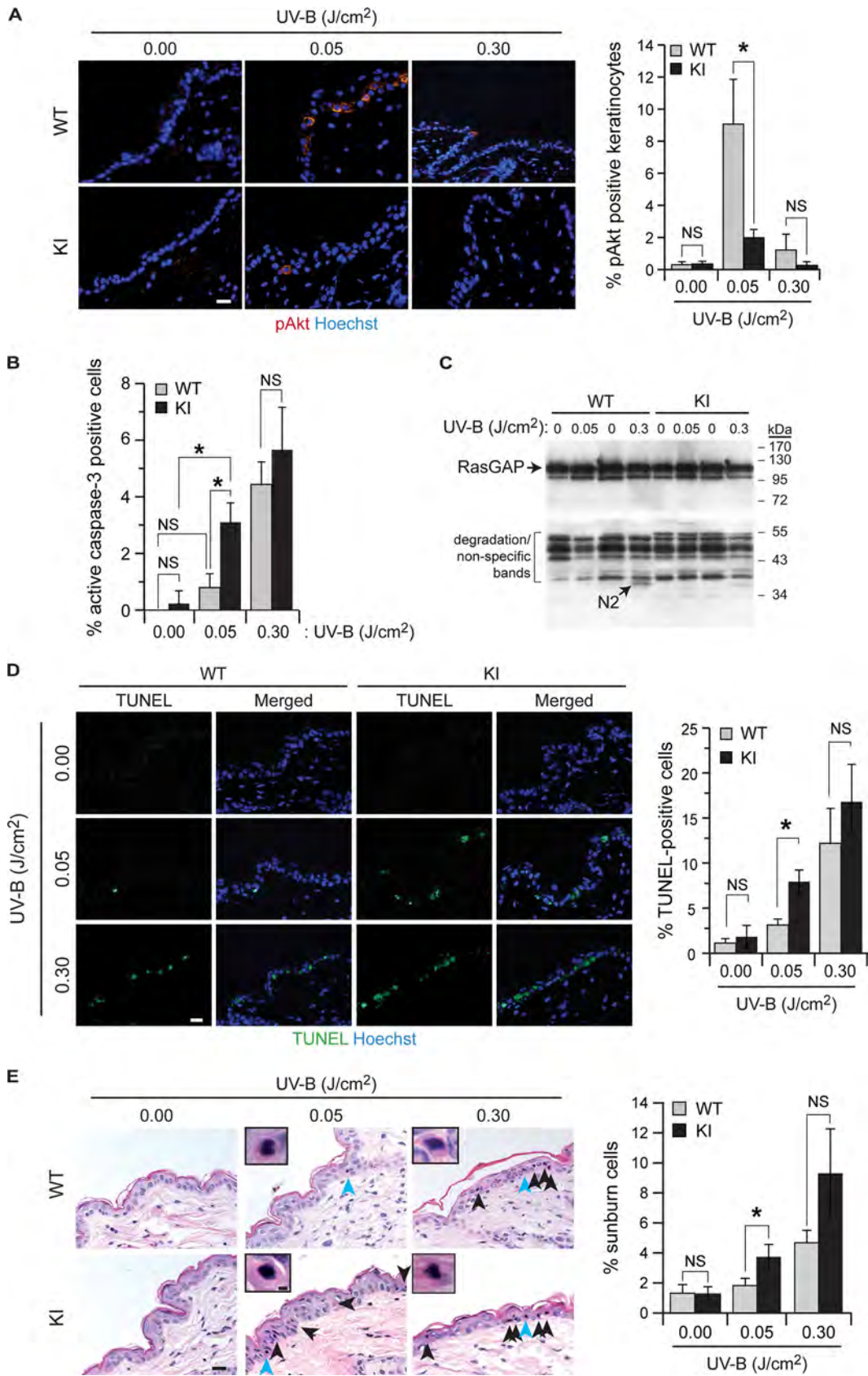
DISCUSSION

The role of caspase-3 in the induction of the antiapoptotic Akt kinase was investigated in adult caspase-3-knockout mice in relation to three different pathophysiological conditions: UV-B skin exposure, doxorubicin-induced cardiomyopathy, and DSS-mediated colitis. Each of these stresses led to Akt activation in the tissues affected by the stress. This was, however, blocked or strongly compromised in mice lacking caspase-3. This impaired Akt activation correlated with augmented cell death, tissue damage, and even lethality. A similar defect in Akt activation was observed in KI mice that expressed a caspase-3-resistant form of p120 RasGAP, and this was accompanied by increased apoptosis and stronger adverse effects: increased number of sunburn cells in UV-B-exposed skin, decreased heart function upon doxorubicin injection, and stronger DSS-mediated colitis development. This study there-

fore identifies a physiological protective mechanism against stress that relies on the activity of an executioner caspase.

Caspase-3 is now known to mediate many nonapoptotic functions in cells (15, 23, 24). It is involved in B cell homeostasis by negatively regulating B cell proliferation following antigen stimulation (46). Caspase-3 is also activated during T cell stimulation (32), and this may participate in T cell proliferation (2, 22). Additionally, caspase-3 is required for erythropoiesis (9). There is thus evidence that caspase-3 plays important functional roles in non-dying hematopoietic cells, but it remains unclear how these cells counteract the apoptotic potential of caspase-3. Cleavage of RasGAP could have been one of the mechanisms allowing these cells to survive following caspase-3 activation. However, T and B cell development occurs normally in the D455A RasGAP KI mice (see Table S1 in the supplemental material). Similarly, the development of mature myeloid and erythroid lineage cells in the bone marrow proceeds normally in the KI mice (see Table S1 in the supplemental material). Therefore, hematopoietic cells use protective mechanisms other than those activated by the cleavage of RasGAP to inhibit apoptosis if caspase-3 is activated during their development.

Caspase-3 is necessary for the development of several tissues.



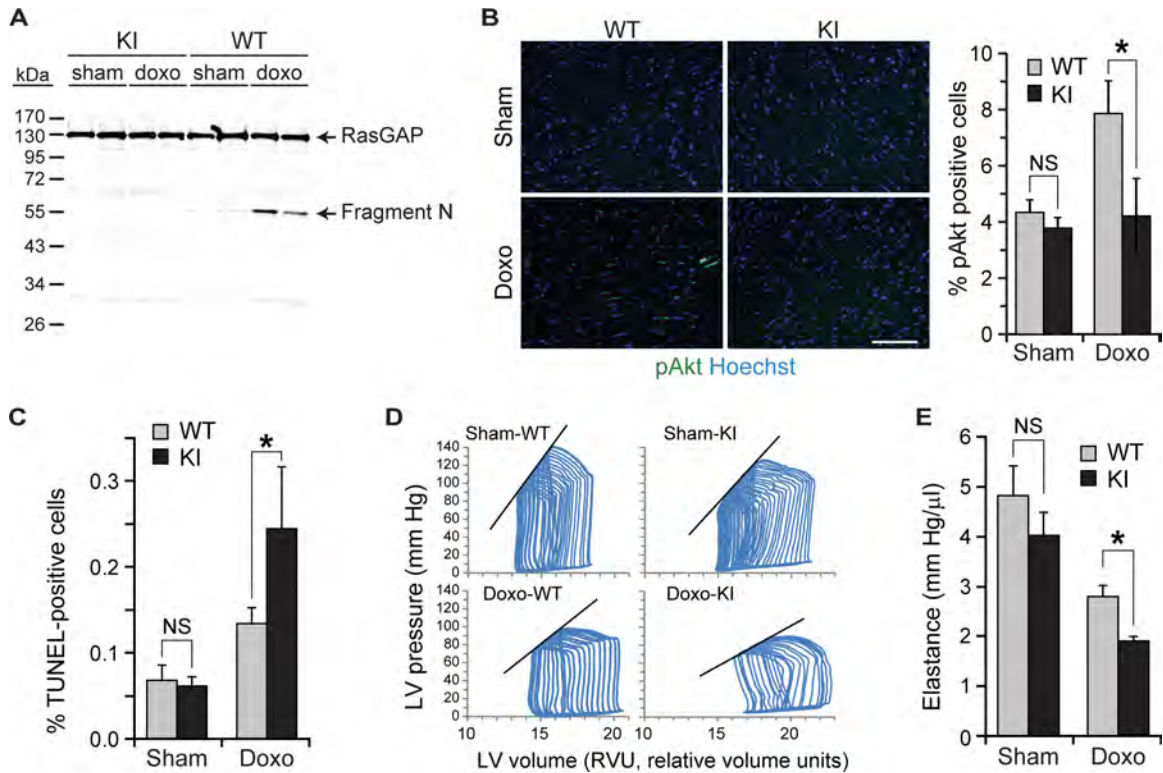


FIG 7 Role of RasGAP cleavage in heart of doxorubicin-treated mice. Wild-type (WT) and RasGAP^{D455A/D455A} (KI) mice were injected with doxorubicin and analyzed 5 days later. (A) Western blot analysis of RasGAP cleavage. This experiment has been repeated once with similar results. (B) Histoimmunofluorescence detection and quantitation of active Akt. Bar, 100 μ m. (C) Assessment of apoptosis by the TUNEL assay. (B and C) Results correspond to the mean \pm 95% CI of measurements performed on 3 animals per condition (three independent experiments). (D) Representative examples of end-systolic left ventricular pressure-volume loops. (E) Heart contractility assessed by end-systolic elastance. Results correspond to the mean \pm 95% CI of measurements performed on 9 to 11 animals per condition (three independent experiments).

Muscle development and osteoblast differentiation are compromised in the absence of caspase-3 (17, 33, 34). Caspase-3 also plays important functions in neurogenesis, synaptic activity, neuronal growth cone guidance, and glial development (7, 16, 37). Histological analyses of muscle, bone, and brain tissues did not reveal any defect in the KI mice (data not shown). Moreover, the growth curve and size of wild-type and KI mice were comparable (Fig. 4D and E). Hence, the mechanisms allowing tissues and organs to withstand caspase-3 activation during development do not rely on RasGAP cleavage and remain to be characterized.

In vitro data provided evidence that low caspase-3 activity induced by mild stress generates fragment N, which was responsible for Akt activation and promotion of cell survival. At higher caspase-3 activity induced by stronger insults, fragment N is further processed into fragments that can no longer stimulate Akt, and this favors apoptosis (47). The data obtained *in vivo* in UV-B-exposed skin are consistent with this model. Low doses of UV-B induced no further cleavage of fragment N (i.e., no production of

fragment N2) in keratinocytes, and this was accompanied by Akt activation and absence of an apoptotic response. In contrast, high UV-B doses generated fragment N2 and Akt was no longer activated, and this led to keratinocyte cell death (Fig. 6). *In vivo*, therefore, RasGAP also functions as a caspase-3 activity sensor to determine whether cells within tissues and organs should be spared or die.

The levels of caspase-3 activation that are required to induce partial cleavage of RasGAP into fragment N are at least an order of magnitude lower than those necessary to induce apoptosis (48). *In vitro*, these low caspase activity levels are not easily detected (47). In response to the stress stimuli used in the present study that led to Akt activation, we could not visualize low caspase-3 activation by Western blotting in any of the tissues investigated, although in response to stronger stresses that did not lead to Akt activation (e.g., 0.3 J/cm² of UV-B [Fig. 6]), caspase-3 activation could be evidenced (Fig. 2A and B). Nonetheless, blocking caspases with chemical inhibitors or using mice lacking caspase-3 prevented Akt

FIG 6 Role of RasGAP cleavage in UV-B exposed skin. Skin of wild-type (WT) and RasGAP^{D455A/D455A} (KI) mice was exposed to the indicated doses of UV-B. Mice were sacrificed 24 h later, and the exposed skin was isolated for biochemical and histological analyses. (A and B) Histoimmunofluorescence detection and quantitation of active Akt (A) and active caspase-3 (B). Results correspond to the mean \pm 95% CI of measurements performed on 4 to 6 animals (three independent experiments). (C) Western blot analysis of RasGAP cleavage (the blot shown is representative of three independent experiments). (D) Assessment of apoptosis by the TUNEL assay. Results correspond to the mean \pm 95% CI of measurements performed on 5 to 9 animals (three independent experiments). (E) Histological assessment of sunburn cells in the epidermis. Results correspond to the mean \pm 95% CI of measurements performed on 9 to 11 animals (three independent experiments). Cells indicated by light blue arrowheads are enlarged in the insets. Bar, 20 μ m.

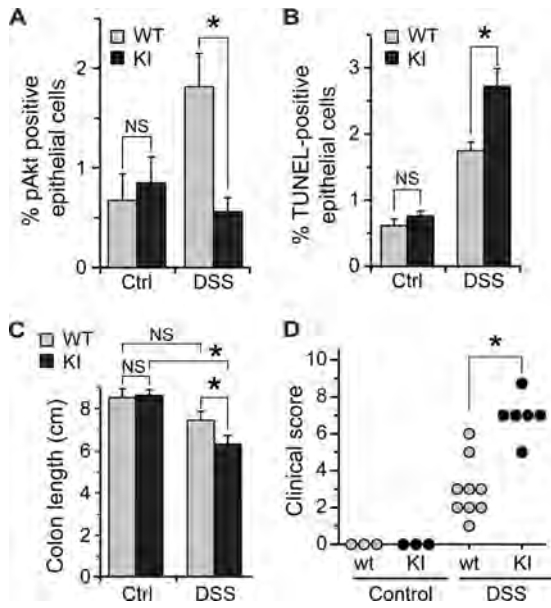


FIG 8 Role of RasGAP cleavage in colon of DSS-treated mice. Wild-type (WT) and RasGAP^{D455A/D455A} (KI) mice were given DSS-containing water for 3 days and normal drinking water for four additional days. The mice were then sacrificed. (A) Quantitation of active Akt on histological sections. Results correspond to the mean \pm 95% CI of measurements performed on 3 to 4 animals per condition (three independent experiments). (B) Assessment of apoptosis by the TUNEL assay. Results correspond to the mean \pm 95% CI of measurements performed on 3 control and 6 to 7 DSS-treated animals per genotype (three independent experiments). (C) Colon damage assessed by variations in colon length. Results correspond to the mean \pm 95% CI of measurements performed on 3 control and 7 to 9 DSS-treated animals per genotype (three independent experiments). (D) Clinical scoring of colitis performed on 7 to 10 animals per condition (three independent experiments). The data were analyzed with a Wilcoxon two-sample two-sided test.

activation induced by low stresses (Fig. 1 and 2). Therefore, caspase-3 exerts an important protective function in tissues and organs in a RasGAP cleavage-dependent manner under conditions where caspase-3 activation may be below the detection threshold of current caspase-3 activation assessment methods.

In conclusion, our study provides the first genetic evidence that in response to various pathology-inducing stresses caspase-3 itself activates the antiapoptotic Akt kinase and that this protective response is mediated through the cleavage of a given caspase-3 substrate, the ubiquitous p120 RasGAP protein. This defense mechanism allows an organism to dampen damage to tissues and organs induced by diverse pathogenic conditions. Hence, procedures aimed at activating the signaling pathways modulated by RasGAP cleavage may represent an attractive strategy to increase the resistance of individuals exposed to environmental or chemical stresses. Additionally, our work has direct implications for therapeutic protocols using caspase inhibitors, as inhibition of caspases could lead to unanticipated adverse effects by decreasing the ability of an organism to cleave RasGAP and defend itself.

ACKNOWLEDGMENTS

This work was supported by Swiss National Science Foundation grants 31003A_119876 and 31003A_141242 1/1 (to C.W.), 310030_135394/1 (to L.L.), and 310030_122012 (to W.H.) and by an Interdisciplinary Research Project subsidiary from the Faculty of Biology and Medicine, University of Lausanne, Lausanne, Switzerland (to C.W. and P.B.).

We thank Andrew Dwyer for critical reading of the manuscript. We thank the Transgenic Animal Facility of the Faculty of Biology and Medicine and the University Hospital (University of Lausanne) for generation of the knock-in mice.

H.K., N.P., and C.W. conceived the study. N.P. performed immunofluorescence experiments. H.K. and N.P. performed histology, TUNEL experiments, and the associated quantitation. J.W. generated the KI mice. J.-Y.Y., G.D., N.P., and C.W. performed the experiments on MEFs *in vitro*. N.G. and W.H. analyzed hematopoiesis and lymphopoiesis in mice. N.P. and P.B. performed the UV-B illumination experiments. H.K. and B.M. performed the DSS experiments. H.K. and L.L. analyzed cardiac functions in mice. C.W. wrote the paper. All authors discussed the results.

We declare that we have no conflict of interest.

REFERENCES

- Abraham MC, Shaham S. 2004. Death without caspases, caspases without death. *Trends Cell Biol.* 14:184–193.
- Alam A, Cohen LY, Aouad S, Sekaly RP. 1999. Early activation of caspases during T lymphocyte stimulation results in selective substrate cleavage in nonapoptotic cells. *J. Exp. Med.* 190:1879–1890.
- Bonnet MC, et al. 2011. The adaptor protein FADD protects epidermal keratinocytes from necroptosis *in vivo* and prevents skin inflammation. *Immunity* 35:572–582.
- Bulat N, et al. 2011. RasGAP-derived fragment N increases the resistance of beta cells towards apoptosis in NOD mice and delays the progression from mild to overt diabetes. *PLoS One* 6:e22609. doi:10.1371/journal.pone.0022609.
- Bulat N, Waeber G, Widmann C. 2009. LDLs stimulate p38 MAPKs and wound healing through SR-BI independently of Ras and PI3 kinase. *J. Lipid Res.* 50:81–89.
- Burguillos MA, et al. 2011. Caspase signalling controls microglia activation and neurotoxicity. *Nature* 472:319–324.
- Campbell DS, Holt CE. 2003. Apoptotic pathway and MAPKs differentially regulate chemotropic responses of retinal growth cones. *Neuron* 37:939–952.
- Candi E, Schmidt R, Melino G. 2005. The cornified envelope: a model of cell death in the skin. *Nat. Rev. Mol. Cell Biol.* 6:328–340.
- Carlisle GW, Smith DH, Wiedmann M. 2004. Caspase-3 has a nonapoptotic function in erythroid maturation. *Blood* 103:4310–4316.
- Caserta TM, Smith AN, Gultice AD, Reedy MA, Brown TL. 2003. Q-VD-OPH, a broad spectrum caspase inhibitor with potent antiapoptotic properties. *Apoptosis* 8:345–352.
- Cuvillier O, et al. 2001. Sphingosine generation, cytochrome c release, and activation of caspase-7 in doxorubicin-induced apoptosis of MCF7 breast adenocarcinoma cells. *Cell Death Differ.* 8:162–171.
- Daniels F, Jr, Brophy D, Lobitz WC, Jr. 1961. Histochemical responses of human skin following ultraviolet irradiation. *J. Invest. Dermatol.* 37:351–357.
- Droin N, et al. 2008. A role for caspases in the differentiation of erythroid cells and macrophages. *Biochimie* 90:416–422.
- Eymin B, et al. 1999. Caspase-induced proteolysis of the cyclin-dependent kinase inhibitor p27Kip1 mediates its anti-apoptotic activity. *Oncogene* 18:4839–4847.
- Feinstein-Rotkopf Y, Arama E. 2009. Can't live without them, can live with them: roles of caspases during vital cellular processes. *Apoptosis* 14:980–995.
- Fernando P, Brunette S, Megeney LA. 2005. Neural stem cell differentiation is dependent upon endogenous caspase 3 activity. *FASEB J.* 19:1671–1673.
- Fernando P, Kelly JF, Balazsi K, Slack RS, Megeney LA. 2002. Caspase 3 activity is required for skeletal muscle differentiation. *Proc. Natl. Acad. Sci. U. S. A.* 99:11025–11030.
- Fujita J, et al. 2008. Caspase activity mediates the differentiation of embryonic stem cells. *Cell Stem Cell* 2:595–601.
- Gaime E, et al. 2006. Caspase-3-derived C-terminal product of synphilin-1 displays antiapoptotic function via modulation of the p53-dependent cell death pathway. *J. Biol. Chem.* 281:11515–11522.
- Holler N, et al. 2003. Two adjacent trimeric Fas ligands are required for Fas signaling and formation of a death-inducing signaling complex. *Mol. Cell. Biol.* 23:1428–1440.
- Jianhui L, et al. 2010. Endotoxin impairs cardiac hemodynamics by

- affecting loading conditions but not by reducing cardiac inotropism. *Am. J. Physiol. Heart Circ. Physiol.* 299:H492–H501.
22. Kennedy NJ, Kataoka T, Tschopp J, Budd RC. 1999. Caspase activation is required for T cell proliferation. *J. Exp. Med.* 190:1891–1896.
 23. Kuranaga E, Miura M. 2007. Nonapoptotic functions of caspases: caspases as regulatory molecules for immunity and cell-fate determination. *Trends Cell Biol.* 17:135–144.
 24. Launay S, et al. 2005. Vital functions for lethal caspases. *Oncogene* 24: 5137–5148.
 25. Leonard JR, Klocke BJ, D'Sa C, Flavell RA, Roth KA. 2002. Strain-dependent neurodevelopmental abnormalities in caspase-3-deficient mice. *J. Neuropathol. Exp. Neurol.* 61:673–677.
 26. Li Z, et al. 2010. Caspase-3 activation via mitochondria is required for long-term depression and AMPA receptor internalization. *Cell* 141:859–871.
 27. Liadis N, et al. 2005. Caspase-3-dependent β -cell apoptosis in the initiation of autoimmune diabetes mellitus. *Mol. Cell. Biol.* 25:3620–3629.
 28. Luciano F, Herrant M, Jacquelin A, Ricci JE, Aubergier P. 2003. The p54 cleaved form of the tyrosine kinase Lyn generated by caspases during BCR-induced cell death in B lymphoma acts as a negative regulator of apoptosis. *FASEB J.* 17:711–713.
 29. Mansilla S, Priebe W, Portugal J. 2006. Mitotic catastrophe results in cell death by caspase-dependent and caspase-independent mechanisms. *Cell Cycle* 5:53–60.
 30. McLaughlin B, et al. 2003. Caspase 3 activation is essential for neuroprotection in preconditioning. *Proc. Natl. Acad. Sci. U. S. A.* 100:715–720.
 31. Michod D, Widmann C. 2007. TAT-RasGAP_{317–326} requires p53 and PUMA to sensitize tumor cells to genotoxins. *Mol. Cancer Res.* 5:497–507.
 32. Miossec C, Dutilleul V, Fassy F, Diu-Hercend A. 1997. Evidence for CPP32 activation in the absence of apoptosis during T lymphocyte stimulation. *J. Biol. Chem.* 272:13459–13462.
 33. Miura M, et al. 2004. A crucial role of caspase-3 in osteogenic differentiation of bone marrow stromal stem cells. *J. Clin. Invest.* 114:1704–1713.
 34. Mogi M, Togari A. 2003. Activation of caspases is required for osteoblastic differentiation. *J. Biol. Chem.* 278:47477–47482.
 35. Newton K, Strasser A. 2003. Caspases signal not only apoptosis but also antigen-induced activation in cells of the immune system. *Genes Dev.* 17:819–825.
 36. Ohkawara T, et al. 2005. Transgenic over-expression of macrophage migration inhibitory factor renders mice markedly more susceptible to experimental colitis. *Clin. Exp. Immunol.* 140:241–248.
 37. Oomman S, Strahlendorf H, Dertien J, Strahlendorf J. 2006. Bergmann glia utilize active caspase-3 for differentiation. *Brain Res.* 1078:19–34.
 38. Pacher P, et al. 2003. Potent metalloporphyrin peroxynitrite decomposition catalyst protects against the development of doxorubicin-induced cardiac dysfunction. *Circulation* 107:896–904.
 39. Pacher P, et al. 2004. Left ventricular pressure-volume relationship in a rat model of advanced aging-associated heart failure. *Am. J. Physiol. Heart Circ. Physiol.* 287:H2132–H2137.
 40. Parcellier A, Tintignac LA, Zhuravleva E, Hemmings BA. 2008. PKB and the mitochondria: AKTing on apoptosis. *Cell. Signal.* 20:21–30.
 41. Peter ME. 2011. Programmed cell death: apoptosis meets necrosis. *Nature* 471:310–312.
 42. Rincheval V, Renaud F, Lemaire C, Mignotte B, Vayssiere JL. 1999. Inhibition of Bcl-2-dependent cell survival by a caspase inhibitor: a possible new pathway for Bcl-2 to regulate cell death. *FEBS Lett.* 460:203–206.
 43. Slee EA, Adrain C, Martin SJ. 2001. Executioner caspase-3, -6, and -7 perform distinct, non-redundant roles during the demolition phase of apoptosis. *J. Biol. Chem.* 276:7320–7326.
 44. Sordet O, et al. 2002. Specific involvement of caspases in the differentiation of monocytes into macrophages. *Blood* 100:4446–4453.
 45. Taylor RC, Cullen SP, Martin SJ. 2008. Apoptosis: controlled demolition at the cellular level. *Nat. Rev. Mol. Cell Biol.* 9:231–241.
 46. Woo M, et al. 2003. Caspase-3 regulates cell cycle in B cells: a consequence of substrate specificity. *Nat. Immunol.* 4:1016–1022.
 47. Yang J-Y, et al. 2004. Partial cleavage of RasGAP by caspases is required for cell survival in mild stress conditions. *Mol. Cell. Biol.* 24:10425–10436.
 48. Yang J-Y, Walicki J, Michod D, Dubuis G, Widmann C. 2005. Impaired Akt activity down-modulation, caspase-3 activation, and apoptosis in cells expressing a caspase-resistant mutant of RasGAP at position 157. *Mol. Biol. Cell* 16:3511–3520.
 49. Yang J-Y, Widmann C. 2001. Antiapoptotic signaling generated by caspase-induced cleavage of RasGAP. *Mol. Cell. Biol.* 21:5346–5358.
 50. Yang J-Y, Widmann C. 2002. The RasGAP N-terminal fragment generated by caspase cleavage protects cells in a Ras/PI3K/Akt-dependent manner that does not rely on NF κ B activation. *J. Biol. Chem.* 277:14641–14646.
 51. Youn HJ, et al. 2005. Induction of caspase-independent apoptosis in H9c2 cardiomyocytes by adriamycin treatment. *Mol. Cell. Biochem.* 270: 13–19.

Supplemental information**Supplemental Tables****Supplemental table 1: Hematopoiesis and lymphopoiesis in wild-type and RasGAP^{D455A/D455A} knock-in mice**

Thymocytes, bone marrow (BM) and spleen cells were exposed to a hypotonic buffer to remove erythrocytes. Cells were then incubated with 2.4G2 (anti-CD16/32) hybridoma supernatant to block FC receptors before staining for multi-color flow cytometry (except for the staining of BM precursors). Dead cells were excluded based on 7-AAD uptake. The following antibodies were used CD3 ϵ (17A2), CD4 (RM4-5), CD8 α (53.6.7), CD11b (Mac1, M1/70), CD16/32 (93), CD19 (1D3/6D5), CD25 (PC-61), CD34 (Ram34), CD43 (S7), CD44 (IM781), CD45R/B220 (RA3-6B2), CD45.2 (104.2), CD71 (R17217), CD117 (2B8), CD127 (A7R34), Sca1 (D7), GR-1 (Ly6G, RB68C5), Ter119 (Ter119), BP-1 (6C3), IgM (11/41 or R6-60.2), TCR β (H57), TCR $\gamma\delta$, CD24. The antibodies were conjugated to appropriate fluorochromes (FITC, PE, PE-Texas red, PE-Cy5, PE-Cy5.5, PerCP-Cy5.5, PE-Cy7, APC, Alexa647, Alexa700, APC-Cy7, APC-Alexa780, Pacific blue, efluor450) at the Ludwig Center for Cancer Research of the University of Lausanne (LICR) or purchased from eBiosciences, Becton Dickinson or Biolegend. A cocktail of PE-Cy7-conjugated anti-TCR β , CD3 ϵ , CD4, CD8 α , CD11 β , GR-1, B220, CD19, Ter119, CD161 (PK136) monoclonal antibodies was used to gate out lineage-positive cells. Samples were run on a LSRII flow cytometer (Becton Dickinson) and analyzed with FlowJo software (Tristar).

Interpretation of the results presented in Supplemental Table 2

The bone marrow of D445A and control mice contained a comparable population of Lin⁻ Sca1⁺ c-kit⁺ (LSK) cells that contains haematopoietic stem cells. Further, myeloid/erythroid (Lin⁻ Sca1⁻ c-kit⁺, LKS⁻) and lymphoid committed common lymphoid progenitors (CLP, Lin⁻ c-kit^{lo} CD127⁺) were also present at comparable numbers. Among the LKS⁻ cells there was a normal distribution of CMP (Common myeloid progenitors), GMP (Granulocyte monocyte progenitors) and MEP (Megakaryocyte erythroid progenitors) (not shown).

		WT	KI
Bone Marrow *	x 10 ⁶	29±3	26±4
lin ⁻ Sca1 ⁺ c-kit ⁺ (LSK)	x 10 ⁴	7.7±2.0	7.1±3.3
lin ⁻ Sca1 ⁻ c-kit ⁺ (LKS ⁻)	x 10 ⁴	57.0±19.6	53.6±10.8
lin ⁻ c-kit ⁺ CD127 ⁺ (CLP)	x 10 ⁴	6.0±2.0	5.1±2.8
Ter119 ⁺ CD71 ⁺	x 10 ⁶	1.8±0.2	1.7±0.3
GR1 ⁺ CD11b ⁺	x 10 ⁶	14.1±2.6	13.0±2.5
GR1 ⁻ CD11b ⁺	x 10 ⁶	2.3±0.2	2.2±0.5
B220 ⁺ CD43 ⁺	x 10 ⁶	1.3±0.1	1.1±0.2
B220 ⁺ CD43 ⁻	x 10 ⁶	6.2±0.6	5.1±1.0
Thymus	x 10 ⁶	80±20	96±18
CD4 ⁻ 8 ⁻ (DN)	x 10 ⁶	2.3±2.2	2.7±1.6
CD4 ⁺ 8 ⁺ (DP)	x 10 ⁶	68.9±16.4	77.7±21.3
CD4 ⁺ 8 ⁻	x 10 ⁶	5.7±1.8	8.0±3.8
CD4 ⁻ 8 ⁺	x 10 ⁶	2.1±0.8	2.2±0.6
TCR $\gamma\delta$ CD4 ⁻ CD8 ⁻	x 10 ⁶	0.17±0.11	0.26±0.15
Spleen	x 10 ⁶	57±22	70±21
B220 ⁺	x 10 ⁶	21.8±3.2	29.9±2.6
CD3 ⁺ CD4 ⁺	x 10 ⁶	12.3±3.4	13.1±1.5
CD3 ⁺ CD8 ⁺	x 10 ⁶	6.2±2.6	7.7±1.1
CD3 ⁻ CD122 ⁺	x 10 ⁶	0.9±0.6	1.2±0.5

Data are the mean absolute number of cells (\pm SD) from 3-5 different mice.

* Cell counts refer to one hind leg

Further, the development of mature myeloid and erythroid lineage cells in the bone marrow was not perturbed, as judged by the normal numbers of granulocytes (GR1⁺CD11b⁺), monocytes (GR1⁻CD11b⁺) and erythroblasts (CD71⁺TER119⁺). With regard to lymphocyte development, the sizes of the B220⁺CD43⁺ and the

B220⁺CD43⁻ populations were comparable. Among immature B220⁺ CD43⁻ cells there were comparable populations of CD19⁻ BP-1⁻, CD19⁺ BP-1⁻ and CD19⁺ BP-1⁺ cells (not shown). Similarly, intrathymic T cell development was also unaffected. This was not only true for TCR $\alpha\beta$ lineage cells but also for CD4⁻CD8⁻ cells expressing TCR $\gamma\delta$.

As expected from the normal presence of immature precursors, the periphery of D445A mice (spleen) contained comparable numbers of B cells (B220), T cells (CD3⁺, both CD4⁺ and CD8⁺ T cells) and NK cells (CD3⁻CD122⁺).

In conclusion, the steady state hematopoiesis and lymphopoiesis was not perturbed in RasGAP^{D455A/D455A} knock-in mice.

Supplemental table 2: Wild-type and RasGAP^{D455A/D455A} knock-in mice hemodynamic parameters injected or not with doxorubicin

Hemodynamic measurements were performed using left ventricular pressure-volume micro-catheters as described in the methods. Doxorubicin induced cardiac dysfunction as shown by reduced left ventricular (LV) systolic pressure, stroke work and dp/dt max, which were related to a depression in contractility, as shown by the significant reduction of end-systolic elastance, an ejection phase measure of contractility. The hearts were not dilated, which is expected in such a short term model of heart failure. Importantly, the reduction of cardiac contractility was significantly more pronounced in RasGAP D455A KI mice, as shown by significantly greater reduction of LV end-systolic pressure, dp/dt max, E_{se}, as well as significant decrease of dp/dt@edv, an isovolumic phase measure of contractility. Results correspond to the mean \pm 95% CI of measurements performed on 9-11 mice per treatment and genotype.

Variable	Sham-WT	Sham-KI	Doxo-WT	Doxo-KI
HR (bpm)	334±30	294±15	245±14†	255±22
Esp (mm Hg)	131±7	115±7	93±4†	75±5†*
Edp (mm Hg)	9.2±1.5	11.7±1.5	9.7±1.3	7.6±1.0
Esv (μl)	15.4±1.1	18.6±1.4	18.3±2.2	23.5±3.2
Edv (μl)	31.5±1.6	36.7±1.8	35.3±2.3	41.1±3.9
SV (μl)	18.5±1.1	20.5±2.0	19.5±1.1	19.8±1.8
CO (μl min ⁻¹)	6173±691	5284±301	4737±370	5130±715
EF (%)	57±2	55±2	55±4	48±4
SW (mm Hg μl)	1791±102	1837±124	1417±124†	1188±123†
dp/dt max (mm Hg sec ⁻¹)	9372±786	7892±326	6724±436†	5173±495†*
Ese (mm Hg μl ⁻¹)	4.8±0.6	4.0±0.5	2.7±0.2†	1.8±0.1†*
dp/dt@edv (mm Hg sec ⁻¹ μl ⁻¹)	185±29	143±11	188±24	82±17†*

† p<0.05 vs sham in the same genotype. *p<0.05 WT vs KI

HR, heart rate; Esp, end-systolic pressure; Edp, end-diastolic pressure; Esv, end-systolic volume; Edv, end-diastolic volume; SV, stroke volume; CO, cardiac output; EF, ejection fraction; SW, stroke work; dp/dt max, first derivative of LV systolic pressure increment; Ese, end-systolic elastance (slope of the end-systolic pressure-volume relationship); dp/dt@edv, dp/dt max corrected for end-diastolic volume.

Supplemental Figures

Figure S1: Schematic representation of the D455A targeting vector construction

The 3' and 5' homology arms of the targeting vector were derived from a RasGAP genomic clone (RP22-250D10) obtained by screening the RPCI-22 129S6/SvEvTac mouse BAC library from the BACPAC Resource Center (Children's Hospital Oakland Research Institute, Oakland, California, USA) (2) with a probe corresponding to nucleotides 7137306-7136366 of *Mus musculus* chromosome 13 genomic contig (accession N° NT_039589.2). This led to the identification of three BAC clones (RP22-250D10, #452; RP22-268I2, #453; RP22-257P13 #454). The DNA prepared from these clones was pooled and digested with *Swa*I. The resulting ~10 kb fragment was sub-cloned in the *Eco*RV restriction site of pBluescript II SK + (Stratagene). A plasmid containing RasGAP exons 9, 10, and 11 was identified by PCR and called **RasGAP exons 9-10-11.blu** (plasmid #419). From this plasmid, a blunt-ended ~6.5 kb *Bst*XI fragment [nucleotides 7139579-7145879 from the *Mus musculus* chromosome 13 genomic contig (accession n° NT_039589.2)] was sub-cloned in the *Eco*RV restriction site of pBluescript II SK + to generate the 5' homology arm composed of parts of introns 8 and 9 and exon 9 (the resulting plasmid was called **RasGAP exon 9.blu**; plasmid #427). A ~2.6 kb *Hind*III fragment from RasGAP exons 9-10-11.blu (nucleotides 7138985-7136418 from the chromosome 13 genomic contig) was sub-cloned in the *Hind*III restriction site of pcDNA3 to generate the 3' homology arm composed of parts of introns 10 and 11 and exon 11 (the resulting plasmid was called **RasGAP exon 11.dn3**; plasmid #421). A 590 bp fragment (called the Vital Region [VR] as it encodes amino acid 455 of RasGAP) containing exon 10 and connecting the 5' and 3' homology arms was PCR-amplified from the BAC clones described above using the *Pwo* polymerase (Roche Applied Science, catalogue n° 04 340 868 001), sub-cloned into the *Sma*I and *Not*I sites of pBluescript II SK+, and sequenced twice to confirm that no PCR-generated errors occurred (the resulting plasmid was called **Lox 66-RasGAP Exon 10.blu**; plasmid #427). The mutation of the caspase cleavage site in exon 10 was done using the megaprimer PCR mutagenesis method(1) using the following primers: 1) a sense primer for the first PCR: AA GTA CTG AAC GAC ACT GTG GCC GGC AAG GAG ATC TAT AAC ACA AT. This corresponds to sequence 641-685 of the *Mus musculus* RasGAP

mRNA (gi 21703899) carrying an A to C mutation (underlined) that destroys the first RasGAP caspase cleavage site by substituting an aspartate (D) residue for an alanine (A) (3) and two additional silent mutations (bold) that, together with the D to A mutation, create a new restriction site recognized by the NaeI and NgoMIV endonucleases (see also Figure 4B). 2) an anti-sense primer for the first PCR: TACCTAGCATGAACAGATTG (a random sequence not found in the plasmid) GCGGCCGC (NotI) GTTCTAAAACCCTGGTTATA (3' terminal sequence of the Vital Region; sequence 42026-42007 of the *Mus musculus* BAC clone RP23-222G16 [gi 29367036]). 3) a sense primer for the second PCR: CGTA CCCGGG (SmaI) AGTAGGTGGGTTTCAGGAGCAG (sequence 42007-42026 of the *Mus musculus* BAC clone). 4) an anti-sense primer for the second PCR: TACCTAGCATGAACAGATTG (the same random sequence found in primer 2).

The mutated PCR product was digested with SmaI and NotI and subcloned into the SmaI/NotI sites of pBluescript II SK + [generating plasmid **RasGAP exon 10 (D455A).blu**; plasmid #428].

The LoxP targeting vector plasmid (**Lox-Neo-Lox.Itv**, plasmid #425) is a derivative of the LTV plasmid (a gift from Olivier Staub, Lausanne University, Switzerland) from which the third LoxP site was removed. This Lox-Neo-Lox.Itv plasmid was used as a backbone to construct the targeting vector. It consists of a neomycin-resistance cassette (PGK-Neo) flanked with two LoxP sites and the Herpes Simplex Virus thymidine kinase gene (HSV-TK). RasGAP Exon 11.dn3 was digested with HindIII and the resulting 2.6 kb fragment was ligated into the HindIII site of LTV (generating plasmid **Lox-Neo-Lox-RasGAP Exon 11.Itv**; plasmid #426). The 0.6 kb SmaI/NotI fragment of RasGAP Exon 10 (D455A).blu was ligated into the SmaI/NotI sites of RasGAP Exon 9.blu, creating plasmid RasGAP Exons 9-10 (D455A).blu. Finally, the Sall/NotI 7 kb fragment of RasGAP Exons 9-10 (D455A).blu was inserted into the Sall/NotI sites of LTV-Lox-Neo-Lox-RasGAP Exon 11 plasmid to obtain the final D455A targeting vector [plasmid **RasGAP Exons 9-10 (D455A)-Lox-Neo-Lox-RasGAP Exon 11**; plasmid #441]. This clone was sequenced to verify that the LoxP sites and the D455A mutation were intact.

The targeting vector electroporation, clone selection and injection into C57/BL6 blastocysts was performed at the Transgenic Animal Facility of the University of Lausanne (<http://www.unil.ch/taf>).

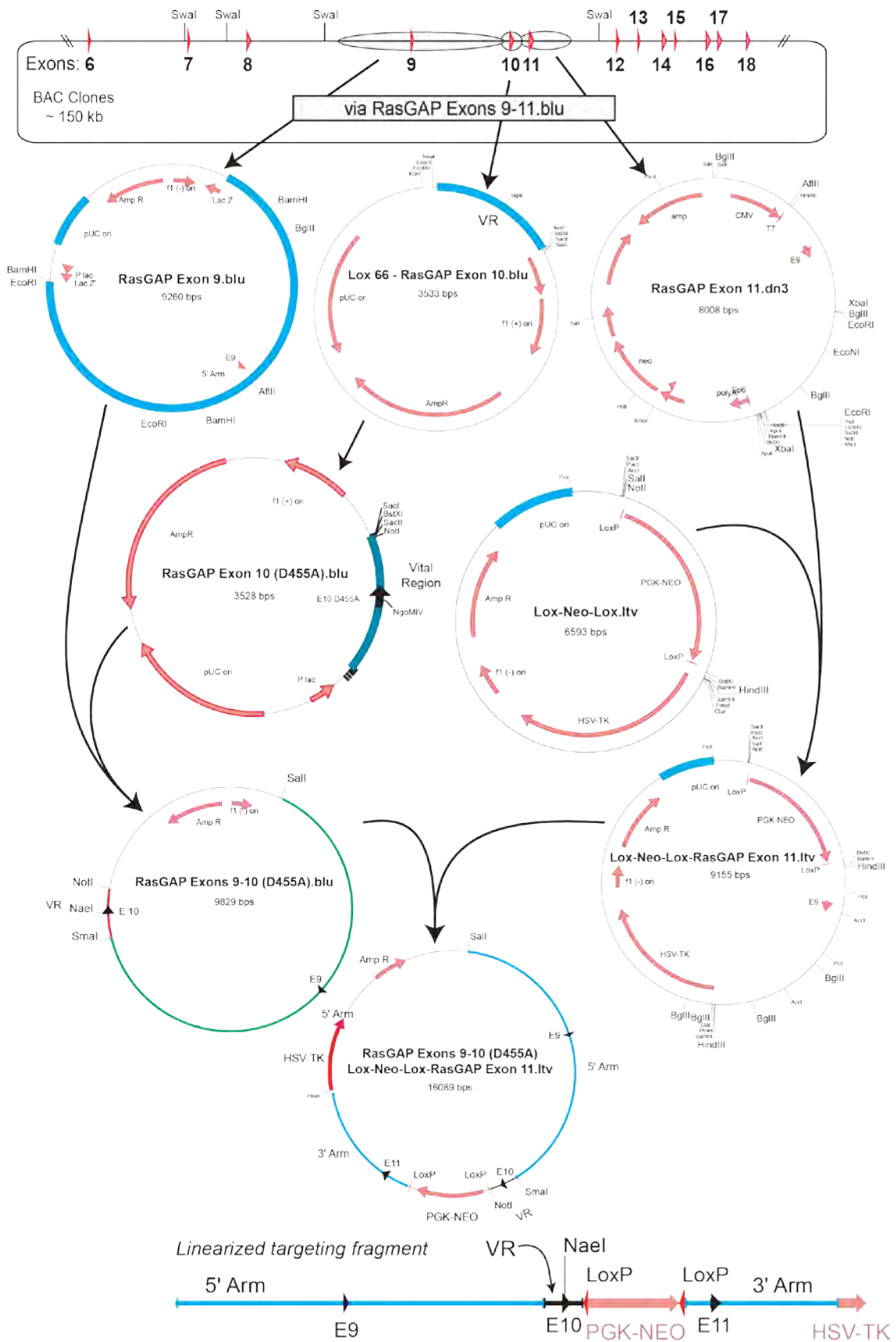


Figure S1

Reference List

1. **Nelson, R. M. and G. L. Long.** 1989. A general method of site-specific mutagenesis using a modification of the *Thermus aquaticus* polymerase chain reaction. *Anal.Biochem.* **180**:147-151.
2. **Osoegawa, K., M. Tateno, P. Y. Woon, E. Frengen, A. G. Mammoser, J. J. Catanese, Y. Hayashizaki, and P. J. de Jong.** 2000. Bacterial artificial chromosome libraries for mouse sequencing and functional analysis. *Genome Res.* **10**:116-128.
3. **Yang, J.-Y. and C. Widmann.** 2001. Antiapoptotic signaling generated by caspase-induced cleavage of RasGAP. *Mol.Cell.Biol.* **21**:5346-5358.

Figure S2: No histological alteration in RasGAP^{D455A/D455A} knock-in mice tissues
Paraffin-embedded hematoxylin and eosin-stained sections of the indicated organs and tissues were prepared from wild-type and knock-in mice homozygous.

Results: Part I

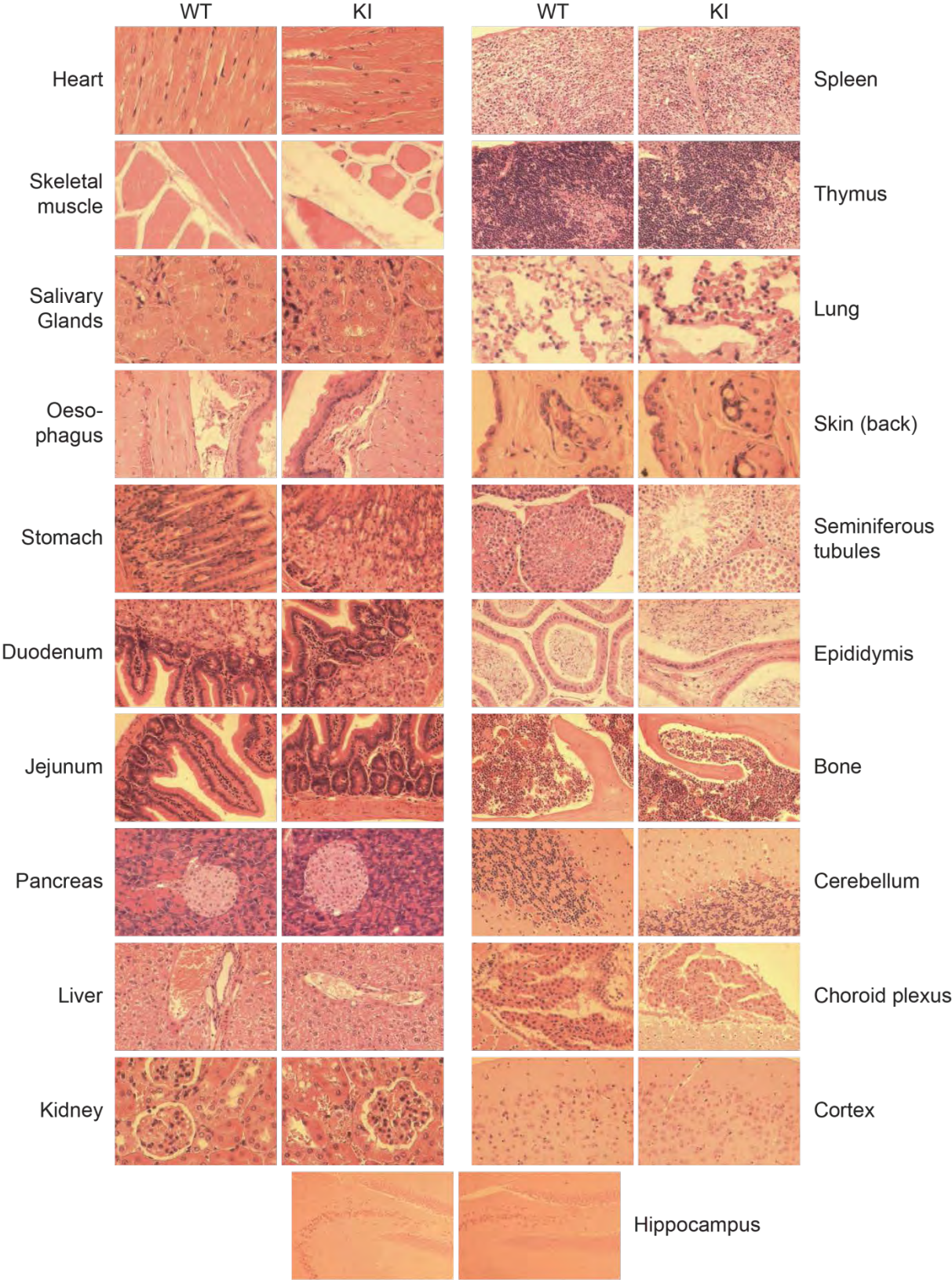


Figure S2

3. Results: Part II

1. Introduction

Peroxynitrite (PN) is a reactive oxidant and nitrating agent that is produced from the reaction between nitric oxide and superoxide anion. PN easily crosses biological membranes and oxidizes target molecules either directly or indirectly. PN induces cardiomyocytes cell death by apoptosis and necrosis (1). *In vitro* PN stimulation leads to either activation or inhibition of a wealth of cellular signal transduction pathways, whose dysregulation plays key roles in the development of cardiovascular pathologies. *In vivo* peroxynitrite generation was demonstrated in various rodent models of myocardial ischemia-reperfusion and heart failure as well as in humans suffering of these pathologies (1;2).

2. Results

RasGAP-derived fragment N was able to protect different cell types treated with various apoptosis inducing stimuli. The capacity of fragment N to protect cells against protein nitration- and oxidation-induced death was investigated. In response to PN stimulation, we observed a rapid cleavage of RasGAP and the consequent generation of both fragment N and N2 simultaneously. This did not allow the endogenous accumulation of fragment N; however, the overexpression of a caspase-resistant form of fragment N was efficient in counteracting PN-induced cell death.

3. Contribution

This work has been published in the journal of Free Radical Biology and Medicine (FRBM). Except the preparation of primary cardiomyocytes which was done by Nathalie Rosentblatt, I performed all the experiments shown in this paper. I wrote the manuscript which was revised and corrected by Christian Widmann.

Reference List

1. Pacher,P., Beckman,J.S., and Liaudet,L. 2007. Nitric oxide and peroxynitrite in health and disease. *Physiol Rev* **87**:315-424.
2. Liaudet,L., Vassalli,G., and Pacher,P. 2009. Role of peroxynitrite in the redox regulation of cell signal transduction pathways. *Front Biosci.* **14**:4809-4814.



Original Contribution

The role of endogenous and exogenous RasGAP-derived fragment N in protecting cardiomyocytes from peroxynitrite-induced apoptosis

Hadi Khalil^a, Nathalie Rosenblatt^b, Lucas Liaudet^c, Christian Widmann^{a,*}^a Department of Physiology, Biology and Medicine Faculty, University of Lausanne, 1005 Lausanne, Switzerland^b Division of Pathophysiology, Centre Hospitalier Universitaire Vaudois and University of Lausanne, Lausanne, Switzerland^c Department of Intensive Care, Centre Hospitalier Universitaire Vaudois and University of Lausanne, Lausanne, Switzerland

ARTICLE INFO

Article history:

Received 26 January 2012

Received in revised form

18 May 2012

Accepted 7 June 2012

Available online 19 June 2012

Keywords:

Peroxynitrite

Caspases

RasGAP

Akt

Apoptosis

Cardiomyocytes

Free radicals

ABSTRACT

Peroxynitrite (PN) is a potent nitrating and oxidizing agent generated during various pathological situations affecting the heart. The negative effects of PN result, at least in part, from its ability to activate caspases and apoptosis. RasGAP is a ubiquitously expressed protein that is cleaved sequentially by caspase-3. At low caspase-3 activity, RasGAP is cleaved into an N-terminal fragment, called fragment N, that protects cells by activating the Ras/PI3K/Akt pathway. At high caspase-3 activity, fragment N is further cleaved and this abrogates its capacity to stimulate the antiapoptotic Akt kinase. Fragment N formation is crucial for the survival of cells exposed to a variety of stresses. Here we investigate the pattern of RasGAP cleavage upon PN stimulation and the capacity of fragment N to protect cardiomyocytes. PN did not lead to sequential cleavage of RasGAP. Indeed, PN did not allow accumulation of fragment N because it induced its rapid cleavage into smaller fragments. No situations were found in cells treated with PN in which the presence of fragment N was associated with survival. However, expression of a caspase-resistant form of fragment N in cardiomyocytes protected them from PN-induced apoptosis. Our results indicate that the antiapoptotic pathway activated by fragment N is effective at inhibiting PN-induced apoptosis (as seen when cardiomyocytes express a caspase-3-resistant form of fragment N) but because fragment N is too transiently generated in response to PN, no survival response is effectively produced. This may explain the marked deleterious consequences of PN generation in various organs, including the heart.

© 2012 Elsevier Inc. All rights reserved.

Introduction

Peroxynitrite (PN)¹, the product of superoxide-mediated nitric oxide oxidation, has toxic and damaging effects in cells [1]. PN-induced cellular damage is mediated by protein nitration and oxidation of tyrosine residues, antioxidant depletion (e.g., inactivation of glutathione peroxidase), and modifications of DNA bases [2]. This has an impact on the modulation of several signal transduction pathways including the phosphoinositide 3-kinase/Akt pathway and mitogen-activated protein kinase pathway [3,4]. PN can also lead to executioner caspase activation and apoptosis [5–8]. PN generation plays an important role in oxidative and nitrosative stress in various pathophysiological situations, including myocardial injury, heart failure, and cardiomyopathy [9].

RasGAP is a ubiquitously expressed, multidomain protein that acts as a regulator of Ras and Rho GTP-binding proteins. RasGAP

contains two conserved caspase-3 cleavage sites [10]. At low caspase-3 activity levels, RasGAP is cleaved at position 455. The resulting N-terminal fragment (fragment N) activates a potent antiapoptotic signaling pathway mediated by the Ras/PI3K/Akt pathway [11], which is crucial for cell survival under low stress conditions [12]. However, at higher caspase-3 activity, fragment N is further cleaved at position 157, abrogating its antiapoptotic activity [13]. The fragments resulting from this second cleavage, in particular fragment N2 (RasGAP 158–455), regulate tumor cell death by sensitizing them to anti-cancer treatment-induced apoptosis [13]. Therefore RasGAP acts as a sensor of caspase activity that controls the balance between cell death and survival. Overexpression of an uncleavable form of fragment N in vitro protects various cell types against genotoxins, death receptor ligands, UV-c, staurosporine, and inflammatory cytokines [12,14]. Moreover, transgenic mice expressing fragment N specifically in pancreatic β cells are more resistant against prodiabetogenic conditions and their β cells experience less apoptosis in such situations [15,16].

The capacity of fragment N to protect cells against protein nitration- and oxidation-induced death has not been investigated yet. Here, we have evaluated how PN modulates the formation

Abbreviations: CI, confidence interval; GFP, green fluorescent protein; HRP, horseradish peroxidase; PBS, phosphate-buffered saline; PFA, paraformaldehyde; PN, peroxynitrite

* Corresponding author. Fax: +41 21 692 5505.

E-mail address: Christian.Widmann@unil.ch (C. Widmann).

of fragment N and how efficient fragment N is in counteracting PN-induced cell death.

Materials and methods

Cells

H9C2 cells, a rat heart clonal cell line (ATCC, Manassas, VA, USA) [17], and HEK 293 cells (ATCC; Catalog No. CRL-1573) were grown in Dulbecco's modified Eagle's medium (DMEM; GIBCO) supplemented with 10% fetal calf serum (Invitrogen), 100 U/ml penicillin, and 0.1 mg/ml streptomycin (Sigma). HeLa cells were maintained in RPMI 1640 (GIBCO) containing 10% fetal calf serum. All these cells were cultured at 37 °C and 5% CO₂.

Primary culture of neonatal mouse cardiomyocytes

Hearts were isolated from 1- to 2-day-old newborn mice killed by decapitation and placed on ice in ADS buffer (116 mM NaCl, 20 mM Hepes, 5.4 mM KCl, 1 mM NaH₂PO₄, 0.84 mM MgSO₄ · 7H₂O, 5.5 mM glucose). Ventricles without atria were digested in ADS containing 0.45 mg/ml collagenase (Worthington Biochemical Corp.) and 1 mg/ml pancreatin (Invitrogen) as described [18]. Briefly, the tissue homogenates were incubated for 15 min at 37 °C with rocking at 700 rpm. The supernatants were collected and the pellets were subjected to two additional rounds of digestion in 1.5 ml ADS containing collagenase and pancreatin. The supernatants collected from the three digestion rounds were mixed and plated in 10-cm culture dishes (10 ventricles per dish) for two rounds of 45-min differential plating at 37 °C and 10% CO₂. Cells in the supernatants of the first differential plating were collected and replated for the second differential plating. The cells in the supernatants of the second plating were collected, washed once in 5 ml of a 3:1 mixture of DMEM and medium 199 (Invitrogen) supplemented with 10% horse serum (Oxoid), 5% fetal calf serum (Invitrogen), 100 U/ml penicillin, and 0.1 µg/ml streptomycin, and centrifuged for 10 min at 192 g at room temperature. Seventy-five thousand cells were seeded onto 0.1% gelatin-coated 24-well plates.

Chemicals and antibodies

Peroxyntirite was supplied as a 50 mM stock in 0.3 M sodium hydroxide (Cayman Chemicals). Hoechst 33342 was from Roche. It was diluted in water at a final concentration of 10 mg/ml and stored at 4 °C in the dark. The anti-RasGAP antibody was from Enzo Life Science (Catalog No. ALX-210-860-R100) and is directed at the fragment N2 moiety of the human protein (amino acids 158–455). The anti-phosphoserine 473–Akt rabbit polyclonal IgG antibody as well as anti-caspase-3 monoclonal antibodies were from Cell Signaling Technology (Catalog Nos. 9271 and 9665, respectively). The mouse polyclonal IgG antibody recognizing sarcomeric α -actinin was from Sigma (Catalog No. A78811). The monoclonal antibody specific for the HA tag was purchased as ascites from Babco (Richmond, CA, USA; Catalog No. MMS-101R). This antibody was adsorbed on HeLa cell lysates to decrease nonspecific binding as previously described [10]. The secondary antibody used in the immunocytochemistry was Cy3-conjugated AffiniPure goat anti-mouse IgG (H+L) from Jackson ImmunoResearch Laboratories. Alexa Fluor 680 goat anti-rabbit IgG (H+L) (Molecular Probes) and IRDye 800-conjugated affinity purified anti-mouse IgG (H+L) (Rockland) were the secondary antibodies used on Western blots. Horseradish peroxidase (HRP)-goat anti-mouse and HRP-goat anti-rabbit antibodies were from Jackson ImmunoResearch. The chemiluminescent HRP substrate was from Witec AG.

Plasmids

HA-hRasGAP[1–455](D157A).liti (No. 353) (previously called N-D157A.liti) is a lentiviral vector encoding the HA-tagged uncleavable form of fragment N [14]. HA-hRasGAP[1–455].liti (No. 769) is a lentiviral vector encoding the HA-tagged wild-type form of fragment N. It was constructed by subcloning the 1423-bp fragment isolated from the BamHI/XhoI digestion of HA-hRasGAP[1–455].dn3 (No. 14) (previously named HA-GAPN.dn3 and described in [10]) into the TRIP-PGK-ATGm-MCS-WHV (No. 349) lentiviral vector opened with the same restriction enzymes. Myr-mAkt1-HA.cmv (No. 249), which encodes a constitutively active form of Akt that bears a Src myristoylation sequence at its N-terminus and an HA tag at its C-terminus, was described earlier under the name myr-Akt.cmv [11]. Plasmid hIkB alpha delta N2.cmv (No. 11) encodes the human $\text{IkB}\alpha$ protein with the Δ N2 deletion (i.e., amino acids 3–71); this construct cannot be phosphorylated by IkB kinases and degraded by the proteasome and therefore functions as an inhibitor of NF- κ B. It has been described before under the name of $\text{IkB}\alpha\Delta$ N2 [11]. The pEGFP-C1 (No. 6) plasmid encoding the green fluorescent protein (GFP) is from Clontech. Stag.dn3 (No. 763) was generated by subcloning the following two oligonucleotides into pcDNA3 (No. 1; Invitrogen) opened with HindIII and XbaI: Oligo 806 [AGCTT (N2–N6 of HindIII site), CCCGGG (SmaI), CCACC (Kozak; N6 of SmaI provides the first nucleotide of the Kozak sequence), ATG (start codon), AAAGAAACCGCTGCTGCTAAATTCGAACGCCAGCACATGGACAGC (S-tag), TAA (stop codon), T (N1 of XbaI site)] and Oligo 807 [CTAGA (N5–N1 of XbaI site), TTA (stop codon), GCTGTCCATGTG CTGGCGTTCGAATTTAGCAGCAGCGTTTCTTT (S-tag), CAT (start codon), GGTGG (Kozak sequence), CCCGGG (SmaI), A (N6 of HindIII site)]. Stag-hRasGAP[158–455].dn3 (No. 754) encodes the S-tagged form of fragment N2 (S-tag-N2) [19].

Lipofectamine transfection

H9C2 cells were cotransfected with a GFP-encoding plasmid in combination with the indicated plasmids using Lipofectamine 2000 (Life Technologies). After transfection, the cells were incubated in serum-containing medium for 48 h at 37 °C, 5% CO₂. At that time, the percentage of GFP-positive H9C2 cells was about 30%.

Apoptosis scoring based on nuclear morphology

Apoptosis was determined by scoring the number of cells displaying pyknotic nuclei as described previously [20].

Apoptosis scoring based on quantitation of cytoplasmic histone-associated DNA fragments

Apoptosis was monitored by quantifying the cytoplasmic histone-associated DNA fragments using Cell Death Detection ELISA Plus from Roche. After the indicated treatments described in Fig. 5, cells in 24-well plates were washed once with ice-cold phosphate-buffered saline (PBS) and then lysed in 200 µl of the kit lysis buffer for 30 min on ice. The lysates were centrifuged at 200g for 10 min. Supernatants contain the cytoplasmic fraction and pellets contain the nuclei and high-molecular-weight non-fragmented DNA. Twenty microliters of the supernatants was transferred to wells of a streptavidin-coated 96-well microplate to which was added 80 µl of an immunoreagent mixture containing two antibodies, a biotin-labeled anti-histone antibody that binds to H1, H2A, H2B, H3, and H4 histones and that will therefore retain histone proteins in the well through biotin-streptavidin binding, and an HRP-labeled anti-DNA-POD antibody that reacts with single- or double-stranded histone-associated DNA. The plates

were then incubated for 2 h at room temperature with gentle shaking (300 rpm). After this incubation period the wells were washed three times with 250 μ l of the incubation buffer, 100 μ l of HRP substrate was added, and the plate was incubated at room temperature for an additional 15- to 20-min period with gentle shaking. The reaction was stopped by adding 100 μ l of stop solution. Absorbance was measured at 405 nm in triplicates. In each experiment a background control (incubation buffer only mixed with the stop solution) and a negative control (untreated cells) were performed. The background value was subtracted from all measurements. An enrichment factor, corresponding to the level of mono- and oligo-nucleosomes released into the cytoplasm, was calculated by dividing the corrected absorbance from the experimental conditions with the corrected negative control value.

Stimulation with PN

Prior stimulation, cells were washed once with PBS. Two milliliter (in the case of 6 well-plates) of freshly prepared PN stimulation buffer (90 mM NaCl, 5 mM KCl, 50 mM Na₂HPO₄, 0.8 mM MgCl₂, 0.2 mM CaCl₂, 5 mM glucose pH 7.4) was then added. PN was delivered to the cells as a single bolus at a 1:100 dilution against one side of the dish, while rapidly swirling the buffer to ensure optimal exposure of the cells to PN, which was used at final concentrations ranging from 12.5 to 500 μ M. The cells were incubated with PN for the indicated periods of time at 37°C. The PN-containing buffer was then replaced with culture medium. The PN concentrations used here are in agreement with those used in previous *in vitro* studies investigating the mechanisms of PN cytotoxicity [4,17,21]. Although such concentrations may appear elevated at first glance, it is noteworthy that, because of the rapid decomposition of PN, the cells are actually exposed to a lower concentration of this agent. Indeed, it has been determined that bolus addition of 50–500 μ M PN to cultured cells resulted in an actual exposure of 5–50 μ M of the oxidant [36,37]. Furthermore, the concentrations of PN used in our study are physiologically relevant, as it has been estimated that the rate of PN generation may reach up to 1 mM min⁻¹ in an inflamed organ such as the lung *in vivo* [38].

Lentiviral infection

Recombinant lentiviruses were produced as described previously [14].

Western blot

Cells were lysed in monoQ-C buffer (70 mM β -glycerophosphate, 0.5% Triton X-100, 2 mM MgCl₂, 100 mM Na₃VO₄, 1 mM dithiothreitol, 20 μ g/ml aprotinin) and protein quantification was performed using the Bradford technique. Equal amounts of proteins were subjected to SDS-PAGE and then transferred onto a nitrocellulose membrane (Bio-Rad Catalog No. 162 0115). The membranes were blocked with TBS-Tween 20 0.1% containing 5% nonfat milk and incubated overnight at 4 °C with the specific primary antibodies. Blots were then washed with TBS-Tween 0.1%, incubated with the appropriate secondary antibody (1:5000 dilution) 1 h at room temperature, and subsequently visualized and quantified with the Odyssey infrared imaging system (Li-Cor Biosciences, Bad Homburg, Germany) or with the Chemidoc XRS+ system (Bio-Rad Laboratories). In some instances, the blots were stripped and reprobed. This was performed by incubating the blots at 50 °C for 30 min in stripping buffer (62.5 mM Tris-base, 100 mM β -mercaptoethanol, 1% SDS, pH 6.7) followed by three 20-min-long washes at room temperature in TBS-Tween 0.1%.

Immunocytochemistry

Cells were grown on glass coverslips, and 2 day postinfection, the cells were fixed and immunocytochemistry was performed as previously described [22].

Statistical analysis

Results are shown as means \pm 95% confidence interval (CI). The statistical analyses used in this study were one-way ANOVAs and paired Student's *t* test. In the latter case, the difference between the indicated conditions was considered significant when $p < 0.05/n$, where p is the probability derived from the *t* test analysis and n is the number of comparisons done (Bonferroni correction). Statistically significant differences are indicated by asterisks.

Ethics statement

Experiments on the mice were carried out in strict accordance with the Swiss Animal Protection Ordinance (OPAn) and in conformation with Directive 2010/63/EU of the European Parliament. The protocol was approved by the Veterinary Office of the state of Vaud, Switzerland (Approval Reference No. 2185).

Results

Pattern of PN-induced RasGAP cleavage in H9C2 cells

To investigate the pattern of RasGAP cleavage upon PN stimulation, we exposed H9C2 embryonic rat heart myoblast cells [23] to a dose of 250 μ M PN for various periods of time (Fig. 1). Consistent with previous studies [8], starting 2 h poststimulation, PN induced increased levels of caspase-3 activation and apoptotic cell death (Fig. 1A and C). This was accompanied by cleavage of RasGAP into fragments N and N2 (Fig. 1B). In subsequent experiments, the 4-h post-PN-stimulation time point was chosen as it allowed PN to efficiently induce its cellular responses.

Exposure of H9C2 cells to increasing doses of PN induced cleavage of caspase (Fig. 2A) and cleavage of RasGAP into fragment N (Fig. 2B). This correlated with Akt activity induction (Fig. 2D). However, there were no conditions under which fragment N was produced without a concomitant generation of fragment N2 (Fig. 2B). Moreover, fragment N production did not correlate with cell survival (Fig. 2C) and caspase-3 activation (Fig. 2A). These results indicate that PN is not able to induce sequential cleavage of RasGAP and accumulation of fragment N in H9C2 cells that would result in a cell protection response.

Cisplatin induces sequential cleavage of RasGAP in H9C2 cells

The absence of sequential cleavage of RasGAP in PN-treated H9C2 cells could be due to a peculiarity of this cell line. To address this point, H9C2 cells were treated with increasing doses of cisplatin, which is known to induce sequential cleavage of RasGAP in other cell types [12]. Fig. 3B shows that low concentrations of this genotoxin (< 10 μ M) led to fragment N generation in H9C2 cells before fragment N2 was substantially produced and that this correlated with cell survival (Fig. 3C) and mild caspase-3 activation (Fig. 3A). Akt stimulation under these conditions was not increased (Fig. 3D). At higher concentrations of cisplatin (> 10 μ M), fragment N2 levels markedly increased (Fig. 3B), caspase-3 was strongly activated (Fig. 3A), levels of active Akt decreased (Fig. 3D), and apoptosis occurred (Fig. 3C). These results demonstrate that partial cleavage of RasGAP into the

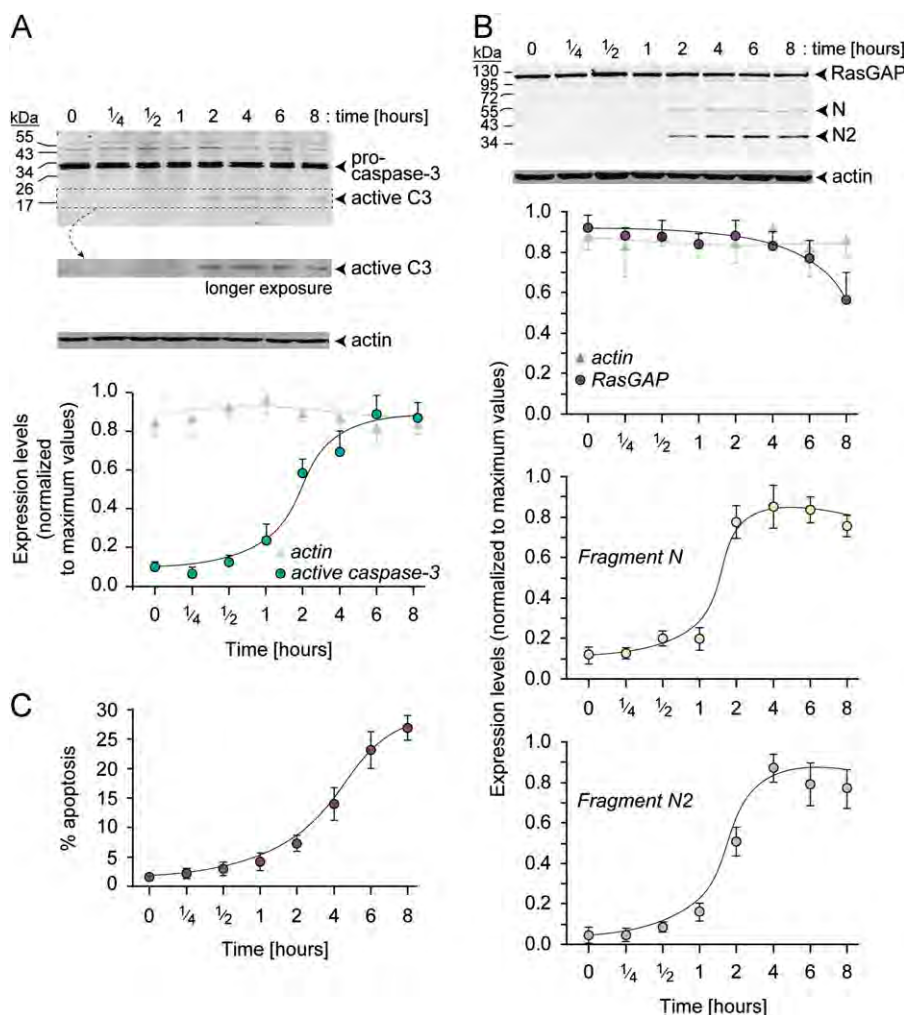


Fig. 1. Apoptosis and RasGAP cleavage kinetics after PN stimulation. One hundred fifty thousand H9C2 cells were seeded in six-well plates and cultured overnight. One day later, the cells were stimulated with 250 μ M PN for 20 min. After PN stimulation, the cells were placed in complete culture medium for the indicated periods of time before being lysed. (A) The levels of caspase-3 activation and (B) the extent of RasGAP cleavage were determined by Western blotting using an antibody recognizing both procaspase-3 and the cleaved, active form of the protease and an antibody recognizing RasGAP fragment N2 sequences, respectively. In both cases, actin levels were also evaluated by reprobing the blots with an actin-specific antibody. The graphs under the blots present the quantitation of the Western blot band intensities normalized to the highest values. (C) Alternatively, the cells were fixed with 2% PFA and apoptosis was determined by scoring cells with pyknotic or fragmented nucleus. Data correspond to the means \pm 95% CI of three independent experiments.

antiapoptotic RasGAP fragment N can occur in H9C2 cells as seen in other cell types [12].

PN induces RasGAP cleavage in a nonsequential manner

To assess whether the inability of PN to induce a sequential cleavage of RasGAP could be observed in cell types other than H9C2 cells, HeLa cells were treated with increasing concentrations of this compound. PN induced a similar pattern of caspase-3 activation, RasGAP cleavage, increased Akt activation, and apoptosis in HeLa cells compared to H9C2 cells (Fig. 4). These results indicate that when PN induces the cleavage of RasGAP and fragment N generation, fragment N is rapidly processed further into smaller fragments. Hence, there are no concentrations of PN that preferentially generate fragment N and that correlate with cell survival, low caspase-3 activity, and Akt activation.

Ectopic expression of a caspase-resistant form of fragment N protects cardiomyocytes from PN-induced apoptosis

One possibility to explain the lack of protection mediated by the endogenously generated fragment N in response to PN is its

rapid cleavage. Therefore, if fragment N were not degraded, it could counteract PN-induced death. To test this possibility, wild-type fragment N and the uncleavable D157A form were ectopically expressed in H9C2 cells (Fig. 5A) before they were challenged with low and high PN concentrations. As hypothesized, wild-type fragment N was degraded in response to PN stimulation, whereas the cleavage-resistant mutant was not (Fig. 5B and C). Overexpression of both fragment N forms inhibited caspase-3 activation and apoptosis induced by low PN concentration (50 μ M) (Fig. 5B and D), although for apoptosis this did not reach statistical significance in the case of wild-type fragment N (Fig. 5D). At high PN concentration (250 μ M), only the D157A fragment N mutant inhibited caspase-3 activation and apoptosis (Fig. 5B and D), indicating that fragment N, if not degraded, efficiently protects cells against PN-induced death.

Fragment N has been shown to activate the prosurvival Akt kinase [11]. To investigate the prosurvival signals induced by fragment N in cardiomyocytes stimulated or not with PN, we monitored the levels of Akt-Ser 473 phosphorylation under conditions where the wild-type and uncleavable D157A forms of fragment N were overexpressed. As expected in control H9C2 cells (i.e., cells not stimulated with PN), both forms of fragment N

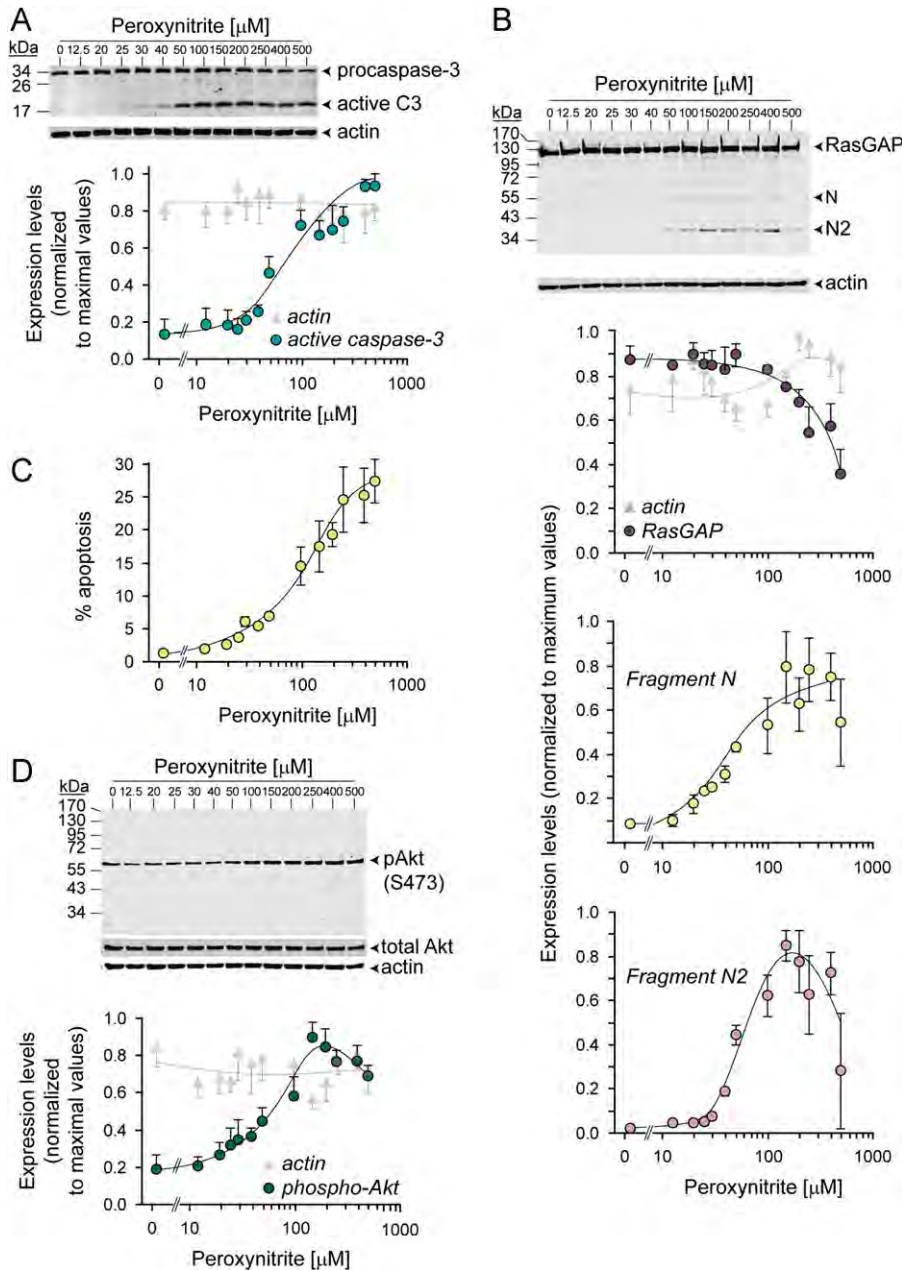


Fig. 2. PN does not induce sequential cleavage of RasGAP in H9C2 cells. H9C2 cells were treated as for Fig. 1 with the indicated PN concentrations for 20 min. After PN stimulation, the cells were placed in complete culture medium for an additional 4-h period before being lysed. (A) Caspase-3 activation, (B) RasGAP cleavage, and (C) apoptosis were assessed as described for Fig. 1. (D) Akt activation was investigated by Western blot analysis using a phosphoserine 473–Akt-specific antibody. The blot was re-probed with an actin-specific antibody. Finally, the blot was stripped and probed with an antibody recognizing total Akt. Quantitation of the Western blot band intensities for caspase-3 and RasGAP was performed as for Fig. 1. Phospho-Akt band intensities were normalized to the total Akt intensities and the resulting ratios were normalized to the highest values. Results correspond to the means \pm 95% CI of three independent experiments.

stimulated Akt phosphorylation (Fig. 5B; compare the 0 μM lanes). PN was found, as reported earlier [4,24], to promote Akt–Ser 473 phosphorylation (Fig. 5B; first three lanes). However, in the presence of 50 μM PN, Akt activation was more pronounced in H9C2 cells overexpressing fragment N (Fig. 5B; compare the 50 μM lanes). In the presence of 250 μM PN, Akt was strongly stimulated and no further increase was seen upon overexpression of fragment N (Fig. 5B; compare the 250 μM lanes).

To clarify the potential role of Akt in protecting cardiomyocytes against PN, H9C2 cells were transfected with a myristoylated constitutively active form of Akt (myr-Akt) and their sensitivity to PN-induced apoptosis was monitored. The myr-Akt protein was, as expected from its constitutive activity, phosphorylated on Ser 473

(Fig. 5E) and was able to inhibit apoptosis induced by low PN concentrations (50 μM). However, at high PN concentrations (250 μM), myr-Akt no longer protected cells (Fig. 5E). These results suggest that Akt activation can mediate the protection induced by fragment N in cardiomyocytes subjected to low concentrations of PN but that there are other prosurvival signals activated by fragment N that allow cardiomyocyte survival at high PN concentrations.

One possibility that could explain the differential capacity of wild-type fragment N and the D157A form of the fragment to protect cardiomyocytes is that the former can be cleaved into smaller fragments (e.g., fragment N2), which have been shown to sensitize tumor cells to apoptosis induced by various stimuli [13,25,26]. We therefore determined whether fragment N2 can

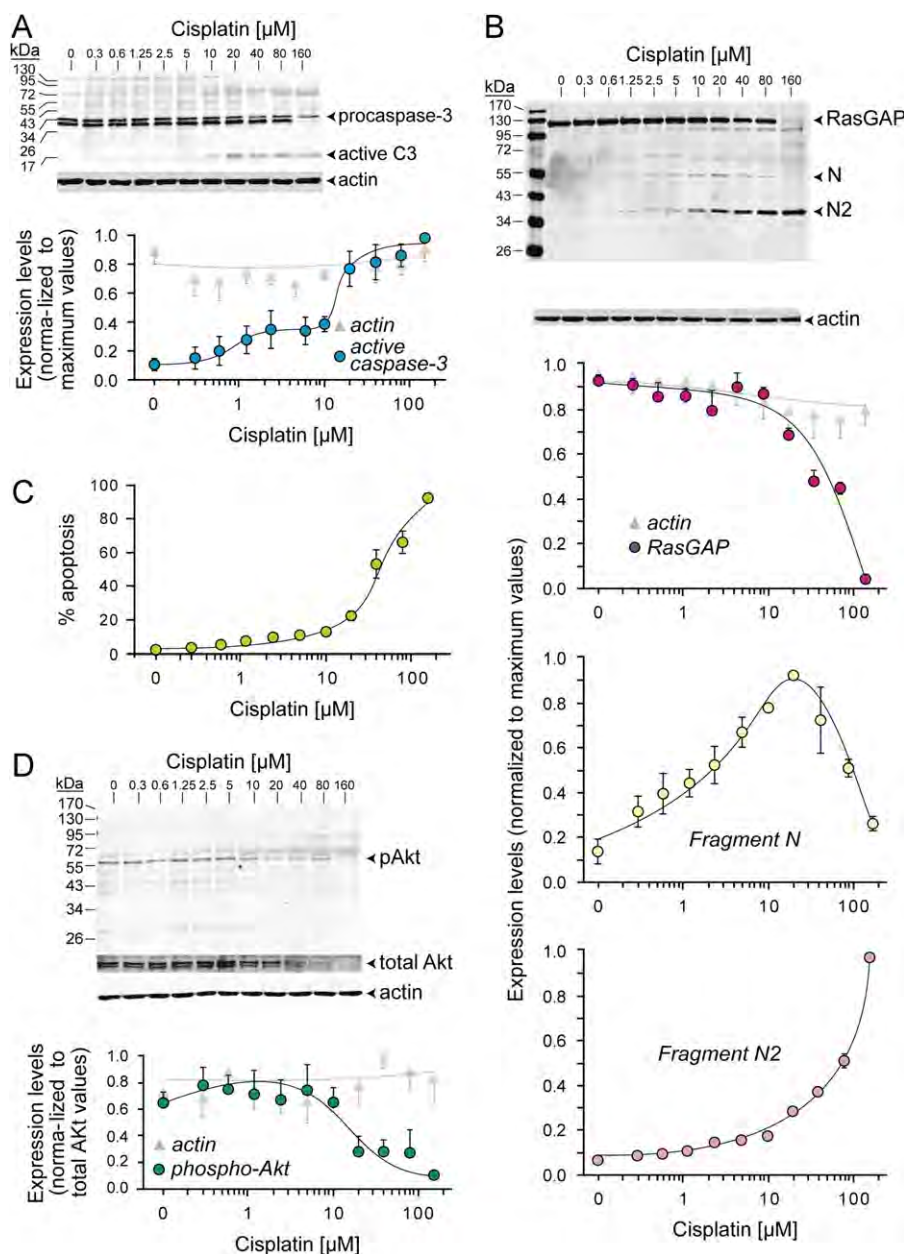


Fig. 3. Cisplatin induces a sequential cleavage of RasGAP in cardiac cells. H9C2 cells were seeded and cultured as for Fig. 1. The cells were then incubated with the indicated concentrations of cisplatin for 24 h. (A) Caspase-3 activation, (B) RasGAP cleavage, (C) apoptosis, and (D) Akt activation were assessed as described for Fig. 2.

sensitize H9C2 cells, which despite having been immortalized are, however, not tumor cells [23], to PN-induced apoptosis. Fig. 5F shows that ectopic expression of fragment N2 in H9C2 cells did not modulate their sensitivity to PN-induced death. This indicates that the lower capacity of fragment N to protect cardiomyocytes from PN-induced apoptosis compared to the uncleavable fragment N mutant probably results from its degradation rather than the generation of proapoptotic fragments such as N2.

Finally, we investigated whether fragment N was able to protect primary cardiomyocytes, the purity of which was assessed by α -actinin staining (Fig. 6A). Ectopic expression of wild-type fragment N and the D157A caspase-resistant form of the fragment both led to Akt activation in primary cardiomyocytes (Fig. 6B; compare the 0 μM lanes). Wild-type fragment N inhibited caspase-3 activation in primary cardiomyocytes stimulated with low, but not high, concentrations of PN. In contrast, the D157A fragment N mutant was able to efficiently reduce caspase-3 activation even at high PN

concentrations. This ability of the D157A form of fragment N to inhibit caspase-3 activation was associated with a marked reduction in PN-induced primary cardiomyocyte apoptosis (Fig. 6C and D). Thus, the pathways activated by fragment N are able to efficiently protect cardiac cells from PN-induced cell death.

Discussion

Earlier work has shown that RasGAP is cleaved by caspase-3 sequentially in response to increasing concentrations or doses of stress-inducing agents. This was seen in various cell types exposed to cisplatin, UV light, Fas ligand, and doxorubicin [12,13]. In contrast we provide evidence here that PN does not promote sequential cleavage of RasGAP whether the cells used are of cardiomyocyte origin or not. No concentration of PN was found that would lead to the partial cleavage of RasGAP into fragment N

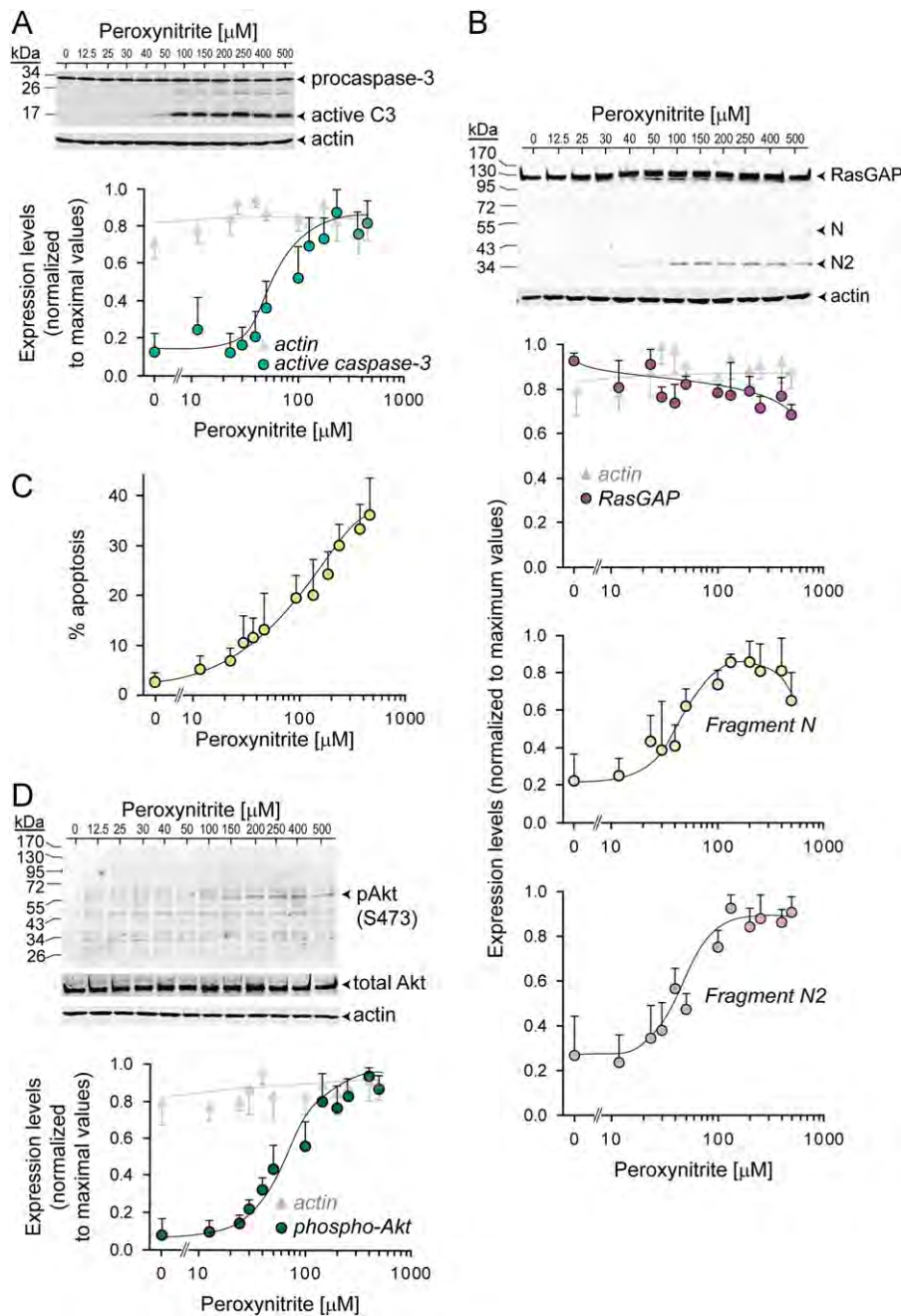


Fig. 4. PN does not induce sequential cleavage of RasGAP in HeLa cells. HeLa cells were treated and analyzed as described for H9C2 cells in the legend to Fig. 2.

and that would be associated with cell survival. Fragment N was generated in cells treated with PN but was apparently immediately degraded further into smaller fragments (N1 and N2) that cannot activate the Akt protective pathway [13]. When the wild-type form of fragment N was ectopically expressed in cells, it failed to inhibit PN-induced apoptosis and this was associated with its degradation. In contrast, a caspase-resistant form of fragment N efficiently protected immortalized (Fig. 5) and primary cardiomyocytes (Fig. 6) against PN-induced death. The antiapoptotic signals generated by fragment N are therefore able to counteract apoptosis induced by PN in cells.

PN has a short half life, ~ 1.9 s at pH 7.4 [27], yet it induces potent and adverse effects on cellular processes by modulating signal transduction pathways involving Akt, MAPKs (ERK, cJNK, p38), protein kinase C, and NF- κ B (reviewed in [3]). Moreover, PN has the potential to activate multiple caspases including caspase-2,

-3, -6, -7, -8, and -9 and thus the cleavage of key cellular proteins such as poly(ADP-ribose) polymerase and lamins [5]. Considering these broad effects on multiple cellular targets, it appears that upon PN stimulation, caspase activation is an all-or-nothing phenomenon. Indeed, PN induces a monophasic caspase-3 activation in which fragment N and fragment N2 are concomitantly produced and apoptosis occurs (Figs. 2 and 4). This contrasts with the situation observed with cisplatin, which induces a biphasic caspase-3 activation: the first phase (low activation) associated with fragment N production, no formation of fragment N2, and cell survival; the second phase (high activation) associated with fragment N degradation into fragment N2 and apoptosis (Fig. 3).

Interestingly, Akt, the PI3K effector kinase that has been demonstrated to mediate fragment N-induced antiapoptotic responses [11,12,14–16], is strongly activated by PN. The ability of PN to modulate Akt is poorly understood. In some cell types

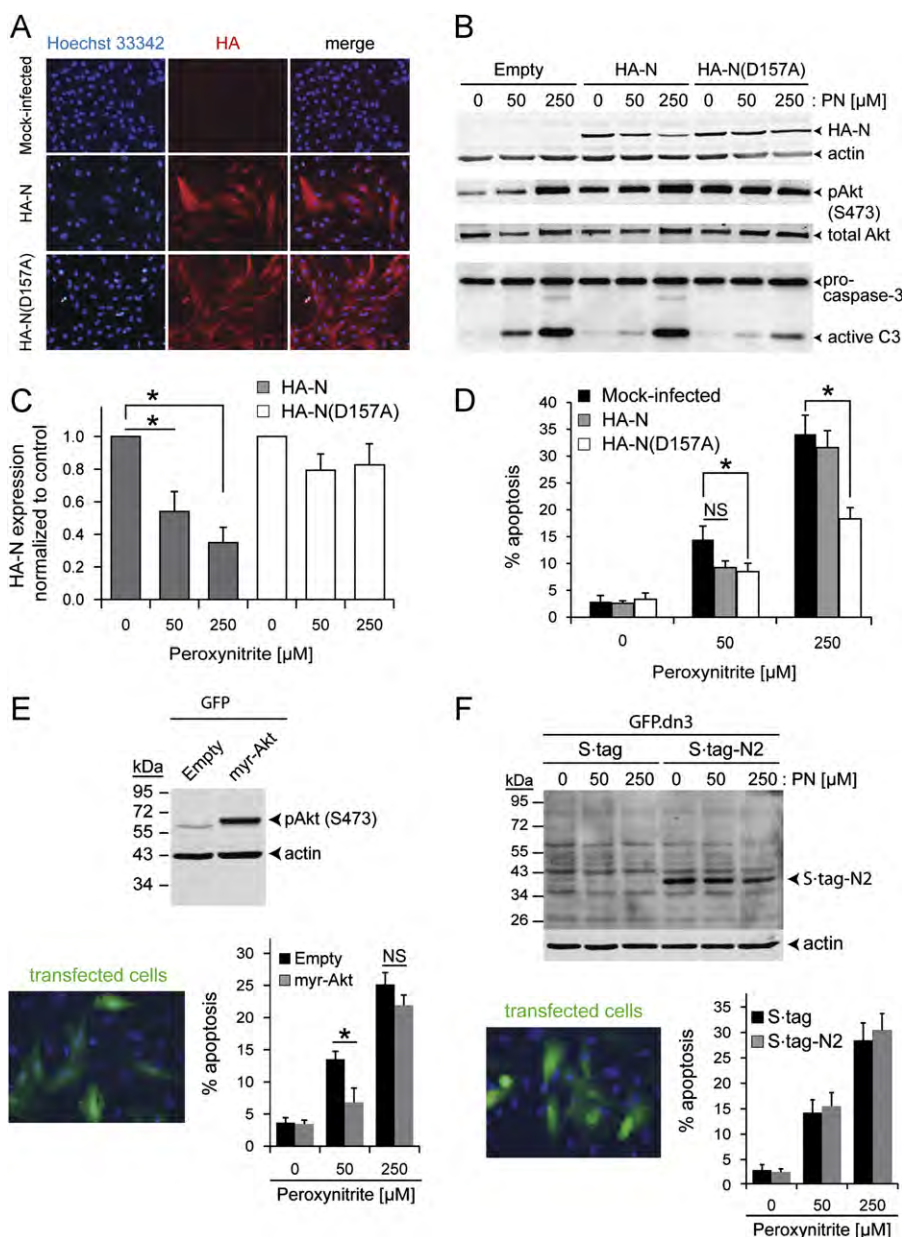


Fig. 5. Fragment N-mediated protection against PN in H9C2 cells. H9C2 cells (80,000) were infected with an empty lentivirus or with lentiviruses encoding the HA-tagged wild-type form (HA-N) or the caspase-resistant D157A form [HA-N(D157A)] of fragment N. (A) Three days after infection the efficiency of fragment N expression was determined by immunocytochemistry. About 85% of the cells were found to express fragment N. (B) The cells were stimulated for 20 min with the indicated concentrations of PN and incubated for a further 7-h period and then starved for 1 h in serum-free medium to ensure low basal Akt-Ser 473 phosphorylation. Finally the cells were lysed and expression of HA-tagged fragment N, the phosphorylation of Akt at serine 473, and caspase-3 cleavage were assessed by Western blotting using the indicated antibodies. (C) The expression levels of HA-N and HA-N(D157A) were normalized to actin and further normalized to the expression value of control cells (0 μM PN). (D) Alternatively, 3 day postinfection, the cells were treated as indicated for (B). The cells were then fixed and the percentage of apoptotic cells was determined. (E) Overexpression of a constitutively active Akt form protects cardiomyocytes against apoptosis induced by intermediate PN doses. H9C2 cells (150,000) were cotransfected with a GFP-expressing plasmid and either an empty vector or a plasmid encoding the constitutively active myr-Akt construct. The expression levels of activated Akt were detected by Western blotting as indicated for Fig. 2. Alternatively the transfected cells were treated with the indicated concentrations of PN for 4 h and apoptosis was then scored in GFP-positive cells. (F) Fragment N2 has no effect on PN-induced apoptosis. H9C2 cells (150,000) were cotransfected with a GFP-expressing plasmid in combination with S-tag- or S-tag-N2-expressing plasmids. S-tag-N2 expression levels were detected by immunoblotting using HRP-conjugated S-protein. Alternatively the transfected cells were treated with the indicated concentrations of PN for 4 h and then apoptosis was scored in GFP-expressing cells. Results in (C–F) correspond to the means \pm 95% CI of three independent experiments performed once each (C and D) or in duplicate (E and F). Statistical significance was assessed by one-way ANOVA.

(pheochromocytoma cells, endothelial cells, macrophages), PN was shown to efficiently inhibit Akt, whereas in others PN exposure resulted in strong stimulation of the kinase (skin fibroblasts, hepatoma cell lines, neural cells) [3,28]. It is suggested that it is the nitration capacity of PN that induces Akt inhibition and it is its oxidative property that mediates Akt activation [3,28]. Our results indicate that cardiomyocytes and HeLa cells fall in the second category, as PN activates Akt in these cells. Nevertheless, activation

of Akt by PN in cardiac cells does not impede apoptosis and may therefore represent a futile protection attempt. Yet, expression of a constitutively active form of Akt in cardiomyocytes inhibits apoptosis induced by low concentrations of PN (Fig. 5E). This could therefore be one mechanism used by fragment N to protect cardiomyocytes when the surrounding concentrations of PN are not too elevated. However, fragment N apparently uses additional means to inhibit apoptosis of cardiomyocytes exposed to high

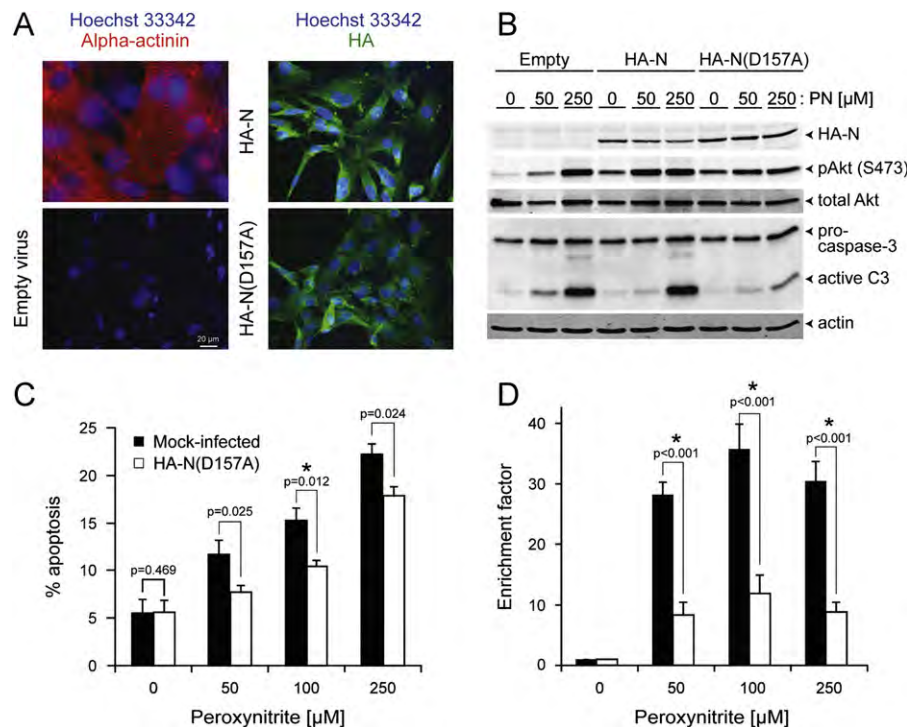


Fig. 6. A caspase-resistant fragment N protects primary cardiomyocytes from PN-induced apoptosis. Seventy-five thousand primary cardiomyocytes were seeded in 24-well plates and cultured for 3 day. (A) The cells were then infected with an empty lentivirus or with lentiviruses encoding the HA-tagged wild-type form (HA-N) or the caspase-resistant D157A form [HA-N(D157A)] of fragment N. The purity of the cardiomyocyte preparation was monitored by immunocytochemistry using an α -actinin-specific antibody, and the efficiency of fragment N expression was assessed by determining the percentage of HA-positive cells. (B) The cells were stimulated for 40 min with the indicated concentrations of PN and then treated and analyzed as indicated for Fig. 5B. Alternatively, the infected cardiomyocytes were left untreated or stimulated for 40 min with 50, 100, or 250 μ M PN. Eight hours later, apoptosis was determined (C) by scoring the percentage of cells with pyknotic or fragmented nuclei or (D) by measuring the extent of DNA-coated histones released from nuclei. Results correspond to the means \pm 95% CI of three independent experiments performed in triplicates. The indicated p values were derived from paired t tests. Asterisks indicate statistically significant differences after Bonferroni corrections.

concentrations of PN because the active form of Akt does not inhibit apoptosis under these conditions (Fig. 5E). Hence, signaling pathways other than, or in parallel to, Akt activation could participate in the protection mediated by caspase-resistant forms of fragment N in cardiac cells. The NF- κ B transcription factor is a downstream target of Akt [29,30]. However, in the presence of fragment N, Akt-mediated NF- κ B activation is inhibited [11,14,16]. NF- κ B activation leads to cell death of β cells [31] and the KB epithelial carcinoma cell line [32]. In the heart the role of NF- κ B is controversial, as it may convey both pro- and antiapoptotic signals [33]. Nevertheless, recent data are consistent with a detrimental role of NF- κ B in heart failure [34]. NF- κ B inhibition might be the other signaling event required for fragment N to protect cardiomyocytes as recently shown in pancreatic β cells [16]. However, inhibition of the NF- κ B pathway did not alter cardiac cell apoptosis induced by either low or high concentrations of PN (Supplementary Fig. S1). This would suggest that fragment N does not use its NF- κ B inhibitory capacity to protect cardiomyocytes against PN-induced death. It cannot, however, be excluded that it is the interplay between Akt activation and NF- κ B inhibition generated by fragment N that induces a more potent survival response than when Akt and NF- κ B are regulated separately. The protective pathways regulated by fragment N need to be better characterized as they represent potential targets for the development of cardiac-protective therapies.

The loss of adult cardiomyocytes by necrosis or apoptosis is a major factor in the initiation and progression of heart failure, as it contributes to the decline in myocardium function [35]. This process is mediated at least in part by PN, which has emerged as a key mediator of cardiomyocyte injury in numerous cardiac pathologies, including myocardial ischemia-reperfusion injury, myocarditis, cardiac allograft rejection, and anthracycline-

induced cardiomyopathy (see [28] for an extended review on this topic). In such conditions, multiple molecular mechanisms have been shown to contribute to peroxynitrite-mediated cytotoxicity, ultimately resulting in the demise of cardiac myocytes, via both the necrotic and the apoptotic pathways [10]. Therefore, in light of our current in vitro findings, future in vivo studies should be designed to assess the importance of fragment N cleavage by PN as a contributing mechanism to cardiomyocyte death in the aforementioned pathological conditions.

Acknowledgments

This work was supported by a grant from CardioMet (Centre des maladies cardio-vasculaires et métaboliques; University of Lausanne and Centre Hospitalier Universitaire Vaudois) (to L.L. and C.W.) and by Swiss National Science Foundation Grants 31003A_119876 and 31003A_141242/1 (to C.W.) and 310030_135394/1 (to L.L.). We thank Sandra Levrand for her technical support.

Appendix A. Supporting information

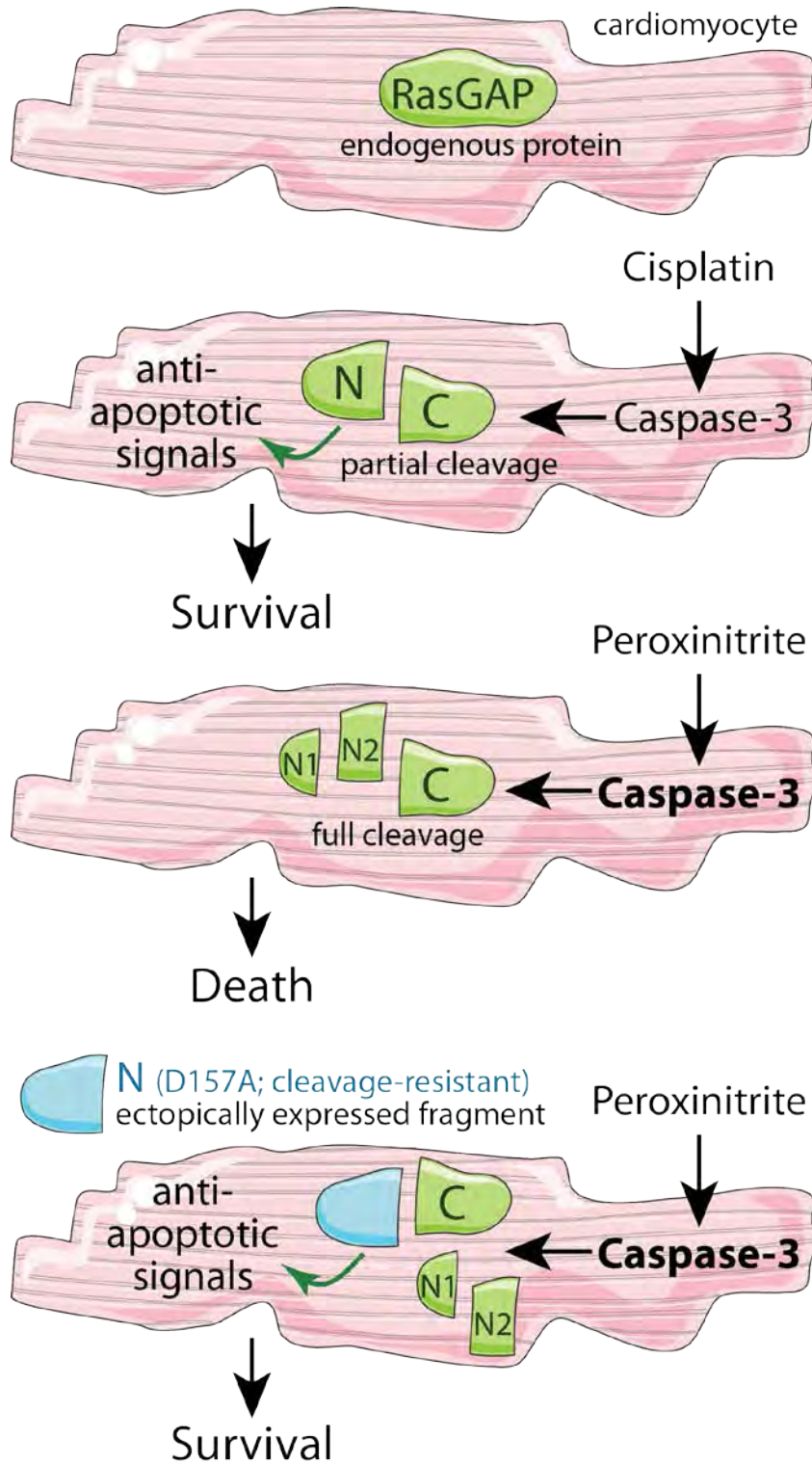
Supplementary data associated with this article can be found in the online version at <http://dx.doi.org/10.1016/j.freeradbiomed.2012.06.011>.

References

- [1] Beckman, J. S.; Koppenol, W. H. Nitric oxide, superoxide, and peroxynitrite: the good, the bad, and ugly. *Am. J. Physiol.* **271**:C1424–C1437; 1996.

- [2] Ducrocq, C.; Blanchard, B.; Pignatelli, B.; Ohshima, H. Peroxynitrite: an endogenous oxidizing and nitrating agent. *Cell. Mol. Life Sci.* **55**:1068–1077; 1999.
- [3] Liaudet, L.; Vassalli, G.; Pacher, P. Role of peroxynitrite in the redox regulation of cell signal transduction pathways. *Front. Biosci.* **14**:4809–4814; 2009.
- [4] Klotz, L. O.; Schieke, S. M.; Sies, H.; Holbrook, N. J. Peroxynitrite activates the phosphoinositide 3-kinase/Akt pathway in human skin primary fibroblasts. *Biochem. J.* **352**:219–225; 2000.
- [5] Zhuang, S.; Simon, G. Peroxynitrite-induced apoptosis involves activation of multiple caspases in HL-60 cells. *Am. J. Physiol. Cell Physiol.* **279**:C341–C351; 2000.
- [6] Zhang, Y.; Wang, H.; Li, J.; Jimenez, D. A.; Levitan, E. S.; Aizenman, E., et al. Peroxynitrite-induced neuronal apoptosis is mediated by intracellular zinc release and 12-lipoxygenase activation. *J. Neurosci.* **24**:10616–10627; 2004.
- [7] Virag, L.; Scott, G. S.; Cuzzocrea, S.; Marmer, D.; Salzman, A. L.; Szabo, C. Peroxynitrite-induced thymocyte apoptosis: the role of caspases and poly (ADP-ribose) synthetase (PARS) activation. *Immunology* **94**:345–355; 1998.
- [8] Levrand, S.; Vannay-Bouchiche, C.; Pesse, B.; Pacher, P.; Feihl, F.; Waeber, B., et al. Peroxynitrite is a major trigger of cardiomyocyte apoptosis in vitro and in vivo. *Free Radic. Biol. Med.* **41**:886–895; 2006.
- [9] Pacher, P.; Schulz, R.; Liaudet, L.; Szabo, C. Nitrosative stress and pharmacological modulation of heart failure. *Trends Pharmacol. Sci.* **26**:302–310; 2005.
- [10] Yang, J. -Y.; Widmann, C. Antiapoptotic signaling generated by caspase-induced cleavage of RasGAP. *Mol. Cell. Biol.* **21**:5346–5358; 2001.
- [11] Yang, J. -Y.; Widmann, C. The RasGAP N-terminal fragment generated by caspase cleavage protects cells in a Ras/PI3K/Akt-dependent manner that does not rely on NFκB activation. *J. Biol. Chem.* **277**:14641–14666; 2002.
- [12] Yang, J. -Y.; Michod, D.; Walicki, J.; Murphy, B. M.; Kasibhatla, S.; Martin, S., et al. Partial cleavage of RasGAP by caspases is required for cell survival in mild stress conditions. *Mol. Cell. Biol.* **24**:10425–10436; 2004.
- [13] Yang, J. -Y.; Walicki, J.; Michod, D.; Dubuis, G.; Widmann, C. Impaired Akt activity down-modulation, caspase-3 activation, and apoptosis in cells expressing a caspase-resistant mutant of RasGAP at position 157. *Mol. Biol. Cell.* **16**:3511–3520; 2005.
- [14] Yang, J. -Y.; Walicki, J.; Abderrahmani, A.; Cornu, M.; Waeber, G.; Thorens, B., et al. Expression of an uncleavable N-terminal RasGAP fragment in insulin-secreting cells increases their resistance toward apoptotic stimuli without affecting their glucose-induced insulin secretion. *J. Biol. Chem.* **280**:32835–32842; 2005.
- [15] Yang, J. Y.; Walicki, J.; Jaccard, E.; Dubuis, G.; Bulat, N.; Hornung, J. P., et al. Expression of the NH2-terminal fragment of RasGAP in pancreatic β-cells increases their resistance to stresses and protects mice from diabetes. *Diabetes* **58**:2596–2606; 2009.
- [16] Bulat, N.; Jaccard, E.; Peltzer, N.; Khalil, H.; Yang, J. Y.; Dubuis, G., et al. RasGAP-derived fragment N increases the resistance of beta cells towards apoptosis in NOD mice and delays the progression from mild to overt diabetes. *PLoS One* **6**:e22609; 2011.
- [17] Levrand, S.; Pesse, B.; Feihl, F.; Waeber, B.; Pacher, P.; Rolli, J., et al. Peroxynitrite is a potent inhibitor of NFκB activation triggered by inflammatory stimuli in cardiac and endothelial cell lines. *J. Biol. Chem.* **280**:34878–34887; 2005.
- [18] Rosenblatt-Velin, N.; Lepore, M. G.; Cartoni, C.; Beermann, F.; Pedrazzini, T. FGF-2 controls the differentiation of resident cardiac precursors into functional cardiomyocytes. *J. Clin. Invest.* **115**:1724–1733; 2005.
- [19] Annibaldi, A.; Dousse, A.; Martin, S.; Tazi, J.; Widmann, C. Revisiting G3BP1 as a RasGAP binding protein: sensitization of tumor cells to chemotherapy by the RasGAP 3127–326 sequence does not involve G3BP1. *PLoS One* **6**:e29024; 2011.
- [20] Michod, D.; Widmann, C. TAT-RasGAP317–326 requires p53 and PUMA to sensitize tumor cells to genotoxins. *Mol. Cancer Res.* **5**:497–507; 2007.
- [21] Pesse, B.; Levrand, S.; Feihl, F.; Waeber, B.; Gavillet, B.; Pacher, P., et al. Peroxynitrite activates ERK via Raf-1 and MEK, independently from EGF receptor and p21Ras in H9C2 cardiomyocytes. *J. Mol. Cell. Cardiol.* **38**:765–775; 2005.
- [22] Annibaldi, A.; Michod, D.; Vanetta, L.; Cruchet, S.; Nicod, P.; Dubuis, G., et al. Role of the sub-cellular localization of RasGAP fragment N2 for its ability to sensitize cancer cells to genotoxin-induced apoptosis. *Exp. Cell Res.* **315**:2081–2091; 2009.
- [23] Kimes, B. W.; Brandt, B. L. Properties of a clonal muscle cell line from rat heart. *Exp. Cell Res.* **98**:367–381; 1976.
- [24] Delgado-Esteban, M.; Martin-Zanca, D.; Andres-Martin, L.; Almeida, A.; Bolanos, J. P. Inhibition of PTEN by peroxynitrite activates the phosphoinositide-3-kinase/Akt neuroprotective signaling pathway. *J. Neurochem.* **102**:194–205; 2007.
- [25] Michod, D.; Yang, J. Y.; Chen, J.; Bonny, C.; Widmann, C. A RasGAP-derived cell permeable peptide potently enhances genotoxin-induced cytotoxicity in tumor cells. *Oncogene* **23**:8971–8978; 2004.
- [26] Pittet, O.; Petermann, D.; Michod, D.; Krueger, T.; Cheng, C.; Ris, H. B., et al. Effect of the TAT-RasGAP317–326 peptide on apoptosis of human malignant mesothelioma cells and fibroblasts exposed to meso-tetra-hydroxyphenylchlorin and light. *J. Photochem. Photobiol. B* **88**:29–35; 2007.
- [27] Beckman, J. S.; Beckman, T. W.; Chen, J.; Marshall, P. A.; Freeman, B. A. Apparent hydroxyl radical production by peroxynitrite: implications for endothelial injury from nitric oxide and superoxide. *Proc. Natl. Acad. Sci. USA* **87**:1620–1624; 1990.
- [28] Pacher, P.; Beckman, J. S.; Liaudet, L. Nitric oxide and peroxynitrite in health and disease. *Physiol. Rev.* **87**:315–424; 2007.
- [29] Kane, L. P.; Mollenauer, M. N.; Xu, Z.; Turck, C. W.; Weiss, A. Akt-dependent phosphorylation specifically regulates Cot induction of NF-κB-dependent transcription. *Mol. Cell. Biol.* **22**:5962–5974; 2002.
- [30] Ozes, O. N.; Mayo, L. D.; Gustin, J. A.; Pfeffer, S. R.; Pfeffer, L. M.; Donner, D. B. NF-κB activation by tumour necrosis factor requires the Akt serine-threonine kinase. *Nature* **401**:82–85; 1999.
- [31] Eldor, R.; Yeffet, A.; Baum, K.; Doviner, V.; Amar, D.; Ben Neriah, Y., et al. Conditional and specific NF-κB blockade protects pancreatic β cells from diabetogenic agents. *Proc. Natl. Acad. Sci. USA* **103**:5072–5077; 2006.
- [32] Barisic, S.; Strozzyk, E.; Peters, N.; Walczak, H.; Kulms, D. Identification of PP2A as a crucial regulator of the NF-κB feedback loop: its inhibition by UVB turns NF-κB into a pro-apoptotic factor. *Cell Death Differ* **15**:1681–1690; 2008.
- [33] Gordon, J. W.; Shaw, J. A.; Kirshenbaum, L. A. Multiple facets of NF-κB in the heart: to be or not to NF-κB. *Circ. Res.* **108**:1122–1132; 2011.
- [34] Hamid, T.; Guo, S. Z.; Kingery, J. R.; Xiang, X.; Dawn, B.; Prabhu, S. D.; Cardiomyocyte, N. F. - κB p65 promotes adverse remodelling, apoptosis, and endoplasmic reticulum stress in heart failure. *Cardiovasc. Res.* **89**:129–138; 2011.
- [35] Gill, C.; Mestril, R.; Samali, A. Losing heart: the role of apoptosis in heart disease—a novel therapeutic target? *FASEB J.* **16**:135–146; 2002.
- [36] Go, Y. M.; Patel, R. P.; Maland, M. C.; Park, H.; Beckman, J. S.; Darley-Usmar, V. M. Evidence for peroxynitrite as a signaling molecule in flow-dependent activation of c-Jun NH2-terminal kinase. *Am. J. Physiol.* **277**:H1647–H1653; 1999.
- [37] White, R.; Crow, J.; Spear, N.; Thomas, S.; Patel, R.; Green, I. Making and working with peroxynitrite. *Methods Mol. Biol.* **100**:215–230; 1998.
- [38] Ischiropoulos, H.; Zhu, L.; Beckman, J. S. Peroxynitrite formation from macrophage-derived nitric oxide. *Arch. Biochem. Biophys.* **298**:446–451; 1992.

Graphical representation



Supplemental information

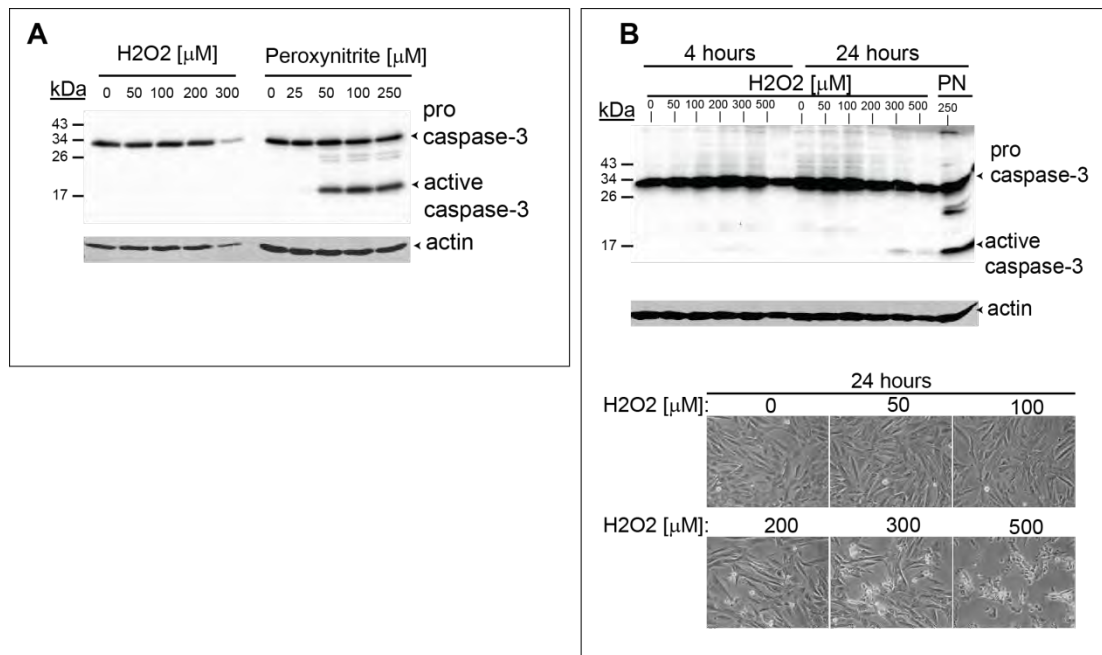


Fig. S1. H₂O₂ induces cellular damage but no or only marginal caspase-3 activation. (A) H9C2 cells (150'000) were treated with the indicated concentrations of H₂O₂ or PN for 4 hours. The cells were then lysed and the levels of caspase-3 cleavage were detected by immune-blotting as described in Figure 1. (B) H9C2 cells were treated as in panel A with H₂O₂ for 4 or 24 hours. Caspase-3 activation was assessed as in panel A. Peroxynitrite (250 μ M) was used as a positive control for caspase-3 activation. Representative images of the cells treated with different concentrations of H₂O₂ are presented under the Western blots.

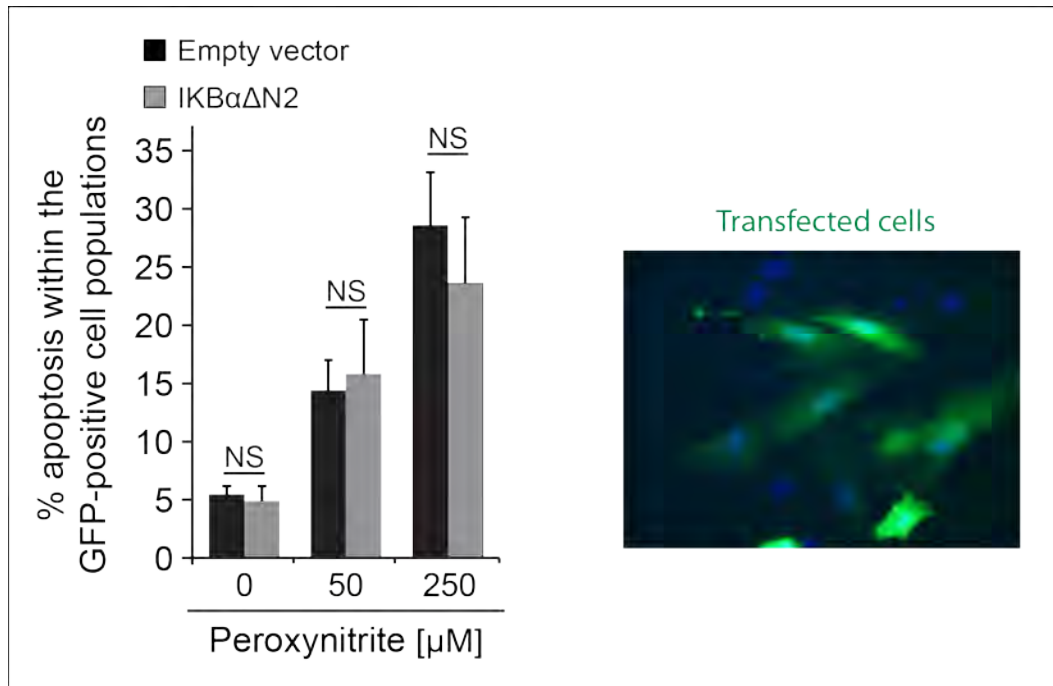


Figure S2

Fig. S2. Inhibition of NF-κB does not affect peroxynitrite-induced apoptosis. H9C2 cells (150'000) were co-transfected with a GFP-expressing plasmid in combination with an empty vector or with an IκBαΔN2-expressing plasmid. The transfected were treated with the indicated concentration of PN for four hours. Apoptosis was then scored in GFP-positive cells. Results correspond to the mean ± 95% CI of quadruplicate determinations. Statistical significance was assessed by one-way ANOVAs (NS, not significant).

3. Results: Part III

1. Introduction

Heart failure represents a major and growing public health concern and it is the leading cause of mortality worldwide. Heart failure is typically induced by a number of common pathology-inducing stimuli such as longstanding hypertension, familial hypertrophic and dilated cardiomyopathies (1;2). Under stress, the heart undergoes a hypertrophic response, which is a compensatory mechanism that aims to improve cardiac contractile function and cardiac output (2;3). Death of cardiomyocytes by necrosis and apoptosis accompanies hypertrophy and represents the irreversible end point of compensatory hypertrophy, which afterwards shifts to heart failure (4-6).

2. Results

Previously we found that, fragment N conserved heart function after doxorubicin-induced cardiotoxicity. Moreover, overexpression of caspase-resistant form of fragment N protected cardiomyocytes against peroxynitrite-induced death. Here we assessed the role of RasGAP cleavage and fragment N generation in protecting the heart against pressure-induced stress. Wild-type and RasGAP KI mice were subjected to transverse aortic arch banding (TAC); the heart parameters were then analyzed by echocardiography at different time points. We found that, the absence of RasGAP cleavage was correlated with exacerbated heart dysfunction. This is summarized by, a drop in the left ventricle contractility and cardiac output, presumably due to the increased myocardial apoptosis and fibrosis.

3. Contribution

The experiments presented in this part are not published yet. Echocardiography measurements were performed by Corrine Berthonneche in the Cardiovascular Assessment Facility (CAF). Real-time qRT-PCR analysis of expression of hypertrophy marker genes was performed by Mohamed Nemir, I partially contributed to these experiments. I was responsible for breeding the mice, and for collecting the tissues after each TAC experiment. I performed the rest of biochemical and histological (Western blot, TUNEL, and fibrosis) analysis and quantifications. I also wrote this manuscript, which was revised by Christian Widmann. Note, this research project is still ongoing.

Reference List

1. Frey,N., and Olson,E.N. 2003. Cardiac hypertrophy: the good, the bad, and the ugly. *Annu Rev Physiol* **65**:45-79.
2. Heineke,J., and Molkentin,J.D. 2006. Regulation of cardiac hypertrophy by intracellular signalling pathways. *Nat Rev Mol Cell Biol* **7**:589-600.
3. Gupta,S., Das,B., and Sen,S. 2007. Cardiac hypertrophy: mechanisms and therapeutic opportunities. *Antioxid. Redox. Signal.* **9**:623-652.
4. Narula,J., Haider,N., Virmani,R., DiSalvo,T.G., Kolodgie,F.D., Hajjar,R.J., Schmidt,U., Semigran,M.J., Dec,G.W., and Khaw,B.A. 1996. Apoptosis in myocytes in end-stage heart failure. *N. Engl. J Med.* **335**:1182-1189.
5. Anversa,P., and Kajstura,J. 1998. Myocyte cell death in the diseased heart. *Circ. Res.* **82**:1231-1233.
6. Fortuno,M.A., Ravassa,S., Fortuno,A., Zalba,G., and Diez,J. 2001. Cardiomyocyte apoptotic cell death in arterial hypertension: mechanisms and potential management. *Hypertension* **38**:1406-1412.

The role RasGAP of cleavage and fragment N generation in heart
protection against pressure-induced overload stress

Hadi Khalil¹, Jiang-Yan Yang¹, Mohamed Nemir², Thierry Pedrazzini²,
and Christian Widmann¹

¹Department of Physiology, Biology and Medicine Faculty, University of Lausanne,
Switzerland; ²Department of Medicine, Experimental Cardiology Unit, University of
Lausanne, Switzerland

Correspondence to Christian Widmann, Department of Physiology, Bugnon 7, 1005
Lausanne, Switzerland, Phone: +41 21 692 5123, Fax: +41 21 692 5505, E-mail:
Christian.Widmann@unil.ch.

1. Introduction

Heart failure is defined as a deficiency in the capability of the heart to adequately pump blood in response to systemic demands. Heart failure represents a major and growing public health concern and it is the leading cause of hospitalization, morbidity, and mortality worldwide. Heart failure is typically induced by a number of common pathology-inducing stimuli including longstanding hypertension, myocardial infarction, valvular insufficiency and stenosis, myocarditis due to an infectious agent, familial hypertrophic and dilated cardiomyopathies, and diabetic cardiomyopathy (1;2). In these cases the myocardium undergoes hypertrophy (excessive growth in size without myocyte proliferation) as a compensatory mechanism to improve the contractile function and cardiac output. Under pathologic conditions, hypertrophy in the adult heart aims to augment pump function and to reduce wall stress (2;3).

In the long term, compensatory cardiac hypertrophy transiently shifts to another phase of pathological hypertrophy that predisposes to heart failure, arrhythmia and sudden death. This transition is accompanied with a decline in the contractile function of the left ventricle associated with a group of myocardial remodeling events marked by reactivation of the fetal gene expression program (4), modifications in the extracellular matrix components leading to myocyte slippage and myocardial fibrosis (5;6), bioenergetically unfavorable changes in contractile protein isoforms, and relative decrease in myocardial vascularization resulting in oxidative stress and death of cardiomyocytes by necrosis and apoptosis (7-9).

Death of cardiomyocytes is the critical irreversible cellular event in the process of left ventricular dysfunction; therefore it would be of extreme interest to define the molecular players that can limit cardiomyocyte cell death. In response to stress, low caspase-3 activities lead to RasGAP cleavage into an amino-terminal fragment called fragment N that efficiently protects a variety of cell types against many different stresses (10). Fragment N-mediated protection is accompanied by the activation of the Ras/PI3K/Akt pathway. Akt is a prosurvival kinase that regulates a variety of downstream targets (refer to introduction for further details). In the heart, expression of the proto-oncogenic serine-threonine kinase is induced by activated Akt. Pim-1 can induce its proliferative signaling but can also mediate cardioprotective effects through

phosphorylation of multiple targets including Bad (11;12). Several mouse models were constructed to decipher the role of Akt activation in heart under various stress conditions. It has been shown for example that cardiac-specific overexpression of myr-Akt (a plasma membrane targeted form of Akt that is therefore constitutively activated), a nuclear targeted form of Akt, as well as E40K-Akt mutant were able to improve cardiac contractile function by decreasing apoptosis and fibrosis (13-15).

It has been shown recently that fragment N protects cardiomyocytes against nitrosative and oxidative stress induced by peroxynitrite (16). Additionally, mice that are unable to cleave RasGAP into fragment N because of a point mutation in RasGAP that destroys its first caspase-3 cleavage site, experience more doxorubicin-induced heart damage and this correlates with a decreased capacity of activating Akt (17)(see also Part I). Here, we have investigated whether generation of fragment N preserves heart function during episodes of myocardial hypertrophy and pressure overload induced by transverse aortic arch constriction (TAC).

2. Results

2.1. Mice that cannot generate fragment N are more susceptible to pressure overload induced-stress

To study the effect of the absence of RasGAP cleavage on cardiac myocytes in pressure overload-induced hypertrophy, wild-type (WT) and RasGAP D455A knock-in (KI) mice were used, the KI mice express mutated alleles of RasGAP that encode a caspase-3-resistant form of the protein. These mice are therefore unable to generate fragment N in response to stress (17). The WT and KI were either sham operated or subjected to trans-aortic constriction (TAC) to induce pressure overload in the left ventricle. As shown earlier, KI mice are viable and fertile, grow normally and show no obvious morphological alterations (Part I, Figure 4). In basal sham conditions, there was no effect of the RasGAP^{D455A} mutation on cardiac parameters (heart rate, cardiac output, aortic velocity and heart weight-to-body weight ratio), as shown by echocardiography measurements performed over an eight week period (Figure 1 and Tables 1, S1 and S2). TAC induced left ventricular hypertrophy that tended to be higher in the KI mice; however this difference did not reach a statistically-significant level (Figure 1F). In TAC-subjected groups interventricular

septal (IVS) dimensions, left ventricular posterior wall (LVPW) thickness, and left ventricular internal diameter (LVID) during systole and diastole, as well as left ventricular mass were comparable in the WT and KI mice (Tables 1, S1 and S2). These results suggest that mice that do not have the capacity to cleave RasGAP experience similar pressure-induced cardiac hypertrophy like WT mice. Strikingly however, a stronger reduction in fractional shortening (%FS) and ejection fraction (%EF) accompanied by a more pronounced decrease in cardiac output and worsened heart dilation, were observed in TAC-subjected KI mice compared to WT controls, which was accompanied by a decrease in cardiac output (Figure 1). Alteration of these parameters is indicative of ventricular remodelling and functional deterioration of the left ventricle, which was evidently exacerbated in KI mice after pressure overload-induced stress.

However, the drop in cardiac output took place while comparable cardiac hypertrophy was observed in TAC-operated mice of both genotypes, suggesting that other pathological alterations such as increased cardiomyocyte death and myocardial fibrosis participated in the exacerbated cardiac dysfunction observed in KI mice hearts.

2.2. Earlier fetal gene reactivation in KI mice stressed hearts

A characteristic feature of hypertrophied heart is the reactivation of the fetal gene program. Hearts exposed to TAC adapt by undergoing a hypertrophic response, which is accompanied by the release of the atrial and brain natriuretic peptides (ANP and BNP respectively), the function of which is to reduce increased blood pressure. Increased ANP and BNP levels represent ventricular hypertrophy and cardiovascular risk (18). ANP and BNP secretion is accompanied by the expression of fetal isoforms of contractile proteins such as α -skeletal actin (ACTA1A) and β -myosin heavy chain (β -MHC) (4;19).

Genotype / treatment	WT Sham	WT TAC	KI Sham	KI TAC
Number of mice	n=8	n=7	n=7	n=9
Body weight (g)	30 ± 4.1	30.61 ± 2.4	30.62 ± 2.6	31.21 ± 1.1
Heart rate (Beats/min)	481 ± 41	491 ± 33	465 ± 29	464 ± 33
IVS;d (mm)	0.76 ± 0.03	1.12 ± 0.09	0.80 ± 0.04	1.10 ± 0.06
IVS;s (mm)	0.981 ± 0.04	1.43 ± 0.12	1.05 ± 0.06	1.35 ± 0.08
LVID;d (mm)	4.14 ± 0.23	4.56 ± 0.27	4.25 ± 0.28	4.50 ± 0.32
LVID;s (mm)	3.13 ± 0.26	3.53 ± 0.2	3.10 ± 0.3	3.79 ± 0.37
LVPW;d (mm)	0.74 ± 0.04	1.09 ± 0.11	0.76 ± 0.33	1.11 ± 0.07
LVPW;s (mm)	0.94 ± 0.05	1.36 ± 0.12	1.04 ± 0.07	1.27 ± 0.06
LVID Trace (CO) (ml/min)	17.93 ± 3.4	20.90 ± 4.4	20.25 ± 3.1	14.28 ± 2.9 *
LVID Trace (SV) (ul)	38 ± 5.6	44 ± 10.3	44 ± 6.7	31 ± 4.6 *
% FS	25 ± 3.8	22 ± 3.6	27 ± 4.5	16 ± 2.9 *
%EF	49 ± 6	45 ± 6	53 ± 7	34 ± 6 *
LV Mass (mg)	116 ± 10	228 ± 35	128 ± 16	225 ± 40
LV Vol;d (ul)	77 ± 10	96 ± 13	82 ± 14	94 ± 17
LV Vol;s (ul)	40 ± 8	53 ± 6	39 ± 11	63 ± 16
HW/BW echo	3.90 ± 0.3	7.47 ± 1.3	4.17 ± 0.5	7.20 ± 2.2
Aortic velocity (mm/s)	715 ± 132	4503 ± 402	826 ± 161	4096 ± 476

Table 1. Echocardiography analysis six weeks after-TAC surgery. The numbers in blue indicate significance between TAC-operated versus Sham mice. (*) p<0.05 between WT and KI mice, n = 7-9 mice per group.

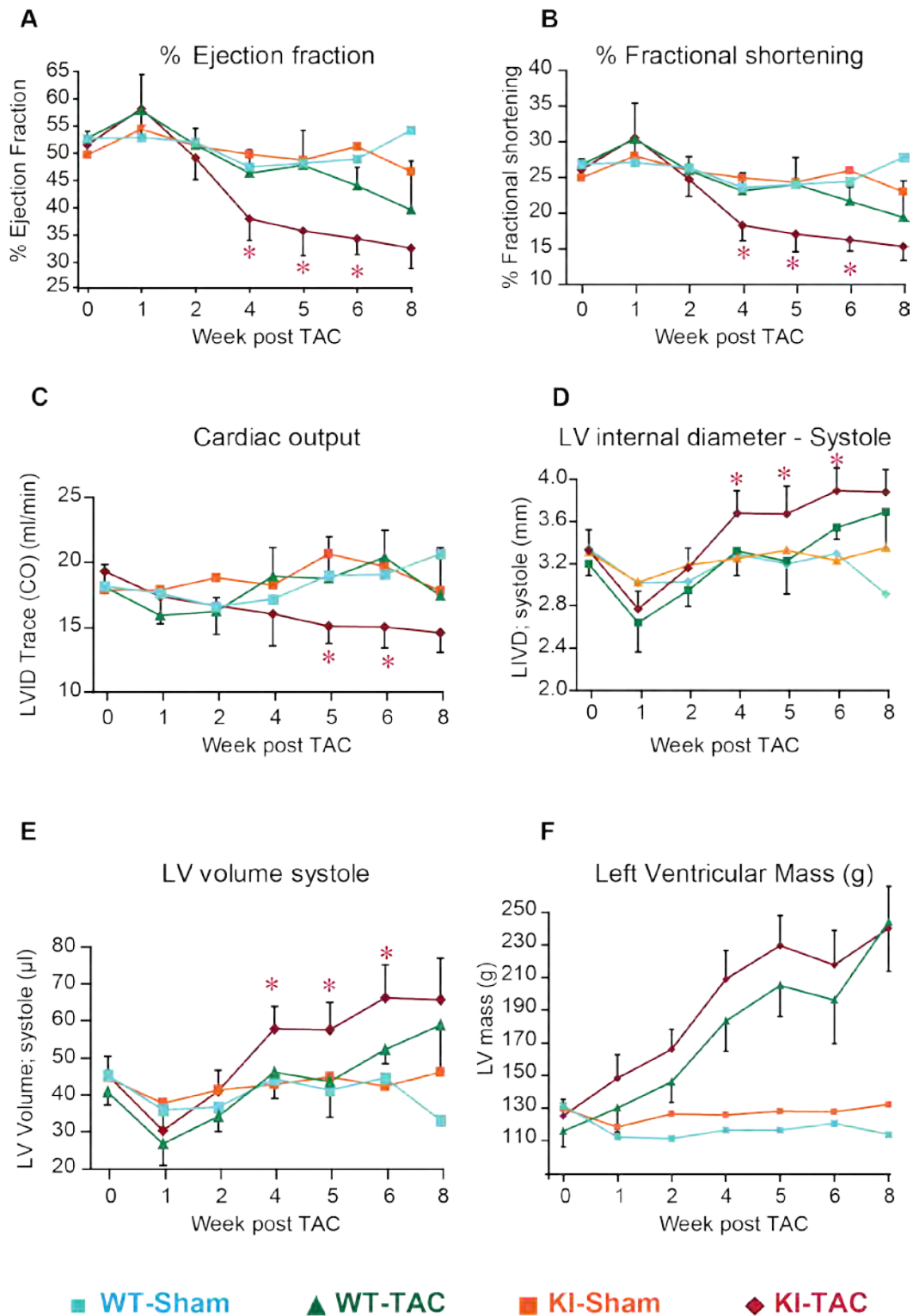


Figure 1. D455A mice experience worsened hear function impairment in response to TAC compared to wild-type mice. The values shown in the figure are extracted from the corresponding echocardiography tables of 5 independent experiments, including table 1, and supplementary tables 1 and 2. **(A, B, C)** Decreased contractility in TAC-operated KI mice. **(D, E)** Increased left ventricular dilation in KI-operated mice. **F.** KI mice tend to show higher signs of left ventricular hypertrophy.

While TAC-operated WT mice showed a non-significant tendency to increase the expression levels of fetal genes compared to sham WT mice two weeks after aortic banding, TAC-subjected KI mice showed significant elevation of fetal gene expression compared to their corresponding KI sham mice (Figure 2A). This indicates that there is stronger myocardial remodeling in KI mice than in WT mice. These results suggest that the KI mice experienced earlier the onset of pressure-induced stress and were therefore undergoing an accelerated myocardial remodeling.

2.3. Increased fibrosis in stressed hearts of KI mice

By inducing cardiac stiffness which alters cardiac contractility, increased cardiac fibrosis contributes to the impairment of cardiac function and correlates with heart failure. Cardiac fibrosis is characterized by excessive deposition of extracellular matrix proteins and inappropriate proliferation of cardiac fibroblasts (20). Heart sections subjected to Van Gieson staining were used to assess the extent of myocardial fibrosis (Figure 2B). Four weeks post TAC; fibrotic lesions were detected in WT and KI mice. Consistent with the echocardiography data and fetal gene reactivation profiles, the TAC-operated KI mice showed a higher percentage of myocardial fibrosis compared to WT mice. This dramatic increase in the areas of fibrotic lesions would increase myocardial stiffness and may explain the reduction in the contractility of the left ventricle and the drop in ejection fraction.

2.4. Increased stress-induced cell death in mice lacking fragment N generation

We have recently shown that the absence of fragment N generation in the KI mice was associated with lower levels of active prosurvival Akt kinase and increased levels of apoptosis in the myocardium of mice injected with doxorubicin (17). In addition, hearts of those mice suffered a decline in the contractility as addressed by a decreased end-systolic elastance. Exacerbated cardiac dysfunction in KI mice subjected to TAC-induced hypertrophy was marked by a drop in left ventricular function, increased expression of fetal genes and higher fibrosis, however with no difference in left ventricular mass. These remodeling events may be explained by increased rates of cardiomyocyte cell death (9;21) with subsequent appearance of fibrotic lesions.

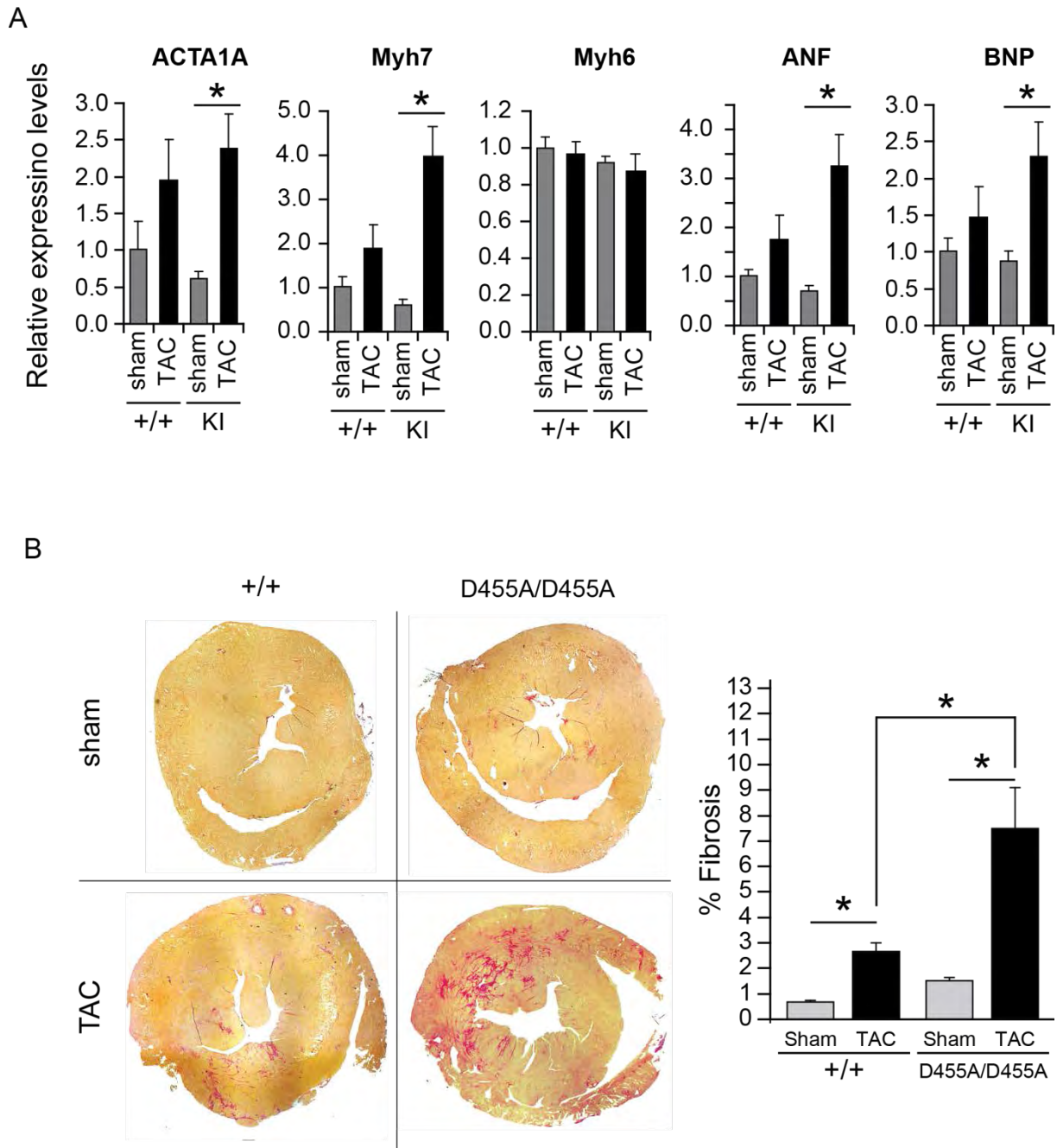


Figure 2. myocardial remodelling and fibrosis

A. Real-time qRT-PCR analysis of expression of hypertrophy marker genes in wild type and D455A KI mice hearts 2 weeks after the TAC. The expression level of Alpha-skeletal actin (ACTA1A), β -myosin heavy chain (Myh7) atrial natriuretic peptide (ANP), brain natriuretic peptide (BNP), and α -myosin heavy chain Myh6 was calculated relative to the housekeeping gene *Gapdh*, and expressed as fold change relative to the WT-Sham group, set to 1 (Mean \pm SEM; * p <0.05; n = 5-6 mice per group)

B. Histological characterization of cardiac fibrosis shown in red with Van Gieson staining in wild type and D455A KI mice after 4 weeks of TAC (original magnification x100). The bar graph on the right represents percentage of fibrotic areas measured on Van-Gieson-stained tissue sections. (Mean \pm SEM; * p <0.05; Sham, n =4, TAC; n =5)

because of massive death of cardiomyocytes which are replaced by extracellular matrix and invading myofibroblasts (5;22). Although the experiments in which we are quantifying myocardial apoptosis are still ongoing, our preliminary data indicated higher levels of myocardial apoptosis in the KI mice one-week post TAC (Figure 3A). Although not significant, there was still a tendency of difference in myocardial apoptosis between KI and WT four weeks after TAC (Figure 3B), which suggests that the early induction of apoptosis is the initial driving event of exacerbated phenotype observed in the KI mice. Nevertheless, after the long term stress (four weeks), both WT and KI mice might have reached comparable levels of apoptosis in the myocardium. Western blot analysis on cardiac protein extracts obtained two weeks after TAC showed lower levels of active Akt kinase and increased activation of caspase-3 in KI compared to WT mice; however preliminary data indicated that this difference was not maintained four weeks after TAC operation (Figure 3D, E). These experiments need to be repeated and quantified in order to obtain a clear cut interpretation. Our data so far showed that the reduced % EF and cardiac output are the consequence of increased myocardial apoptosis and fibrosis. These results suggest that, independently of the progress of myocardial hypertrophy the early augmentation in the rate of myocardial apoptosis plays an important role in driving a faster transition from compensated myocardial hypertrophy to heart failure.

3. Discussion

In normal physiological conditions, RasGAP cleavage is not indispensable for normal development in mice. RasGAP cleavage appears not essential for heart development and function, since, under baseline conditions, most of the structural and functional cardiac parameters are not different between WT and KI mice. Moreover no signs of the heart alteration in aged mice were detected based on echocardiography data obtained from measurements performed on non-stressed aged (>40 weeks) WT and KI littermates (not shown). Consistent with previously described data in skin and colon, the importance of RasGAP cleavage in the heart becomes fully evident under stress conditions. Our results support that the absence of fragment N generation plays a role in the drop of the contractile function of the heart upon doxorubicin induced cardiotoxicity (Part I, Figure 7 and Table S2) (17).

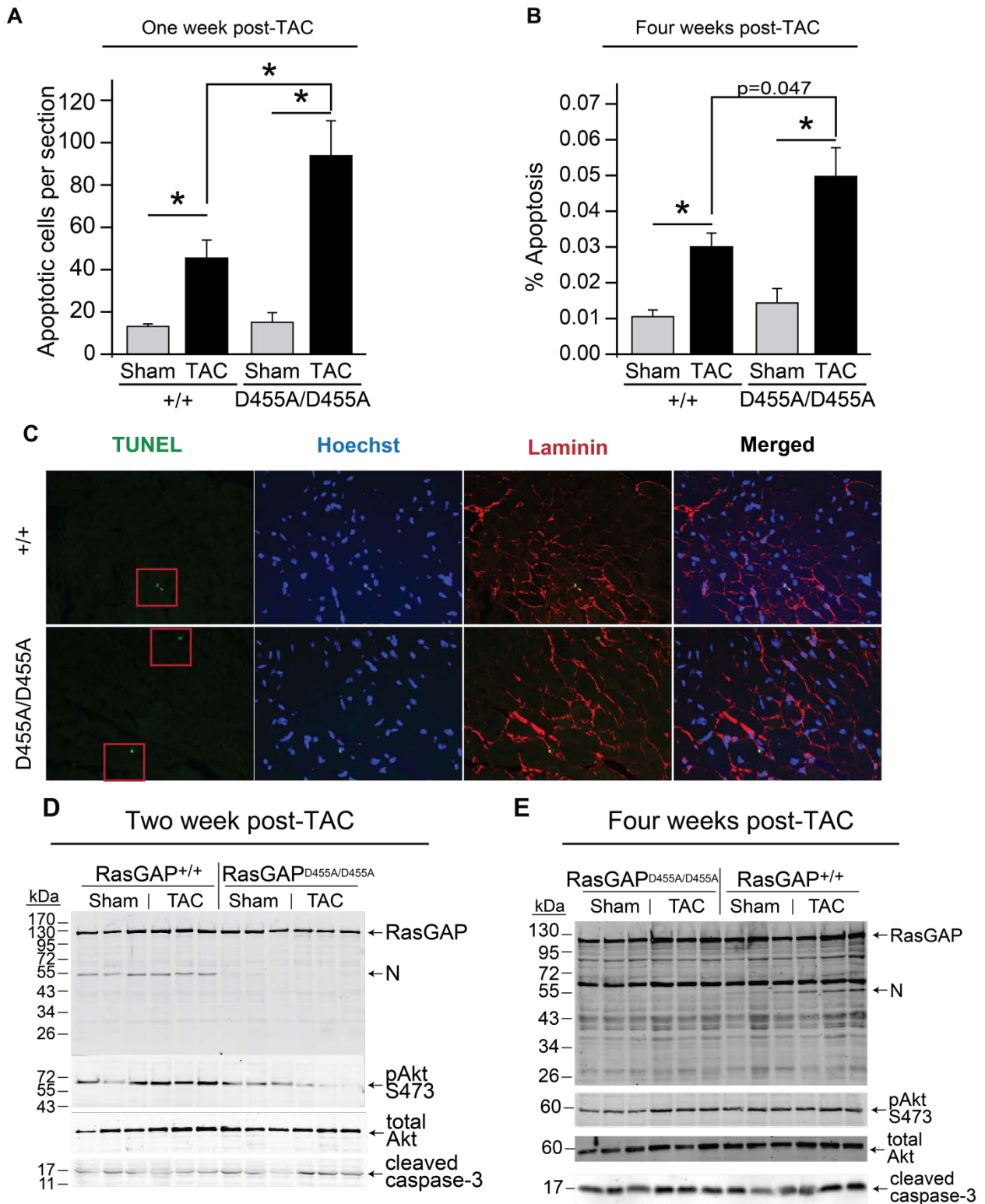


Figure 3. D455A KI mice display higher apoptosis levels and lower activation of Akt

A-B. Quantitative analysis of apoptosis in heart tissue sections from WT and KI mice 1 week (data expressed as the number of TUNEL/DAPI-positive cells per heart section) and 4 weeks (data expressed as the number of TUNEL/Laminin/DAPI-positive cells per heart section) after Sham or TAC operation. Paraffin-embedded heart tissue sections were subjected to TUNEL assays to reveal apoptotic cells, which were counted and expressed as number of

apoptotic cells per heart section. The number of pyknotic nuclei displayed represents the average of three heart sections at different levels per mouse. **C.** Representative images of triple staining (TUNEL/Hoechst/Laminin). **D-E.** Heart tissues from wild type mice or D455A KI mice subjected or not to TAC procedure, homogenized in lysis buffer, and the proteins were subsequently subjected to Western blotting using antibodies against the indicated proteins. The extent of RasGAP cleavage, caspase-3 cleavage and Akt activation were determined by western blot analysis.

The cleavage of RasGAP resulted in a slight, but not significant effect on the evolution of left ventricular hypertrophy, as indicated by comparable echocardiography parameters (IVS, LVPW, LVID, LV mass) in the WT and KI mice. The TAC procedure induced comparable stress on both mouse groups as demonstrated by the similar aortic velocity (Table 1). Strikingly, a stronger reduction in cardiac output, %FS and %EF was observed in TAC-subjected KI mice (Table 1). Ventricular remodeling was evident in mice that suffered pressure overload. Compared to the sham groups the KI mice showed a significant increase in the expression of fetal genes two weeks after TAC (Figure 2A). However, no significant differences were detected between the two genotypes. Preliminary data showed that indeed both WT and KI TAC-subjected mice induce a similar fetal gene re-expression profile compared to their sham groups one week after TAC surgery. This suggests that compensatory mechanisms were more efficient in WT mice, which were responsible to restore fetal genes to the basal level.

The transition from compensated hypertrophy to heart failure accompanied with a decline in the contractile function of the left ventricle is usually associated with modifications in the extracellular matrix components leading to myocyte slippage and myocardial fibrosis (5;6). Cardiac fibrosis is characterized by excessive deposition of extracellular matrix proteins. Fibrosis increases myocardial stiffness and alterations in cardiac conductivity, a criterion which is related to extracellular matrix (ECM) quality. The myocardial ECM is composed mainly of collagen type I (Col I) and collagen type III (Col III), which make scaffolding support for the myocytes and maintain the integrity of the heart. (6). Interestingly, TAC-induced hypertrophy led to an increase in myocardial fibrosis in both WT and KI mice; however the increase was more important in the KI mice. It will be very informative to analyse the relative expression of coll I and col III, and myocardial fibrosis in early time points (one week post-

surgery) in addition, these data may indicate a role of RasGAP cleavage specifically in inhibition of fibrosis process.

Based on our previous data, we estimated a higher rate of cell death in KI mice which could be the main factor leading to these pathological alterations. We have previously shown that cells expressing a caspase-insensitive RasGAP mutant were rendered more sensitive to low stress conditions, caused by the inability of cells to cleave RasGAP and induce the associated cell survival pathway (23). In addition, the overexpression of a caspase-3-resistant form of fragment N protected cardiomyocytes efficiently against peroxynitrite induced oxidative-nitrosative stress, which lead to apoptosis (17). One critical patho-physiological nodal point in the process of hypertrophy decompensation and heart failure is the induction of apoptosis (17;24;25). As expected, we detected a higher level of active caspase-3 (Figure 3D) and an increased rate of apoptotic cell death in KI stressed mice after one week of TAC surgery compared to WT (Figure 3A). These preliminary results, expressed as the number of TUNEL positive cells per heart section, are now being finalized and the percentage of apoptotic cell death will be reported in the final manuscript. These results link cardiomyocyte apoptosis with ventricular remodeling and functional deterioration during the transition from compensated pressure overload hypertrophy to heart failure, and identify induction of RasGAP cleavage and fragment N generation as a critical molecular event, which decrease cardiac myocyte apoptosis during pressure overload. The protection against apoptosis is not very potent after four weeks of TAC, since after such long term of stress, a protection tendency was still observed, but the differences in the myocardial apoptosis were not significant between WT and KI mice (Figure 4). Functionally, this was correlated with detrimental effects on heart performance. This can be explained by the fact that excessive cleavage of fragment N might have taken place due to the chronic stress. Surprisingly, despite of the increased apoptosis and fibrotic lesions, the echocardiography data did not detect any signs of thinning of left ventricular wall in the KI mice six weeks post-TAC (Table 1).

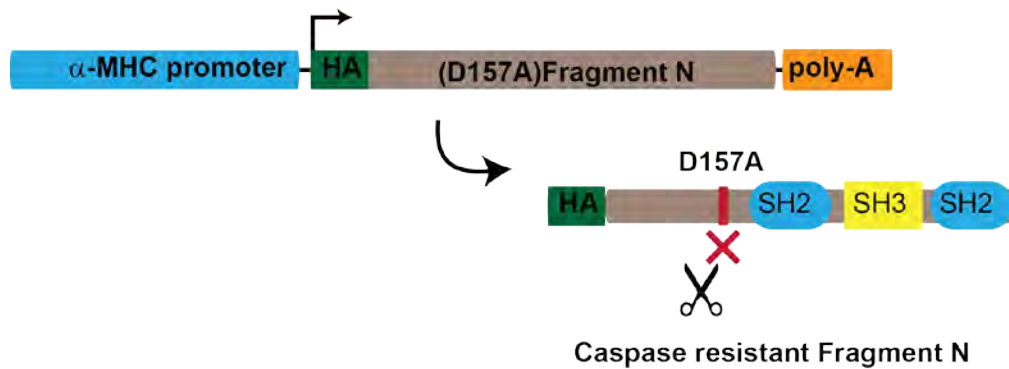


Figure 4. Schematic representation of the transgene construct to achieve cardiac-specific expression of caspase-resistant fragment N.

Cardioprotection is mediated by PI3K/Akt pathway activation, which plays an important role in the regulation of cardiomyocyte growth and survival (3;11;26). Our data show a lower activation of the prosurvival kinase Akt in KI mice at the early stages of the hypertrophic response (Figure 4D-E). Nevertheless, these experiments need to be confirmed and quantified at different time points.

It is worth to mention that the efficacy of cardiomyocyte protection by fragment N-mediated apoptosis inhibition, under these experimental conditions might not be the ideal situation due to the possibility of further processing of fragment N into fragments N1 and N2 which do not induce any pro-survival advantage. To overcome the later scenario of fragment N further fragmentation, and to verify the protective functions of fragment N in an *in vivo* setting, we have generated transgenic mice expressing an HA-tagged caspase resistant form of fragment N, under the control of the α -myosin heavy chain promoter (Figure 4). Currently the mice are being characterized for the expression of fragment N and the transmission of the transgene. The same set of experiments performed earlier in this chapter will be repeated in this new *in vivo* model.

4. Supplemental data

Supplemental table 1. RasGAP^{D455A/D455A} KI mice have increased heart dysfunction following TAC (Four weeks).

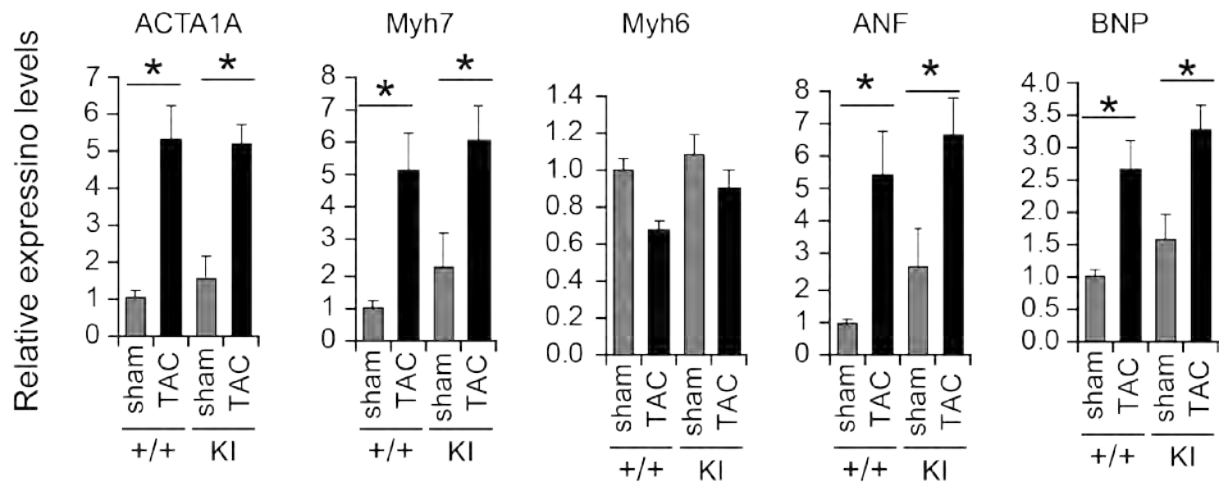
Wild-type and RasGAP^{D455A/D455A} were left untreated or subjected to TAC. The table represents different parameters measured by echocardiography. WT: control mice; KI: mice unable to generate fragment N. n=4-7 animals per group. The numbers in blue indicate significance between TAC-operated versus Sham mice. (#) indicates significant differences between WT and KI mice. # p < 0.05

Genotype	WT Sham	WT TAC	KI Sham	KI TAC
Body weight (g)	29.4 ± 2.3	31.5 ± 2.7	30.5 ± 2.2	30.6 ± 1.9
Heart rate (Beats/min)	457 ± 76	525 ± 68	566 ± 35	465 ± 59
IVS;d (mm)	0.82 ± 0.08	1.08 ± 0.11	0.85 ± 0.18	1.13 ± 0.23
IVS;s (mm)	1.05 ± 0.06	1.39 ± 0.12	1.12 ± 0.17	1.37 ± 0.2
LVID;d (mm)	4.00 ± 0.32	3.88 ± 0.49	4.16 ± 0.21	4.19 ± 0.22
LVID;s (mm)	2.94 ± 0.40	2.83 ± 0.58	3.02 ± 0.30	3.41 ± 0.20
LVPW;d (mm)	0.75 ± 0.05	1.21 ± 0.17	0.85 ± 0.14	1.20 ± 0.26
LVPW;s (mm)	1.02 ± 0.10	1.47 ± 0.26	1.09 ± 0.12	1.45 ± 0.28
% FS	26.6 ± 4.9	27.6 ± 6.9	27.7 ± 3.9	18.6 ± 4.3 #
%EF	52.3 ± 8.0	53.8 ± 11.3	53.9 ± 5.9	38.7 ± 7.7 #
LV Mass (mg)	108.3 ± 11.1	184.4 ± 30.9	135.8 ± 31.8	216.1 ± 58.1
HW:BW echo	3.7 ± 0.3	5.9 ± 1.0	4.4 ± 0.7	7.1 ± 2.1

Supplemental table 2.**No significant differences in hypertrophy parameters between Wild-type and RasGAP^{D455A/D455A} KI mice one week following TAC.**

Wild-type and RasGAP^{D455A/D455A} were left untouched, or subjected to sham or TAC surgery. The table represents different parameters measured by echocardiography one week after operation. WT: control mice; KI: mice unable to generate fragment N. n=5-7 animals per group. The numbers in **blue #** indicate significance between TAC-operated versus Sham mice. **#** p < 0.05. No differences were detected between WT and KI animals, Hence Untouched animals are not shown to simplify the presentation of data.

Genotype	WT	WT	KI RasGAP	KI RasGAP
Condition	Sham	TAC	Sham	TAC
Number of mice	n=6	n=6	n=5	n=9
ECHO	Mean	Mean	Mean	Mean
Body weight (g)	27.39 ± 1.42	27.01 ± 1.58	25.9 ± 2.83	25.68 ± 2.88
Heart rate (Beats/min)	454.5 ± 29.4	448.33 ± 26.4	441.2 ± 47.4	431.44 ± 23.8
IVS;d (mm)	0.754 ± 0.033	1.038 ± 0.092#	0.755 ± 0.063	1.03 ± 0.11#
IVS;s (mm)	0.984 ± 0.081	1.35 ± 0.163 #	1.00 ± 0.063	1.34 ± 0.15#
LVID;d (mm)	4.135 ± 0.139	3.675 ± 0.293	4.15 ± 0.579	3.718 ± 0.35
LVID;s (mm)	3.017 ± 0.346	2.524 ± 0.634#	3.019 ± 0.63	2.53 ± 0.49
LVPW;d (mm)	0.735 ± 0.03	1.037 ± 0.126#	0.757 ± 0.091	1.015 ± 0.122#
LVPW;s (mm)	0.970 ± 0.077	1.340 ± 0.126#	1.004 ± 0.051	1.254 ± 0.123#
LVID Trace (CO) (ml/min)	17.57 ± 2.58	14.21 ± 2.68	17.80 ± 6.10	15.08 ± 2.93
LVID Trace (SV) (ul)	40.45 ± 7.29	33.61 ± 5.2	40.1 ± 10.2	35.35 ± 5.36
% FS	27.0 ± 7.32	32.13 ± 12.77	27.93 ± 6.02	32.46 ± 8.63
%EF	52.55 ± 10.5	59.22 ± 17.25	54.09 ± 9.5	60.661 ± 10.7
LV Mass (mg)	112.84 ± 9.72	147.8 ± 25.2#	118.89 ± 34.25	147.9 ± 27.3
LV Vol;d (ul)	75.82 ± 6.06	57.703 ± 10.5#	78.68 ± 26.9	59.5 ± 12.1
LV Vol;s (ul)	36.142 ± 9.26	24.91 ± 12.97	37.82 ± 19.5	24.43 ± 8.7
HW/BW echo	4.125 ± 0.382	5.49 ± 1.06#	4.57 ± 1.12	5.76 ± 0.95#
Aortic velocity (mm/sec)	733.6 ± 84.5	4478.3 ± 404 #	769.25 ± 246	4325 ± 653#
Body weight (g)	26.79 ± 1.33	26.47 ± 1.74	25.17 ± 2.58	25.2 ± 2.38
Heart weight (mg)	126.66 ± 13.2	158.66 ± 20.41	131.8 ± 31.5	160.2 ± 18.2
Tibial length TL (mm)	18.41 ± 0.204	18.183 ± 0.29	18.37 ± 0.5	18.2 ± 0.33
HW/ BW	4.746 ± 0.632	6.00 ± 0.8#	5.21 ± 0.98	6.385 ± 0.76 #
HW/ TL	6.87 ± 0.70	8.739 ± 1.24 #	7.16 ± 1.62	8.79 ± 0.95 #



Supplemental Figure 1.

Real-time qRT-PCR analysis of expression of hypertrophy marker genes in wild type and D455A KI mice hearts one week after the TAC. The expression level of Alpha-skeletal actin (ACTA1A), β -myosin heavy chain (Myh7) atrial natriuretic peptide (ANP), brain natriuretic peptide (BNP), and α -myosin heavy chain Myh6 was calculated relative to the housekeeping gene *Gapdh*, and expressed as fold change relative to the WT-Sham group, set to 1 (Mean \pm SEM; * p <0.05; n= 5-7 mice per group).

5. Materials and methods

The WT and KI mice strains were used were described in Part I.

5.1 Trans-aortic constriction (TAC)

Mice are anesthetized by injection of a mixture of ketamin/xylazine/acepromazin and placed on warming pad for maintenance of body temperature. In the supine position, endotracheal intubation is performed and the mouse is placed on artificial ventilation with a mini-rodent ventilator. The thorax of the animal is shaved and disinfected. A small horizontal incision is made at the level of the cranial sternum allowing visualization of the aortic arch. A suture is placed around the aorta between the origin of the right inoinate and left common carotid artery. Transaortic constriction (TAC) is created using a 7.0 silk suture tied twice around the aorta and a predetermined-gauge needle size (standardly 27 gauge). The needle is then gently retracted, the incision is closed and the skin is sutured. A local antiseptic is applied to the skin. The animal is kept under artificial respiration until spontaneous breathing resumes. For animals undergoing a sham operation, the ligature is placed in an identical location but not tied.

5.2. In vivo transthoracic cardiac imaging with echocardiography

Transthoracic echocardiography was performed using a 30 MHz probe and the Vevo 770 Ultrasound machine (VisualSonics, Toronto, ON, Canada). Mice were lightly anesthetized with 1-1.5% isoflurane, maintaining heart rate at 400-500 beats per minute. The mice were placed in decubitus dorsal on a heated 37°C platform to maintain body temperature. A topical depilatory agent was used to remove the hair and ultrasound gel was used as a coupling medium between the transducer and the skin. The heart was imaged in the 2D mode in the parasternal long-axis view. From this view, an M-mode cursor was positioned perpendicular to the interventricular septum and the posterior wall of the left ventricle at the level of the papillary muscles. Diastolic and systolic internal ventricular septum (IVS;d and IVS;s), diastolic and systolic left ventricular free posterior wall thickness (LVPW;d and LVPW;s), and left ventricular internal end-diastolic and end-systolic chamber (LVID;d and LVID;s) dimensions were measured. The measurements were taken in three separate M-mode images and averaged. Left ventricular fractional shortening (%FS) and ejection fraction (%EF) were also calculated. Fractional shortening was assessed from M-

mode based on the percentage changes of left ventricular end-diastolic and end-systolic diameters. %EF was derived from the formula of $(LV\ vol;d - LV\ vol;s) / LV\ vol;d * 100$.

5.3. Histology

For histological analysis, hearts were dissected free from atria and vessels and fixed in 4% formalin. Staining included standard histological staining with hematoxylin and eosin. Fibrosis was assessed by staining with Van Gieson reagent. Quantification of the fibrotic red labeled area was scored by counting the number of red pixels using Adobe Photoshop program (Adobe Systems Inc.).

5.4. TUNEL staining

The methodology is detailed in Part I material and in Methods section (apoptosis scoring).

5.5. RNA Isolation and quantitative RT-PCR

Total RNA was purified from tissues using Trizol reagent (Invitrogen). Aliquots consisting of 4 μ g of total RNA were reverse-transcribed into cDNAs using MMLV reverse transcriptase and oligo dT primers. The cDNAs were subsequently amplified by quantitative TaqMan using Gene Expression Assays, on ABI 7500 Thermal Cycler following manufacturer's instructions (Applied Biosystems). Expression levels were normalized relative to those housekeeping gene Gapdh. The relative expression levels were calculated according to the $\Delta\Delta$ Ct method, using reference samples as indicated in individual experiments.

Reference List

1. Frey,N., and Olson,E.N. 2003. Cardiac hypertrophy: the good, the bad, and the ugly. *Annu Rev Physiol* **65**:45-79.
2. Heineke,J., and Molkentin,J.D. 2006. Regulation of cardiac hypertrophy by intracellular signalling pathways. *Nat Rev Mol Cell Biol* **7**:589-600.
3. Gupta,S., Das,B., and Sen,S. 2007. Cardiac hypertrophy: mechanisms and therapeutic opportunities. *Antioxid. Redox. Signal.* **9**:623-652.
4. Kuwahara,K., Nishikimi,T., and Nakao,K. 2012. Transcriptional regulation of the fetal cardiac gene program. *J Pharmacol. Sci.* **119**:198-203.
5. Berk,B.C., Fujiwara,K., and Lehoux,S. 2007. ECM remodeling in hypertensive heart disease. *J Clin. Invest* **117**:568-575.
6. Shirwany,A., and Weber,K.T. 2006. Extracellular matrix remodeling in hypertensive heart disease. *J Am. Coll. Cardiol.* **48**:97-98.
7. Narula,J., Haider,N., Virmani,R., DiSalvo,T.G., Kolodgie,F.D., Hajjar,R.J., Schmidt,U., Semigran,M.J., Dec,G.W., and Khaw,B.A. 1996. Apoptosis in myocytes in end-stage heart failure. *N. Engl. J Med.* **335**:1182-1189.
8. Anversa,P., and Kajstura,J. 1998. Myocyte cell death in the diseased heart. *Circ. Res.* **82**:1231-1233.
9. Fortuno,M.A., Ravassa,S., Fortuno,A., Zalba,G., and Diez,J. 2001. Cardiomyocyte apoptotic cell death in arterial hypertension: mechanisms and potential management. *Hypertension* **38**:1406-1412.
10. Yang,J.-Y., Michod,D., Walicki,J., Murphy,B.M., Kasibhatla,S., Martin,S., and Widmann,C. 2004. Partial cleavage of RasGAP by caspases is required for cell survival in mild stress conditions. *Mol. Cell Biol.* **24**:10425-10436.
11. Miyamoto,S., Rubio,M., and Sussman,M.A. 2009. Nuclear and mitochondrial signalling Akts in cardiomyocytes. *Cardiovasc. Res* **82**:272-285.
12. Muraski,J.A., Rota,M., Misao,Y., Fransioli,J., Cottage,C., Gude,N., Esposito,G., Delucchi,F., Arcarese,M., Alvarez,R. et al 2007. Pim-1 regulates cardiomyocyte survival downstream of Akt. *Nat Med* **13**:1467-1475.
13. Rota,M., Boni,A., Urbanek,K., Padin-Iruegas,M.E., Kajstura,T.J., Fiore,G., Kubo,H., Sonnenblick,E.H., Musso,E., Houser,S.R. et al 2005. Nuclear targeting of Akt enhances ventricular function and myocyte contractility. *Circ. Res.* **97**:1332-1341.
14. Shiojima,I., Sato,K., Izumiya,Y., Schiekofer,S., Ito,M., Liao,R., Colucci,W.S., and Walsh,K. 2005. Disruption of coordinated cardiac hypertrophy and angiogenesis contributes to the transition to heart failure. *J Clin. Invest* **115**:2108-2118.

15. Ceci,M., Gallo,P., Santonastasi,M., Grimaldi,S., Latronico,M.V., Pitisci,A., Missol-Kolka,E., Scimia,M.C., Catalucci,D., Hilfiker-Kleiner,D. et al 2007. Cardiac-specific overexpression of E40K active Akt prevents pressure overload-induced heart failure in mice by increasing angiogenesis and reducing apoptosis. *Cell Death Differ* **14**:1060-1062.
16. Khalil,H., Rosenblatt,N., Liaudet,L., and Widmann,C. 2012. The role of endogenous and exogenous RasGAP-derived fragment N in protecting cardiomyocytes from peroxynitrite-induced apoptosis. *Free Radic. Biol. Med.* **53**:926-935.
17. Khalil,H., Peltzer,N., Walicki,J., Yang,J.Y., Dubuis,G., Gardiol,N., Held,W., Bigliardi,P., Marsland,B., Liaudet,L. et al 2012. Caspase-3 Protects Stressed Organs against Cell Death. *Mol. Cell Biol.* **32**:4523-4533.
18. Fagard,R., Bielen,E., Lijnen,P., and Amery,A. 1993. Cardiac variables and blood pressure as determinants of left ventricular inflow velocities. *J Hum. Hypertens.* **7**:7-12.
19. Izumo,S., Nadal-Ginard,B., and Mahdavi,V. 1988. Protooncogene induction and reprogramming of cardiac gene expression produced by pressure overload. *Proc. Natl. Acad. Sci. U. S. A* **85**:339-343.
20. Cohn,J.N., Ferrari,R., and Sharpe,N. 2000. Cardiac remodeling--concepts and clinical implications: a consensus paper from an international forum on cardiac remodeling. Behalf of an International Forum on Cardiac Remodeling. *J Am Coll. Cardiol.* **35**:569-582.
21. Teiger,E., Than,V.D., Richard,L., Wisnewsky,C., Tea,B.S., Gaboury,L., Tremblay,J., Schwartz,K., and Hamet,P. 1996. Apoptosis in pressure overload-induced heart hypertrophy in the rat. *J Clin. Invest* **97**:2891-2897.
22. Manabe,I., Shindo,T., and Nagai,R. 2002. Gene expression in fibroblasts and fibrosis: involvement in cardiac hypertrophy. *Circ. Res* **91**:1103-1113.
23. Yang,J.-Y., Michod,D., Walicki,J., Murphy,B.M., Kasibhatla,S., Martin,S., and Widmann,C. 2004. Partial cleavage of RasGAP by caspases is required for cell survival in mild stress conditions. *Mol. Cell Biol.* **24**:10425-10436.
24. Diwan,A., Wansapura,J., Syed,F.M., Matkovich,S.J., Lorenz,J.N., and Dorn,G.W. 2008. Nix-mediated apoptosis links myocardial fibrosis, cardiac remodeling, and hypertrophy decompensation. *Circulation* **117**:396-404.
25. Gill,C., Mestril,R., and Samali,A. 2002. Losing heart: the role of apoptosis in heart disease--a novel therapeutic target? *FASEB J* **16**:135-146.
26. Matsui,T., Nagoshi,T., and Rosenzweig,A. 2003. Akt and PI 3-kinase signaling in cardiomyocyte hypertrophy and survival. *Cell Cycle* **2**:220-223.

3. Results: Part IV

1. Introduction

NF- κ B-dependent transcription is tightly controlled, and the regulation of NF- κ B activation is adequately achieved at different levels throughout the signaling cascade. Although swift activation of NF- κ B is required for a successful immune response, such response should not last forever and thus it needs to be properly switched off to avoid tissue damage. Several human diseases result from both loss and gain of function in NF- κ B signaling. Inhibition of NF- κ B is accompanied by severe immune deficiency, increased susceptibility to infection and profound effects on tissue homeostasis in both immune and non-immune cell (1-3). Uncontrolled NF- κ B activation can lead to chronic inflammation; increase the risk of cancer, autoimmune diseases (e.g. rheumatoid arthritis), atherosclerosis and neuro-degenerative disorders (1;3;4).

2. Results

RasGAP-derived fragment N mediates its anti-apoptotic properties through the activation of Ras/PI3K/Akt pathway (5). Several downstream targets of Akt are activated or repressed by direct or indirect phosphorylation. Despite the fact that the NF- κ B pathway can induce anti-apoptotic responses, fragment N induced-Akt does not require NF- κ B activation (8). In addition, fragment N inhibits NF- κ B activation of *in vivo* and *in vitro* (9-11). In this paper we show the cellular mechanism of a novel NF κ B cellular inhibitor. In a caspase-3-dependent manner, fragment N prevents NF κ B accumulation in the nucleus by favoring the nuclear export of NF- κ B in various cell types.

3. Contribution

This work is unpublished. Experiments presented in Figures 1-4 were performed by Nouredine Loukili. The rest of the experiments I carried out. I wrote the manuscript which was revised and corrected by Christian Widmann.

Reference List

1. Courtois,G. 2005. The NF-kappaB signaling pathway in human genetic diseases. *Cell Mol. Life Sci.* **62**:1682-1691.
2. Pasparakis,M. 2009. Regulation of tissue homeostasis by NF-kappaB signalling: implications for inflammatory diseases. *Nat Rev Immunol.* **9**:778-788.
3. Wong,E.T., and Tergaonkar,V. 2009. Roles of NF-kappaB in health and disease: mechanisms and therapeutic potential. *Clin Sci (Lond)* **116**:451-465.
4. Ben-Neriah,Y., and Karin,M. 2011. Inflammation meets cancer, with NF-kappaB as the matchmaker. *Nat. Immunol.* **12**:715-723.
5. Yang,J.-Y., and Widmann,C. 2002. The RasGAP N-terminal fragment generated by caspase cleavage protects cells in a Ras/PI3K/Akt-dependent manner that does not rely on NFκB activation. *JBC* **277**:14641-14646.
6. Ozes,O.N., Mayo,L.D., Gustin,J.A., Pfeffer,S.R., Pfeffer,L.M., and Donner,D.B. 1999. NF-kappaB activation by tumour necrosis factor requires the Akt serine-threonine kinase. *Nature* **401**:82-85.
7. Kane,L.P., Mollenauer,M.N., Xu,Z., Turck,C.W., and Weiss,A. 2002. Akt-dependent phosphorylation specifically regulates Cot induction of NF-kappa B-dependent transcription. *Mol Cell Biol* **22**:5962-5974.
8. Yang,J.-Y., and Widmann,C. 2002. The RasGAP N-terminal fragment generated by caspase cleavage protects cells in a Ras/PI3K/Akt-dependent manner that does not rely on NFκB activation. *JBC* **277**:14641-14646.
9. Yang,J.Y., Walicki,J., Abderrahmani,A., Cornu,M., Waeber,G., Thorens,B., and Widmann,C. 2005. Expression of an uncleavable N-terminal RasGAP fragment in insulin-secreting cells increases their resistance toward apoptotic stimuli without affecting their glucose-induced insulin secretion. *J Biol Chem* **280**:32835-32842.
10. Bulat,N., Jaccard,E., Peltzer,N., Khalil,H., Yang,J.Y., Dubuis,G., and Widmann,C. 2011. RasGAP-derived fragment N increases the resistance of beta cells towards apoptosis in NOD mice and delays the progression from mild to overt diabetes. *PLoS. One.* **6**:e22609.
11. Yang,J.Y., Walicki,J., Jaccard,E., Dubuis,G., Bulat,N., Hornung,J.P., Thorens,B., and Widmann,C. 2009. Expression of the NH(2)-terminal fragment of RasGAP in pancreatic beta-cells increases their resistance to stresses and protects mice from diabetes. *Diabetes* **58**:2596-2606.

Caspase-3 generates a RasGAP-derived NF- κ B repressor in response to stress

Hadi Khalil¹, Nouredine Loukili¹, Alexandre Regamey², Marcel Huber², and Christian Widmann¹

¹Department of Physiology, Biology and Medicine Faculty, University of Lausanne, Switzerland; ²Department of Dermatology, Lausanne University Hospital, Lausanne, Switzerland

Running head: RasGAP fragment N inhibits NF- κ B

Correspondence to Christian Widmann, Department of Physiology, Bugnon 7, 1005 Lausanne, Switzerland, Phone: +41 21 692 5123, Fax: +41 21 692 5505, E-mail: Christian.Widmann@unil.ch.

1. Abstract

The NF- κ B transcription factor is a master regulator of inflammation. It is activated in response to a multitude of stresses, including infection with diverse pathogens, wounding, oxidative stress, and DNA damage. Short-term stress-induced NF- κ B activation is generally beneficial. However, sustained NF- κ B may be detrimental directly causing apoptosis in certain cell types or leading to a persistent damaging inflammation response. NF- κ B activity in stressed cells needs therefore to be controlled for homeostasis maintenance but how this is achieved is poorly understood. Here we show that the N-terminal fragment of RasGAP (called fragment N) that is produced by caspase-3 in mildly stressed cells is a potent NF- κ B inhibitor. Fragment N does not alter the upstream events leading to NF- κ B translocation to the nucleus, i.e. I κ B is degraded similarly and nuclear import is not affected in cells expressing fragment N. However, NF- κ B does not accumulate in the nucleus because fragment N promotes NF- κ B nuclear export. Cells that are unable to generate fragment N because of a point mutation in the caspase-3 cleavage site of RasGAP, in contrast to wild-type cells, do not repress NF- κ B activation in response to stress. Finally, knock-in mice bearing the uncleavable mutant of RasGAP generate a stronger inflammatory response compared to control mice in response to experimental colitis. Our study provides biochemical and genetic evidence of the importance of RasGAP cleavage by caspase-3 in the control of stress-induced NF- κ B activation.

2. Introduction

Nuclear factor Kappa B (NF- κ B) was discovered and characterized as a transcription factor which binds to a site in the promoter of the immunoglobulin κ chain and that is required for B lymphocyte-specific gene expression. However; subsequent studies showed that NF- κ B could be activated in various cells types (1). NF- κ B is ubiquitously expressed and serves as a critical regulator of expression of many genes (2). The NF- κ B family in mammalian cells comprises five different members: p65 (RelA), RelB, c-Rel, NF- κ B1 (p50/p105) and NF- κ B2 (p52/p100). RelA, RelB, and c-Rel, are synthesized as transcriptionally active proteins; while p50/p105 (NF- κ B1) and p52/p100 (NF- κ B2) are synthesized as longer precursor molecules of 105 and 100 kDa respectively that are then processed by proteolytic cleavage into the smaller, transcriptionally active, p50 and p52 forms [reviewed extensively by (2-4);(5);(6)]. NF- κ B homo- or heterodimers are sequestered in the cytosol of unstimulated cells via non-covalent interactions with a class of inhibitory proteins called Inhibitors of κ B (I κ Bs) (2;7;8). Signals that induce NF- κ B activation trigger the activation of the upstream I κ B kinase complex (IKK), containing the IKK α and IKK β catalytic subunits and the IKK γ (also called Nemo) regulatory subunit. This complex then phosphorylates I κ B proteins, leading to their degradation. NF- κ B is thus no longer sequestered in the cytoplasm and is then free to translocate to the nucleus where it can regulate expression of genes containing NF- κ B binding elements (9;10).

NF- κ B is a critical regulator of immune responses, maturation of immune cells, and development of secondary lymphoid organs. Sustained activation of NF- κ B might lead to chronic inflammation which is implicated in pathogenesis including cancer, ALI (acute lung injury), neurodegenerative disorders, and autoimmune diseases (e.g. rheumatoid arthritis) and atherosclerosis (11). In addition recent studies addressed an important function of NF- κ B in non-immune cells. Increased NF- κ B activation triggers cytokine expression by the epithelial cells, resulting in exacerbated tissue inflammatory responses (12).

RasGAP is an unconventional caspase substrate because, depending on the extent of its cleavage by caspase-3, either induces an anti-apoptotic response (13) or favors cell death (14). At low levels of caspase-3 activity, RasGAP is cleaved at position 455, generating an N-terminal fragment (fragment N) that induces the anti-apoptotic Akt pathway (13;15;16). At higher levels of caspase-3 activity, fragment N is further cleaved at position 157 shutting off its capacity to stimulate Akt (14). Several downstream targets of Akt are activated or repressed by direct or indirect phosphorylation. Akt can mediate the activation of NF- κ B by directly phosphorylating IKK α at threonine 23 (17), or indirectly through Cot (cancer osaka thyroid) a serine/threonine kinase of the mitogen-activated protein kinase kinase kinase (MAP3K) family (18). However, despite the fact that fragment N activates Akt, its ability to protect cells does not depend on NF- κ B (15). In fact in beta cells, fragment N appears to inhibit NF- κ B activation (19-21). Here we show that fragment N is a general NF- κ B repressor in stressed cells. This inhibitory activity relies on the promotion of NF- κ B nuclear export. Fragment N generation is required to control the extent of inflammation in mouse model of colitis. Cleavage of RasGAP by caspase-3 represents therefore a newly described mechanism used by cells and tissues to regulate NF- κ B-dependent responses activated by stress.

3. RESULTS

3.1. Fragment N inhibits Akt-mediated NF-kB activation

The RasGAP-derived fragment N induces an anti-apoptotic response through the activation of Ras/PI3K/Akt pathway (15). Even though fragment N simulates Akt, which has the ability to activate NF-kB, fragment N expression in cells does not lead to NF-kB stimulation (15). This raises the possibility that fragment N inhibits Akt-induced NF-kB stimulation. To test this assumption, Akt was stimulated by expression of the constitutively active V12Ras mutant and with fragment N. This led to similar Akt stimulation as assessed by its phosphorylation on Ser⁴⁷³ and phosphorylation of GSK3 β , one of its downstream targets (22) (Figure 1A; quantitation shown in Figure 1B-C). Activation of Akt by fragment N is Ras-dependent as it was completely abolished by the overexpression of the dominant negative N17Ras mutant (Figure S1). V12Ras, as expected, stimulated NF-kB activity (Figure 1D). Not only did fragment N not activate NFkB, it inhibited V12Ras- (Figure 1D) and myr-Akt- (Figure 1E) mediated NF-kB activation. The capacity of myr-Akt to stimulate NF-kB was mild. The Cot kinase has been shown to mediate strong Akt-induced NF-kB activation (23). Even in this condition did fragment N potently inhibit NF-kB activity (Figure 1F). These results indicate that fragment N, while able to activate Akt, prevents the latter to stimulate NFkB.

3.2. Fragment N inhibits the activation of NF-kB in response to a variety of stimuli

To determine whether NF-kB inhibition mediated by fragment N is specific to Akt-dependent signals or whether it has a broader effect, we tested the ability of fragment N to inhibit NF-kB induction by a variety of NF-kB inducing stimuli that operate through either the canonical or non-canonical NF-kB pathways. Figure 2A-B shows that expression of fragment N in cells prevented NF-kB activation induced by the TNF α and IL-1 β cytokines and by the lipopolysaccharide (LPS) bacterial toxin. Ectopic expression of intracellular proteins that mediate NF-kB

stimulation in response to ligand stimulation of cytokines and bacterial toxin receptors can lead to NF- κ B activation. For example, expression of TRAF2 and TRAF6 cells induces NF- κ B stimulation via the canonical IKK $\alpha/\beta/\gamma$ pathway (24). Over-expression of the ectodermal dysplasia receptor (EDAR) also leads to NF- κ B activation through the canonical pathway (25). Ectopic expression of the NIK kinase, on the other hand, can induce NF- κ B stimulation via either the canonical or the non-canonical IKK α/α pathway. Figure 2C shows that in each of these cases, fragment N expression in HeLa cells led to significant reduction in NF- κ B activity. Similar results were obtained in a different cell line (Figure S2).

We then monitored the nuclear translocation of GFP-tagged p65 in different cell types stimulated with TNF α (Figure 3A-B) or in conditions where NIK was overexpressed (Figure 3C-E). This led to an increase in nuclear location of GFP-p65. However, when fragment N was present, TNF α and NIK-induced p65 nuclear translocation was significantly decreased. These data show that fragment N is a general NF- κ B blocker that prevents nuclear accumulation of NF κ B.

3.3. Repression of NF- κ B activation in stressed cells requires caspase activity and fragment N generation

As fragment N is generated in mildly stressed cells in response to a weak caspase-3 activation, a prediction based on the data presented above is that stressed cells should be impaired in their ability to activate NF- κ B in the presence of a low stress unless caspases are inhibited or unless cells are unable to generate fragment N because of a point mutation in their first caspase-3 cleavage site. We therefore exposed cells to a low dose of UV-C and tested their capacity to stimulate NF- κ B in response to TNF α . Figure 4A shows that UV-C pretreatment prevented TNF α -mediated NF- κ B activation. However, UV-C pretreatment was unable to prevent NF- κ B stimulation when cells were exposed to the pan-caspase MX1013 inhibitor (26)(Figure 4B). Similarly, MEFs that express the RasGAP caspase-3 cleavage resistant D455A mutant, and hence

that are unable to generate fragment N (Figure 4C, upper part; see also (16)), were still able to activate NF- κ B despite UV pretreatment (Figure 4C).

3.4. Fragment N neither inhibits I κ B degradation nor binds to NF- κ B dimers

NF- κ B dimers are sequestered in the cytoplasm through binding to I κ B proteins that mask their nuclear localization sequences (27). Upon stimulation the activated IKK complex phosphorylates I κ B α . This targets I κ B α for proteasome-dependent degradation, releasing NF- κ B that can then translocate to the nucleus and regulate gene expression (28). To determine whether fragment N inhibits I κ B α degradation, we monitored the pattern of I κ B degradation induced by TNF α in the presence or in the absence of fragment N. Figure 5A shows that 30 minutes after TNF α stimulation, degradation of I κ B α took place regardless of whether fragment N was present or not. I κ B α expression is regulated by NF- κ B and is therefore re-expressed rapidly *de novo* following its degradation (see time 60' and 90' in the control condition in Figure 5A). As expected from the ability of fragment N to inhibit NF- κ B activation, I κ B re-expression was inhibited in TNF α -treated cells expressing fragment N (Figure 5A). Therefore, fragment N does not inhibit I κ B α degradation but, as a consequence of fragment N-mediated NF- κ B inhibition, *de novo* synthesis of I κ B α is delayed. One mechanism by which fragment N could modulate NF- κ B activation is through direct interaction with NF- κ B subunits (p50, p65) in a I κ B-like manner. To assess this possibility, the presence of p65 and p50 in fragment N immuno-precipitates was determined. Figure 5B and 5C show that, in conditions where p65 and p50 co-immunoprecipitated with I κ B α , no binding was detected with fragment N. Possibly, fragment N could only interact with NF- κ B once it has been freed from I κ B. We therefore repeated the above experiment using cells stimulated with LPS or with TNF α for 30 minutes. In these cases again, no interaction was detected between fragment N and p65 or p50 (Figure S2). These results indicate that the I κ B-degradation is not modulated by fragment N and that NF- κ B dimers are not sequestered in the cytoplasm by direct interaction with fragment N.

3.5. Fragment N does not affect NF- κ B import but favors nuclear export

TNF α -stimulated p50/p65 heterodimer nuclear import is specifically mediated by importin α 3 and importin α 4 (29). Therefore, we tested whether fragment N competes for p50/p65–importin complex formation through direct interaction with importins. Immunoprecipitation experiments (Figure S4) showed that no direct interaction takes place between fragment N and importin α 3 or importin α 4, suggesting that the NF- κ B importing machinery is not affected by fragment N. To further assess this point, nuclear accumulation of GFP-p65 was monitored. As nuclear location of p65 is determined by the balance of nuclear import and nuclear export, we used the nuclear export inhibitor Leptomycin B (LMB)(30) to insure that the presence of p65 in the nucleus only depended on nuclear import. Figure 6 shows that LMB induced GFP-p65 nuclear accumulation that was independent of fragment N expression. As a control, a non-degradable form of I κ B, I κ B $\alpha\Delta$ N2 completely blocked LMB-induced GFP-p65 nuclear accumulation. These results suggest that fragment N does not affect NF κ B nuclear import.

Since there is less NF- κ B located in the nucleus in cells expressing fragment N (Figure 3) but fragment N does not hamper NF- κ B nuclear import, one must come to the conclusion that fragment N favors NF- κ B nuclear export. To directly test this assertion, fluorescence recovery after photo-bleaching (FRAP) was performed to monitor nuclear export of GFP-tagged p65 in conditions where fragment N is expressed in cells or not. In control cells, GFP-p65 nuclear export was readily detected but this nuclear export was strongly promoted when cells expressed fragment N (Figure 7). The nuclear membrane integrity of the recorded cells was not affected by procedure as determined by the total absence of nuclear export of GFP-p65 in the presence of LMB (Figure 7 and supplemental video).

Crm1, which is inhibited by LMB, is the main receptor for the export of proteins out of the nucleus and may therefore be targeted by fragment N to increase NF- κ B nuclear export (31). However, no interaction between fragment N and CRM1 could be detected (data not shown). Additionally, fragment N did not modulate Crm1 expression levels (Figure 8). Altogether, these results demonstrate that

fragment N inhibits NF- κ B activity by promoting its export from the nucleus but it does not do so by directly interacting with Crm1.

3.6. The role of RasGAP cleavage and fragment N formation in dampening the extent of inflammation *in vivo* (ongoing)

Experimental colitis is induced by dextran sodium sulfate (DSS). Mice fed with DSS polymers in the drinking water suffer of colitis characterized by diarrhoea, bloody faeces, weight loss and a histological picture of inflammation and ulceration as seen in human inflammatory bowel disease(32). Wild-type and RasGAP KI mice were treated with 5% DSS in the drinking water over 72 hours and the clinical scores were calculated (part I figure 8). The clinical scores obtained predict an exacerbated inflammatory response in the KI mice. Currently we are performing the experiments to assess the expression levels of pro-inflammatory cytokines including IL-1 β , IL-6, TNF α in the colon.

4. Discussion

NF- κ B transcription factor is involved in a variety of important cellular and physiological responses, including modulation of cell survival and the coordination of immune response. The control of NF- κ B activity is therefore of considerable importance for tissue homeostasis. Hence, NF κ B-dependent transcription is tightly controlled, and regulation of its activation is adequately achieved at different levels throughout the signaling cascade.

Inhibition NF- κ B signaling is mediated mainly by sequestering the NF- κ B dimers in the cytosol through the formation of NF κ B-I κ B complexes. Besides I κ B family members, few NF- κ B cellular inhibitors have been identified, such as RelA-associated inhibitor (RAI) (33) and TNAP (TRAFs and NIK associated protein) (34). Here we report RasGAP-derived fragment N as a newly described stress-induced NF- κ B inhibitor. Negative regulation of NF- κ B can be achieved by post-translational modifications of signaling proteins that mainly control the activation

of the IKK complex. For instance, the A20 deubiquitinase enzyme, the expression of which is induced by NF- κ B, removes the polyubiquitin chains from Rip1 and IKK γ and this destabilizes the IKK-activating complex (35). Similar effects are mediated by the CYLD (cylindromatosis) tumour suppressor that inhibits both NF- κ B and JNK kinase activation by removing Lys63-linked polyubiquitin chains from BCL3, RIP1, TRAF2, TRAF6 and NEMO (11). Fragment N, however, does not affect the upstream activation events that lead to NF- κ B nuclear translocation. However, we did not monitor whether fragment N modulates the post translational modifications which may affect transcriptional activity, nuclear localization and stability of NF- κ B members (36). Rather, fragment N increases the rate of NF- κ B nuclear export, allowing less NF- κ B dimers to reside in the nucleus. This consequently inhibits the ability of NF- κ B to regulate the expression of the downstream target genes.

Human diseases may result from either loss or gain of function in NF- κ B signaling. For example sustained inhibition of NF- κ B is accompanied by severe immune deficiency, increased susceptibility to infection and profound effects on tissue homeostasis in both immune and non-immune cell (11;37;38). Uncontrolled NF- κ B activation can lead to chronic inflammation; increase the risk of cancer (39), autoimmune diseases (e.g. rheumatoid arthritis), atherosclerosis and neurodegenerative disorders (11;37;40). Human inflammatory bowel diseases (IBDs), including ulcerative colitis and Crohn's disease, are chronic inflammatory conditions that result from dysregulation of the mucosal immune system in the gastrointestinal tract (41). Increased expression of pro-inflammatory cytokines IL-1 β , IL-6, and TNF α is detected in active IBDs and correlates with the severity of inflammation. NF- κ B is known to regulate the expression of these pro-inflammatory cytokines (8), therefore, the inhibition of NF- κ B in these conditions might be extremely useful in minimizing the severity of inflammation associated with IBDs.

caspase-3 in mildly stressed cells generates fragment N that protects cells through activating the Ras/PI3K/Akt pathway (42). Nevertheless, fragment N inhibits the activation of NF- κ B. Similarly, a caspase-cleaved form of Lyn inhibited the NF- κ B signaling pathway without any modifications in I κ B proteins, or on the nuclear translocation of NF- κ B (43). Akt kinases play a role in diverse signaling cascades that regulate cell proliferation, survival, invasiveness, and angiogenesis. Aberrant regulation of these processes is considered as a hallmark of cancer (44). Akt induced NF- κ B activation is beneficial in certain cases where NF- κ B inhibits the apoptosis of dendritic cells (45;46). Whereas it is detrimental in other cases, NF- κ B functions as tumor promoter in hepatocellular carcinoma that commonly develops in the background of chronic hepatitis. In addition, In pancreatic β -cells, strong NF- κ B activation favours β -cells death (47). It is probably essential that the persistent fragment N-mediated activation of Akt requires a negative modulation of prosurvival signals conveyed by NF- κ B to minimize the chances of tumor formation. Indeed, the overexpression of fragment N in pancreatic β under the control of rat insulin promoter (RIP) activated Akt but did not induce insulinoma formation in those mice (48). On the contrary, when Akt was constitutively activated in the RIP-myr-Akt transgenic mice, those mice were more susceptible for spontaneous insulinoma formation (49).

The precise molecular mechanism by which fragment N favours the nuclear export of NF- κ B is not fully elucidated. Crm1-mediated nuclear export depends on the formation of the multiprotein export complex that contains the GTP-binding protein Ran and Ran binding protein 3 (RanBP3). Active nuclear export depends on the availability of GTP-bound form of Ran that is essential for the translocation of RNA and protein by the nuclear pore complex. The exchange of Ran GDP-bound into GTP-bound state is mediated by the chromatin-associated GEF known as the regulator of chromosome condensation 1 (RCC1). RanBP3 plays an important role in stabilizing the export complex formation containing Crm1 in Ran.GTP and RCC1 (50). Future experiments will be directed to study the effect of fragment N on nuclear export complex formation mainly by

monitoring any modifications favored by fragment N on the expression levels of RanGTP and RanBP3. Additional experiments should be carried out to evaluate the role of fragment N in the formation of nuclear export complex and to validate whether fragment N favours the export of other transcription factors including STAT1, NFAT, and c-Fos.

5. Figure legends

Figure 1: Fragment N activates Akt in a Ras-dependent manner but hampers the ability of Akt to mediate NF- κ B activation.

A-C. HeLa cells were co-transfected with an empty vector (pcDNA3) or with a V12Ras-encoding plasmid (V12Ras), with or without a fragment N-encoding plasmid (N). Lysates were then analyzed by Western blot for the presence of the indicated proteins (panel A). Quantitation of the phospho-Akt and phospho-GSK-3 α / β is shown in panel B and C, respectively (mean \pm 95% CI of 3 experiments performed in duplicate). **D-F.** HeLa cells were transfected with 0.25 μ g prLUC, a NF- κ B reporter plasmid and 0.25 μ g of pRL-TK renilla luciferase-encoding plasmid together with plasmids encoding the indicated constructs. NF- κ B activity was measured by luciferase assay and expressed as a fold increase over basal (Mean \pm 95% CI of 3 experiments).

Figure 2: Fragment N blocks NF- κ B activation in response to various stimuli

A. HeLa cells were transfected with the combination of 0.25 μ g prLUC, NF- κ B reporter plasmid and 0.25 μ g of pRL-TK renilla luciferase-encoding in addition to empty plasmid (pcDNA3), or HA-tagged fragment N-encoding plasmid (N) as indicated. Cells were then stimulated with IL1 β , hTNF α or LPS as indicated. NF- κ B activity is expressed as a fold increase over basal (mean \pm S.E. of duplicate determinations). **B.** HeLa cells were transfected with a combination of 0.25 μ g prLUC, NF- κ B reporter plasmid and 0.25 μ g of pRL-TK renilla luciferase-encoding in addition to empty plasmid (pcDNA3), and plasmids encoding the expression of proteins TRAF2, TRAF6, EDAR or NIK, in the presence or absence of HA-tagged fragment N-encoding plasmid (N) as indicated. NF- κ B activity was measured as indicated in panel A. **C.** HeLa cells were transfected or not with HA-tagged fragment N, 24 hours after transfection cells were treated or not with 25 ng/ml of hTNF alpha for 30 minutes. 5 μ g of nuclear proteins were

subjected to electrophoretic mobility shift assay (EMSA) using a DNA probe containing NF- κ B binding element.

Figure 3: Fragment N prevents p65 nuclear accumulation

A. INS1 cells were plated on cover slips and transfected with a GFP-p65-encoding plasmid (GFP-p65), in the presence or in the absence of an HA-tagged fragment N-encoding plasmid (N). After 20 hours, cells were then stimulated for 30 minutes with 25 ng/ml TNF α . Cells were fixed and the nuclei were stained with Hoechst 33342. Immunocytochemistry was performed using an anti-HA antibody and the cells were photographed using a Zeiss confocal microscope. **B-D.** INS1, HeLa, and U2OS cells were transfected with plasmids encoding the indicated constructs. In panel B, the cells were further stimulated or not for 30 min with 25 ng/ml human TNF α . The cells were then photographed as above and the percentage of GFP-p65 levels in the nucleus was determined as described in the method section. The cross in a box indicates the mean; the red line in a box indicates the median; the box contains 50% of values (i.e. 25% of those above and 25% of those below the median); whisker's length corresponds to 1.5 time of the box's length (if shorter, the length of the whisker reaches the lowest or the highest value of the data set). Small squares represent outlier values (i.e. outside the range covered by the box and the whiskers).

Figure 4: Stresses that induce the formation of fragment N blunt NF- κ B activation in a caspase-dependent manner.

A. HeLa cells were transfected as described in Figure 1A. The cells were then illuminated or not with UV (46 J/m²) and 24 hours later, the cells were stimulated or not for 30 minutes with 25 ng/ml of human TNF α . NF- κ B activity was then determined as described in Figure 2A. The results correspond to the mean plus or minus SD of three experiments performed in duplicate. **B.** HeLa cells were transfected as described in Figure 1A. The cells were then pre-incubated or not

with 10 μ M of the caspase inhibitor MX103, followed by UV illumination and TNF α stimulation as described in panel A. NF-kB activity was then determined as described in Figure 2A. **C.** Wild type or RasGAP D455A MEFs were treated as described in Panel A. (Upper panel), cells were then lysed and the pattern of RasGAP cleavage were analyzed by western blot using antibody that detects full-length as well as fragments N and N2. (Lower panel), alternatively the extent of NF-kB activation was monitored by electrophoretic mobility shift assay as described in Figure 2C.

Figure 5: Fragment N does not inhibit I κ B alpha degradation, neither bind to NF-kB

A. Fragment N does not inhibit I κ B degradation. HeLa cells were infected with an empty virus or with an HA-tagged fragment N-encoding virus (N). 72 hours after infection, cells were stimulated for 30 minutes with 25 ng/ml TNF α and then lysed with monoQC lysis buffer. The levels of fragment N expression and I κ B α were measured by western blot using antibodies directed toward HA and the endogenous form of I κ B respectively. **B. Immunoprecipitation p65.** Two-million 293T cells were transfected with empty pcDNA3, V5-tagged fragment N (V5-N) or V5-tagged I κ B α (V5-I κ B α) with HA-tagged p65 (HA-p65). 500 μ g of cell lysates were then immunoprecipitated with 1 μ g of anti-V5 antibody. Lysates and the immunoprecipitated material were analysed by Western blot using a RasGAP (upper panel), p65 (middle panel) and anti-V5 body (lower panel) or an anti-p50 antibody. Star indicates a non-specific band. **C. Immunoprecipitation p50.** Two-million 293T cells were transfected with empty pcDNA3, V5-tagged fragment N (V5-N) or V5-tagged I κ B α (V5-I κ B α). 500 μ g of cell lysates were then immunoprecipitated with 1 μ g of V5 antibody. The initial lysates and the immunoprecipitated material were analysed by Western blot using a RasGAP (upper panel), p50 (middle panel) and anti-V5 body (lower panel). Note that anti p50 antibody recognizes the p105 as well.

Figure 6: 250,000 HeLa cells were transfected with empty plasmid, I κ B α . Δ N2, or fragment N encoding plasmid in combination with GFP-p65 encoding plasmid. After 24 hours the cells were treated with 2 ng/ml of Leptomycin B for one hour. The cells were then fixed and immunocytochemistry was performed as described before. The levels of nuclear and cytoplasmic signals were analyzed by Nikon Eclipse 90i automated microscope.

Figure 7: Fragment N favors NF- κ B nuclear export

Two hundred fifty thousand HeLa cells were transfected with an mCherry-encoding plasmid or with an mCherry-tagged fragment N-encoding plasmid together with a GFP-p65-encoding plasmid. Prior to cytoplasmic photo-bleaching cells were treated for 30 minutes with hTNF α to promote nuclear accumulation of GFP- tagged p65. Nuclear export of NF- κ B was recorded for 28 minutes by FRAP as indicated in the method section (panel A). When indicated, cells were treated with 2 ng/ml of Leptomycin B for one hour prior to TNF α stimulation. Panel B depicts representative images of cells at different times during the FRAP experiment.

Figure 8: Fragment N does not affect CRM1 expression

Two hundred thousand HeLa cells were infected with an empty virus or with an HA-tagged fragment N-encoding virus (N). Three days later, cells were stimulated or not for 24 hours with 25 ng/ml TNF α and then lysed in RIPA lysis buffer. The levels of fragment N expression and CRM1 were measured by Western blot using anti-HA and anti-Crm1 antibodies, respectively.

Figure S1: Fragment N activates Akt in a Ras-dependent manner

Hela cells were transfected with empty vector (pcDNA3) or N17Ras encoding plasmid (N17Ras), with or without fragment N encoding plasmid (N). The cells were then washed twice with 1x PBS and starved for 48 hours, and then lysed. 50 µg of proteins were analysed by western blotting using antibodies detecting HA, Akt and phospho (S473) Akt.

Figure S2: Fragment N inhibits NF-κB in various cell types

293T cells were transfected with the combination of 0.25 µg prLUC, NF-κB reporter plasmid and 0.25 µg of pRL-TK renilla luciferase-encoding in addition to empty plasmid (pcDNA3), and plasmids encoding the expression of proteins TRAF2, or p65 in the presence or absence of HA-tagged fragment N-encoding plasmid (N) as indicated. NF-κB activity is expressed as a fold increase over basal as in (mean +/- S.E. of duplicate determinations).

Figure S3: Fragment N does not bind to p65 or p50 in TNF α - or LPS-stimulated cells

A: 293T cells were transfected as indicated in figure 5B, however cells were treated with 25 ng/ml TNF α or 1 µg/ml LPS for 30 minutes before lysis, then 500µg of proteins were immunoprecipitated as explained in figure 5B.

C: 293T cells were transfected as indicated in figure 5C, however cells were treated with 25 ng/ml TNF α or 1 µg/ml LPS for 30 minutes before lysis, then 500µg of proteins were immunoprecipitated as explained in figure 5C.

Figure S3: Fragment N does not bind to importin- α 3 and α 4

Two-million 293T cells were transfected with empty pcDNA3, HA-tagged fragment N (HA-N) or HA-tagged p65 (HA-p65) with V5-tagged p65 (V5-Imp α 3). 500 µg of cell lysates were then immunoprecipitated with 1 µg of anti-HA antibody. Lysates and the immunoprecipitated material were analysed by Western blot using an HA (upper panel), and anti-V5 body (lower panel). **B:** Two-

million 293T cells were transfected with empty pcDNA3, HA-tagged fragment N (HA-N) or HA-tagged p65 (HA-p65) with V5-tagged p65 (V5-Imp α 4). 500 μ g of cell lysates were then immunoprecipitated with 1 μ g of anti-HA antibody. Lysates and the immunoprecipitated material were analysed by Western blot using an HA (upper panel), and anti-V5 body (lower panel).

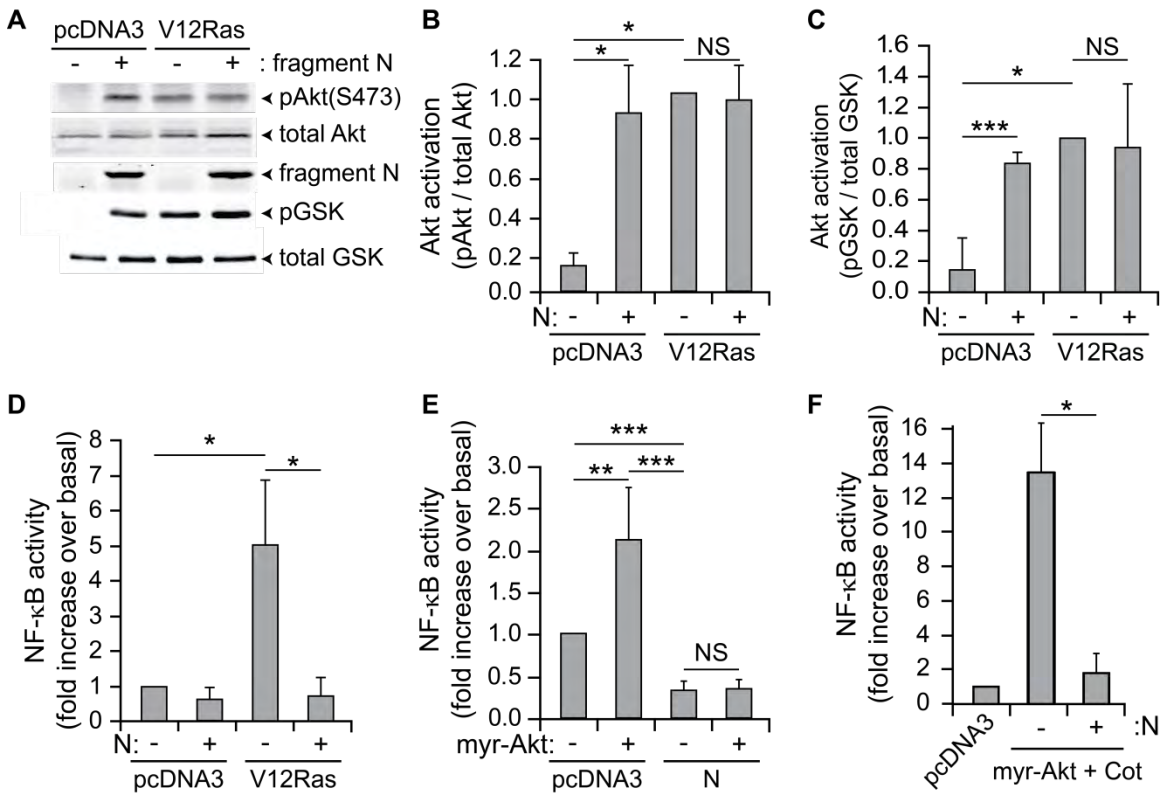


Figure 1

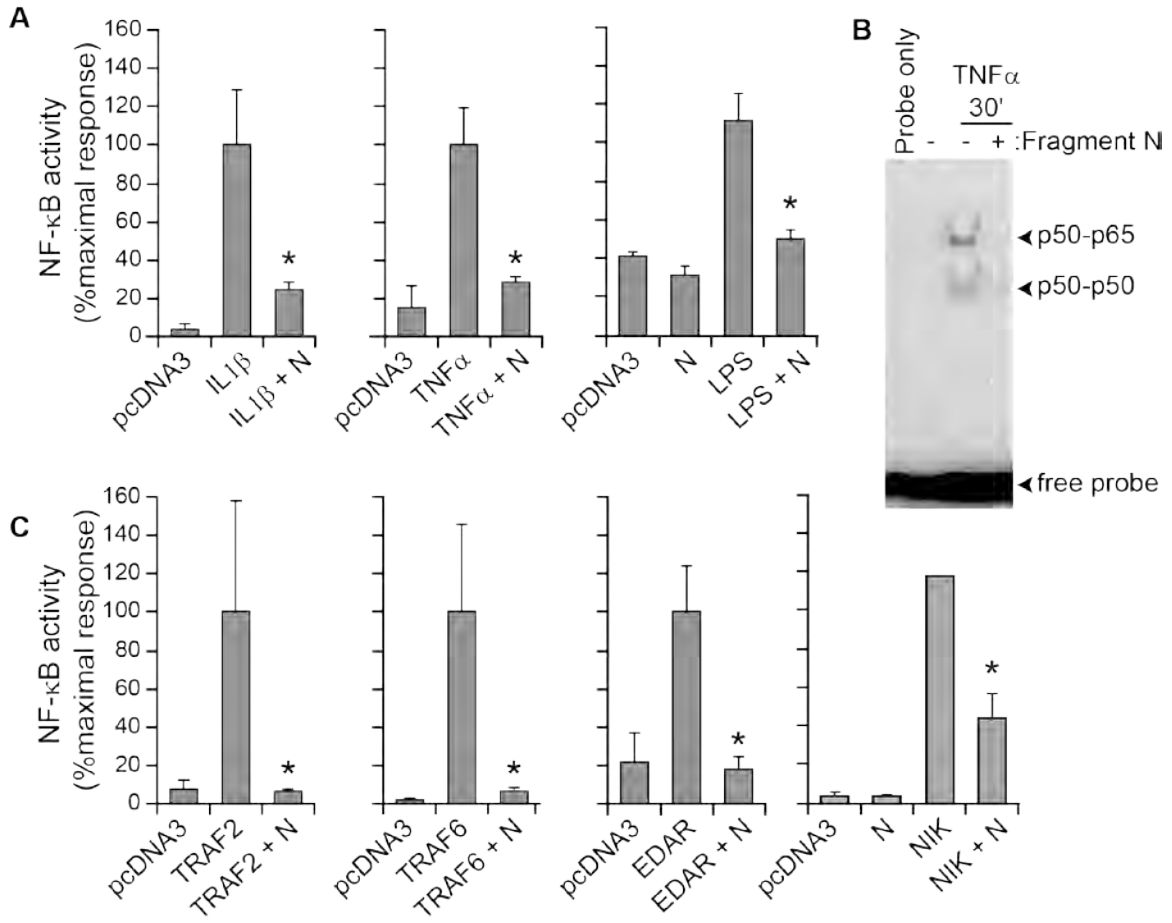


Figure 2.

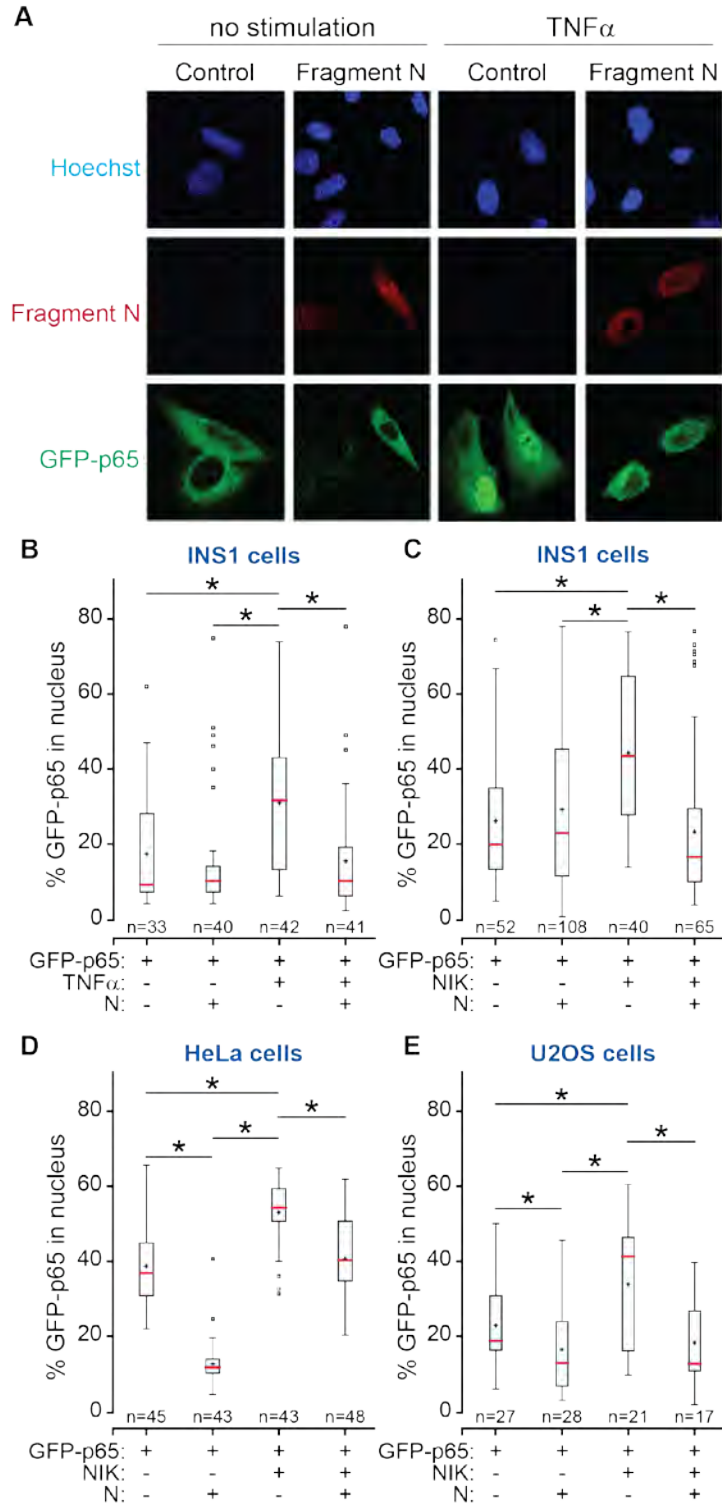


Figure 3.

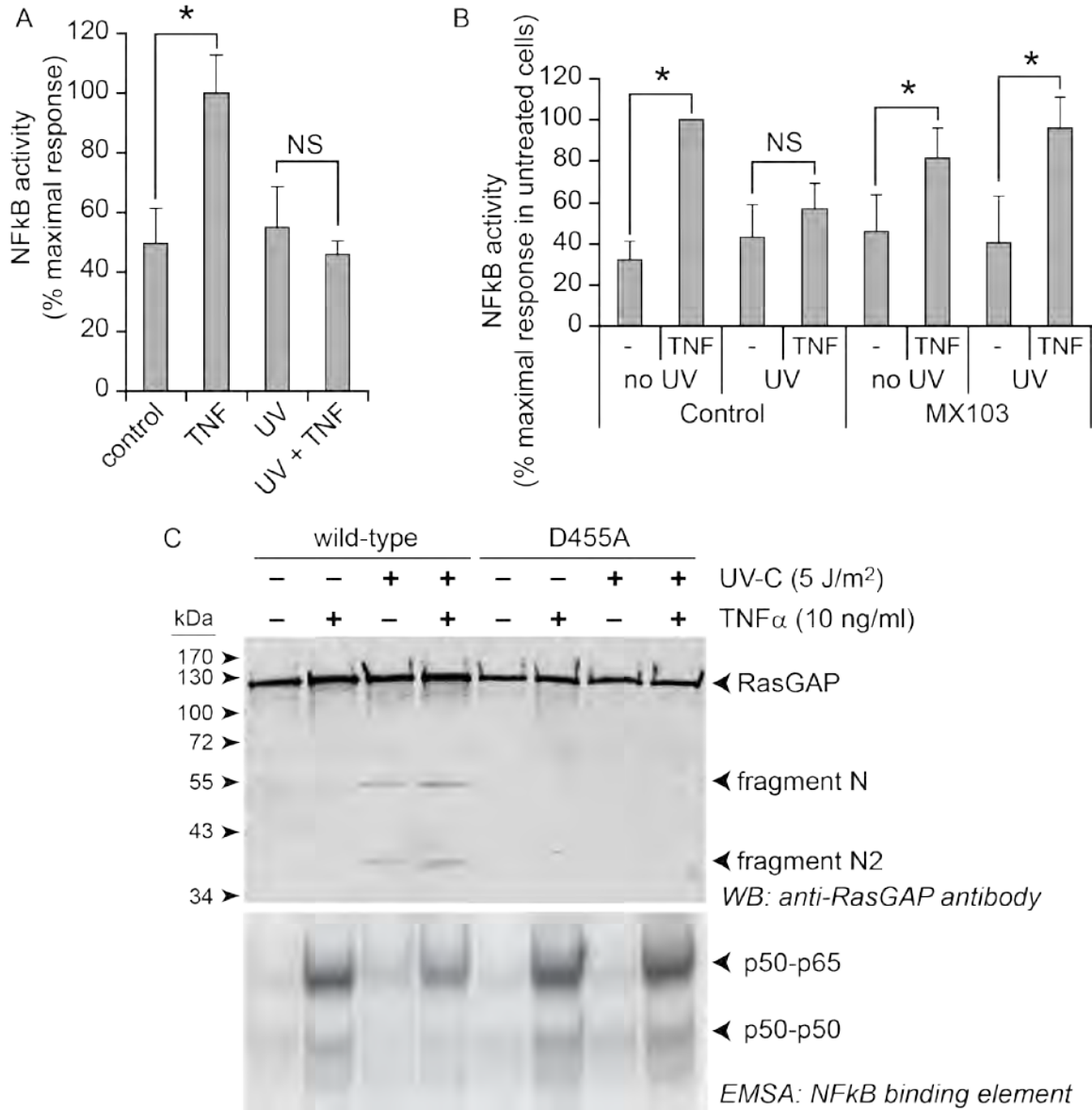
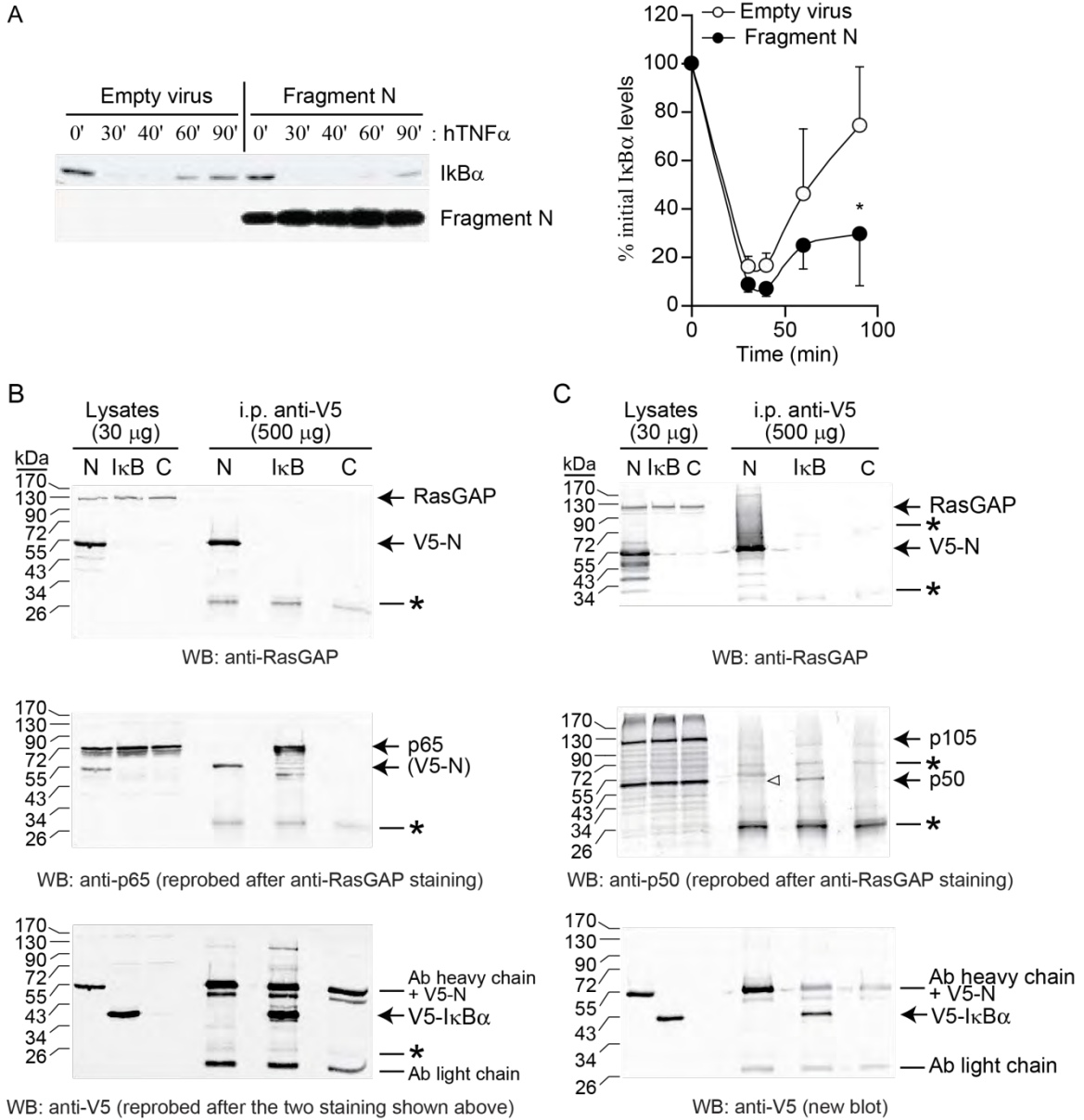


Figure 4.



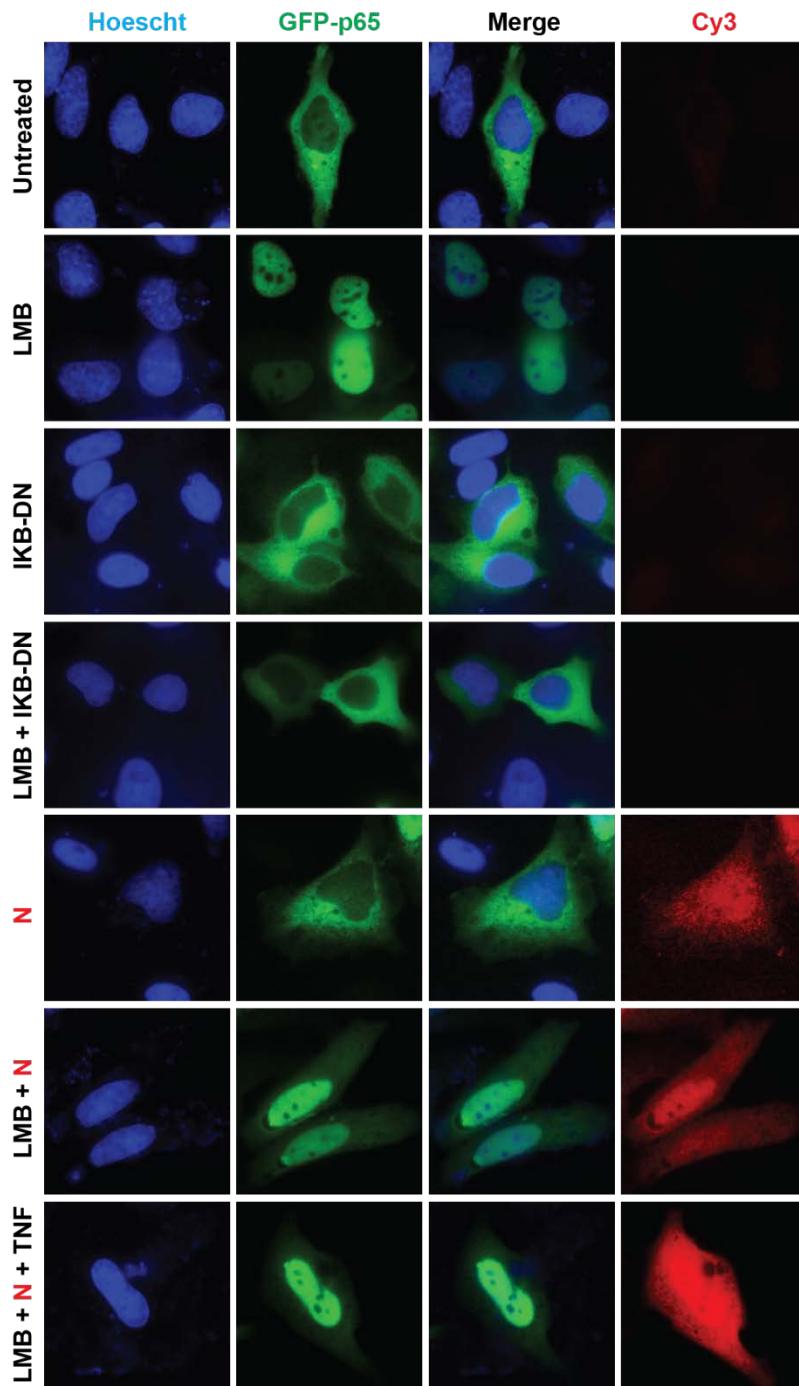


Figure 6

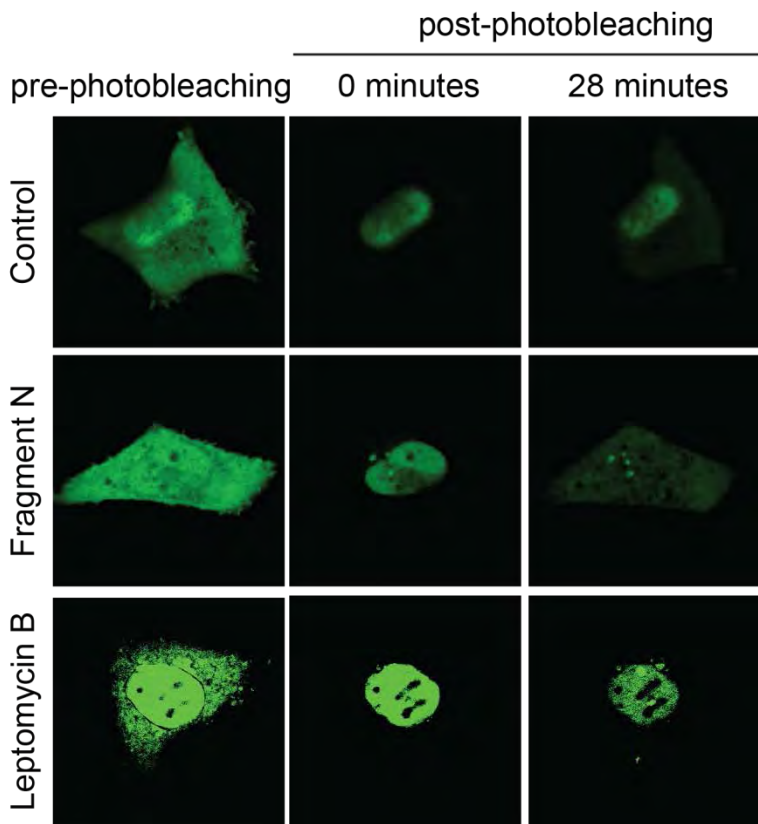
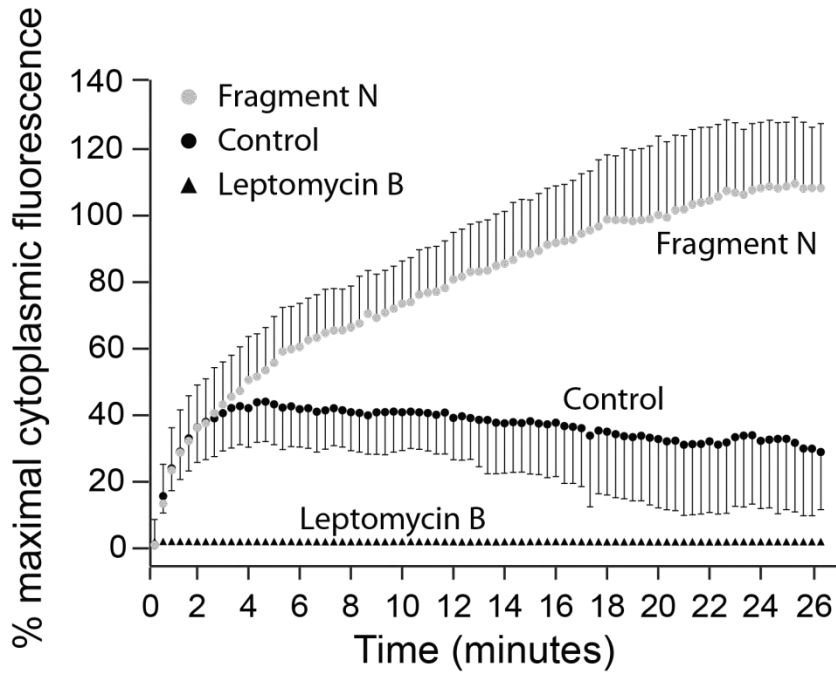


Figure 7.

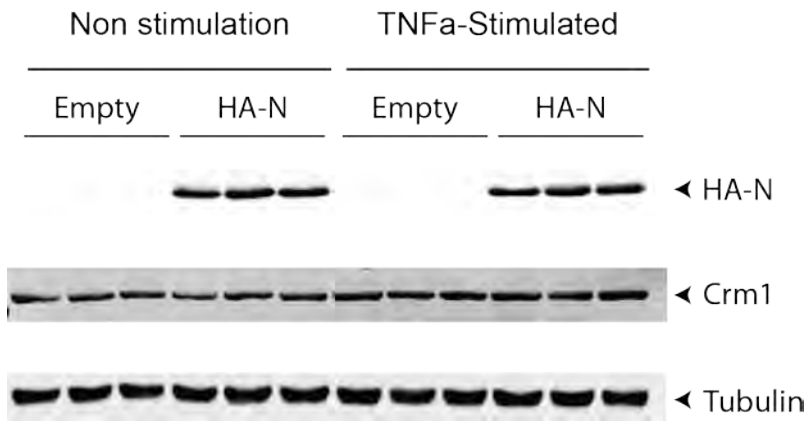


Figure 8.

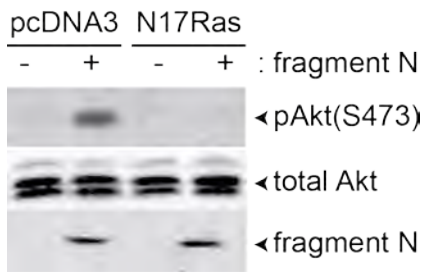


Figure S1.

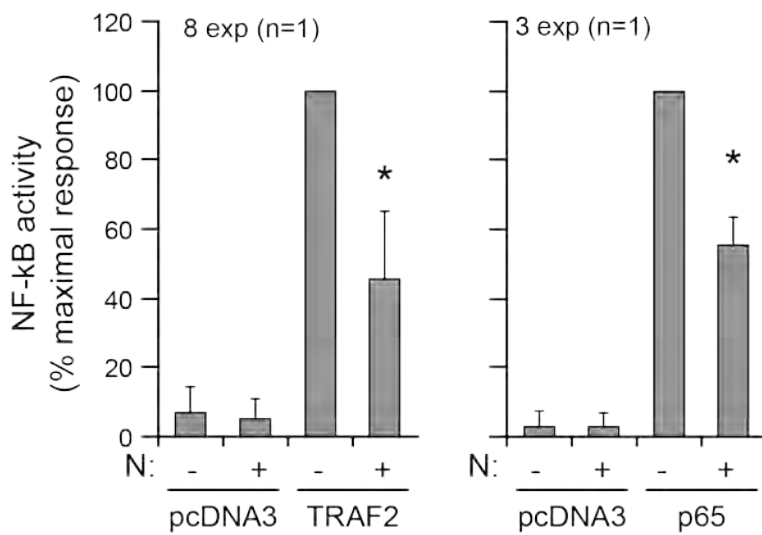


Figure S2.

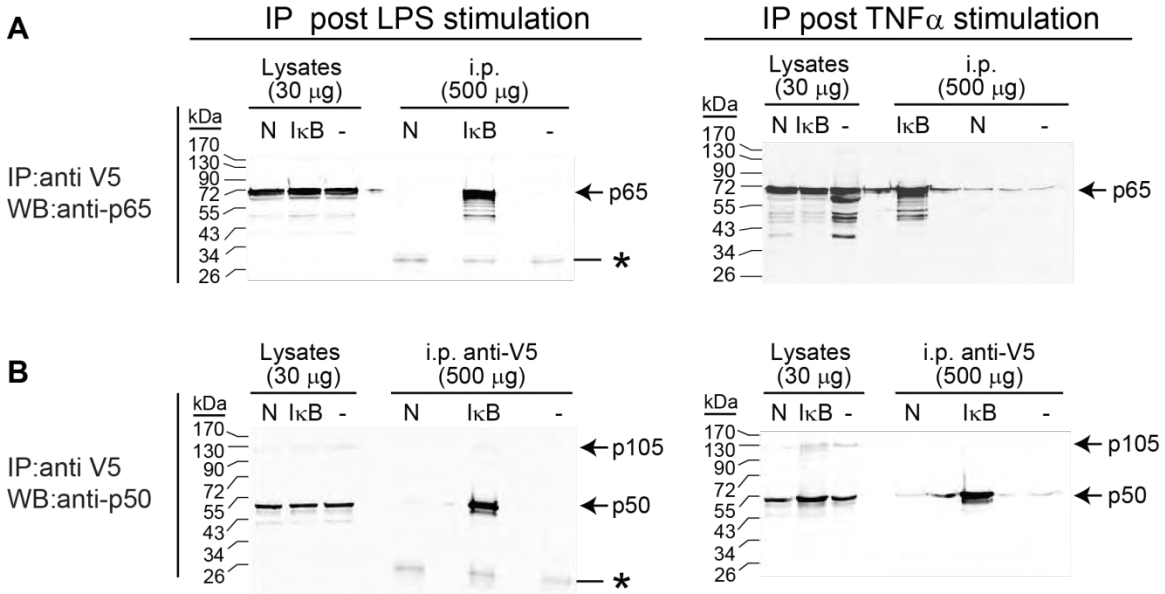


Figure S3.

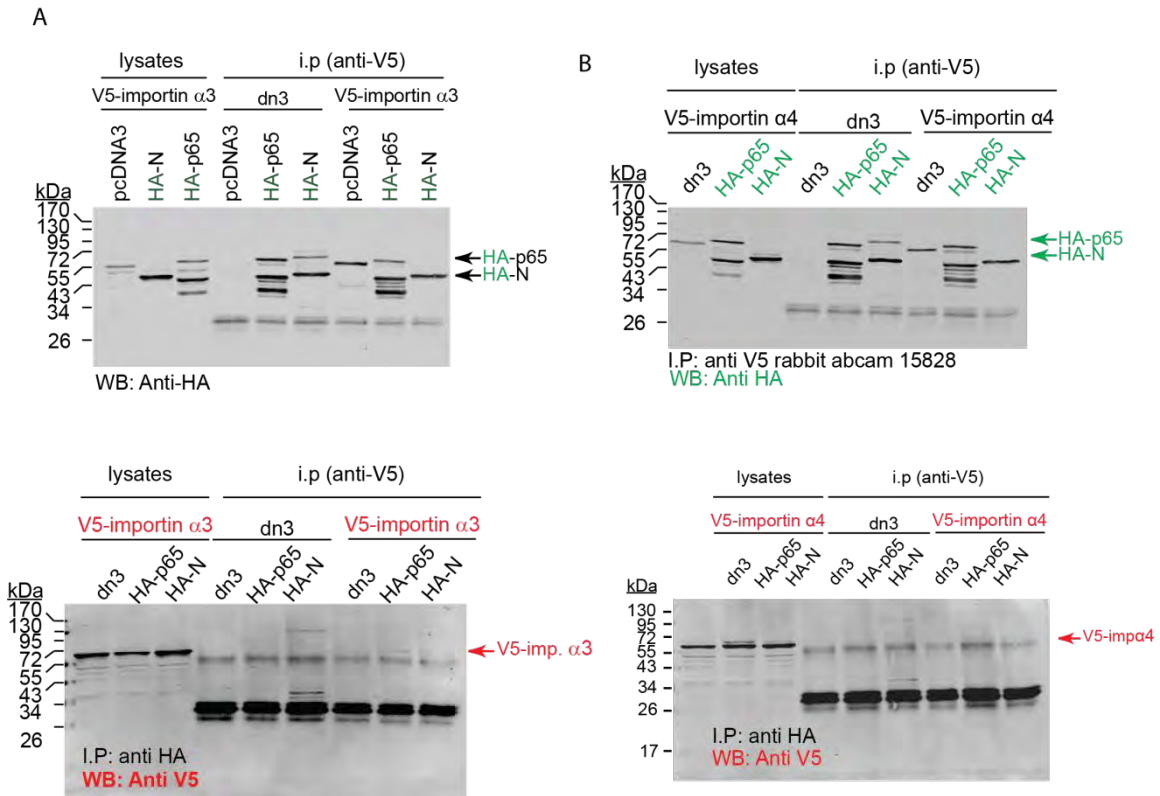


Figure S4.

6. Materials and methods

Cells and transfection

HEK 293 cells (ATCC, Manassas, VA catalog n°CRL-1573) were grown in Dulbecco's modified Eagle's medium (DMEM; GIBCO, catalog n°61965) supplemented with 10% fetal calf serum (Invitrogen, catalog n° 41Q2174K), 100 units/ml penicillin, and 0.1 mg/ml streptomycin (Sigma, catalog n° P0781). HeLa cells were maintained in RPMI 1640 (GIBCO catalog n° 61870-10) containing 10% fetal calf serum. INS1 cells were maintained in RPMI 1640 containing 10% fetal calf serum and 50 μ M β -mercaptoethanol. All these cells were cultured at 37°C and 5% CO₂. INS1 and HeLa cells were transfected with the indicated plasmids using lipofectamine 2000 (Life Technologies; catalog n°11668-019). HEK 293T cells were transfected using the calcium/phosphate precipitation procedure (51). Eight hours after transfection, the medium containing the DNA precipitates was replaced with fresh serum-containing culture medium.

Chemicals and Antibodies

Human TNF α was from Roche (cat. n° 11 088 939 001). Mouse recombinant IL1 β and lipopolysaccharide (LPS) were from Sigma (cat. n° I5271 and L6529 respectively). Leptomycin B was from Calbiochem (cat. n° 431050). Hoechst 33342 was from Roche (catalog n°H-1399). It was diluted in water at a final concentration of 10 mg/ml and stored at 4°C in the dark. Mouse anti-V5 antibody was from Invitrogen (cat. n° R960-25). Rabbit anti-V5 antibody was from Abcam (cat. n° 15828). HA tag-specific antibodies were purchased as ascites from Babco (Richmond,CA; catalog n°MMS-101R). This antibody was adsorbed on HeLa cell lysates to decrease non-specific binding as previously described (13). The anti-RasGAP antibody was from Enzo Life Science (catalog number ALX-210-860-R100) and is directed at the fragment N2 moiety of the human protein (amino acids 158-455). The anti-phospho serine 473-Akt rabbit polyclonal IgG antibody was from cell signaling (catalog n°9271). The rabbit polyclonal IgG antibody recognizing Akt1/2 was from Santa Cruz Biotechnology (cat. n° SC-

8312). The anti-I κ B α , anti-p50/p105 and anti-p65 antibodies were from Cell Signaling (cat. n° 9242, and 3035 and 3034 respectively). The anti-Crm1 antibody was from Abcam (cat. n° ab24189). The secondary antibody used in immunocytochemistry experiments was a Cy3-conjugated AffiniPure Goat anti-mouse IgG (H+L) from Jackson Immuno Research Laboratories (catalog n°115-165-146). Alexa Fluor 680 goat anti-rabbit IgG (H+L) (Molecular Probes; catalog n°A21109) and IRDye 800-conjugated affinity purified anti-Mouse IgG (H+L) (Rockland catalog n°610-132-121) were the secondary antibodies used for Western blots.

Plasmids

dn3, *cmv*, *cr3* and *rk5* extensions in the names of some of the plasmids used in this study indicate that the backbone vector is pcDNA3 (Invitrogen), pCMV4/5 (Progmega), pCR3 (Invitrogen: catalog n°V1.0-140711sa), and pRK-5 (Pharmingen: catalog n°556104), respectively. The eukaryotic expression vector pcDNA3 (#1) was from Invitrogen (catalog n°A-150228). **pmCherry-N1** (#685) encoding for red fluorescent protein (RFP) and **pEGFP-C1** (#6) encoding the green fluorescent protein (GFP), were from Clontech (catalog n°632523 and 6084-1 respectively). **pRL-TK**, encoding the *Renilla reniformis* luciferase, was from Promega (catalog n°E2241). **prLUC** (#49) is an NF- κ B reporter plasmid. It contains two NF- κ B responsive elements (AGGGGACTTTCCGA) and a minimal cFos promoter (nucleotides 498–662 of the mouse cFos gene; locus MMCFOS) upstream of the firefly luciferase(20). The **h-H-Ras(G12V).dn3** (#182) plasmid codes for a constitutive active form of H-Ras (described previously as V12Ras.dn3 (15)). **h-H-Ras(S17N).cmv** (#159) encodes a dominant negative form of H-Ras (described previously as N17Ras.cmv (13)). **HA-hRasGAP[1-455](D157A).dn3** (#352) encodes the HA (MGYPYDVPDYAS)-tagged version of a caspase-resistant form of RasGAP fragment N (RasGAP sequences 1-455) (described previously as N-D157A.dn3 (13)). **HA-hRasGAP[1-455](D157A).Iti** (#353) is a lentiviral vector encoding the uncleavable form of fragment N (described previously as N-D157A.Iti (52)). **V5-hRasGAP[3-455](D157A).dn3**

(#585) encodes the V5 (MGKPIPPLLGLDST)-tagged version of the caspase-resistant form of fragment N lacking the first two amino acids (53). **HA-hRasGAP[1-455](D157A)-no stop.dn3** (#365) bears the HA-tagged version of caspase-resistant fragment N lacking the stop codon. It was constructed by PCR amplifying HA-hRasGAP[1-455](D157A).dn3 (#352) (20) with the sense oligonucleotide #71 [GCGTGGATAGCGGTTTACTC (nucleotides 644-664 of pcDNA3)] and the anti-sense oligonucleotide #333 [AAAAAAAA (feeder) GCGGCCGC (NotI) GTC GAC TGT GTC ATT GAG TAC (human RasGAP D455-V449; last 6 nucleotides encoding for Sall restriction site)]. The PCR fragment was then cut with Bsu36 and NotI and the resulting 784 bp fragment subcloned into HA-hRasGAP[1-455](D157A).dn3 opened with the same enzyme. **HA-hRasGAP[1-455](D157A)-mCherry.dn3** (#784) codes for a fusion protein between the HA-tagged version of caspase-resistant fragment N and mCherry (a mutant fluorescent protein derived from the tetrameric *Discosoma sp.* red fluorescent DsRed protein). This plasmid was constructed by PCR amplification of pmCherry-N1 (#685) with the sense oligonucleotide #813 [AAAAAAA (feeder) CTCGAG (XhoI) CC (a two-nucleotide insertion that maintains the reading frame) ATGGTGAGCAAGGGCGAGGA (the first 20 nucleotides of the mCherry coding sequence) and the anti-sense oligonucleotide # 816 [TTTTTTT (feeder) TCTAGA (XbaI) CTAATTGTACAGCTCGTCCATGCCGCC (C-terminal sequence of mCherry)]. The resulting PCR product was digested with XhoI and XbaI and inserted into plasmid HA-hRasGAP[1-455](D157A)-no stop.dn3 (#365) cut with the same enzyme. The **myr-mAkt1-HA.cmv** (#249) plasmid encodes a constitutively active form of Akt that bears a Src myristoylation sequence (MGSSKSKPK) at its N-terminus and an HA tag at its C-terminus. It was described earlier under the name myr-Akt.cmv (15). **hIkB alpha.tb7** (#526) bears the human IkB α cDNA (nucleotides 2-1448 from NCBI entry NM_020529 but with T1228C and G1535C substitutions in the 3' untranslated region). It was obtained from RZPD (Deutsches Ressourcenzentrum for Genomforschung GmbH (accession number: IRAUp969B0119D6). **hIkB alpha.dn3** (#643) contains the same insert of hIkB alpha.tb7 but placed in the pcDNA3 eukaryotic expression

vector. It was constructed by sub-cloning the blunted *Sma*I/*Bam*HI *hIkB* alpha.tb7 fragment into pcDNA3 opened with the same enzymes and blunted. **V5-hIkB alpha.dn3** (#650) encodes a V5-tagged version of human I κ B α . It was constructed by PCR amplification of plasmid *hIkB* alpha.dn3 with the sense oligonucleotide #653 [CGC (feeder) GGATCC (*Bam*HI) GCCACC (Kozak) ATG GGC AAG CCA ATC CCT AAT CCA CTC CTC GGC CTC GAC AGT ACT (V5 tag) ATG TTC CAG GCG GCC (complementary sequence to nucleotides 95 to 109 of the human I κ B alpha mRNA; NCBI entry NM_020529)] and the anti-sense oligonucleotide #677 [AAAAAA (feeder) GAA GTG CCT CAG CAA TTT CTG GCT (complementary sequence to nucleotides 485 to 462 of the human I κ B alpha mRNA; NCBI entry NM_020529)]. The resulting 441 bp PCR product was digested with *Bam*HI and *Bbv*CI and inserted into plasmid *hIkB* alpha.dn3 that was linearized with the same restriction enzymes. **hIkB alpha delta N2.cmv** (#11) encodes the human I κ B α protein with the Δ N2 deletion (i.e. amino acid 3–71). This construct cannot be phosphorylated by I κ B kinases and degraded by the proteasome and therefore functions as an inhibitor of NF κ B. It has been described before under the name of I κ B α Δ N2 (15). **V5-hIkB alpha delta N2.mCherry** (#687) was constructed by PCR amplifying *hIkB* alpha delta N2.cmv with oligonucleotide #814 [AAAAAA (feeder) CTCGAG (*Xho*I) GCCACC (Kozak) ATG GGA AAA CCA ATA CCA AAT CCA CTA CTA GGC CTA GAC AGT ACA (V5 tag) ATG TTC GAG GAC GGG GAC TCG (sequence complementary to the first 7 codons of I κ B α Δ N2)] and oligonucleotide #815 [AAAAAA (feeder) GGATCC (*Bam*HI) GC (2 nucleotides added to maintain the reading frame with mCherry) TGC (stop codon mutated to alanine) TAA CGT CAG ACG CTG GCC TCC AA (last 23 nucleotides of the coding sequence of human I κ B alpha)]. The resulting 818 bp PCR product was digested with *Bam*HI and *Xho*I and inserted into plasmid pmCherry-N1 (#685) that was linearized with the same restriction enzymes. The **myc-hRelA.cr3** (#524) plasmid encodes a myc (EQKLISEEDL)-tagged version of human RelA. An NRSPGEFCRYP-coding intervening sequence is located between the myc tag and RelA. **GFP-hRelA.dn3** (#561) encodes a fusion protein between the green fluorescent protein (GFP) and

human RelA. It was constructed as follow. The myc-hRelA.dn3 plasmid was digested with XhoI, blunt-ended with Klenow, and then digested with HindIII. The resulting 1780 bp fragment was inserted into pEGFP-C3 (#98) opened with BamHI, blunt-ended with Klenow, and then digested with HindIII. The resulting plasmid (**GFP-stop-myc-hRelA**; #553) contains a stop codon between the GFP- and the myc-RelA-coding sequences. The stop codon and the myc tag were removed by a Scal/EcoRV digestion and self-ligation, generating plasmid GFP-hRelA.dn3. **hNIK-HA.cmv** (#498) encodes the human NFkB-inducing kinase (NIK) bearing an HA tag (MGYPYDVPDYAS) at its C-terminus. **FLAG-hTRAF2.cr3** (#539) encodes the human TNFR-associated factor 2 protein (nucleotides 64-1563 of NCBI entry BC043492; first 2 codons missing) bearing a FLAG tag (MDYKDDDDK) at its N-terminus. **FLAG-mTRAF6.dn3** (#518) encodes the mouse TNFR-associated factor 6 protein (nucleotides 371-1999 of NCBI entry NM_009424) bearing a FLAG tag at its N-terminus. The **mEDAR.dn3** (#517) plasmid contains the mouse ectodysplasin A receptor cDNA (nucleotides 260-1604 of NCBI entry NM_010100). **Myc-hCot.rk5** (#477) bears myc-tagged human Cot.

Fluorescence recovery after photobleaching (FRAP)

Two-hundred thousand HeLa cells were seeded in 35 mm glass bottom micro-well dish (MatTek, catalog n°P35G-1.5-14-C). Twenty-four hours later the cells were co-transfected with the indicated plasmids. After an additional 24-hour period, the cells were treated for 30 minutes with hTNF α to promote GFP-p65 nuclear accumulation. FRAP was then performed using a Zeiss confocal microscope (Carl Zeiss/LSM710) piloted by the ZEN 2009 software and equipped with a 40X objective (EC Plan-neofluar 40x/1.30 Oil DIC M27). Photo-bleaching was achieved by simultaneous laser excitation at three wavelengths 458, 488 and 514 nm for 20 seconds. Cytoplasmic fluorescence recovery was automatically recorded by the ZEN 2009 software (one image was taken every 20 seconds during 28 minutes). The cytoplasmic intensity values (i.e. the total fluorescence intensity values in the whole cytoplasmic surface) were normalized

to the nuclear fluorescence intensity at time 0 (i.e. the nuclear value found in the first image recorded after photobleaching). For a given experiment, the resulting ratios were normalized to the maximal recorded ratio, which in the present study is obtained when cells express fragment N.

NF- κ B luciferase reporter assay

Cells cultured in six-well plates were transfected with the plasmids of interest in the presence of 0.25 μ g of prLUC (#49), an NF- κ B firefly luciferase expressing reporter plasmid (54) and 0.25 μ g of pRL-TK (#402), a plasmid encoding the Renilla luciferase. The total amount of DNA used in the transfection was always kept to 3 μ g by the addition of empty pcDNA3 when required. Twenty-four hours after transfection, the cells were lysed. In some cases, the cells were treated for 30 minutes with TNF α or IL1 β before lysis. Luciferase assay was performed using the Dual-Luciferase Reporter Assay from Promega (cat. no. E1910). Lysis was performed by the addition of 200 μ l of passive lysis buffer (PLB) provided by the manufacturer and incubated 30 min on ice. The lysates were then cleared by centrifugation at 16'000 g for 15 min. The firefly luciferase activity was recorded by mixing 25 μ l of the lysate with 25 μ l of the LARII Reagent and the Renilla luciferase activity was recorded by adding to the previous mix 25 μ l of the Stop and Glo reagent. For each measurement, light emission was quantified during 12 s using a Lumat LB 9501 luminometer (Berthold Technologies, Zurich, Switzerland). Results are expressed as the ratio of the firefly luciferase signal normalized to *Renilla* luciferase signal.

Akt kinase Assay

HeLa cells were cultured and transfected with the indicated plasmids as indicated above. Cells were then starved for 48 hours and the Akt kinase activity was measured using a kinase assay from Cell Signaling (catalog n°9840) as per the manufacturer's instructions. Briefly, the cells were lysed in 0.5 ml mono-Qc buffer (70 mM β -glycerophosphate, 0.5% Triton X-100, 2 mM MgCl₂, 100 mM Na₃VO₄, 1 mM dithiothreitol, 20 μ g/ml aprotinin) (13). After clearing the lysates by

centrifugation at 16'000 g for 15 min, Akt was immunoprecipitated from 300 µg of cell lysates proteins with an anti-Akt antibody linked to agarose beads overnight at 4°C. The immunoprecipitates were then washed 3 times with mono-Qc buffer and resuspended in 50 µl kinase buffer (2.5 mM Tris pH7.5, 0.5 mM β-glycerolphosphate, 0.2 mM DTT, 10 µM Na₃VO₄, 1 mM MgCl₂) supplemented with 200 µM ATP and 1 µg of glycogen synthase kinase-3 fusion protein. After 30 min at 30°C the reaction was stopped by the addition of 25 µl of 3X SDS sample buffer (187.5 mM Tris HCl (pH 6.8), 6% SDS, 30% glycerol, 150 mM DTT, 0.03% bromophenol blue), and the extent of glycogen synthase kinase-3 phosphorylation was analyzed by Western blotting using a specific anti-phospho-glycogen synthase kinase-3 antibody.

Western blot analysis

Cells were lysed in monoQ-C buffer and protein quantification was performed by the Bradford technique. Equal amounts of proteins were subjected to SDS PAGE and then transferred onto a nitrocellulose membrane (Biorad catalog n°162 0115). The membranes were blocked with TBS-Tween 20 0.1% containing 5% non-fat milk and incubated over night at 4°C with the specific primary antibodies. Blots were then washed with TBS-Tween 0.1%, incubated with the appropriate secondary antibody (1:5000 dilution) 1 hour at room temperature and subsequently visualized and quantified with the Odyssey infrared imaging system (LICOR Biosciences, Bad Homburg, Germany). In some instances, the blots were stripped and reprobated. This was performed by incubating the blots at 50°C for 30 minutes in stripping buffer (62.5 mM Tris-base, 100 mM β-mercaptoethanol, 1% SDS, pH to 6.7) followed by three 20 minute-long washes at room temperature in TBS-tween 0.1%.

Immuno-cytochemistry

Cells were grown on glass coverslips, post specified transfection and treatment, the cells were fixed and immuno-cytochemistry was performed as previously described(55).

Immunoprecipitation

Two million HEK 293T cells were seeded in 10-cm plates and the following day transfected using the calcium/phosphate precipitation procedure (51). After an additional 24 hour period, cells were lysed in lysis buffer (50 mM Tris pH 7.4, 150 mM NaCl, 1% NP-40) and 500 µg of the lysates were incubated with 1 µg of the specified antibody for 12 hours at 4°C. Thirty µl of G sephrose beads (Amersham Bio-Sciences cat n°17-0618-01) were then added to the samples and the incubation resumed for 2 additional hours. Immunoprecipitate complexes were then washed 3 times with PBS and solubilised in 30 µl sample buffer (250 mM Tris-HCl pH 7, 10% SDS, 30% glycerol, 5% β- mercaptoethanol) and subjected to SDS page subsequently.

Electrophoretic mobility shift assay (EMSA)

Cells were washed in ice-cold PBS and then resuspended in buffer A (10 mM Hepes, pH7.9, 10 mM KCl, 0.1mM EDTA, 0.1mM EGTA, 1mM dithiothreitol, 1mM phenylmethylsulfonyl fluoride) (400 µl/well for 6-well plates). Cells were kept 15 minutes on ice, then 12.5 µl of 10% NP40 was added, and the cells were pelleted 2 min at 16'000 g. The pellet was washed with 100 µl of buffer A and resuspended in 50 µl buffer C (20 mM Hepes, pH 7.9, 0.4 M NaCl, 1 mM EDTA, 1 mM EGTA, 1mM dithiothreitol, 1 mM phenylmethylsulfonyl fluoride PMSF). After 20 min of incubation on ice, the cells were centrifuged 5 min at 16'000 g, and the supernatants (nuclear extracts) were transferred to a new tube and frozen at -80°C. A probe containing a NF-κB binding site (underlined) was prepared by annealing the complementary nucleotides GGC AGT TGAA GGGGACTTTCC CAGG and GGT AGCCT GGGAAAGTCCCC TTCA. The annealed probe was labelled with ³²P-dCTP (5 µCi) using Klenow DNA polymerase (2 U/µl; Promega cat. n° M2201). Four ng of the labeled probe and 10 µg of nuclear extracts were mixed in binding buffer (10 mM Hepes, pH 7.9, 25 mM KCl, 0.25 mM EDTA 0.05% NP40, 0.5 mg/ml BSA, 2.5% glycerol, 0.2 µg/µl poly (deoxyinosine-deoxycytidine) (Amersham bioscience 27-7880-01), 1 mM

PMFS, 1 mM DTT), incubated at room temperature for 20 min, and then separated in a 0.5X TBE, 5% polyacrylamide native gel. The dried gel was analyzed using a Phosphoimager (Bio-Rad).

Lentiviral infection

Recombinant lentiviruses were produced as described previously (52).

Quantitation of the percentage of nuclear GFP-p65

Quantification of the nuclear GFP-RelA was performed by measuring the mean intensity of GFP fluorescence in cytoplasm and in the nucleus then calculating the ratio using Image J software.

Statistical analysis

Results are shown as mean \pm SD. The statistical analyses used in this study were one-way ANOVAs and paired Student's test. In the latter case, the difference between the indicated conditions was considered significant when $p < 0.05/n$, where p is the probability derived from the t test analysis and n is the number of comparisons done (Bonferroni correction). Statistically significant differences are indicated by asterisks.

Acknowledgements

We thank the late Jürg Tschopp, Fabio Martinon, and Arthur Weiss for the gift of plasmids myc-hRelA.cr3, hNIK-HA.cmv, and Myc-hCot.rk5, respectively.

Reference List

1. Sen,R., and Baltimore,D. 1986. Inducibility of kappa immunoglobulin enhancer-binding protein Nf-kappa B by a posttranslational mechanism. *Cell* **47**:921-928.
2. Baldwin,A.S., Jr. 1996. The NF-kappa B and I kappa B proteins: new discoveries and insights. *Annu Rev Immunol.* **14**:649-683.
3. Barnes,P.J. 1997. Nuclear factor-kappa B. *Int J Biochem. Cell Biol* **29**:867-870.
4. Verma,I.M., Stevenson,J.K., Schwarz,E.M., Van,A.D., and Miyamoto,S. 1995. Rel/NF-kappa B/I kappa B family: intimate tales of association and dissociation. *Genes Dev.* **9**:2723-2735.
5. May,M.J., and Ghosh,S. 1998. Signal transduction through NF-kappa B. *Immunology Today* **19**:80-88.
6. Kopp,E.B., and Ghosh,S. 1995. NF-kappa B and rel proteins in innate immunity. *Adv Immunol.* **58**:1-27.
7. Li,Q., and Verma,I.M. 2002. NF-kappaB regulation in the immune system. *Nat Rev Immunol.* **2**:725-734.
8. May,M.J., and Ghosh,S. 1998. Signal transduction through NF-kappa B. *IT* **19**:80-88.
9. Oeckinghaus,A., Hayden,M.S., and Ghosh,S. 2011. Crosstalk in NF-kappaB signaling pathways. *Nat. Immunol.* **12**:695-708.
10. Bonizzi,G., and Karin,M. 2004. The two NF-kappaB activation pathways and their role in innate and adaptive immunity. *Trends Immunol.* **25**:280-288.
11. Wong,E.T., and Tergaonkar,V. 2009. Roles of NF-kappaB in health and disease: mechanisms and therapeutic potential. *Clin Sci (Lond)* **116**:451-465.
12. Pasparakis,M. 2012. Role of NF-kappaB in epithelial biology. *Immunol. Rev.* **246**:346-358.
13. Yang,J.-Y., and Widmann,C. 2001. Antiapoptotic signaling generated by caspase-induced cleavage of RasGAP. *Mol. Cell. Biol.* **21**:5346-5358.
14. Yang,J.-Y., Walicki,J., Michod,D., Dubuis,G., and Widmann,C. 2005. Impaired Akt activity down-modulation, caspase-3 activation, and apoptosis in cells expressing a caspase-resistant mutant of RasGAP at position 157. *Mol. Biol. Cell* **16**:3511-3520.
15. Yang,J.-Y., and Widmann,C. 2002. The RasGAP N-terminal fragment generated by caspase cleavage protects cells in a Ras/PI3K/Akt-dependent manner that does not rely on NF-kB activation. *J. Biol. Chem.* **277**:14641-14646.

16. Yang,J.-Y., Michod,D., Walicki,J., Murphy,B.M., Kasibhatla,S., Martin,S., and Widmann,C. 2004. Partial cleavage of RasGAP by caspases is required for cell survival in mild stress conditions. *Mol. Cell Biol.* **24**:10425-10436.
17. Ozes,O.N., Mayo,L.D., Gustin,J.A., Pfeffer,S.R., Pfeffer,L.M., and Donner,D.B. 1999. NF-kappaB activation by tumour necrosis factor requires the Akt serine-threonine kinase. *Nature* **401**:82-85.
18. Kane,L.P., Mollenauer,M.N., Xu,Z., Turck,C.W., and Weiss,A. 2002. Akt-dependent phosphorylation specifically regulates Cot induction of NF-kappa B-dependent transcription. *Mol Cell Biol* **22**:5962-5974.
19. Yang,J.Y., Walicki,J., Abderrahmani,A., Cornu,M., Waeber,G., Thorens,B., and Widmann,C. 2005. Expression of an uncleavable N-terminal RasGAP fragment in insulin-secreting cells increases their resistance toward apoptotic stimuli without affecting their glucose-induced insulin secretion. *J Biol Chem* **280**:32835-32842.
20. Bulat,N., Jaccard,E., Peltzer,N., Khalil,H., Yang,J.Y., Dubuis,G., and Widmann,C. 2011. RasGAP-derived fragment N increases the resistance of beta cells towards apoptosis in NOD mice and delays the progression from mild to overt diabetes. *PLoS. One.* **6**:e22609.
21. Yang,J.Y., Walicki,J., Jaccard,E., Dubuis,G., Bulat,N., Hornung,J.P., Thorens,B., and Widmann,C. 2009. Expression of the NH(2)-terminal fragment of RasGAP in pancreatic beta-cells increases their resistance to stresses and protects mice from diabetes. *Diabetes* **58**:2596-2606.
22. Cross,D.A., Alessi,D.R., Cohen,P., Andjelkovich,M., and Hemmings,B.A. 1995. Inhibition of glycogen synthase kinase-3 by insulin mediated by protein kinase B. *Nature* **378**:785-789.
23. Kane,L.P., Mollenauer,M.N., Xu,Z., Turck,C.W., and Weiss,A. 2002. Akt-dependent phosphorylation specifically regulates Cot induction of NF-kappa B-dependent transcription. *Mol Cell Biol* **22**:5962-5974.
24. Chung,J.Y., Park,Y.C., Ye,H., and Wu,H. 2002. All TRAFs are not created equal: common and distinct molecular mechanisms of TRAF-mediated signal transduction. *J Cell Sci.* **115**:679-688.
25. Kumar,A., Eby,M.T., Sinha,S., Jasmin,A., and Chaudhary,P.M. 2001. The ectodermal dysplasia receptor activates the nuclear factor-kappaB, JNK, and cell death pathways and binds to ectodysplasin A. *J. Biol. Chem.* **276**:2668-2677.
26. Jaeschke,H., Farhood,A., Cai,S.X., Tseng,B.Y., and Bajt,M.L. 2000. Protection against TNF-induced liver parenchymal cell apoptosis during endotoxemia by a novel caspase inhibitor in mice. *Toxicol. Appl. Pharmacol.* **169**:77-83.
27. Huxford,T., Huang,D.B., Malek,S., and Ghosh,G. 1998. The crystal structure of the IkkappaBalpha/NF-kappaB complex reveals mechanisms of NF-kappaB inactivation. *Cell* **95**:759-770.

28. Ben-Neriah, Y. 2002. Regulatory functions of ubiquitination in the immune system. *Nat. Immunol.* **3**:20-26.
29. Fagerlund, R., Kinnunen, L., Kohler, M., Julkunen, I., and Melen, K. 2005. NF- κ B is transported into the nucleus by importin α 3 and importin α 4. *J. Biol. Chem.* **280**:15942-15951.
30. Kudo, N., Matsumori, N., Taoka, H., Fujiwara, D., Schreiner, E.P., Wolff, B., Yoshida, M., and Horinouchi, S. 1999. Leptomycin B inactivates CRM1/exportin 1 by covalent modification at a cysteine residue in the central conserved region. *Proc. Natl. Acad. Sci. U. S. A* **96**:9112-9117.
31. Hutten, S., and Kehlenbach, R.H. 2007. CRM1-mediated nuclear export: to the pore and beyond. *Trends Cell Biol.* **17**:193-201.
32. Okayasu, I., Hatakeyama, S., Yamada, M., Ohkusa, T., Inagaki, Y., and Nakaya, R. 1990. A novel method in the induction of reliable experimental acute and chronic ulcerative colitis in mice. *Gastroenterology* **98**:694-702.
33. Yang, J.P., Hori, M., Sanda, T., and Okamoto, T. 1999. Identification of a novel inhibitor of nuclear factor- κ B, RelA-associated inhibitor. *J Biol Chem* **274**:15662-15670.
34. Hu, W.H., Mo, X.M., Walters, W.M., Brambilla, R., and Bethea, J.R. 2004. TNAP, a novel repressor of NF- κ B-inducing kinase, suppresses NF- κ B activation. *J Biol Chem* **279**:35975-35983.
35. Ruland, J. 2011. Return to homeostasis: downregulation of NF- κ B responses. *Nat. Immunol.* **12**:709-714.
36. Perkins, N.D. 2006. Post-translational modifications regulating the activity and function of the nuclear factor kappa B pathway. *Oncogene* **25**:6717-6730.
37. Courtois, G. 2005. The NF- κ B signaling pathway in human genetic diseases. *Cell Mol. Life Sci.* **62**:1682-1691.
38. Pasparakis, M. 2009. Regulation of tissue homeostasis by NF- κ B signalling: implications for inflammatory diseases. *Nat Rev Immunol.* **9**:778-788.
39. Pikarsky, E., Porat, R.M., Stein, I., Abramovitch, R., Amit, S., Kasem, S., Gutkovich-Pyest, E., Urieli-Shoval, S., Galun, E., and Ben Neriah, Y. 2004. NF- κ B functions as a tumour promoter in inflammation-associated cancer. *Nature* **431**:461-466.
40. Ben-Neriah, Y., and Karin, M. 2011. Inflammation meets cancer, with NF- κ B as the matchmaker. *Nat. Immunol.* **12**:715-723.
41. Podolsky, D.K. 2002. Inflammatory bowel disease. *N. Engl. J Med.* **347**:417-429.
42. Yang, J.-Y., Michod, D., Walicki, J., Murphy, B.M., Kasibhatla, S., Martin, S., and Widmann, C. 2004. Partial cleavage of RasGAP by caspases is required for cell survival in mild stress conditions. *Mol. Cell Biol.* **24**:10425-10436.

43. Marchetti,S., Gamas,P., Belhacene,N., Grosso,S., Pradelli,L.A., Colosetti,P., Johansen,C., Iversen,L., Deckert,M., Luciano,F. et al 2009. The caspase-cleaved form of LYN mediates a psoriasis-like inflammatory syndrome in mice. *EMBO J* **28**:2449-2460.
44. Testa,J.R., and Tsichlis,P.N. 2005. AKT signaling in normal and malignant cells. *Oncogene* **24**:7391-7393.
45. Riol-Blanco,L., Delgado-Martin,C., Sanchez-Sanchez,N., Alonso,C., Gutierrez-Lopez,M.D., Del Hoyo,G.M., Navarro,J., Sanchez-Madrid,F., Cabanas,C., Sanchez-Mateos,P. et al 2009. Immunological synapse formation inhibits, via NF-kappaB and FOXO1, the apoptosis of dendritic cells. *Nat Immunol.* **10**:753-760.
46. Widera,D., Mikenberg,I., Kaltschmidt,B., and Kaltschmidt,C. 2006. Potential role of NF-kappaB in adult neural stem cells: the underrated steersman? *Int J Dev Neurosci* **24**:91-102.
47. Tuttle,R.L., Gill,N.S., Pugh,W., Lee,J.P., Koeberlein,B., Furth,E.E., Polonsky,K.S., Naji,A., and Birnbaum,M.J. 2001. Regulation of pancreatic β -cell growth and survival by the serine/threonine protein kinase Akt1/PKB α . *Nat. Med.* **7**:1133-1137.
48. Yang,J.Y., Walicki,J., Jaccard,E., Dubuis,G., Bulat,N., Hornung,J.P., Thorens,B., and Widmann,C. 2009. Expression of the NH(2)-terminal fragment of RasGAP in pancreatic beta-cells increases their resistance to stresses and protects mice from diabetes. *Diabetes* **58**:2596-2606.
49. Alliouachene,S., Tuttle,R.L., Boumard,S., Lapointe,T., Berissi,S., Germain,S., Jaubert,F., Tosh,D., Birnbaum,M.J., and Pende,M. 2008. Constitutively active Akt1 expression in mouse pancreas requires S6 kinase 1 for insulinoma formation. *J Clin Invest* **118**:3629-3638.
50. Hutten,S., and Kehlenbach,R.H. 2007. CRM1-mediated nuclear export: to the pore and beyond. *Trends Cell Biol.* **17**:193-201.
51. Jordan,M., Schallhorn,A., and Wurm,F.M. 1996. Transfecting mammalian cells: optimization of critical parameters affecting calcium-phosphate precipitate formation. *Nucleic Acids Res.* **24**:596-601.
52. Yang,J.-Y., Walicki,J., Abderrahmani,A., Cornu,M., Waeber,G., Thorens,B., and Widmann,C. 2005. Expression of an uncleavable N-terminal RasGAP fragment in insulin-secreting cells increases their resistance toward apoptotic stimuli without affecting their glucose-induced insulin secretion. *J. Biol. Chem.* **280**:32835-32842.
53. Annibaldi,A., Dousse,A., Martin,S., Tazi,J., and Widmann,C. 2011. Revisiting G3BP1 as a RasGAP binding protein: sensitization of tumor cells to chemotherapy by the RasGAP 317-326 sequence does not involve G3BP1. *PLoS. One.* **6**:e29024.
54. Bulat,N., Jaccard,E., Peltzer,N., Khalil,H., Yang,J.Y., Dubuis,G., and Widmann,C. 2011. RasGAP-derived fragment N increases the resistance of beta cells towards apoptosis in NOD mice and delays the progression from mild to overt diabetes. *PLoS. One.* **6**:e22609.

55. Annibaldi,A., Michod,D., Vanetta,L., Cruchet,S., Nicod,P., Dubuis,G., Bonvin,C., and Widmann,C. 2009. Role of the sub-cellular localization of RasGAP fragment N2 for its ability to sensitize cancer cells to genotoxin-induced apoptosis. *Exp Cell Res* **315**:2081-2091.

3. Results: Part V

1. Introduction

RasGAP-derived fragment N was shown to activate the Ras/PI3K/Akt prosurvival pathway (1). Indeed, Fragment N efficiently protects cells against stress inducing stimuli and plays a role in the maintenance of organ functionality (2). Besides, Fragment N inhibits the activation of the transcription factor NF- κ B by increasing the rate of NF- κ B nuclear export. However, the precise molecular mechanism by which fragment N operates is not fully defined. To identify the potential binding partners of fragment N, we performed a pull down of an overexpressed caspase-resistant form of fragment N and we analysed the pull-down precipitates by mass spectrometry.

2. Results

The mass spectrometry results revealed a list of potential candidates which might bind to fragment N. these proteins (Table 1) are:

- SH2 domain-containing adapter protein B (Shb), a 55 kDa SH2-containing protein that is implicated in several cellular processes including cell proliferation and apoptosis.
- 3-Hydroxyacyl CoA dehydrogenase (27 kDa), an oxidoreductase It is involved in fatty acid metabolic processes.
- Glucocorticoid receptor DNA-binding factor 1 (GRLF1) also known as p190RhoGAP (171 kDa). GRLF1 associates with the promoter region of the glucocorticoid receptor gene and represses the transcription of glucocorticoid receptor (3).
- Pyrroline-5-carboxylate reductase 3 (29 kDa), which is an oxidoreductase that plays a role in arginine and proline metabolism (4)
- Insulin receptor substrate 4 (IRS4) (134 kDa), which binds to insulin receptor and plays a role in growth, reproduction, and glucose homeostasis (5).

- The small GTPase (RAB6A) (24 kDa), of the RAB family, which belongs to the small GTPase superfamily RAB6A is located at the Golgi apparatus and regulates protein trafficking (6).

2.1 Shb binds to fragment N

Shb was identified with the highest hits in mass spectrometry analysis. Therefore we decided to validate this possible interaction between Shb and fragment N . Originally, SH2-containing protein was described in the insulinoma β TC-1 cell line (origin of Shb nomenclature). However, Shb was later found to be ubiquitously expressed (7). Shb binds and protein which operates downstream of several tyrosine kinase receptors. Shb N-terminus contains proline-rich motifs, which are followed by potential tyrosine/serine phosphorylation sites. The C-terminus bears the SH2 domain (8;9). Two putative in-frame translation initiator methionine codons are found in the Shb mRNA, therefore two translation products of 64 kDa and 56 kDa may potentially be generated. The differences between these two isoforms are found in the proline-rich motifs. Shb is implicated in cell proliferation, survival, apoptosis, migration and differentiation (10;11) . Specifically Shb binds to Grb2 (9;12) which is known to associate with the GEF SOS, which is known to activate Ras (13). Therefore Shb is an interesting target that may play an important role in modulating the function of fragment N. We validated the interaction between fragment N and Shb (Figure 1 from master project; Darko Maric) and currently the characterization of this binding is followed by a PhD student in the lab.

3. Contribution

I performed the pull down experiments prior to mass spectrometry which was performed in the protein analysis facility (University of Lausanne, Epalinges, Switzerland). The validation of fragment N and Shb interaction was carried out by Darko Maric under my supervision together with Christian Widmann.

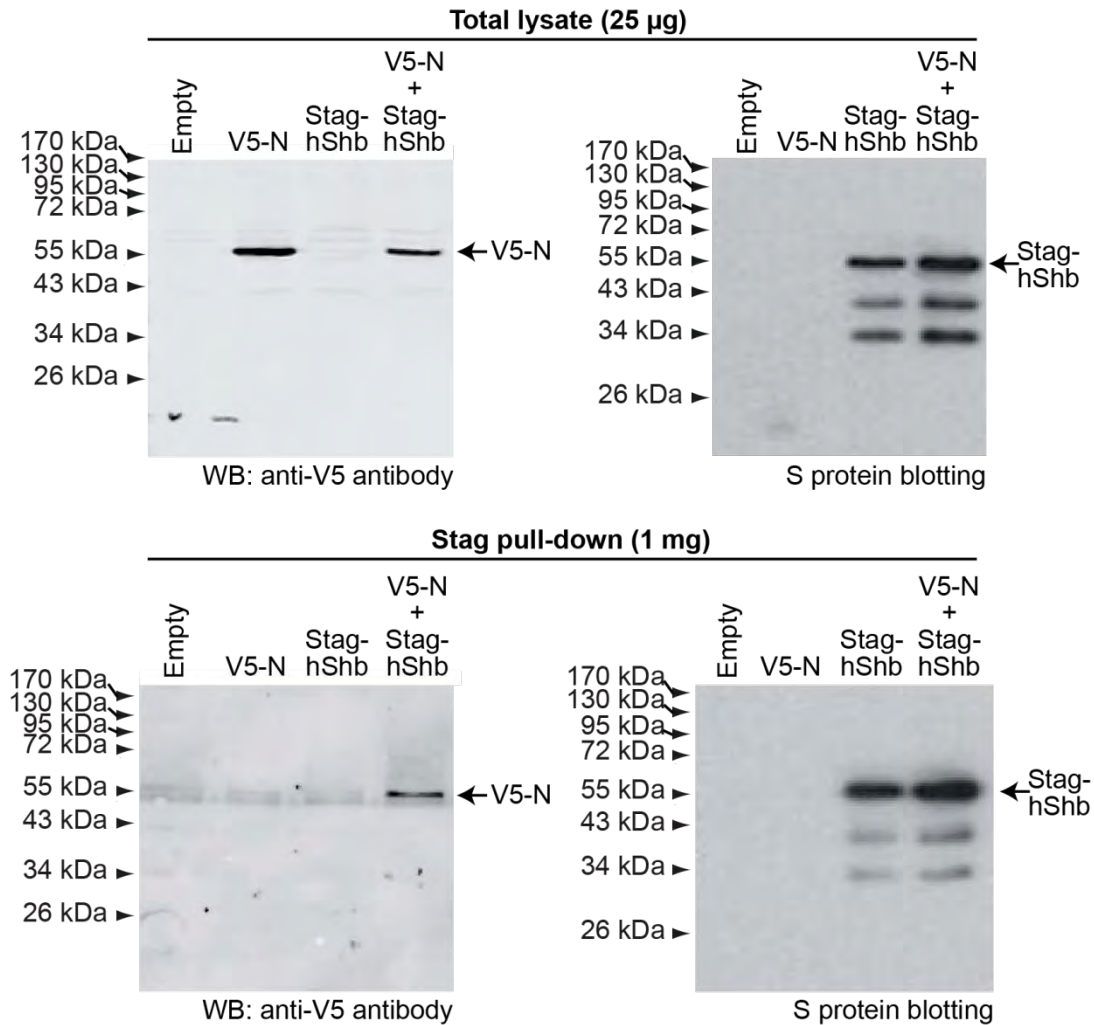


Figure 1. Shb interacts with fragment N. HEK293T cells were seeded at 2 million cells per 8.4 cm dish. Twenty-four hours later, the cells were transfected with 2.5 µg of plasmids encoding for the indicated constructs. Twenty-four hours later, the cells were lysed in RIPA buffer and the lysates analyzed by Western blotting for the presence of fragment N (~55 kDa) and Shb (~56 kDa) using a monoclonal mouse anti-V5 antibody or HRP-conjugated S-protein, respectively (upper blots). Alternatively, 1 mg of lysate was pull-downed using G protein beads and 0.5 mg of an anti-V5 rabbit antibody. The pull-downed material was analyzed for the presence of fragment N as described for the total lysates or using S-protein HRP for the detection of Shb (lower blots).

Reference List

1. Yang,J.-Y., and Widmann,C. 2002. The RasGAP N-terminal fragment generated by caspase cleavage protects cells in a Ras/PI3K/Akt-dependent manner that does not rely on NFκB activation. *JBC* **277**:14641-14646.
2. Khalil,H., Peltzer,N., Walicki,J., Yang,J.Y., Dubuis,G., Gardiol,N., Held,W., Bigliardi,P., Marsland,B., Liaudet,L. et al 2012. Caspase-3 protects stressed organs against cell death. *Mol. Cell Biol.*
3. LeClerc,S., Palaniswami,R., Xie,B.X., and Govindan,M.V. 1991. Molecular cloning and characterization of a factor that binds the human glucocorticoid receptor gene and represses its expression. *J Biol. Chem.* **266**:17333-17340.
4. Dougherty,K.M., Brandriss,M.C., and Valle,D. 1992. Cloning human pyrroline-5-carboxylate reductase cDNA by complementation in *Saccharomyces cerevisiae*. *J Biol. Chem.* **267**:871-875.
5. Fantin,V.R., Wang,Q., Lienhard,G.E., and Keller,S.R. 2000. Mice lacking insulin receptor substrate 4 exhibit mild defects in growth, reproduction, and glucose homeostasis. *Am. J Physiol Endocrinol. Metab* **278**:E127-E133.
6. Young,J., Stauber,T., del,N.E., Vernos,I., Pepperkok,R., and Nilsson,T. 2005. Regulation of microtubule-dependent recycling at the trans-Golgi network by Rab6A and Rab6A'. *Mol. Biol. Cell* **16**:162-177.
7. Welsh,M., Mares,J., Karlsson,T., Lavergne,C., Breant,B., and Claesson-Welsh,L. 1994. Shb is a ubiquitously expressed Src homology 2 protein. *Oncogene* **9**:19-27.
8. Anneren,C., Reedquist,K.A., Bos,J.L., and Welsh,M. 2000. GTK, a Src-related tyrosine kinase, induces nerve growth factor-independent neurite outgrowth in PC12 cells through activation of the Rap1 pathway. Relationship to Shb tyrosine phosphorylation and elevated levels of focal adhesion kinase. *J Biol. Chem.* **275**:29153-29161.
9. Welsh,M., Songyang,Z., Frantz,J.D., Trub,T., Reedquist,K.A., Karlsson,T., Miyazaki,M., Cantley,L.C., Band,H., and Shoelson,S.E. 1998. Stimulation through the T cell receptor leads to interactions between SHB and several signaling proteins. *Oncogene* **16**:891-901.
10. Welsh,N., Makeeva,N., and Welsh,M. 2002. Overexpression of the Shb SH2 domain-protein in insulin-producing cells leads to altered signaling through the IRS-1 and IRS-2 proteins. *Mol. Med.* **8**:695-704.
11. Lu,L., Holmqvist,K., Cross,M., and Welsh,M. 2002. Role of the Src homology 2 domain-containing protein Shb in murine brain endothelial cell proliferation and differentiation. *Cell Growth Differ.* **13**:141-148.
12. Wange,R.L. 2000. LAT, the linker for activation of T cells: a bridge between T cell-specific and general signaling pathways. *Sci. STKE.* **2000**:re1.

13. Chardin,P., Camonis,J.H., Gale,N.W., van,A.L., Schlessinger,J., Wigler,M.H., and Bar-Sagi,D. 1993. Human Sos1: a guanine nucleotide exchange factor for Ras that binds to GRB2. *Science* **260**:1338-1343.

4. Discussion and perspectives

Discussion and perspectives

Apoptosis is orchestrated primarily by members of caspase family. Caspase-3 in addition to other executioner caspases-6 and -7 are the major effectors known to carry out the proteolysis events during apoptosis. Previous work in our lab has shown that RasGAP is cleaved sequentially by caspase-3 in response to increasing doses of apoptosis-inducing agents. Low caspase-3 activity induced by mild stress generates fragment N that is responsible for Akt activation and promotion of cell survival. Higher caspase-3 activity induced by stronger insults leads to fragment N further processing into fragments that can no longer stimulate Akt and this favors apoptosis (1). In agreement with our data, it is now known that caspase-3 can mediate many non-apoptotic functions in cells (2-4) including T and B cell homeostasis (5;6), muscle (7), monocyte (8), bone marrow stromal stem cell (9), and erythroid cell differentiation (10). These studies indicate that caspase-3 plays important functional roles in non-dying cells but the main question remains to be answered: how these cells bypass the apoptotic potential of caspase-3?

In our study (Results, Part I) we investigated the role of caspase-3 in the induction of anti-apoptotic signaling pathways, in particular the anti-apoptotic kinase Akt. Caspase-3 knock-out mice were subjected to various patho-physiological stimuli: UV-B skin exposure, doxorubicin-induced cardiomyopathy, and DSS-mediated colitis. We found that stress-induced Akt activation was blunted in mice lacking caspase-3 (Part I, Figures 1, 2, and 3). This defect was presumably responsible for the increased sensitivity to stress and deteriorations in organs function. We observed a similar defect in Akt activation in KI mice that express a caspase-3-resistant form of p120 RasGAP. In

addition to their inability to activate Akt in response to stress, the KI mice showed an increased rate of apoptosis and greater organ dysfunction (Part I Figures 6, 7, and 8). Therefore our study validates the *in vitro* mechanism of Akt activation mediated by RasGAP-derived fragment N (1;11) in two *in vivo* systems and provides the evidence of a physiological protective mechanism against stress that relies on the activity of caspase-3 and RasGAP cleavage (12).

The pre-described protective mechanism seems to be general and to operate in various organs (skin, colon, and heart) upon different stress stimuli; however, there are situations where the protection against caspase-3 apoptotic activity is independent of RasGAP cleavage. Caspase-3 is activated during T cell stimulation (13) and this may participate in T cell proliferation (14;15). Additionally, caspase-3 is required for erythropoiesis (16). T and B cell development, as well as mature myeloid and erythroid lineage development occur normally in the RasGAP KI mice (Part I, Supplemental table 2). Therefore RasGAP cleavage does not seem to be essential for allowing these cells to survive following caspase-3 activation, which suggest that in hematopoietic cells, other protective mechanisms apart from RasGAP cleavage might be responsible for protection against caspase-3 apoptotic activity.

Caspase-3 is necessary for the development of several tissues (7;9;17). For instance, caspase-3 is playing important functions in neurogenesis, synaptic activity, neuronal growth cone guidance, and glial development (18-20). In contrast, RasGAP cleavage does not seem to be crucial for development. Histological analyses of several tissues including muscle, bone, and brain did not reveal any defect in the tissues of unstressed

KI mice (Part I, Supplemental figure 2). Moreover, the growth curve and size of wild-type and KI mice were comparable (Part I, Figure 4D-E). In particular, inhibition of RasGAP cleavage in normal conditions did not affect heart growth and function, homeodynamic parameters measured by micro-catheter (Part I, Supplemental table 2) or echocardiography in young or aged animals (Part III, Table 1) did not indicate any significant differences of heart function between wild-type and KI mice.

We utilized the KI mice to study thoroughly in two different *in vivo* models the effect of RasGAP cleavage and fragment N formation on heart function under stress induced by doxorubicin (21;22) and pressure overload mediated by transverse aortic arch banding (TAC). As seen previously in skin and colon (Part I, Figures 6, and 8), when a stress is applied on the heart, the cleavage of RasGAP, and subsequent generation of fragment N tend to be indispensable for adequate heart function. Fragment N is generated in response to doxorubicin cardiotoxicity (Part I, Figure 7A), as well as in condition of hypertrophy induced by TAC (Figure 3D-E). The absence of fragment N in the KI mice was associated with the exacerbated drop of the contractile function of the heart during the episode of stress (Part I Figure 7 and Part III, Table 1) (12). These data indicate a pivotal role of fragment N in preserving the heart function during episodes of stress by inhibiting cardiomyocyte apoptosis (Part I, Figure 7C and Part III figure 3A-B). As discussed earlier the protection of fragment N is mainly mediated by the activation of Akt, which was found to be blunted in the KI mice (Part I, Figure 7B). Nevertheless, Western blot analysis showed that Akt activation reached comparable levels in wild-type and KI TAC-subjected mice after a chronic stress (4 week TAC) which suggests that Akt

activation might not be the only pro-survival mechanism modulated by fragment N to favor heart protection.

It is known that the loss of adult cardiomyocytes by necrosis or apoptosis is a major factor in the initiation and progression of heart failure as it contributes to the decline in myocardial function (23). In a hypertrophied heart the compensated hypertrophy is shifted to pathological heart failure once cardiomyocyte cell death is augmented. Hypertrophy took place in a similar pattern in both wild-type and KI mice, which indicates that RasGAP cleavage does not have any detectable effect on the evolution of cardiac hypertrophy. However, signs of adverse myocardial remodeling events appeared earlier in the KI mice, as observed by the increase of relative expression levels of fetal genes and the higher myocardial fibrosis (Part III, Figure 3A-B). These experiments need to be finalized and confirmed by different readouts, but the data we have so far has shown a massive increase in fibrotic lesions in hearts of TAC-operated KI mice. These findings highlight a possible role of fragment N in inhibiting the evolution of fibrosis process. Further experiments in this area need to be performed to investigate this hypothesis.

Peroxynitrite (PN), an oxidant and nitrating agent is a key mediator of cardiomyocyte injury in numerous cardiac pathologies, including myocardial ischemia reperfusion injury, myocarditis, cardiac allograft rejection and anthracycline-induced cardiomyopathy (24). PN induces potent and adverse effects on cellular processes by modulating signal transduction pathways involving Akt, MAPKs (ERK, c-jun, p38) (25). Moreover, PN has the potential to activate multiple caspases including caspase-2, -3, -6, -7, -8 and -9 and

thus the cleavage of key cellular proteins such as poly(ADP-ribose) polymerase and lamins (26). PN-mediated cytotoxicity results in the demolition of cardiac myocytes, both via the necrotic and apoptotic pathways [10]. Our *in vitro* data demonstrated that PN induces a rapid non-sequential cleavage of RasGAP, which did not allow the accumulation of fragment N, apparently because PN induced fragment N rapid cleavage into smaller fragments (only Fragment N2 was detected Part II, Figures 1 and 3)(27). However, a caspase-resistant form of fragment N efficiently protected immortalized (Part II, Figure 5) and primary cardiomyocytes (Part II, Figure 6) against PN-induced death, and increased active Akt levels (27).

These results showed that the anti-apoptotic signals generated by fragment N are therefore able to counteract apoptosis induced by PN in cells. Nevertheless, overexpression of a constitutively active form of Akt (myr-Akt) was inefficient to inhibit PN-induced apoptosis, which illuminates that the activated Akt we detected after PN stimulation was a futile protection attempt. These results suggest that fragment N does not rely only on the activation of Akt activation in protecting cardiomyocytes against PN-induced death, and that other prosurvival pathways might be activated as well. Further experiments in this area need to be conducted to evaluate and characterize potency of fragment N in protecting cardiomyocytes against other stimuli such as doxorubicin and angiotensin II and to decipher thoroughly other possible prosurvival pathways regulated by fragment N.

In conclusion, our *in vitro* data showed a crucial role of fragment N in protecting cardiomyocytes against damaging agents (in particular PN) associated with pathological situations and contribute to heart dysfunction (27). Additionally, the *in vivo* studies

conducted on the KI mice hearts indicated a protective role of fragment N in the heart, where its absence was associated with adverse effect on the contractile activity and remodeling of the heart. In light of these findings, a transgenic mouse model where cardiac-specific expression of a caspase-3-resistant form of fragment N under the control of myosin heavy chain alpha [α MyHC-HA-(D157A)N] was generated. This model will be a very useful tool to validate our data in an additional *in vivo* setup and to decipher the protective mechanisms modulated by fragment N in the heart. The experiments performed earlier (i.e. doxorubicin-induced cardiotoxicity and TAC-induced hypertrophy) will be repeated to evaluate heart protection by fragment N overexpression under these challenging conditions. Once this system is validated to be functional, it will be extremely interesting and informative to attempt to restore heart function in caspase-3 knock-out and RasGAP KI mice hearts by crossing to [α MyHC-HA-(D157A)N] mice.

Ras/PI3K/Akt pathway is the only protective mechanism identified so far and known to be modulated by fragment N. Several downstream targets of Akt are activated or repressed by direct or indirect phosphorylation (detailed in introduction). In particular, Akt can mediate the activation of NF- κ B activation by directly phosphorylating IKK α at threonine 23 (Ozes et al., 1999), or indirectly through Cot (cancer Osaka thyroid) a serine/threonine kinase of the mitogen-activated protein kinase kinase kinase (MAP3K) family (28). Sustained NF- κ B activation is correlated with severe inflammatory responses and increased resistance to apoptosis in cancerous cells (29). Despite the fact that fragment N activates Akt, its ability to protect cells does not depend on NF- κ B (30). In fact in beta cells, fragment N inhibits detrimental NF- κ B activation (31-33). Our

data (Part IV) show that fragment N is a general NF- κ B repressor in stressed cells (Part IV, Figures 1-4) and this inhibitory activity relies on the enhancement of NF- κ B nuclear export (Part IV, Figures 6,7). Therefore, cleavage of RasGAP by caspase-3 represents a new mechanism used by cells to regulate NF- κ B-dependent responses activated by stress. Additionally, we observed that Fragment N generation is required to control the extent of inflammation in DSS-induced colitis mouse model (Part I, Figures 1, 8). The clinical scores obtained from wild-type and KI mice treated with DSS predict an augmented inflammatory response in the KI mice. However, the profiles of pro-inflammatory cytokines and the histological analysis are not yet performed to firmly confirm this assumption. Additional *in vivo* experiments will be performed to determine the efficacy of fragment N anti-inflammatory potential by intranasal inhalation of LPS to induce a local inflammation in the lung of wild-type and KI mice (34;35). Results of these future experiments will determine the efficiency of fragment N in limiting the uncontrolled and harmful inflammatory responses under stress and will open a new episode of research about the anti-inflammatory properties of fragment N. In addition, they will evaluate the possible use of fragment N as an inhibitor of systemic inflammation. The mechanism by which fragment N enhances NF- κ B nuclear export of is not fully understood and it remains also to be investigated whether this effect is specific to NF- κ B or generalized to other transcription factors such as Stat1, and NF-AT.

Fragment N has a homogenous distribution in cells (36) and therefore might function at different cellular levels. Unpublished data indicated that fragment N does not bind to RasGAP or Akt. The interaction map of fragment N is partially revealed by mass spectrometry analysis. Results (Part V) identified few potential binding partners of

fragment N, of which we verified the interaction of SH2-adaptor protein (Shb) with fragment N. Shb localizes to activated receptor tyrosine kinases and interacts with Grb2 which on the other hand binds to the guanine nucleotide exchange factor (GEF) Son of Sevenless (SOS), the known activator of Ras (37). Shb was found to bind to fragments N and N2, but very weakly to RasGAP. This suggests that certain signaling events are driven by fragment N are independent of RasGAP. Recently a PhD project was initiated to determine the exact domains essential for this interaction and investigate its possible role in modulating fragment N function.

In summary, this work provided the genetic evidence and identified a protective mechanism induced by caspase-3 under mild stress. This protective response is mediated through the cleavage of RasGAP/ fragment N generation, and activation of pro-survival kinase Akt, which is needed to protect organs and preserve their function. Further, we identified fragment N as a general inhibitor of NF- κ B and a facilitator of NF- κ B nuclear export. Finally, we identified a direct interaction between fragments N and Shb adaptor protein, which binds to receptor tyrosine kinases and regulate downstream signaling events. In addition, other potential binding proteins need to be verified. These findings will facilitate the future understanding of the mechanism by which fragment N operates, which may lead to the development of promising treatments based on fragment N protective properties in order to increase the resistance of individuals exposed to environmental or chemical stresses.

Reference List

1. Yang,J.-Y., Michod,D., Walicki,J., Murphy,B.M., Kasibhatla,S., Martin,S., and Widmann,C. 2004. Partial cleavage of RasGAP by caspases is required for cell survival in mild stress conditions. *Mol. Cell Biol.* **24**:10425-10436.
2. Feinstein-Rotkopf,Y., and Arama,E. 2009. Can't live without them, can live with them: roles of caspases during vital cellular processes. *Apoptosis.* **14**:980-995.
3. Kuranaga,E., and Miura,M. 2007. Nonapoptotic functions of caspases: caspases as regulatory molecules for immunity and cell-fate determination. *Trends Cell Biol.* **17**:135-144.
4. Launay,S., Hermine,O., Fontenay,M., Kroemer,G., Solary,E., and Garrido,C. 2005. Vital functions for lethal caspases. *Oncogene* **24**:5137-5148.
5. Newton,K., and Strasser,A. 2003. Caspases signal not only apoptosis but also antigen-induced activation in cells of the immune system. *Genes Dev.* **17**:819-825.
6. Woo,M., Hakem,R., Furlonger,C., Hakem,A., Duncan,G.S., Sasaki,T., Bouchard,D., Lu,L., Wu,G.E., Paige,C.J. et al 2003. Caspase-3 regulates cell cycle in B cells: a consequence of substrate specificity. *Nat. Immunol.* **4**:1016-1022.
7. Fernando,P., Kelly,J.F., Balazsi,K., Slack,R.S., and Megeney,L.A. 2002. Caspase 3 activity is required for skeletal muscle differentiation. *Proc. Natl. Acad. Sci. USA* **99**:11025-11030.
8. Sordet,O., Rebe,C., Plenchette,S., Zermati,Y., Hermine,O., Vainchenker,W., Garrido,C., Solary,E., and Dubrez-Daloz,L. 2002. Specific involvement of caspases in the differentiation of monocytes into macrophages. *Blood* **100**:4446-4453.
9. Miura,M., Chen,X.D., Allen,M.R., Bi,Y., Gronthos,S., Seo,B.M., Lakhani,S., Flavell,R.A., Feng,X.H., Robey,P.G. et al 2004. A crucial role of caspase-3 in osteogenic differentiation of bone marrow stromal stem cells. *J. Clin. Invest* **114**:1704-1713.
10. Droin,N., Cathelin,S., Jacquelin,A., Guery,L., Garrido,C., Fontenay,M., Hermine,O., and Solary,E. 2008. A role for caspases in the differentiation of erythroid cells and macrophages. *Biochimie* **90**:416-422.
11. Yang,J.-Y., and Widmann,C. 2001. Antiapoptotic signaling generated by caspase-induced cleavage of RasGAP. *MCB* **21**:5346-5358.
12. Khalil,H., Peltzer,N., Walicki,J., Yang,J.Y., Dubuis,G., Gardiol,N., Held,W., Bigliardi,P., Marsland,B., Liaudet,L. et al 2012. Caspase-3 protects stressed organs against cell death. *Mol. Cell Biol.*
13. Miossec,C., Dutilleul,V., Fassy,F., and Diu-Hercend,A. 1997. Evidence for CPP32 activation in the absence of apoptosis during T lymphocyte stimulation. *J. Biol. Chem.* **272**:13459-13462.

14. Alam,A., Cohen,L.Y., Aouad,S., and Sekaly,R.P. 1999. Early activation of caspases during T lymphocyte stimulation results in selective substrate cleavage in nonapoptotic cells. *J. Exp. Med.* **190**:1879-1890.
15. Kennedy,N.J., Kataoka,T., Tschopp,J., and Budd,R.C. 1999. Caspase activation is required for T cell proliferation. *J. Exp. Med.* **190**:1891-1896.
16. Carlile,G.W., Smith,D.H., and Wiedmann,M. 2004. Caspase-3 has a nonapoptotic function in erythroid maturation. *Blood* **103**:4310-4316.
17. Mogi,M., and Togari,A. 2003. Activation of caspases is required for osteoblastic differentiation. *J. Biol. Chem.* **278**:47477-47482.
18. Fernando,P., Brunette,S., and Megeney,L.A. 2005. Neural stem cell differentiation is dependent upon endogenous caspase 3 activity. *FASEB J.* **19**:1671-1673.
19. Campbell,D.S., and Holt,C.E. 2003. Apoptotic pathway and MAPKs differentially regulate chemotropic responses of retinal growth cones. *Neuron* **37**:939-952.
20. Oomman,S., Strahlendorf,H., Dertien,J., and Strahlendorf,J. 2006. Bergmann glia utilize active caspase-3 for differentiation. *Brain Res.* **1078**:19-34.
21. Singal,P.K., Li,T., Kumar,D., Danelisen,I., and Iliskovic,N. 2000. Adriamycin-induced heart failure: mechanism and modulation. *Mol. Cell Biochem.* **207**:77-86.
22. Mukhopadhyay,P., Rajesh,M., Batkai,S., Kashiwaya,Y., Hasko,G., Liaudet,L., Szabo,C., and Pacher,P. 2009. Role of superoxide, nitric oxide, and peroxynitrite in doxorubicin-induced cell death in vivo and in vitro. *Am. J. Physiol Heart Circ. Physiol* **296**:H1466-H1483.
23. Gill,C., Mestri,R., and Samali,A. 2002. Losing heart: the role of apoptosis in heart disease--a novel therapeutic target? *FASEB J.* **16**:135-146.
24. Pacher,P., Beckman,J.S., and Liaudet,L. 2007. Nitric oxide and peroxynitrite in health and disease. *Physiol Rev.* **87**:315-424.
25. Liaudet,L., Vassalli,G., and Pacher,P. 2009. Role of peroxynitrite in the redox regulation of cell signal transduction pathways. *Front Biosci.* **14**:4809-4814.
26. Zhuang,S., and Simon,G. 2000. Peroxynitrite-induced apoptosis involves activation of multiple caspases in HL-60 cells. *Am. J. Physiol Cell Physiol* **279**:C341-C351.
27. Khalil,H., Rosenblatt,N., Liaudet,L., and Widmann,C. 2012. The role of endogenous and exogenous RasGAP-derived fragment N in protecting cardiomyocytes from peroxynitrite-induced apoptosis. *Free Radic. Biol. Med.* **53**:926-935.
28. Kane,L.P., Mollenauer,M.N., Xu,Z., Turck,C.W., and Weiss,A. 2002. Akt-dependent phosphorylation specifically regulates Cot induction of NF-kappa B-dependent transcription. *Mol Cell Biol* **22**:5962-5974.

29. Ben-Neriah, Y., and Karin, M. 2011. Inflammation meets cancer, with NF-kappaB as the matchmaker. *Nat. Immunol.* **12**:715-723.
30. Yang, J.-Y., and Widmann, C. 2002. The RasGAP N-terminal fragment generated by caspase cleavage protects cells in a Ras/PI3K/Akt-dependent manner that does not rely on NFkB activation. *JBC* **277**:14641-14646.
31. Yang, J.-Y., Walicki, J., Abderrahmani, A., Cornu, M., Waeber, G., Thorens, B., and Widmann, C. 2005. Expression of an uncleavable N-terminal RasGAP fragment in insulin-secreting cells increases their resistance toward apoptotic stimuli without affecting their glucose-induced insulin secretion. *J. Biol. Chem.* **280**:32835-32842.
32. Yang, J.Y., Walicki, J., Jaccard, E., Dubuis, G., Bulat, N., Hornung, J.P., Thorens, B., and Widmann, C. 2009. Expression of the NH(2)-terminal fragment of RasGAP in pancreatic beta-cells increases their resistance to stresses and protects mice from diabetes. *Diabetes* **58**:2596-2606.
33. Bulat, N., Jaccard, E., Peltzer, N., Khalil, H., Yang, J.Y., Dubuis, G., and Widmann, C. 2011. RasGAP-derived fragment N increases the resistance of beta cells towards apoptosis in NOD mice and delays the progression from mild to overt diabetes. *PLoS. One.* **6**:e22609.
34. Szarka, R.J., Wang, N., Gordon, L., Nation, P.N., and Smith, R.H. 1997. A murine model of pulmonary damage induced by lipopolysaccharide via intranasal instillation. *J. Immunol. Methods* **202**:49-57.
35. Mizgerd, J.P., Lupa, M.M., and Spieker, M.S. 2004. NF-kappaB p50 facilitates neutrophil accumulation during LPS-induced pulmonary inflammation. *BMC Immunol.* **5**:10.
36. Annibaldi, A., Michod, D., Vanetta, L., Cruchet, S., Nicod, P., Dubuis, G., Bonvin, C., and Widmann, C. 2009. Role of the sub-cellular localization of RasGAP fragment N2 for its ability to sensitize cancer cells to genotoxin-induced apoptosis. *Exp Cell Res* **315**:2081-2091.
37. Chardin, P., Camonis, J.H., Gale, N.W., van, A.L., Schlessinger, J., Wigler, M.H., and Bar-Sagi, D. 1993. Human Sos1: a guanine nucleotide exchange factor for Ras that binds to GRB2. *Science* **260**:1338-1343.

5. Methods

Reagents

1. HEPES buffer (2X) pH 7.05 (23°C):

- 1.1. Important note: always calibrate the pH meter before starting preparing the HEPES buffer.
 1.2. Composition.

Chemicals	Final concentration	Source/Company	Code/quantities
NaCl	280 mM	Fluka	71380 (1 kg)
KCl	10 mM	Fluka	60130 (1 kg)
Na ₂ HPO ₄	1.5 mM	Merck	1.06586.0500 (500 g)
D-glucose•H ₂ O	12 mM	Merck	1.08342.1000 (1 kg)
HEPES	50 mM	Fluka	54461 (250 g)

1.3. Recipe.

Chemicals	For 500 ml
NaCl	8 g
KCl	0.38 g
Na ₂ HPO ₄	0.1 g
D-glucose•H ₂ O	1.1 g
HEPES	5 g
Adjust pH with NaOH (1 N, then 0.1 N) to 7.05 (23°C)	See 1.4

- 1.4. Add ddH₂O to about 450 ml, then adjust to pH 6.8-6.9 with 1 N NaOH, and finally to pH 7.05 with 0.1 N NaOH. Complete to 500 ml with ddH₂O. Control that the pH is still at 7.05.
 1.5. Sterilize through a 0.22 µm 500 ml Stericups (Millipore #SCGPU05RE). Under a sterile hood, aliquot in 50 ml tubes (40 ml per tube). Write the lot number and the date on the tubes (**the lot number should be indicated in your laboratory book**). Store at -20°C.

2. Others

Chemicals	Source/Company	Code/quantities	Solvent	[stock]	Storage	Sterile
NaOH	Fluka	#71690 (500 g)	ddH ₂ O	10 N	Room temp.	no
Chloroquine	Sigma	C6628 (25g)	PBS	25 mM	-20°C	yes
CaCl ₂ •2H ₂ O (MW 147.02)	Acros	207780010 (1 kg)	ddH ₂ O	2.5 M	4°C	yes
Gelatin	Fluka	48722 (500 g)	PBS	0.1%	4°C	yes
DMEM, glutamax I, 4.5 g/l glucose, sans sodium pyruvate	Gibco	61965026 (500 ml)				
Newborn calf serum (NBCS), heat inactivated	Gibco	26010041 (500 ml)				

2.1. Preparation of NaOH solutions.

NaOH can cause irreversible damage to the eyes. It is thus mandatory to wear glasses when preparing or using NaOH solutions. The preparation of 10 N NaOH involves a highly exothermic reaction, which can cause breakage of glass container. Prepare this solution with extreme care in plastic beakers. To 80 ml of H₂O, slowly add 40 g of NaOH pellets, stirring continuously. As an added precaution, place the beaker on ice. When the pellets have dissolved completely, adjust the volume to 100 ml with H₂O. Store the solution in a plastic

container at room temperature (plastic containers are to be used because NaOH slowly dissolves glassware). Sterilization is not necessary.

- 2.2. Preparation of a 25 mM chloroquine solution.
 In a 50 ml Falcon tube, add 0,645 gr of chloroquine and complete to 50 ml with ddH₂O. Transfer to a 50 ml syringe and sterilize through a 0.22 µm filter (Millex – GV filters [Millipore #SLGV025LS]). Under a sterile hood, aliquote in 15 ml tubes (10 per tube). Write the lot number and the date on the tubes (**the lot number should be indicated in your laboratory book**).
- 2.3. Preparation of a 2.5 M CaCl₂ solution.
 In a 50 ml Falcon tube, add 18.4 g of CaCl₂•2H₂O and complete to 50 ml with ddH₂O. Transfer to a 50 ml syringe and sterilize through a 0.22 µm filter (Millex – GV filters [Millipore #SLGV025LS]). Under a sterile hood, aliquote in 15 ml tubes (10 per tube). Write the lot number and the date on the tubes (**the lot number should be indicated in your laboratory book**).
- 2.4. Preparation of a PBS/0.1% gelatin solution (500 ml).
 Add 0.5 g gelatin and 50 ml PBS 10X to 450 ml ddH₂O in a glass bottle. Autoclave and store at 4°C.

Procedure

Day 0.

1. Plate cells in appropriate medium (use gelatinized dishes if required).

Cells	Number per 10 cm dish	Number per well (6 well-plates)	medium	Gelatinized dish
HEK 293 and derived cell lines	2 · 10 ⁶	350'000	DMEM; 10% NBCS	yes
COS cells	?????		DMEM; 10% NBCS	no

- 1.1. Gelatinization of the dishes.
 Place the indicated volume of PBS/0.1% gelatin in the dish (tilt the plate to cover the entire surface with the solution). Wait at least 10 min. Just before adding the cells to the plates, aspirate the PBS/0.1% gelatin (do not allow the plates to dry).

Dish size	Volume of PBS/01% gelatin
10 cm	2-5 ml
6 well plates	0.5 ml

Day 1.

2. Prewarm the HEPES 2X buffer in a 37°C water bath (at least 20 min). In case the buffer is thawed, mix very well before using.
3. Add the DNA in the indicated volume of H₂O. Add the corresponding volume of 2.5 M calcium solution. Mix **10 times** by pipetting the solution up and down. Allow 20-30 min the solution to equilibrate.

Cells	Dish size	Volume of medium in the dish	DNA amount	Volume of water in which the DNA is added	Volume of 2.5 M calcium to be added
HEK293	10 cm	10 ml	5-20 µg	450 µl	50 µl
	6 well plate	2 ml	2 µg	90 µl	10 µl
	12 well plate	?	?	?	?
	24 well plate	?	?	?	?

4. Add 25 µM chloroquine to the cell culture medium (not necessary to change the medium).
 Note: if the cells are grown in RPMI medium (e.g. HeLa cells), you have to replace it with DMEM because RPMI medium is not compatible with the present transfection technique.

Dish size	Volume of medium	Volume of stock
10 cm	10 ml	10 µl
6 well plates	2 ml	2 µl

5. Place the plates back in the incubator for at least 10 min.
6. Add the indicated volume of prewarmed (37°C) 2X HEPES buffer to the DNA/calcium solution, mix 5 times by pipetting the solution up and down. Incubate for 1 minute exactly (starting from the moment the HEPES has been added to the DNA; not from the time when the mixing is finished). Put the DNA-HEPES mix in the culture medium (rock the plate left to right and up and down 2 times).

Dish size	Volume of HEPES 2X to be added
10 cm	500 µl
6 well plate	100 µl

7. Incubate the cells at 37°C for 8-16 hours (**always mention this time of incubation in your laboratory book**). Replace the transfection medium with normal culture medium containing penicillin and streptomycin [use a 1:100 dilution of a Penicillin-Streptomycin Glutamine 100X solution (10'000 units/ml penicillin G; 10 mg/ml streptomycin sulfate; 29,2 mg/ml L-glutamine; 10 mM sodium citrate; 0.14% NaCl {GibcoBRL #10378-016})] to avoid contamination (the DNA used for the transfection is generally not sterile!).

8. Expected transfection efficiencies (count at least 500 cells).

Cells	Transfection efficiency
HEK293	30-80%
COS	30-40%

9. **In your laboratory book, always mention how long after step 7 were the cells analyzed.**

References

1. Jordan et al. - Nucl. Acid Res. (1996) **24**:596 (#3461)

Quantitation of Western blot signals using the BioRad Fluor-S imager**Apparatus**

BioRad Fluor-S™ MultiImager.

Contact person:

Agostino Campanielli, service manager

(tél. 061 – 717 95 55;

Email: Agostino_Campanielli@bio-rad.com)

Fig. 8-1. Fluor-S MultiImager.

Materials and reagents1. *Plastic sheets and commercial Enhanced chemiluminescence (ECL) solution.*

Materials and reagents	Source/Company	Code/quantities
Plastic sheets Kapak Tubular Roll Stock [9.5''x250' #5 Scotchpak (2 Mil)].	Kapak Parkdale Drivewe, Minneapolis, Minnesota 55416 • 1681	?
ECL reagent Supersignal West Femto Substrate	Pierce	#34095

2. *Home-made ECL solution.*

2.1. Composition of the luminol and coumaric acid stocks.

Chemicals	Final concentration	Source/Company	Code/quantities
Luminol (3-aminophthalhydrazide)	250 mM	Sigma	A-8511 (1 g)
P-coumaric acid	90 mM	Acros	12109-0250 (25 g)
Tris	1 M pH 8.5	Boehringer Mannheim	708976 (1 kg); IBCM stock
H ₂ O ₂ 30%		Merck	1.07210.0250 (250 ml)

The H₂O₂ 30% solution has to be kept in a fridge at 4°C.

2.2. Luminol stock preparation:

Warning: luminol is light sensitive. Work in the dark as much as possible.

Dissolve 1g (the whole content of the bottle) in a few ml of DMSO. When well dissolved, transfer to a 50 ml Falcon tube and complete to a final volume of 22.7 ml with DMSO. Make 1.5 ml aliquots in 2 ml Eppendorf tubes and store at –80°C.

2.3. P-coumaric acid stock preparation:

Weigh 0.5 g of coumaric acid and place it in 50 ml Falcon tube. Add 33.3 ml DMSO. Make 660 µl aliquots in 1.5 ml Eppendorf tubes and store at –80°C.

2.4. Tris 1 M pH 8.5 stock preparation:

2.5. Solution 1.

Chemicals	For 150 ml
Luminol 250 mM stock	1.5 ml
P-coumaric acid 90 mM stock	660 µl
Tris 1 M pH 8.5	15 ml

Quantitation of Western blot signals using the BioRad Fluor-S imager

ddH ₂ O	133 ml

Thaw the luminol aliquote in the dark.

2.6. Solution 2.

Chemicals	For 150 ml
H ₂ O ₂ 30%	90 µl
Tris 1 M pH 8.5	15 ml
ddH ₂ O	135 ml

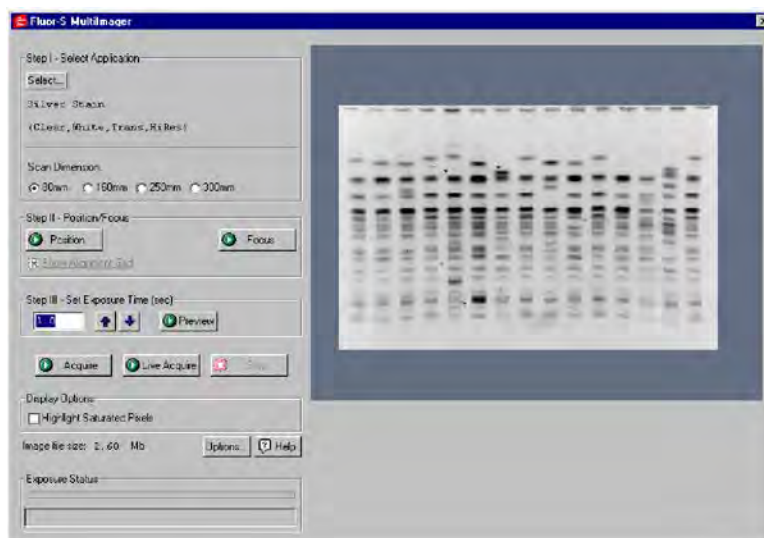
Procedure

1. Preparation of the ECL reagent.
Mix 3 volumes of each home-made solutions 1 and 2 with one volume of each “Pierce” solutions 1 and 2. The resulting ECL reagent mix should be used within one hour (there is no need to rush at this point).
2. Camera settings.
The BioRad Fluor-S imager settings should be adjusted before starting the incubation of the blot with the ECL reagent. Use gloves to manipulate the PC and the imager since they may be contaminated.

For best results select fit the CCD camera with the 50 mm lensⁱ Use the following settingsⁱⁱ:

- 2.1. For placing the membrane and taking a picture of the molecular weight markers:
Focal distance: 2.5 ft; aperture: f:5.6
- 2.2. For imaging the ECL signal:
Focal distance: 4.0 ft; Aperture: f:1.4

3. BioRad Fluor-S imager settings.
Before adding the ECL reagent:
 - 3.1. Turn the lens rings to the “2.1” settings
 - 3.2. On the Fluor-S MultiImager main window, set the “Highlight Saturated Pixels” option on.
 - 3.3. On the Fluor-S MultiImager main window, click on the “Select... -> Blotting -> Chemiluminescence -> High Sensitivity” if the optimal conditions for your antibody/antigen



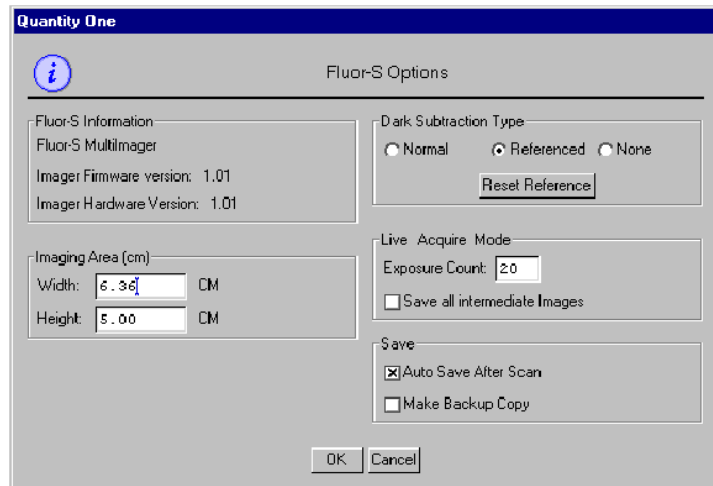
ⁱ Be aware that this lens will give an imaging surface of about 12x9 cm that is smaller than the membrane used for blotting a large gel. If possible, use minigels or cut you membrane into two and take two separate pictures. A drawback is that measurements from each of these two pictures cannot be compared with each other. This means that the appropriate controls or references have to be included in each picture.

ⁱⁱ The focal distance corresponds to that of the membrane placed on the lower surface of the imager cabin. Notice that the focal distance is different for the “visible” light and for the ECL emitted light.

Quantitation of Western blot signals using the BioRad Fluor-S imager

system have not be tested yet. If the signal is known to be strong the “High resolution” option can be selected. Verify that the main window displays now the selected options (e.g. “Chemiluminescence / High Sensitivity”).

- 3.4. Verify that the Dark Subtraction settings are correct. Click on the “Options” button: The “Dark Subtraction Type” should be set to “Referenced”. Click the “Reset Reference” button. The “Dark Exposure Time” should be 600 secondsⁱⁱⁱ. If this is the case, click on the “Cancel” button. If by mistake you click the OK button, or the time has to be reset to 600 seconds take a reference dark image immediately after as described in footnote 3, to avoid having to wait during the actual imaging of your blot.
- 3.5. Go back to the main screen and under “Step III - Set Exposure Time (sec)” indicate the exposure time. If the optimal conditions for your antibody/antigen system have not be tested, choose 30 sec.
- 3.6. Especially for long exposures and also to economize reagents, it is better to cover the membrane with plastic during the imaging of the ECL reaction. Cut a piece of plastic tubular role larger than the blot and open it on one side. Scotch it to a support at the side in which both leaflets are sealed together and scotch at the opposite side only the lower leaflet to the support thus leaving the upper leaflet as a sort of lid.



4. BioRad Fluor-S imager settings. Recording the fluorescence:

Since the BioRad system is not extremely sensitive, the following steps should be performed rapidly for best results.

- 4.1. Take the membrane from the last wash and drain it briefly of excess moisture on a paper towel.
- 4.2. Place the membrane into a as small as possible plastic box and pour the ECL reagent min on it. Flush the reagent several times onto the membrane with a pipette. In general, 30 seconds are enough, especially if the signal is strong.
- 4.3. In the mean time, you can already click on the “Step II – Position/Focus -> Position” button to switch on the lights inside the FluorS cabin.
- 4.4. Place the membrane inside the plastic sandwich scotched onto the support and transfer this inside the cabin as to have the membrane within the imaging area.

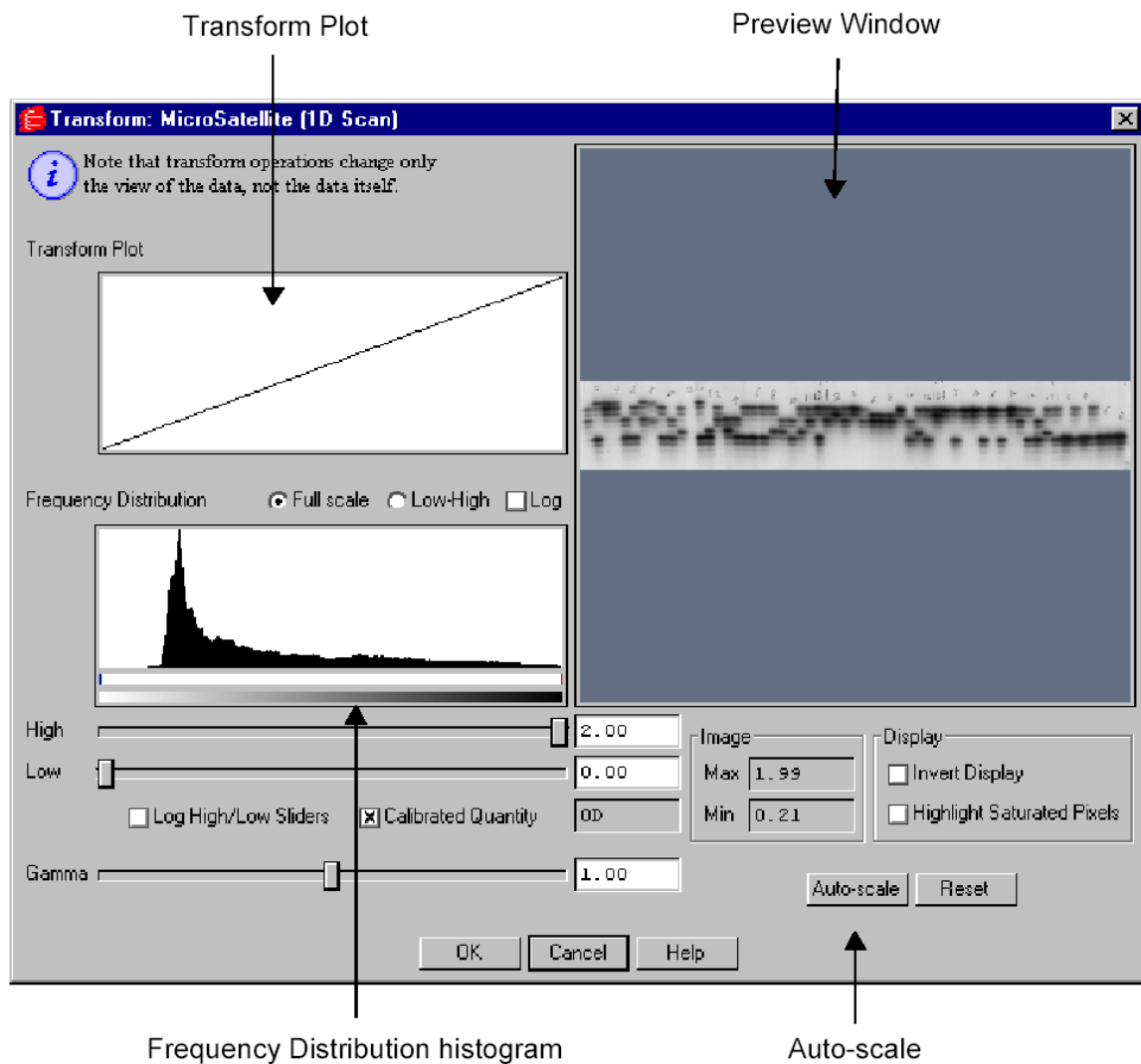
ⁱⁱⁱ Every time you take a picture, a dark subtraction will be performed automatically. This means that the background noise (BN) data will be subtracted to the ECL signal (ES) data. This can be performed either by measuring the BN every time, or by using a referenced BN that is stored in the machine. In any case, the dark subtraction time should be at least as long as the exposure time. If the former is shorter than the latter, errors in image correction may occur. Resetting of dark noise is only necessary if you think that the environmental conditions have changed: big temperature changes or if you obtain an overall strong background noise even with relatively short exposure times (e.g. less than 5 min). BN recording is independent from ES recording: during BN measurements, the shutter closes and no “visible” light enters the CCD camera through the lens. The software allows however, BN recording to take place only after taking “a picture”. It is however possible to take a blank picture during just one second and request a long measurement of the dark noise. If necessary, this can be done hours or days before taking the actual picture. BN recording should be performed for at least as long as your ECL signal recordings. Since having a dark noise recording period longer than the ECL recording period will not affect the quality of the background compensation, it is better to perform a BN measurement during at least 300 seconds.

Quantitation of Western blot signals using the BioRad Fluor-S imager

- 4.5. Turn lens rings to the “2.2” settings. The image on the screen will turn red due to over-exposure (this is a good visual cue to verify that you opened the aperture). Close the cabin door.
- 4.6. Click on the “Position” button again to shut off the lights inside the cabin.
- 4.7. Click on the “Acquire” button (do **not** perform a preview or a Live Acquire!!!).
5. BioRad Fluor-S imager settings. **Enhancing the signal:**

Once the image has been recorded, the background compensation will be performed instantaneously. The corrected picture will appear on the screen. Unless the signal is fairly strong, the picture will appear completely black. In order to enhance the image follow the following steps:

- 5.1. Press Ctrl+b or select “Image -> Transform...” from the main menu.
- 5.2. Check the “Invert Display” option on (white background).
- 5.3. Move the “High” slider to the left until the bands appear in the Preview Window.
- 5.4. If necessary, move the “Low” slider to the right to reduce background noise.
- 5.5. Play with the “Gamma” slider in order to obtain the best contrast. Notice that these changes will only affect the visualization of the picture but will not introduce any changes into the raw data.
- 5.6. Assess visually whether additional pictures have to be taken. Vary the exposure time and/or the sensitivity. You can select high resolution (on the Fluor-S window “Select... -> Blotting -> Chemiluminescence -> High Resolution”) if the signal is strong in order to improve the image quality.



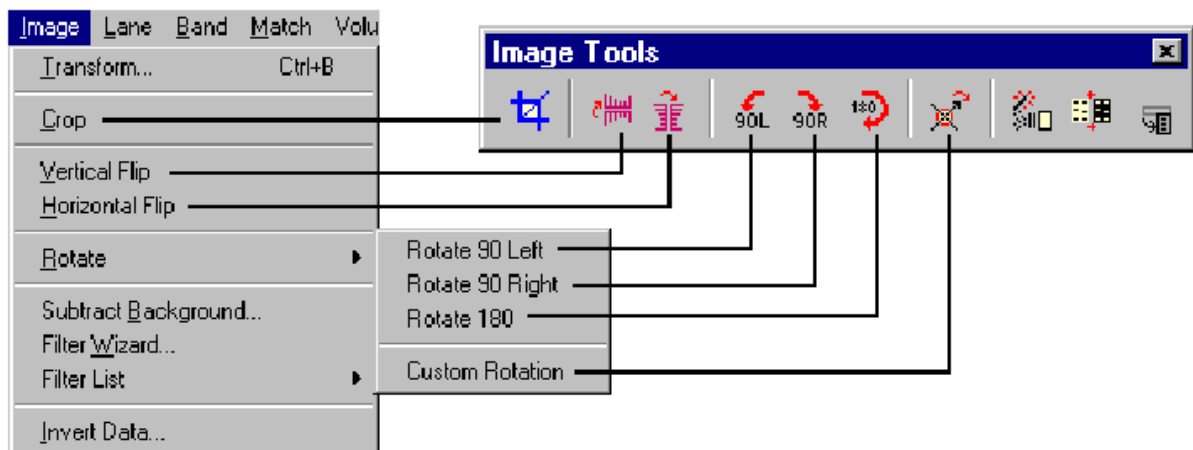
Quantitation of Western blot signals using the BioRad Fluor-S imager

6. BioRad Fluor-S imager settings. **Positioning the markers:**

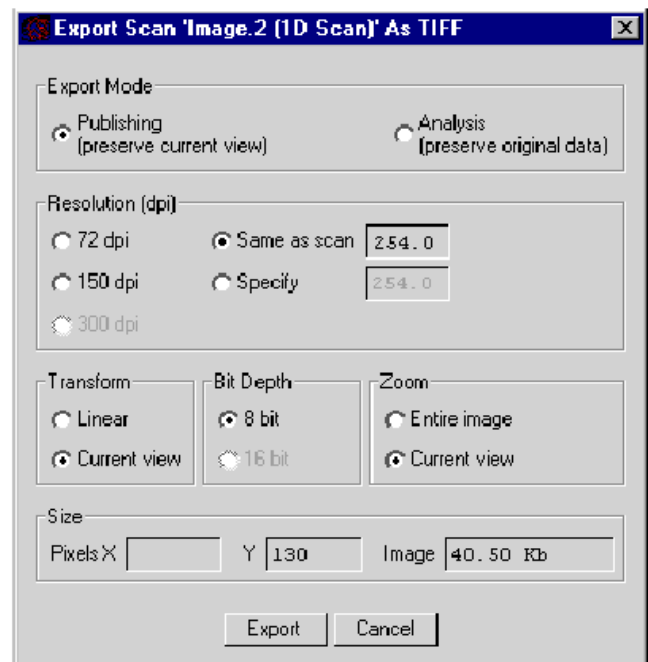
Once you have finished, a regular picture should be taken of the membrane in order to have a reference of the position of the molecular weight markers.

- 6.1. On the Fluor-S window “Select... -> Blotting -> Colorimetric”.
- 6.2. Turn lens rings to the “2.1” settings.
- 6.3. Set the exposure time to one second and click on “Acquire”. It may happen that the image is partially overexposed. Repeating the imaging without changing the settings may however yield a good picture. Alternatively, try shorter exposure times or close the lens aperture one point f: 5.6 -> f:8).

7. **Transforming, saving, printing and exporting** the image to a TIFF file.



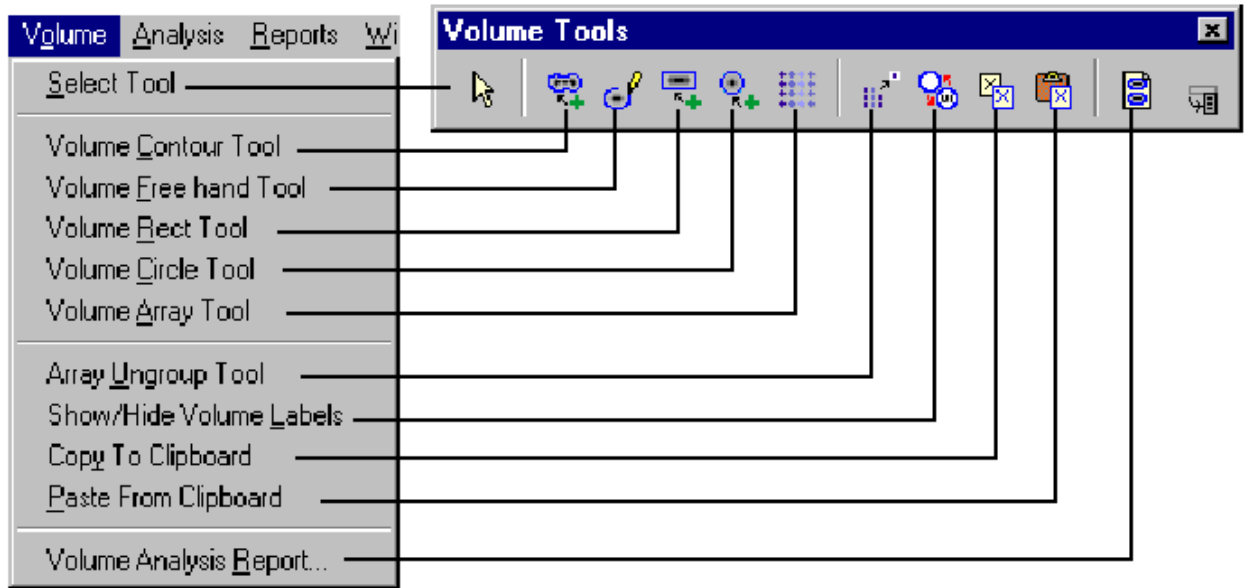
- 7.1. If necessary, the image can be cropped, rotated etc, using the Image Tools.
- 7.2. By default, the file is not saved automatically. Save it in you own folder in the D disk partition (contact the person responsible for the machine if you have none). NEVER save any data on the C partition.
- 7.3. There are three options for printing: “File -> Print -> Print Image (=Ctrl+P)” fits the image to a whole A4 page; “File -> Print -> Print Actual Size...” prints the blot at about the same size as the original; “File -> Print -> Print Scan Report...” prints the blot at about the same size as the original plus all the information concerning the imaging conditions (date, folder pathway where the file was stored, exposure time, resolution, etc) plus any changes introduced to the original data (e.g., if you cropped the picture). Print in any case this report plus eventually the image in one of the other formats^{iv}.
- 7.4. Exporting to TIFF (File ->Export to TIFF...) allows the image to be opened with a graphic utility (e.g. Photoshop). Select “Publishing” as “Export Mode” and “Same as scan” for the “Resolution”, “Current view” for “Transform”, and an “8 bit “as” Bit Depth.



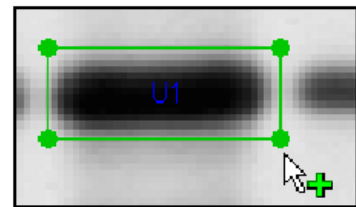
^{iv} Take into account that if you perform an integration of the intensity of the bands you will be able to print again the image along with the values.

Quantitation of Western blot signals using the BioRad Fluor-S imager

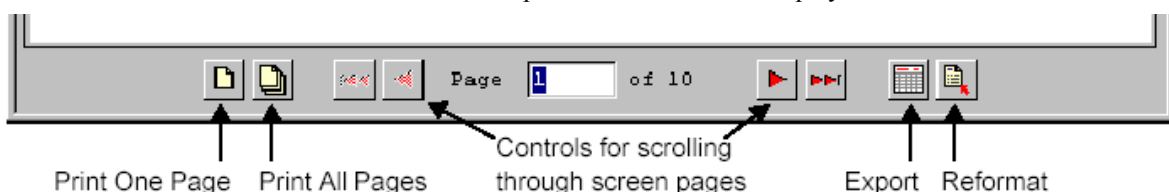
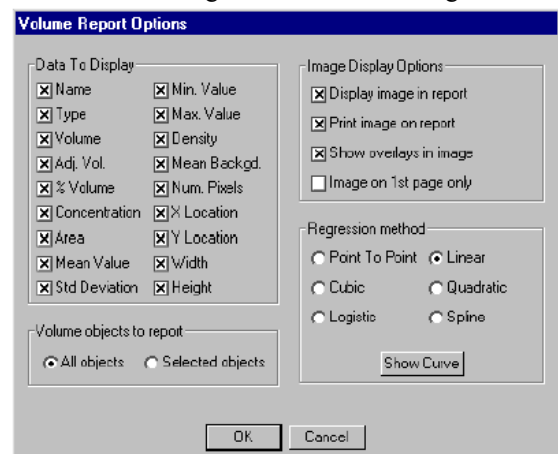
8. Quantitation of bands.



- 8.1. Maximize the size of the window containing the picture of the blot.
- 8.2. On the Volume Toolbar click on the “2. Zoom Box” and drag the cursor over the area containing the bands.
- 8.3. On the Volume Toolbar click on the “5. Volume Rect Tool”. Drag a rectangle around the first, left-most band. To resize the box, click on it to select it, then position the cursor on one corner anchor point and drag. To move the selected volume, position your cursor over the selection and drag.
- 8.4. If each of the bands can be enclosed within such a rectangle, the easiest way to proceed is to clone this rectangle onto the next band and repeat the procedure from left to right until all the bands to be quantified are enclosed within a volume box. In order to do this, hold down the CTRL key while dragging the selected volume onto the next band.
- 8.5. Define the background volume(s). This can be done in two ways.
 - 8.5.1. If all volume areas are equal for all the bands AND the background noise is homogeneous all over the blot:



- 8.5.1.1. Clone the last defined volume onto a region of the blot with an “average gray”.
- 8.5.1.2. Double-click this volume and when the “Volume Properties” window appears check “Background” as “Volume Type”.
- 8.5.1.3. Click on the “Volume Analysis Report...” button of the “Volume Tools” box. The “Volume Report Options” dialog box will pop up, allowing you to specify the data that will appear in your report. Select Name, Volume and Adjusted volume. Deselect the other options under “Data to Display”.



Quantitation of Western blot signals using the BioRad Fluor-S imager

8.5.1.4. If there are more than 10 volumes select “Small” as “Font Size” and “Very Small” as “Line Spacing”. Leave the other (default) options unchanged

8.5.1.5. Click OK. The report will be displayed in a standard report window. The “Adj. Vol.” column contains the band intensity values after subtraction of the background. Click on the “Print All Pages” at the bottom on the Report window in order to obtain a hard copy.

8.5.1.6. You can export your data to spreadsheet applications by clicking on the “Export” button at the bottom of the window. The “Export Report” dialog box will appear. The options selected by default are OK for exporting the data into Excel. Click OK and save the data either on a server in which this application has been installed or to a diskette.



8.5.1.7. If you change your mind about the data to display in your report window, click on the “Reformat” button. This will reopen the “Volume Report Options” dialog box.

8.5.2. If all bands are not defined by a volume of the same area OR the background is not homogeneous all over the blot.

8.5.2.1. Click on the “Select Tool” (the white arrow) and drag the cursor over all the volumes to select them.

8.5.2.2. Clone the volumes by dragging them while holding down the CTRL key and place the new volumes near to the original volumes at a region which you consider to be representative of “local background” but keeping them well aligned with the corresponding lanes. Check that these “reference volumes” do not overlap with those from which they were originated.

8.5.2.3. Click on the “Volume Analysis Report...” button of the “Volume Tools” box. The “Volume Report Options” dialog box will pop up, allowing you to specify the data that will appear in your report. Select only “Name” and “Volume”. Deselect the other options under “Data to Display”.

8.5.2.4. Select “Small” as “Font Size” and “Very Small” as “Line Spacing”. Leave the other (default) options unchanged

8.5.2.5. Proceed as described under points 8.5.1.5-8.5.1.7. Notice that the “empty” volumes cloned from the “band volumes” appear in inverted order, from right to left. Therefore, after importing these data into Excel, the best is to invert their order by selecting the corresponding block of values and clicking on “Data -> Sort... -> Descending”. In such a way both the band volumes and the corresponding background volumes will appear in the same order. Subtracting the latter to the former will yield the band intensities corrected for their local background values.

References

1. Jordan et al. - Nucl. Acid Res. (1996) **24**:596 (#3461)
 2. The Discovery Series. User Guide for Version 4. (Can be found in the small cupboard next to the BioRad apparatus.)
-

Western blot**Apparatus**

Transfer tank located in the drawers next to Christian's office door. It is the transparent tank containing red-black electrode module inside. Gel cassettes and sponges are either in the drawer above the one containing the tanks or above the sink in the middle of the lab.

Materials and reagents1. *Plastic sheets, commercial Enhanced chemiluminescence (ECL) solution and other reagents.*

1.1. Materials and reagents.

Materials and reagents	Source/Company	Code/quantities
Plastic sheets Kapak Tubular Roll Stock [9.5''x250' #5 Scotchpak (2 Mil)].	Kapak Parkdale Drivewe, Minneapolis, Minnesota 55416 • 1681	
Tris	Sigma	T1503 5Kg
Tween	Acros	p7949 100ml
Milk		
ECL reagent Supersignal West Femto Substrate	Pierce	#34095
Ponceau S	Acros	161470250 (25 g)

1.2. **Ponceau S Staining Solution [0.1%(w/v) Ponceau S in 5% (v/v) acetic acid]**

- 1g Ponceau S
 - 50ml acetic acid
 - Make up to 1 liter with ddH₂O
- Store at 4°C. Do not freeze.

Alternative recipe: 0.2% (w/v) Ponceau S in 3% (v/v) acetic acid.

1.3. **Tris-buffer saline (TBS; 18 mM HCl, 130 mM NaCl, 20 mM Tris pH 7.2)**

- 30ml HCl
- 152g NaCl
- 48g Tris base
- Up to 1L dH₂O

1.4. **TBS/tween**

- 19L dH₂O
- 1L 20X TBS
- 0.1% Tween (final concentration)

1.5. **TBS/milk**

- 5% powdered milk (25g for 500ml of TBS/tween)
- TBS/tween
- Alternatively some primary antibodies work better if they are diluted in 5% BSA (5%BSA in TBS/tween)

Western blot2. *Home-made ECL solution.*

2.1. Composition of the stocks.

Chemicals	Stock concentration	Final concentration	Source/Company	Code/quantities
Luminol (3-aminophthalhydrazide)	250 mM (1 g in 22.7 ml DMSO). Make 1.5 ml aliquotes	1.25 mM	Sigma	A-8511 (1 g)
P-coumaric acid	90 mM (0.5 g in 33.3 ml DMSO). Make 660 µl aliquotes.	0.2 mM	Acros	12109-0250 (25 g)
Tris	1 M pH 8.5	100 mM	Boehringer Mannheim	708976 (1 kg); IBCM stock
H ₂ O ₂ 30%	30%	0.01%	Merck	1.07210.0250 (250 ml)

Solution 1: 2.5 mM luminol and 0.4 mM coumaric acid in 100 mM Tris pH 8.5.

Solution 2: 0.02% H₂O₂ in 100 mM Tris pH 8.5.

3. *Home-made enhanced ECL solution Note: for the moment this is not working (use the above recipe instead).*

3.1. Composition of the stocks.

Chemicals	Stock concentration	Final concentration	Source/Company	Code/quantities
Luminol (3-aminophthalhydrazide)	250 mM	1.25 mM	Sigma	A-8511 (1 g)
p-iodophenol	(in DMSO)	50 µM		
Tris	1 M pH 8.5	100 mM	Boehringer Mannheim	708976 (1 kg); IBCM stock
H ₂ O ₂ 30% (8.82 M)	30%	2 mM	Merck	1.07210.0250 (250 ml)

Procedure

1. General remarks.

- 1.1. The conditions of incubation of the blots have to be adapted for each antigen and each antibody used. Therefore, the procedures presented in the following sections have to be considered as general guidelines and should not be assumed to work in all cases. Indications of possible improvements when the conditions are not found optimal will be mentioned.
- 1.2. Always centrifuge the tubes containing the antibodies before usage.
- 1.3. In principle, do not incubate two blots in the same bag.
- 1.4. Never touch the blot with bare hands. Use gloves and move the blots with tweezers.
- 1.5. The following procedure should be considered only for the small gels (see SOP12.1).

Western blot

2. Migration on gels.

Percentage of acrylamide	Separation
8%	40-200 kDa
10%	30-200 kDa
12%	20-200 kDa
4-20%	7-250 kDa
8-16%	15-250 kDa

3. Transfer to membranes.

3.1. After migration, proteins are transferred to nitrocellulose filters (Schleicher and Schuell, BA83 0.2, μm , no. 401380) or PVDF membranes. Instruction on how to do this can be found in the same drawer as the material used for the transfer and for the SDS-PAGE (see SOP 12.1).

3.2. Transfer buffers.

David has recently tested the two following buffers. According to him, transfer buffer II works better.

Composition of transfer buffer I.

Chemicals	Stock solution	Final concentration	Source/Company	Code/quantities
CAPS	1M pH11	10 mM	Acros	172621000 (100 g)
Methanol		10%	Fluka	65543 (5 l)

CAPS 1M stock solution (500 ml): 110 g CAPS (MW 221.3) and 20 g NaOH in water. The pH should be 11. Store in the dark at 4°C.

Prepare the transfer buffer (5 liters) directly in the transfer tank (50 ml CAPS 1M, 500 ml methanol, and water up to 5 liters).

Methanol evaporation ensures that the buffer does not heat too much. Therefore the transfer buffers cannot be used too many times. Without methanol, the buffer would boil during the transfer!

Transfer o/n at 600 mA.

Composition of the transfer buffer II.

Chemicals	10X stock (1 liter)	Final concentration (1X transfer buffer)	Source/Company	Code [quantities]
Tris	30.2 g	1 mM	Biosolve ltd	20092388 [4 kg]
Glycine	144 g	8 mM	ACROS	120070050 [5 kg]
SDS	10 ml of a 10% solution in water	0.001%	Biosolve ltd	19822359 [0.5 kg]

Prepare the transfer buffer 1X (5 liters) directly in the transfer tank.

Add 500 ml of the 10X buffer, 1 liter of methanol and water up to 5 liters.

Transfer 5 hours at 660 mA.

Currently the situation with the transfer buffers is like this: they are located above the sink were other materials for the transfer can also be found (sponges, etc.), There are several bottles of 10x transfer buffer. In order to make 1x transfer buffer, mix 100 ml of the 10X preparation with 700ml of water and 200ml of some alcohol (methanol or ethanol).

3.3 After preparing the transfer tank, place the top on and plug it into a power supply machine (make sure that the plus and minus plugs are connected right: you do not want your proteins to be released on the wrong side directly into the transfer buffer). Transfer is usually preformed at 250 mA (constant amperage) for one hour or one hour and twenty minutes.

Western blot

- 3.4 Check if the protein markers have been transferred (one should see the markers on the membrane and not on the gel).
4. This protocol should be used when there are no particular problems to get a strong signal
 - 4.1. Ponceau S Stain for Western blots.

Background. *This is a rapid and reversible staining method for locating protein bands on Western blots. Sensitivity is somewhat less than Coomassie blue and produces reddish pink stained bands; minor components may be difficult to resolve. The stain is useful because it does not appear to have a deleterious effect on the sequencing of blotted polypeptides and is therefore one method of choice for locating polypeptides on Western blots for blot-sequencing. The stain binds strongly to nylon-based filter media but is fine for nitrocellulose and PVDF membranes. Incubate the membrane for up to an hour in staining solution with gentle agitation. Rinse the membrane in distilled water until the background is clean. The stain can be completely removed from the protein bands by continued washing. Stain solution can be re-used up to 10 times.*

How we use it in the laboratory. Incubate the blot in Ponceau for 2-3 min to visualize the proteins and to determine whether the transfer was homogeneous. With a pen, mark the position of the molecular weight markers. The blots are then subjected to the following incubations.
 - 4.2. wash 3x 20 min at room temperature with TBS/0.1% Tween 20 (TBS/Tween; found in the big tank next to the sink near the entrance of the laboratory).
 - 4.3. 45-60 min at room temperature with TBS/5% powdered milk (TBS/milk).
 - 4.4. overnight with the primary antibody (in TBS/milk) at 4°(in a cold room).
 - 4.5. 3x 20 min at room temperature with TBS/Tween.
 - 4.6. 45 min at room temperature with TBS/milk.
 - 4.7. 45 min with the secondary antibody (in TBS/milk) at room temperature (if the secondary antibody bears a fluorochrome sensitive to light [e.g. antibodies required for the odyssey detection; see SOP 17], make sure that incubation is performed in a black box).
 - 4.8. 3x 20 min at room temperature with TBS/tween (in the dark).
5. Detection of the secondary antibodies on films.
 - 5.1. This method should be used only for antibodies and antigens that do not generate strong signals. If this is not the case, detect the secondary antibodies with the BioRad Fluor-S imager (refer to SOP 2.0) or even better with the Odyssey apparatus (see SOP 17).
 - 5.2. Check that the developer has been turned on and is ready to be used.
 - 5.3. Prepare a cassette that should contain a fluorescent ladder (to position your film on the blot later on).
 - 5.4. Wash a glass plate thoroughly (first with soap, rinse with water and finally with ethanol).
 - 5.5. Prepare the ECL reagent by mixing equal volumes of solutions I and II. You need about 1 ml for each 10 cm² of your blot.
 - 5.6. Cut some Kappak plastic sheet that will be used to contain your blot during the exposure to films. Seal it but leave one side open.
 - 5.7. Take the blot with tweezers and touch some absorbing paper with one of its corner to remove the liquid in excess. Place the blot on the glass plate with the transferred proteins up. Pour the ECL reagent on the blot. Check that the whole surface is covered and wait one minute.
 - 5.8. With tweezers, transfer the blot in the Kappak bag. Remove the bubbles and seal the bag. Using absorbing paper, remove the liquid on the exterior of the bag. Place the bag in the cassette as close as possible to the fluorescent ladder. Tape the bag on one side.
 - 5.9. Immediately, go to the dark room with the sealed blot, the films and a cassette. Place a film on the blot. Close the cassette. Wait one minute. Remove the first film that you insert in the developer. While the first film develops, place a second one on the blot and close the cassette. When the first film comes out, check the intensity of the signal. If it is weak, expose the second film for 5-15 min. If it is too strong, develop the second film immediately (it will of course be too dark too) and expose a third film to 5-15 seconds. If the film has to be exposed for 1-2 seconds, tape it on the other side of the cassette. This will ensure that when you close the lids, the film will not move. Note again that if the signal is strong, you should not use this technique (see point 3.1).
 - 5.10. Keep all the films (the overexposed ones are often used to position the molecular weight markers). All the films should be labeled (**do it immediately**) with the date, the experiment number, the exposure time, the type of ECL used, and the experimental conditions for each lane. Also try (when possible) to identify the bands on your blots.
6. Detection of the secondary antibodies with the BioRad Fluor-S imager.

Western blot

- 6.1. Refer to SOP 2.0.
 - 6.2. In this case also, the images obtained should be labeled: date, the experiment number, the exposure time, the type of ECL used, and the experimental conditions for each lane. Also try (when possible) to identify the bands on your blots.
 7. Quantitation of the ECL signal.
 - 7.1. In principle, quantitation should not be performed using films because the signal on films is not linear (you need more than one photon to activate the silver grains) and saturates rapidly.
 - 7.2. If possible, quantitation should be performed using the BioRas Fluor-S imager. Please refer to SOP 2.0.
 8. Detection of the secondary antibodies using the Odyssey system (Licor).
 - 8.1. Refer to SOP 17.
 9. No signal
 - 9.1. Increase the incubation with the antibodies: o/n incubation with the first antibody and 2-4 hours with the secondary antibody. Perform the incubations at 4°C.
 - 9.2. Reduce the “stringency” of the incubation buffer. Milk containing buffer can possibly quench a fraction of the antibody. The following buffers are ranked from highest to lowest stringency: milk-containing buffer, BSA containing-buffer, tween-containing buffer, PBS or Tris buffer.
 10. How to store antibodies.
 - 10.1. It is possible to reuse antibodies many times and this should be done whenever the antibody is rare and not available commercially. The solution containing the antibody needs to contain 0.05% azide (NaN₃) and 10 mM EDTA.
 11. Very important: after completion of the Western blot procedure, always store the nitrocellulose membranes in Kappak bags at -20°C for further potential use.
-

References

1. Widmann et al. *Biochem. J.* (1995) **310**:203 (#3461)
2. Yang et al. *Mol. Cell Biol.* (2001) **21**:5346 (#3666)

Immunocytochemistry

Day 1

Put two coverslips per well in a 6 well plate and incubate 30 minutes with gelatine 0.1%. After this time remove the gelatine and put the cells over them. Make sure the coverslip is well attached to the surface of the well (push it down softly with a tip).

Day 2

1. Put 1 coverslip / well in a new 6 well plate and wash with 2 ml of PBS 1x
2. Fix the cells to the coverslip surface by treating with PAF 2% (paraformaldehyde diluted in PBS) for 15 minutes
3. Wash once with PBS
4. In order to permeabilize the membranes, incubate the coverslips with triton 0.2% (diluted in PBS) for 10 minutes
5. Wash once with PBS
6. To block unspecific binding sites of the antibody incubate 15 minutes with DMEM + 10% FCS
7. Dilute the antibody in DMEM + 10% FCS (see dilution in the datasheet of each antibody). Put a drop of 60 ul in a parafilm very well straightened over the bench and place the coverslip upside down over the drop (the cells have to be in contact with the antibody solution). Incubate 1 hour at room temperature in a humid environment. We usually use a polystyrene box with a wet absorbing paper stick inside and cover the coverslips with this box.
8. Remove the excess of the antibody solution by touching an absorbing paper with the border of the coverslip and place it with the cells facing up in a new well. Wash with PBS 1x.

Sometimes the antibody solution can be recycled, add 0.05% azide to avoid contamination and store it at 4°C

9. Dilute the secondary antibody in DMEM + 10% FCS, according to experimental experience, usually it's between 1/300-1/500

If we use an antibody coupled to a fluorophore, from now on everything has to be done in low light conditions

10. Proceed as in step 7
11. Proceed as in step 8. Wash extensively, around 4 washes of 20 minutes each.
12. Incubate the coverslips with Hoechst diluted in PBS 1x (1/1000) for 10 minutes
13. Mounting of the slides: More than one coverslip per slide can be placed. Put 2 ul of per coverslip) Vectashield (mounting medium) and place the coverslip very carefully upside down (cells facing towards the vectashield) over it.
14. Seal the coverslips with nail polishing. Store at 4°C and away from the light.

Apparatus

Spectrophotometer Beckmann Life Science DU®530

Materials and reagents

Chemicals	Source/Company	Code/quantities
Bovine serum albumin (BSA)	Sigma	A-7906
Orthophosphoric acid	Acros	201140010
Coomassie blue	Acros	191480250
Ethanol	Biosolve	20655
Whatman paper	Whatman	3030917
Plastic microcuvettes 1.5ml	Brand	7590.15
NaOH	Fluka	71690

BSA standard

Concentration (mg/ml)	µl of stock (10 mg/ml)	µl of water
0.0	0	1000
0.5	50	950
1.0	100	900
1.5	150	850
2	200	800

Standards are kept at -20°C. Each person makes her/his own standards.

Bradford reagent

Reagents	Quantity	µl of water
Orthophosphoric acid	400 ml	
Coomassie blue	0.4 g	
Ethanol 95%	200 ml	
Water	Up to 4 l	

Important: Add the Coomassie Brilliant Blue powder only at the end, after preparing the whole solution!!!!

Filter through WHATMAN

Cuvettes:

Disposable cuvettes

1.5 semimicro

Dimensions 12.5 x 12.5 x 45mm

Brand cat : 7590.15

Measure of the concentration of proteins:

	Standard (duplicate)	Samples (duplicate)	Blank
NaOH 0.2N	200ul	200ul	
Lysate		3.3ul	
Standard	10ul		
Bradford's reagent	1.8ml	1.8ml	1.8ml

Bradford' reagent has a dispenser ready with 1.8ml

- Keep in dark before to measure min. 15 minutes (not necessary)
- Standards and samples must be measured twice.
- Read the absorption at 590-600nm:
- `Main menu` `fixed λ` `Blank`
- Make an average of standards
- Read the samples
- Put the paper, online, print
- Make an average of your samples and the difference between of them should be less as 5%
- Use the excel program to calculate yours concentrations

Another way to measure the protein concentrations is as follow:

Introduce the values into the spectrophotometer twice:

`Main menu` `Protein assay` `bradford` `enter` `STD curve` `enter` `more` `enter` `create table` `enter` `0` `enter` `0`
`enter` `0.5` `enter` `0.5` `enter` `1.0` `enter` `1.0` `enter` `1.5` `enter` `1.5` `enter` `entry done.`

Zero with Bradford's reagent

Lecture of standards, when we have the curve: `entry done`

`Dil 1.00` Changer and put factor 3.00 `enter`

Read yours samples and you have directly the protein's concentration then is the same thing as the possibility number one.

IMPORTANT NOTE

The viral supernatants produced by these methods might, depending upon your retroviral insert, contain potentially hazardous recombinant virus. The user of these systems must exercise due caution in the production, use and storage of recombinant retroviral virions, especially those with amphotropic and polytropic host ranges. This consideration should be applied to all genes expressed as amphotropic and polytropic pseudotyped retroviral vectors. Appropriate guidelines should be followed in the use of these recombinant retrovirus production systems.

The user is strongly advised NOT to create retroviruses capable of expressing known oncogenes in amphotropic or polytropic host range viruses.

According to the Swiss Legislation all the manipulations done using lentiviruses, must be performed in a P2 security Laboratory.

For details and authorization for using the P2 Lab, contact Sylvain Lengacher at the Institute of Physiology (tel. 021 692 55 46, email: Sylvain.Lengacher@unil.ch)

For some additional information concerning the Lentiviral Systems you can check the following websites.

Garry Nolan's Lab website at Stanford University: <http://www.stanford.edu/group/nolan/>

Didier Trono's Lab website at Geneva University: <http://www.tronolab.com/>

Reagents.

Hexadimethrine bromide (Polybrene), Fluka (Sigma Cat. N° 52495)

Sucrose, Fluka (Sigma Cat. N° 84100)

Paraformaldehyde 95 %, (Sigma Cat. N° 441244)

Penicillin-Streptomycin Glutamine 100x solution, (GibcoBRL Cat N° 10378-016)

0.45 µm filters, Millex-HN, 0.45µm, 25mm, stérile, 50/PK (Milian Cat N° SLHN025NS)

0.22 µm filters, Millex-GN, 0.22µm, 25mm, stérile, 50/PK (Milian Cat N° SLGN025NS)

Chloroquine (Sigma Cat. N°C6628).

Laminin, mouse (1 mg) (BD Bioscience Cat. N° 354232)

Poly-D-Lysine (20 mg) (BD Bioscience Cat. N° 354210)

Biocidal ZF (1 l) (WAK Chemie Cat N° WAK-ZF-1)

Solutions.

1X Phosphate Buffered Saline (PBS)

NaCl,	8 g
KCl,	0.2 g
Na ₂ PO ₄ ,	1.44 g
KH ₂ PO ₄	0.24 g
H ₂ O	800ml

Adjust pH to 7.4 with HCl.

Adjust volume to 1 liter with additional distilled H₂O. Sterilize by autoclaving.

Tris-EDTA (TE) buffer. (10 mM Tris; 1 mM EDTA; pH 8.0)

1 M Tris pH 8.0	1 ml
0.5 M EDTA pH 8.0	0.2 ml
H ₂ O	98.8 ml

Autoclave

Polybrene 5 mg/ml (10 ml).

Dissolve 5 mg of Polybrene in 10 ml of PBS. Filter through a 0.22 µM filter, aliquot in eppendorf tubes (1 ml per tube) and store either at 4°C or at -20°C.

Chloroquine 25 mM (50 ml).

Dissolve 399.8 mg of Chloroquine in 50 ml of PBS. Filter through a 0.22 µM filter, aliquot in 15 ml falcon tubes (10 ml per tube) and store at -20°C.

Sodium Acetate 3 M pH 5.2 (100 ml).

To 24.6 gr of sodium acetate (Sigma Cat. N° S-2889), add 90 ml of nanopure water. Adjust the pH to 5.2 (with glacial acetic acid) and complete to 100 ml.

Fixation Solution (2% Paraformaldehyde 3% Sucrose).

- a. Weigh 0.2 gr paraformaldehyde in a 15 ml tube.
- b. Add 6 ml PBS.
- c. Warm up to 60°C and vortex.
- d. Add drops of 0.5 M NaOH, warm up to 60° C and vortex until it dissolves.
- e. Add 0.3 gr of Sucrose and make up the volume to 10 ml with PBS.
- f. Make sure the final solution is neutral.

Procedure

Note: for details on the transfection protocol, refer to SOP001 *Transfection (calcium-phosphate)*.

Day 0.

1. Prepare five 10 cm gelatinized Petri dishes containing 2 - 2.5x10⁶ HEK293T cells in 10 ml medium.

Gelatinization of the dishes.

Place between 2 to 5 ml of PBS/0.1% gelatin in the dish [See SOP001] (tilt the plate to cover the entire surface with the solution). Wait at least 10 min. Just before adding the cells to the plates, aspirate the PBS/0.1% gelatin (do not allow the plates to dry).

Day 1.

2. Prewarm all the solutions in a 37°C water bath (at least 20 min). In case the buffer is thawed, mix very well before using.
3. Add 25 µM chloroquine (10 µl of the 25 mM solution) to the cell culture medium (not necessary to change the medium). Place the plates back in the incubator for at least 10 min.

The addition of chloroquine to the medium appears to increase retroviral titer by approximately two fold. This effect is presumably due to the lysosomal neutralizing activity of the chloroquine (3). It is extremely important that the length of chloroquine treatment does not exceed 12 hours. Longer periods of chloroquine treatment have a toxic effect on the cells causing a decrease in retroviral titers.

4. In a 15 ml Falcon tube prepare the following master mix:

	Volume or quantities
H ₂ O	Variable
pCMV delta R8.91	37,5 µg
pMD.G	12,5 µg
Lentiviral vector (e.g. Prom.lti) encoding the gene of interest	50 µg
CaCl ₂	250 µl
2xHepes	2500 µl
FINAL VOLUME	5 ml

All the plasmid should be prepared using Qiagen or Genomed Maxiprep kits and ethanol precipitated. In case the yield of the plasmid is not very high it should be purified using the CsCl purification method.

- Ethanol Precipitation:
 - a- Carefully calculate the volume of your DNA solution.
 - b- Add 1/10 volume of 3 M Sodium Acetate pH 5.2, mix well.
 - c- Add 2 volumes of cold absolute ethanol.
 - d- Keep at -20° C for at least 1 hour.
 - e- Centrifuge 10' at maximum speed.
 - f- Discard supernatant and wash pellet with ethanol 70 % three times.
 - g- Air dry and resuspend in TE.
 - h- Measure DNA concentration.
5. Mix well, by passing 5 times the solution through a 5 ml pipette.
 6. Exactly 60 seconds after mixing the 2xHepes with the CaCl₂-DNA mixture, add 1 ml precipitate per plate.
 7. Incubate for 6-8 hours in an incubator (37°C - 5% CO₂).
 8. Remove medium, wash once with PBS and put fresh medium containing penicillin and streptomycin to avoid contamination (the DNA used for the transfection is generally not sterile!).
 9. 48 hours after the transfection, collect the supernatant of the plates in a 50 ml Falcon Tube.
 10. Centrifuge for 5' at 1500 rpm (~400 g) at 4°C to pellet the detached cells (ALC PK 130 centrifuge, rotor N° T535).
 11. Filter the cleared virus-containing supernatant through a 0.45 µm filter, wrapping everything in a towel humidified with biocidal to avoid aerosols.
 12. Once the virus is filtered, aliquot in 15 ml falcon tubes.

Note: The size of the aliquots may change according the use you will give to your virus.

13. Keep the virus at -80°C.

Freezing does not appear to cause more than a 2-fold drop in titer, as long as the cells do not undergo more than one freeze/thaw cycle. If the cells undergo more than one freeze/thaw cycle, there is a significant drop in retroviral titer.

14. If the virus encodes for a protein that can be detected, calculate functional titer by immunocytochemistry (See SOP011 *Immunocytochemistry*), as detailed below [for siRNA encoding lentiviruses you may calculate your functional titer by monitoring by western blot the conditions that lead to the best decrease of the targeted proteins, (See SOP006.1 *Western Blot*)].

1. Laminin-Polylysine coating

PolyLysine.

Comes as 20 mg/vial. Add sterile H₂O to the vial to a final volume of 1 ml to make a 1 mg/ml stock solution (in a 50 ml falcon tube). Make 1 ml (=1 mg) aliquots. Store at -20 C.

Laminin.

Comes as 1 mg/vial. Add sterile H₂O to the vial to a final volume of 1 ml to make a 1 mg/ml stock solution. Make 100 µl (=100 µg) aliquots. Store at -70 C.

Coating Coverslips.

1. Thaw 1 tube of polylysine and laminin solution.
2. Add laminin, poly-lysine to 25 ml of sterile H₂O.
3. Use 50 µl solution for each coverslips. Place at 37° C for 2 hrs.
4. Rinse 3x with PBS, and use to plate cells.

2. Plate the appropriate number of cells (according to your cells type) in six-well dishes, with two laminin-coated coverslips in each well.

Cells	Number per well (6 well-plates)	Medium	Coating
GAP ^{+/+} and derived cell lines	3-5 · 10 ⁴	DMEM; 10% NBCS	Polylysine /Laminin
HEK 293 and derived cell lines	35 · 10 ⁴	DMEM; 10% NBCS	Polylysine /Laminin
β-Tc-Tet and derived cell lines	10 ⁵	DMEM (without L-Glu); 15% Horse Serum (Heat decomplexed); 2,5% FCS; 2 mM L-Glu; 10 mM Hepes pH 8; 1 mM Na-Pyruvate	Polylysine /Laminin

3. Incubate cells at 37°C, for 12-18 hours.

Important: infect cells when they are not more than 50% confluent.

- The following day, thaw the frozen virus at 37°C (shake often) and once nearly completely thawed, keep on ice. The virus should stay at 0°C all the time.
- Add various amounts of viruses according to the table below, add 2 µl of a 5 mg/ml polybrene stock solution and complete with fresh medium to 3 ml.

Cell #	0 ml	0.25 ml
0.5 ml	1 ml	2 ml

- Immediately thereafter, seal the plates with parafilm and centrifuge them 45' at 2'500 rpm (~800 g) (ALC PK 130 centrifuge, rotor N° T537).
- Incubate overnight in incubator (37°C - 5% CO₂).
- Change medium after 24 hours.
- Remove medium 72 hs after infection and rinse once with 2 ml of PBS.
- Fix cells by adding 1 ml of PBS-2% paraformaldehyde-3% Sucrose, for 15 minutes.
- The following immunocytochemistry steps can be performed on the bench (*See SOP011*).
- Knowing the number of cells at the moment of infection and the smallest volume that leads to expression of the gene of interest in ~100% of the cells, you can estimate the number of infective particles per ml.

References

- Jordan et al. - Nucl. Acid Res. (1996) **24**:596. For transfection.
- Dull, T. et al. - *J.Virol.* 72.11 (1998): 8463-71. For 3rd generation lentiviral vectors.
- Mulligan, R.C. and Berg, P. - PNAS 78, 2072-2076 (1981)

Author : Alessandro Annibaldi

Introduction.

In molecular biology Cell Fractioning is a laboratory technique used to break cells and separate their molecular and structural components. Cell Fractioning can be divided in two steps: Homogenization and Fractionation. The Homogenization phase, whose purpose is to break the cell, is obtained either by the osmotic alteration of the media where cells are broken open through the utilization of an hypotonic buffer or by mechanical disruption. The Fractionation phase relies on the utilization of centrifugations at different speeds and times to separate cellular components on the basis of their size.

Cell Fractioning (Nuclei/Cytoplasm).

Day 0

Spread at least $2 \cdot 10^6$ in a 10 cm plate. If you want to look at the localization of one or more exogenous protein transfect your cells according to either SOP 1.0 or SOP 3.0, depending on the cell type with which you are working.

Day 1

1. Wash your 10 cm plate with PBS.
2. Add 400 μ l of lysis buffer 0.5% Triton X-100.
3. Scrape cells and incubate on ice for 20 minutes.
4. Centrifugate at 13.000 rpm (16'100 x g) in the Eppendorf centrifuge 5415R located in the lab.
5. Transfer the supernatant (membrane/cytoplasm fraction) into a new Eppendorf tube and keep the pellet.
6. Quantitate the protein concentrations of your samples using the Eppendorf Biophotometer located in the lab (see SOP 13.0 [Bradford]).
7. After completing the quantitation, add the loading buffer according to the amount of protein you want to load. At this point your **Cytoplasmic fraction** is ready to be loaded or alternatively you can store it at -20 °C.
8. Rinse the pellet representing the nuclear/mitochondrial fraction with the lysis buffer once and resuspend in the lysis buffer containing 0.5% SDS. Shear the released genomic DNA by sonication. The sonicator (Heischer DmbH) is now located downstairs, in a room that is in front of Peter Clark's group cell culture room. The settings you have to use are the followings:
Cycle (representing the number of cycles per second): 0.8-0.9.
Amplitude: 80%
9. Once there you have to insert the metallic tip of the sonicator inside your Eppendorf tube and press the black button located on the top of the sonicator for 10 seconds. Two sonications are enough to completely break the DNA. After each sonication place the sample back on ice for a few seconds. Before processing the next sample, wash the metallic tip of the sonicator first with ethanol 70% and then with water. Dry the tip with a clean tissue.
10. After sonication, centrifuge at 13.000 rpm (16'100 x g) in the Eppendorf centrifuge 5415R and transfer the supernatant in a new Eppendorf.

11. Quantitate the protein concentrations of your samples using the Eppendorf Biophotometer located in the lab (see SOP 13.0 [Bradford]).
12. After completing the quantitation, add the loading buffer according to the amount of protein you want to load. At this point your **Nuclear fraction** is ready to be loaded or alternatively you can store it at -20 °C.

Cell Fractioning (Nuclei, Mitochondria, Cytoplasm and Membrane)

Day 0

Start from at least 10^6 using 10 cm plates. If you want to look at the localization of one or more exogenous protein transfect your cells according to either SOP 1.0 or SOP 3.0, depending on the cell type with which you are working.

Day 1

1. Wash your 10 cm plate with PBS.
2. Add 300 µl of hypotonic lysis buffer.
3. Scrape cells and incubate on ice for 20 minutes.
4. Centrifugate at 300 x g 5 minutes at 4 °C in the Eppendorf centrifuge 5415R to pellet nuclei.
5. Transfer the supernatant in a new eppendorf and wash the pellet twice with the lysis buffer. For each wash add 250 µl of lysis buffer, centrifugate at 300 x g and discard the supernatant.
6. Resuspend the pellet in 200 µl of lysis buffer + Triton X100 1%.
7. Quantitate the protein concentrations of your samples using the Eppendorf Biophotometer located in the lab (see SOP 13.0 [Bradford]).
8. After completing the quantitation, add the loading buffer according to the amount of protein you want to load. At this point your **Nuclear fraction** is ready to be loaded or alternatively you can store it at -20 °C.
9. For the mitochondrial fraction start from point number 5. After transferring the supernatant in a new Eppendorf tube, centrifugate at 10'000 x g in the Eppendorf centrifuge 5415R located in the lab for 10 minutes at 4 °C to pellet mitochondria.
10. Transfer the supernatant in a new Eppendorf tube and resuspend the pellet in 200 µl of lysis buffer + Triton X100 1%.
11. Sonicate as described above.
12. Quantitate the protein concentrations of your samples using the Eppendorf Biophotometer located in the lab (see SOP 13.0 [Bradford]).
13. After completing the quantitation, add the loading buffer according to the amount of protein you want to load. At this point your **Mitochondrial fraction** is ready to be loaded or alternatively you can store it at -20 °C.
14. Take the supernatant you transferred in a new Eppendorf tube (point number 10) and centrifugate at 100'000 x g 1.5 hours at 4 °C. For this centrifugation, you have to use the ultra-centrifuge named Centrikon T-108 located in the P2 lab. The rotor, 'Kontron 18425', is

located in the fridge in front of Romano Regazzi's lab. Tubes that suit the rotor are provided from Beckman and the maximum volume you can put in the tubes is 1 ml. After the centrifugation (as well as before using it) clean it with ethanol 70% and water. Do not forget to put the rotor back to its storage place.

15. Transfer the supernatant in a new Eppendorf tube.
16. Quantitate the protein concentrations of your samples using the Eppendorf Biophotometer located in the lab (see SOP 13.0 [Bradford]).
17. After completing the quantitation, add the loading buffer according to the amount of protein you want to load. At this point your **Cytoplasmic fraction** is ready to be loaded or alternatively you can store it at -20 °C.
18. Resuspend the pellet in 150 µl of lysis buffer + Triton X100 1%.
19. Sonicate as described above.
20. Quantitate the protein concentrations of your samples using the Eppendorf Biophotometer located in the lab (see SOP 13.0 [Bradford]).
21. After completing the quantitation, add the loading buffer according to the amount of protein you want to load. At this point your **Membrane fraction** is ready to be loaded or alternatively you can store it at -20 °C.

Materials and reagents	Source/Company	Code
TRIS (Trizma base)	Sigma	T1503
Triton X-100	Fluka	93426
NaCl	Acros	207790050
Glycerol	Fluka	49780
MgCl ₂	MERCK	TA 808932
KCl	Fluka	60130
SDS (sodium dodecyl sulphate)	Sigma	L4390
HEPES	AppliChem	A3724
Centrifuge tubes 11 x 34 mm	Beckman	343778

Lysis buffer (0.5% Triton X-100, 500 mM Tris-HCl pH 7.5, 137 mM NaCl, 10% glycerol, 0.5% Triton X-100)

For 10 ml

5 ml of Tris-HCl pH 7.5 1M

274 µl of NaCl 5M

1 ml of glycerol 100%

50 µl of Triton X-100

Up to 10 ml with water

Hypotonic lysis buffer (10 mM HEPES pH 7.4, 10 mM MgCl₂, 42 mM KCl)

For 10 ml

200 µl of HEPES pH 7.4 500 mM

100 µl of MgCl₂ 1 M

420 µl of KCl 1 M

Up to 10 ml with water

Materials and reagents

Materials and reagents	Source/Company	Code
Coplin Jar (Figure 1)		
Ethanol	Merck	K38929083
Xilene		
Tris 1M pH7.6	Sigma	1297640
BSA	Sigma	A7906
Tween 20	Acros	233360010
Citric acid	Sigma	C8532
EDTA pH8	Fluka	03620
Liquid blocker	Daido Sangyo Co.	22309
Hoechst		
Vectashield Mounting medium	Reactolab	H-1000
Incubation chamber	Plastic flat box with wet tissue on the bottom	
Coverslips	Menzel-Glaser	Available in the DBCM stock



Figure 1: Coplin Jar. In the laboratory, we have jars accommodating 8 and 12 slides.

Buffers**20X TBS (1M Tris base, 18% NaCl, pH 7.6)**

Weigh 122 g of Tris and 180 g NaCl dissolve in 800 ml of distilled water. Adjust the pH to 7.6 with HCl 37%. The volume of HCl to add is approximately 65 to 70 ml. Add water to 1000 ml. Store this solution at room temperature. Dilute 1:20 with distilled water before use and adjust pH if necessary.

I) IHC with fluorescence

Buffer 1: TBS 1x pH 7.6

Dilute TBS 20X, 1:20 with distilled water

Buffer 2: TBS 1x pH 7.6+ Tween 20 0.5%

Dilute TBS 20X, 1:20 with distilled water and add 5 ml of Tween 100% (0.5%).

Buffer 3: TBS 1x pH 7.6 + Tween 20 0.5% + BSA 0.2%

Dilute TBS 20X, 1:20 with distilled water. Add 5 ml of Tween 100% and 2 g of BSA.

Experimental protocol

Slide deparaffinization.

Put the slides on a plate and incubate at 60°C until the paraffin is completely dissolved. Immediately after this (it has to be fast because the paraffin can solidify again), immerse the slides in the first incubation solution described below and then proceed with the subsequent washes.

Incubate sections sequentially in:

- 1°_ xylene 5'
- 2°_ xylene 3'
- 3°_ Ethanol 100% 3'
- 4°_ Ethanol 100% 2'
- 5°_ Ethanol 90%, 2'
- 6°_ Ethanol 75%, 2'
- 7°_ Ethanol 50%, 2'
- 8°_ Wash with water from the sink, distilled water is not necessary.

These solvents are located in a hood besides the radio in Peter Clarke's lab. Turn on the aeration system (top left) of the hood before starting with deparaffinization.

If you have problems of detachment there is an alternative deparaffinization protocol in the annexe.

The slides are now ready for the IHC

Antigen retrieval

The antigen retrieval protocol should be assessed for each antibody. There are cases where no antigen retrieval is needed but this has to be tested for each particular antibody. In the attached table there is a list of already standardised antigen retrieval protocols.

The following two protocols are the most common ones.

Tris-EDTA Buffer (10 mM Tris Base, 1 mM EDTA, 0.01% Tween 20, pH 9)

Tris-base	1.21 g
EDTA	0.37 g
Distilled H ₂ O	1000 ml

Adjust the pH to 9 and then add 0.1 ml of Tween 20. Mix well.

Prepare 1000 ml and put it in a pressure casserole and heat until the second red line is seen on the pressure marker (approximately 10 minutes but it's better to be there before in case there is liquid spilling out the casserole, in this case, remove the recipient from the heating plaque immediately). At this point wait 2 minutes and take the casserole out of the heating plaque. Release the pressure (by pushing down the pressure indicator) and place the casserole in the sink. Pour cold water on the cover without opening it.

Once the vapour is all out open the casserole and take the slides out. Wash immediately with tap water and begin with the immunohistochemistry staining.

Immunohistochemistry (IHC) in fluorescence on paraffin sections

Sodium Citrate Buffer (10 mM Sodium citrate pH 6.0)

Tri-Sodium citrate (dehydrate)	2.94 g
Distilled H ₂ O	1000 ml

Adjust the pH to 6 with HCl and mix well.

This buffer is commonly used and works perfectly well with most antibodies. It gives very nice intense staining with very low background.

This buffer can be used either with the pressure casserole or in the microwaves.

Usually I use it in the microwave. Put the slides into 1000 ml of buffer in a microwave-resistant recipient with a cover. Use the highest power setting until the liquid boils (takes about 7 to 8 minutes). Once the buffer is boiling, lower the power to the minimum and keep heating for 11 minutes. Once the procedure is finished, leave the slides to cool down in the same buffer for at least one hour with agitation. To shorten this period of time, ice can be placed into the recipient. For certain antibodies, there is no need to let the buffer get completely cold.

Wash with tap water before starting the immuno-histochemistry procedure.

Immunostaining

Before starting, surround the samples about to be stained with liquid blocker to ensure a minimal area in which the incubations will be done. Air dry the liquid blocker for a few seconds (but do not dry out the sample!). The liquid blocker should be kept at 4°C.

1. Incubate the slides in a Coplin jar with buffer 1 for 5 minutes on a shaker. Repeat this washing step with buffer 2. All the washing steps should be done on the shaker.
2. Blocking of unspecific sites: add 100 µl of blocking solution (buffer 3) onto the section and into the area delimited by the liquid blocker. Incubate the slides in a humid chamber for at least 30 minutes at room temperature. The humid chamber is a plastic box with a wet tissue inside; keep it close to maintain humidity. If desired 15% of serum of the species in which the secondary antibody was made, can be added to the blocking solution (for example, if the secondary antibody is a goat anti-mouse antibody, you have to choose goat serum). Adding serum is not essential but it can be important when doing a double or triple staining.
3. Incubation with the first antibody: Add 100 µl per slide of the primary antibody diluted in buffer 3 according to the datasheet of the given antibody. Incubate in a humid chamber for 1 hour at room temperature. For some antibodies you can increase the signal by incubating the slides over night at 4°C. To avoid evaporation of the liquid you can cover the slide (with the antibody solution) with parafilm (just put it over it without pressing). This will also ensure a homogeneous spreading of the liquid.
4. Washings: wash the slides three times in buffer 2 for 5 minutes or two times for 10 minutes.

Immunohistochemistry (IHC) in fluorescence on paraffin sections

5. Incubation with secondary antibody: put 100 μ l per slide of the secondary antibody diluted in buffer 3. Usually, the dilution is between 1/200 and 1/500 but this should be tested when new antibodies are employed. Incubate the slides in a humid and dark chamber for 1 hour at room temperature. Secondary antibodies are located on the first freezer you find when entering the lab, in the top right drawer.
6. Wash the samples extensively in a dark or covered Coplin Jar. Perform at least 6 washes of 20 minutes each, in buffer 2. An overnight washing at 4°C is recommended but not essential.
7. Nucleus staining: Dilute the Hoechst dye (located in the first fridge you find when entering in the culture room) 1:1000 in buffer 2 and put 100ul per slide. Incubate in a humid and dark chamber for 10 minutes at room temperature (longer incubation time can result in a saturated staining)
8. Mount the slides with Vectashield mounting medium. This is a special medium used to conserve the fluorescence for longer time. Anyway do not wait too much to observe the slides as the quality would not be as good as if you look at them within one week. The volume of Vectashield to be used should be between 5 μ l, for small samples, to 20 μ l, for big ones. Place a coverslip over it trying to avoid the formation of bubbles
9. Surround the coverslip with nail polish in order to protect the samples from drying out. Keep the slides at 4°C in the dark.

Annexe**Alternative deparaffinization protocol**

Put the slides over a plate at 60°C until the paraffin is completely dissolved. Soon after this, immerse the slides on the first incubation solution described below.

Incubate sections sequentially in:

- 1°_ xylene 5'
- 2°_ xylene 3'
- 3°_ Ethanol 100% 3'
- 4°_ Ethanol 80%, 2'
- 5°_ Put the slides over the plate at 60°C until they dry out completely
- 6°_ Wash with water from the sink, distilled water is not necessary.

Antigen retrieval protocol for some antibodies used in the laboratory

Antibody	Company	Antigen retrieval protocol
Survivin	Cell signalling (2808)	Citrate buffer + microwave
Cytokeratin 5 (MK5)	Covance (PRB-160P)	Citrate buffer + microwave
Cytokeratin 10 (MK10)	Covance (PRB-159P)	Citrate buffer + microwave
Active caspase-3	Cell signalling (9664)	Citrate buffer + microwave
KI-67	Dako (M7249)	Tris-EDTA + pressure

pAkt (Ser473)*	Cell signalling (9271)	Citrate buffer + microwave + TSA amplification system
----------------	------------------------	---

***For this antibody another protocol is needed that uses the TSA plus amplification system.**

Protocol according to manufacturer's instructions (Perkin Elmer)

Comments:

There is an alternative staining method that uses the peroxidase enzyme to visualize the stained structures.

This technique is useful if it is important to see the structure of the tissue you are working with.

Pull-down for mass spectrometry analysis:

1-Transfection

- 2×10^6 HEK293T cells were transfected with $5\mu\text{g}$ of either empty vector Stag-V5.pcdn3 (negative control), or Stag-V5-N (D157A).dn3
(35 plates* 2Million = total 70 million cells per condition)
- Six hours after transfection the medium was changed, and the cells were incubated for 24 hours at 37°C , 5% CO_2 .

2-Lysis

- 24 hours after transfection cells were washed once with 1X PBS.
- Lysed in 500 μl 1% NP40 lysis buffer:
25 mM Tris pH 7.5
150 mM NaCl
1% NP 40
Adjust pH to 7.4.

Lysis step performed on ice.

- Lysates were centrifuged at 13000rpm for 10 minutes.
- 10 μl of each lysate were retained in order to check transfection efficiency by western blot, 20 μg of each sample were loaded 10% gel and protein expression was checked by western blot.
- Supernatant collected and pooled down together: total 18ml of lysates (per condition).

3-Pull-down

- 15 μl of S-protein (Novagen Cat: 69218) were added and the samples were left rotating gently at 4°C 9rpm overnight. (S-protein will recognize Stag in a similar manner to antibody-epitope recognition.
- 12 hours later a centrifugation step was done for 20min at 13000rpm, 4°C in order to get rid of undesired aggregates (N.B Aggregates similar to DNA precipitate seen in Maxipreps could be seen clearly after this centrifugation step)
- 120 μl of 50% Beads (streptavidin sepharose High performance Cat: 17-5113-01) were added to the samples which were incubated rotating at 4°C for 4 further hours at 9 rpm. (before using the beads were washed 1X with PBS centrifuged at 800rpm for 1 min and resuspended in 1/1 volume of PBS)

4-Washing

- The mixture (beads-Sprotein-Protein samples) were washed 5X with 0.1% Tween-20 PBS

(Washing = 500 μ l 0.1% Tween-20 PBS, mix, centrifuge for 2min at 1000 rpm / 4°C).

- 1/10 of the total beads were retained for silver staining and the rest 9/10 were frozen and sent to LC-MC proteomics facility.

5-Elution

- For the 1/10 of pulldown product: 30 μ l of 2X SDS-loading buffers were added, the samples were vortexed, boiled for 5 min at 95 °C, and centrifuged .
- 5 μ l of the pulldown product were loaded on 10% gel and checked by western blot to confirm the Pulldown of stag- fragment N.
- The rest of the pulldown product were loaded on the another 10% gel in parallel for silver staining.